Oleg V. Petrov
Morten Smelror *Editors*

Tectonics of the Arctic

Springer Geology

The book series Springer Geology comprises a broad portfolio of scientific books, aiming at researchers, students, and everyone interested in geology. The series includes peer-reviewed monographs, edited volumes, textbooks, and conference proceedings. It covers the entire research area of geology including, but not limited to, economic geology, mineral resources, historical geology, quantitative geology, structural geology, geomorphology, paleontology, and sedimentology.

More information about this series at http://www.springer.com/series/10172

Oleg V. Petrov · Morten Smelror
Editors

Tectonics of the Arctic

Springer

Editors
Oleg V. Petrov
Russian Geological Research Institute
St. Petersburg, Russia

Morten Smelror
Geological Survey of Norway
Trondheim, Norway

Acknowledgements

Introduction

The Arctic is a geologically unique region where the North American, Eurasian and Pacific lithospheric plates come together, and a new Arctic Ocean is born on the continuation of the North Atlantic. The northern geographical and magnetic poles are located in the Arctic. Large ore deposits have been discovered in the Arctic regions, and the shelves contain large hydrocarbon resources. The interest in Arctic research, which has increased in the last decade, is associated with geopolitical interests of the Arctic states to expand their areas at the expense of the deep marine shelf within the scope of the UN Commission on the Law of the Sea. Not only the Arctic states—Denmark, Canada, Russia, the USA, Norway, but also such leading countries of the world as France, Germany, Great Britain, China, the Republic of Korea have an increased focus on the region.

Until recently, the Arctic remained one of the most unexplored places on the planet. Over the last 10–15 years, new geological and geophysical information on the Central Arctic and adjacent shelves has been obtained due to high-latitude scientific trips under national and international programs (e. g., Outer Limits of the Continental Shelf, IODP), international combined expeditions to the islands of the Russian and Canadian Arctic, and as a result of drilling and seismic surveys aimed at the assessment of the oil and gas potential of the Arctic shelf.

Ambitious international project **Atlas of 1: 5M Geological Maps of the Circumpolar Arctic** was launched to generalize recent geological and geophysical information. It has been carried out since 2003 by the Geological Surveys of Norway, Canada, Russia, the USA, Denmark, Sweden, Germany and France under the auspices of the Commission for the Geological Map of the World/UNESCO, with the participation of experts from national academies and universities. As part of this project, the following potential maps were compiled and published: Potential Fields Map (2008, coordinated by Norway), Geological Map (2009, coordinated by Canada), Ore Deposits Map (2012, coordinated by Norway) and Tectonic Map (2018, coordinated by Russia).

Geological Map. The assembly of the Circum-Arctic geological bedrock map at 1: 5M scale and related database was launched as part of the International Polar Year 2007–2008, under the aegis of the Commission for the Geological Map of the World (CGMW).
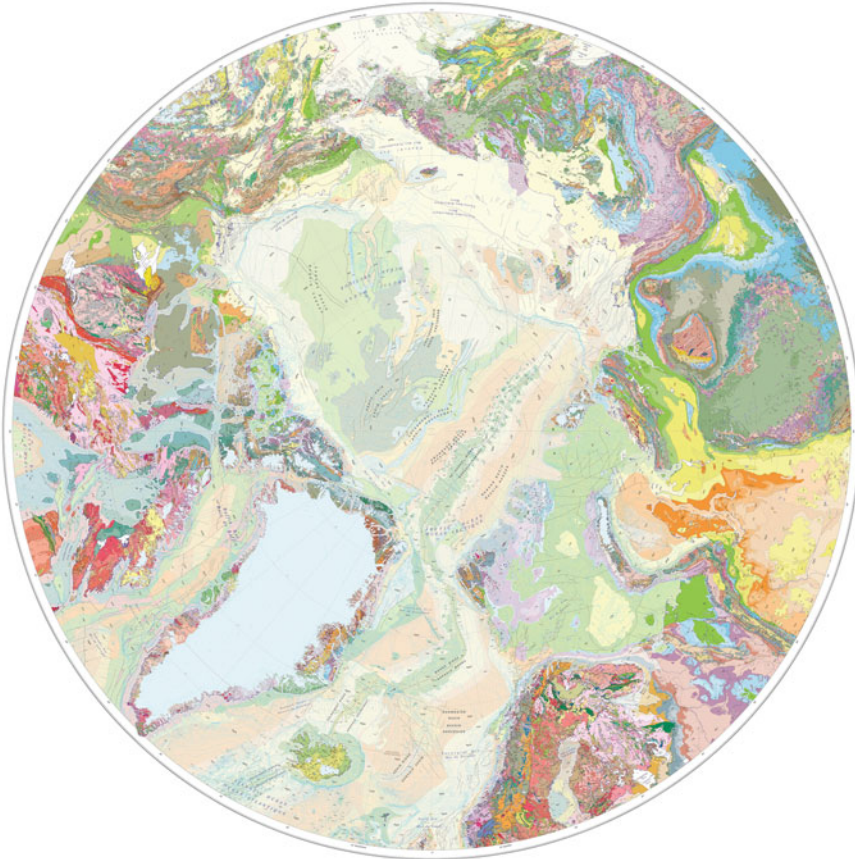
Fig. 1. The bedrock map of the Arctic (Harrison et al. 2011a) (http://geoscan.nrcan.gc.ca/starweb/geoscan/servlet.starweb?path=geoscan/downloade.web&search1=R=287868)

The Circum-Arctic geological map (Fig. 1) combines a large body of new geological information for land areas and new data on bathymetry, dredged samples and available seismic and potential field data for the Arctic Ocean basins. This information was obtained by geological projects carried out in different countries as well as during several international expeditions pursuing investigation of the geology of northern continental margins and Arctic islands—the only places where bedrock buried beneath the younger sediments in the Arctic Ocean are exposed and can be observed.

The map compilation was led by J. C. Harrison and a Canadian team based in Calgary and Ottawa, with the active participation of scientific and technical staff from the geological surveys of Canada, Denmark, Norway, Russia, Sweden and the USA. Project work began in February 2006, and a completed draft in hard copy was presented as intended at the 33rd International Geological Congress in Oslo in 2008.

The map was completed in preliminary form by October 2008 and published by Geological Survey of Canada (GSC) in November the same year (Harrison et al. 2008b). The final map was formally released in 2011 as Geological Survey of Canada Map 2159A and is freely available in digital format from NRCan's Geogratis web site (Harrison et al. 2011a). The map is presented in North Polar stereographic projection, using the WGS 84 datum, and includes complete geological coverage for all onshore and offshore areas down to latitude 60°N. The final printed map is 1.3 m in diameter and is one of the most intricate maps of its kind ever produced by the Geological Survey of Canada. The map consists of five different sheets: The bedrock map at 1: 5M scale with explanatory notes and the list of contributors, the Legend, the Precambrian correlation chart; and two Phanerozoic correlations charts (Harrison et al. 2008a, b, 2009, 2011a, b).

Studied together with known resource occurrence datasets, the new bedrock map and database can be used for project planning and evaluation of mineral and energy resource potential in a wide range of geological settings. This archive of digital spatial data for the Circum-Arctic further represents an important source for the production of formal digital products and also informal user-defined map products accessed via the worldwide web. Collectively, these data can serve as a model for other digital maps from elsewhere in the world.

Compilations of the magnetic and gravimetric maps that will be described in Chapter 2 was coordinated by the Geological Survey of Norway, and Carmen Gaina was chosen as the leader of the "Circum-Arctic Mapping Project—Gravity and Magnetic Maps" (CAMP-GM) working group.

Mineral Resource Map (Fig. 2). The Arctic and high-north areas have a significant potential for metallogenic resources, as well as holding large volumes of prospective industrial minerals. Major new discoveries are still being made in the Arctic, both beyond the regions that are already well known and within provinces where there already operating mines, where the use of modern exploration methods has revealed "new" ore bodies underneath surface Quaternary deposits or at greater depth in the Earth's crust.

There has been a continuing discovery of major new deposits in the Arctic, some in known metallogenic provinces but others in regions not previously recognized as having a major mineral potential. One key issue for the increased mineral exploration in the Arctic relates to increased need for and access to critical mineral resources: Major deposits of many of the critical minerals occur in the Arctic. Another factor is the improved access to the resources due to the more consistent, longer-term opening of shipping lanes such as the Northern Sea Route (North-East Passage) and the North-West Passage combined with greater access to ice-classified cargo vessels and ice-breakers.

Informations on Arctic and high-north mineral resources are available in the archives and databases of the geological surveys and other national agencies. Based on these records, a new joint database and maps showing major metals and mineral deposits of the Arctic were complied. Information on the individual deposits is provided the database accessible online at the project website: www.ngu.no/camet.
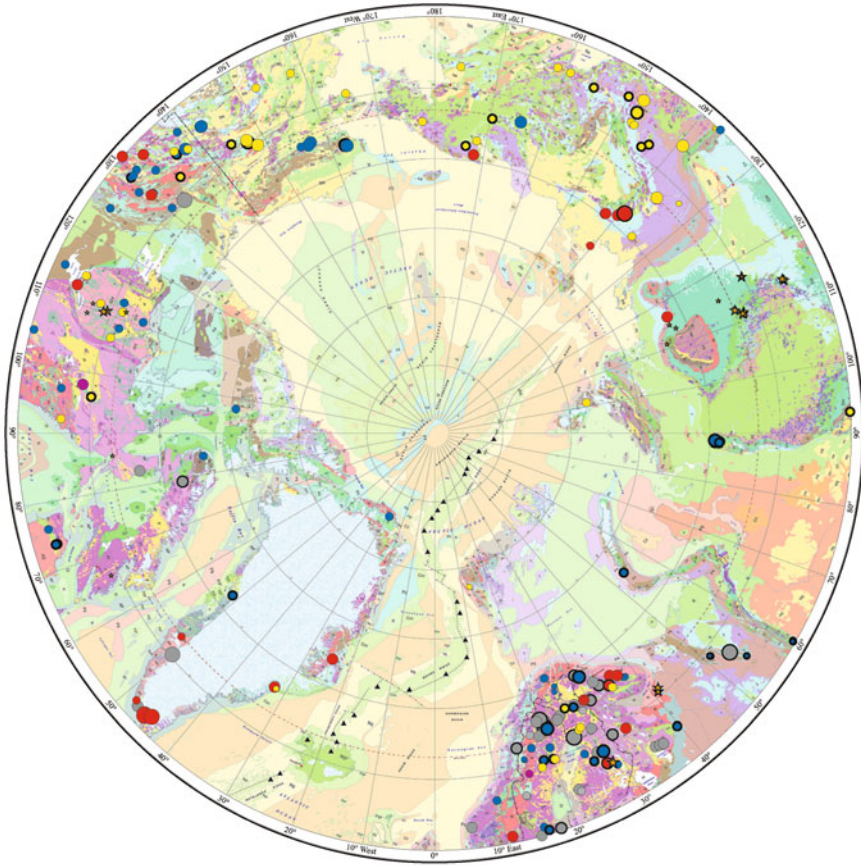
Fig. 2. Metal and mineral deposits of the Arctic, scale 1: 10 000 000. The map is compiled from a database compiled by Jochen Kolb, Frands Schjøth, Símun Olsen, Lars L. Sørensen (GEUS), Lesley Chorlton, Christopher Harrison (GSC), Jouni Vuollo, Taina Eloranta, Pasi Eilu (GTK), Terje Bjerkgård, Jan-Sverre Sandstad (NGU), Anders Hallberg (SGU), Frederic Wilson (USGS) and Artem Terekhov, Anatoly Molchanov, Vitaly Shatov (VSEGEI) (Nordahl et al. 2016)

The new database was compiled by Jochen Kolb, Frands Schjøth, Símun Olsen, Lars L. Sørensen (GEUS), Lesley Chorlton, Christopher Harrison (GSC), Jouni Vuollo, Taina Eloranta, Pasi Eilu (GTK), Terje Bjerkgård, Jan-Sverre Sandstad (NGU), Anders Hallberg (SGU), Frederic Wilson (USGS) and Artem Terekhov, Anatoly Molchanov, Vitaly Shatov (VSEGEI) (Nordahl et al. 2016). The Fennoscandian Ore-Deposit Database (FODD) project implemented by the Finnish, Norwegian and Swedish geological surveys and geological authorities in Murmansk and Karelia regions in NW Russia for the area underlain by the Fennoscandian Shield (http://en. gtk.fi/informationservices/databases/fodd/index.html) has had great importance for the Circum-Arctic project. The database developed in the FODD project, which is available at the above site, has functioned as a template for the Circum-Arctic project

database, though the Circum-Arctic project includes, for numerous practical reasons, only the deposits in the three largest size categories of the FODD system—Large, Very Large and Potentially Large.

Tectonic Map. Tectonic Map is supplemented by a set of maps covering the deep structure of the Arctic, including the Arctic Basin and the North Atlantic, with their continental margins north of 60°N. The map reflects the new understanding of the continental nature of the Alpha-Mendeleev Ridge System based on the latest seismic data interpretation, results of studying rock samples collected from sea bottom exposures by means of a submarine and deep-water drilling by Russian researchers (Expeditions 2012, 2014 and 2016), which allowed identification of close geological relationships of the deep-water Central Arctic Elevations with the structures of the adjacent shallow-water shelves. The new geological and geophysical data used in the map show that the mid-oceanic Gakkel Ridge continues onto the Laptev Sea shelf as the Aptian-Cenozoic rift structure, which coincides with the boundary of the North American and Eurasian lithospheric plates.

A new stage in the generalization of new geological data on the Arctic is the international *Tectonostratigraphic Atlas of the Northeast Atlantic Region* (edited by John R. Hopper et al.) published by the Geological Survey of Denmark (GEUS 2014). It contains large amounts of information on bathymetry, potential fields, crustal structure, seismic stratigraphy, tectonics, heat flow, volcanism and the mantle structure of the North Atlantic and the Eurasian ocean basin with their continental margins and islands.

Tectonostratigraphic Atlas of the Eastern Regions of Russia and Adjacent Areas contains geological and geophysical data on the eastern Eurasian continental margin of the Arctic Ocean and the adjacent water areas of the Arctic basin from the Barents-Kara margin to the Chukchi Plateau. It also contains geological maps, stratigraphic charts, potential fields maps, digital bank of correlated seismic profiles and research results of bottom rock samples from the Mendeleev Rise.

Geological map of the Eastern Arctic and the adjacent deep-water areas takes advantage of 1: 1M State geological maps and unified legend and is correlated with seismic profiles in the area of the Central Arctic Elevations. Tectonostratigraphic charts of sedimentary and magmatic complexes of Arctic islands and continental land describe sedimentation and its relation to main stages of tectonic evolution of the Eastern Arctic. To build these charts, data obtained during international expeditions to the New Siberian Islands and Wrangel Island with the participation of geologists from Russia, Germany, Sweden and other countries was used. Paleomagnetic studies, carried out on the New Siberian Islands for the first time, showed that the Anjou Archipelago and the De Long Archipelago belonged to the common Late Precambrian block during the pre-Mesozoic.

Interrelated structural maps of main reflecting horizons on seismic profiles constructed using CDP seismic reflection lines, maps of seismic complexes' thickness and seismic-facies analysis based on them made it possible to create paleogeographic reconstructions for the Cretaceous, Paleogene and Neogene.

Information on research results of deep-sea sampling of the Mendeleev Rise presented in the Tectonostratigraphic Atlas shows that the consolidated sedimentary cover of the Central Arctic Elevations zone is mainly represented by Vendian to Permian terrigenouscarbonate epiplatform sediments. The upper weakly lithified part of the cover is represented by Meso-Cenozoic sediments, which host magmatic intrusive and effusive rocks of the trappean formation.

Tectonostratigraphic Atlas of the Eastern Regions of Russia and Adjacent Areas was published in Russian in 2019. This book partially repeats the contents of this Atlas, but is largely supplemented by other material.

Tectonic Map of the Arctic (TeMAr), Tectonostratigraphic Atlases of the northeastern Atlantic region and eastern regions of Russia and adjacent areas provided a base for the creation of the present-day platetectonic model of the Arctic region. According to this model, the recent tectonic structure of the Arctic is controlled by the interaction of three lithospheric plates: two continental plates (North American and Eurasian) and the Pacific Oceanic Plate. The Pacific Oceanic Plate, submerging with variable velocities beneath the North American and Eurasian plates, largely determined the kinematics and the age of the boundaries of the lithospheric plates in the Late Mesozoic and Cenozoic.

According to the plate tectonic model, the region of the Central Arctic Elevations corresponds to the marginal part of the North American Continental Plate, and all recent tectonic processes within it are intraplate. At present, it is safe to say that the Neoproterozoic (Epigrenvillian) craton, complicated by Mesozoic-Cenozoic structures, occupies the entire polar region, including islands, shelves and the Central Arctic Elevations of the Amerasian basin. This plate tectonic model fully confirms assumptions of academicians N. S. Shatsky, Yu. M. Pushcharovsky, V. E. Khain, L. P. Sonnenschein, L. M. Natapov and other Soviet and Russian scientists, who in the middle of the last century identified there the Hyperborean Platform, known in later literature as Arctida.

Oleg V. Petrov
Morten Smelror

Contents

New Tectonic Map of the Arctic

O. V. Petrov, M. Pubellier, S. P. Shokalsky, A. F. Morozov, Yu. B. Kazmin, S. N. Kashubin, V. A. Vernikovsky, M. Smelror, H. Brekke, V. D. Kaminsky, and I. I. Pospelov

Abstract The Tectonic Map of the Arctic (TeMAr) that has been compiled under the International project Atlas of Geological maps of the Circumpolar Arctic in scale 1:5 M. The TeMAr working group coordinated by Russia (VSEGEI) includes leading scientists from Geological Surveys, universities and national Academies of Sciences of Denmark, Sweden, Norway, Russia, Canada, the USA, France, Germany and Great Britain. The Tectonic Map compilation activities were aimed at acquiring thorough understanding of deep-water geological formations of the Arctic and Norwegian-Greenland basins, shelves of the marginal seas and the adjacent continental onshore areas of the oceans. The Tectonic Map is supplemented with a set of geophysical maps, schematic maps and sections that illustrate the deep structure of the Earth's crust and upper mantle of the Circumpolar Arctic.

O. V. Petrov (✉) · S. P. Shokalsky · S. N. Kashubin · I. I. Pospelov
Russian Geological Research Institute (VSEGEI), 74 Sredny Prospect, St Petersburg 199106, Russia
e-mail: vsgdir@vsegei.ru

M. Pubellier
French National Centre for Scientific Research (CNRS), 3 Rue Michel Ange, 75016 Paris, France

A. F. Morozov · Yu. B. Kazmin
Federal Agency for Mineral Resources (Rosnedra), 4/6 Gruzinskaya, Moscow 125993, Russia

V. A. Vernikovsky
Institute of Petroleum Geology and Geophysics, Russian Academy of Sciences (IPGG SB RAS), 3 Koptug ave., Novosibirsk 630090, Russia

M. Smelror
Geological Survey of Norway (NGU), Torgarden, 7491 Trondheim, Norway

H. Brekke
Norwegian Petroleum Directorate, 4003 Stavanger, Norway

V. D. Kaminsky
Russian Research Institute for Geology and Mineral Resources of the Ocean (VNIIOKEANGEOLOGIA), 1 Angliyskiy av., St Petersburg 1190121, Russia

1 History of the Tectonic Map Compilation

The Tectonic Map of the Arctic (TeMAr) is based upon the Polar Stereographic Projection (WGS 84) (Fig. 1). In the south the map is bounded by 60 °N. The shadow relief base of the map was compiled using superposed images, synthesized from the Landsat 7 ETM+ (in three bands: 7 (2.08–2.35 µm), 4 (0.76–0.90 µm and 2 (0.52–0.60 µm) and a digital landform model. The landform model has been constructed from the SRTM radar data (Shuttle Radar Topographic Mission with 900 m = 30″ resolution) and the IBCAO chart (version 2.23 with 2 km resolution) in the off shore areas.

The compilation of the 1:5 M Tectonic Map of the Arctic was based on its legend constructed by the following principles:
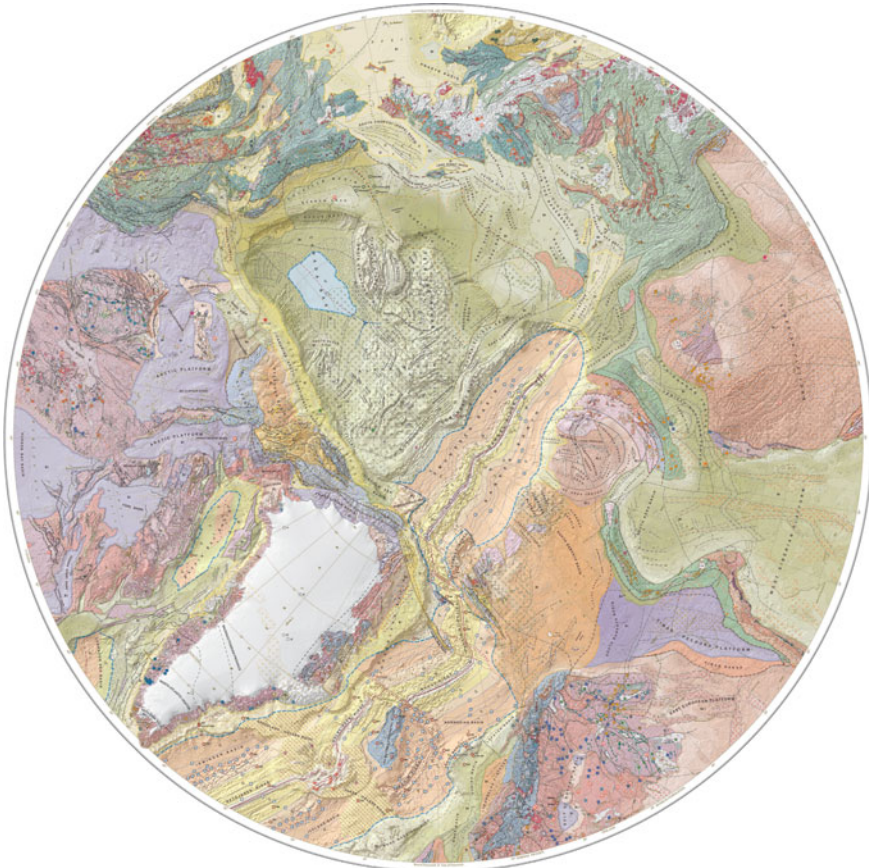
Fig. 1 Tectonic Map of the Arctic at 1:10 M scale (Petrov et al. 2019). The map with the legend and additional maps and schemes are available on the site of VSEGEI: http://www.vsegei.com/en/intcooperation/temar-5000

- integral cartographic representation of geological structures in deepwater parts of the Arctic and Norwegian-Greenland basins, shelves and onshore areas of the ocean margins, allowing structures correlation;
- two main types of the Earth's crust: oceanic and continental;
- in oceanic domains—spreading zones, crust of various ages and intraplate volcanic structures with a thickened crust (oceanic plateaus and aseismic ridges);
- in structures with continental crust—two groups of geological complexes—indicators of the main tectonic processes of a continental crust accretion and its destruction with formation of large igneous provinces (LIPs) that mark the Paleocontinents break-up episodes;
- sedimentary covers are shown as an independent group of mapped objects (70% of the total area);
- tectonic map is accompanied by a set of additional digital maps (as a single GIS project), depicting the region deep structure, its basement tectonic subdivision and thickness of the sedimentary cover, nature of the Earth crust and large igneous provinces. Deep geological and geophysical cross–sections are provided as well.

The legend of the Tectonic Map. The legend of the Tectonic Map of the Arctic has been compiled by two CGMW Subcommissions (for Tectonic Maps and Northern Eurasia), applying an experience in legend construction for newest tectonic maps under the aegis of CGMW and UNESCO.

In this Tectonic Map of the Arctic the latest data obtained by ECS national programs on the delimitation of the continental Arctic shelf outer boundaries have also been used.

At the first stage, the existing legends of the Structural maps Atlantic and Indian oceans as well as tectonic and geological maps of continents were analyzed. Possible approaches were discussed by experts from CGMW, VSEGEI, VNIIOkeangeologia, Sevmorgeo and GIN RAS (workshop on January 11–13, 2010, St. Petersburg) to construct the legend for TeMAr. Some drafts of it and the map fragments have been prepared basing on the workshop results.

Then the legend was tested internationally at the workshop on the Tectonic Map of the Arctic (April 7–9, 2010 in St. Petersburg) attended by participants from 20 organizations (geological surveys and scientific institutions) from the Arctic countries (Russia, Canada, Norway, Denmark) with representatives from France, Sweden, Great Britain, Germany, and Leaders of the Commission for the Geological Map of the World (CGMW). Discussion on the Legend revealed different approaches of national tectonic schools and showed a necessity of settling a unified position and resolving of major contradictions.

At this workshop, an international working group has been formed with the head O. V. Petrov (CGMW Vice-president for Northern Eurasia), S. P. Shokalsky (Secretary General of the CGMW Subcommission for Northern Eurasia), Yu. G. Leonov (President of the CGMW Subcommission for Tectonic Maps), I. I. Pospelov (Secretary General of the CGMW Subcommission for Tectonic Maps), Philippe Rossi (CGMW President), Manuel Pubellier (CGMW Secretary General).

The first version of the legend on eight sheets with an explanation has been sent to all the working group members. Then a written discussion followed, revealing disagreements in the approaches to the compilation of the tectonic map and its database. It took another round of coordination of the positions of Russian, American and European geologists. It has been decided to display in the most disputable Amerasian Basin region a distribution of the Cretaceous High Arctic Large Igneous Province (HALIP), overlapping the basement structures, whose continental nature was disputed by some authors of the map.

After a series of additional discussions and transformations, the legend to the Tectonic Map was finally approved and adopted at the workshop of the international working group (CGMW, Paris, April 15, 2011). In July 2011, the CGMW experts tested the database of the map digital version. Then in November 2011, the updated legend, database and digital fragment of the map of the Russian part have been provided to members of the international working group to compile national map fragments.

The first draft of the Tectonic Map of the Arctic with inset maps of deep structure and tectonic zoning, and with the Transarctic Geotransect were discussed at the Austrian Geological Survey workshop (Vienna, April 24, 2012). The legend and the first map draft have been suggested to be ready.

This TeMAr draft was presented and discussed in August 2012 at a session of the 34th International Geological Congress in Brisbane.

After that, the draft of the Tectonic Map of the Arctic was regularly updated by introduction of new geological and geophysical data obtained in Central Arctic, New Siberian Islands, Franz Josef Land, and Severnaya Zemlya Archipelago.

In February 2014, the 5th meeting of the TeMAr international working group with participants from Canada, France, the USA, Denmark, Norway, Sweden, Germany, and Russia was held at the Gene ral Assembly of the Commission for the Geological Map of the World in Paris. There the Russian party presented an updated draft of the Tectonic Map of the Arctic.

Canadian, Danish and Swedish geologists delivered new regional fragments of the map to be incorporated into the Tectonic Map of the Arctic, with the exception of the Alaska, contiguous shelf of the Chukchi Sea and the Alaska North Slope. Since April 2014, Russian and CGMW experts have been working on the compilation of these missing fragments of the Tectonic Map using materials of Thomas Moore and Stephen Box (US Geological Survey).

Later the Russian TeMAr group compilers came into a close contact with colleagues from Norway, Denmark, Canada and the USA participating in national programs on definition of outer limits of the continental shelf (ICAM-VI–VIII in 2014–2018). When compiling and correcting the map draft, new seismic data and results of dredged bottom material study (2008–2016) have been introduced.

Regular General Assembly was held during the European Geological Union (EGU) in Vienna in April 2016. This meeting was devoted to a discussion of the state-of-the-art and further promotion of TeMAr. At the meeting, the latest draft of the Tectonic Map of the Arctic was demonstrated and discussed, and the issue of

geological correlation of structures of the Northeast of Russia, Alaska and Arctic Canada was thoroughly debated.

The TeMAr Review Meeting Workshop took place in February 2017 in Paris at the CGMW Headquarters. The Expert Council included the leaders of the CGMW, Subcommissions for Northern Eurasia, Tectonic maps and North America, representatives of Geological Surveys of the USA, Canada, and Germany, as well as the Russian Academy of Sciences. The Expert Council approved the latest changes in the tectonic map legend regarding structures of the Northeast Russia and Alaska. It was noted in the Minutes that the Tectonic map of the Arctic may be submitted to the international geological community at the General Assembly of the European Geosciences Union (Vienna) in April 2017.

In March 2017, a short workshop was held at the CGMW Headquarters to review a GIS version of the Tectonic Map of the Arctic.

In 2018, during the CGMW General Assembly (Paris, February 2018), results of the work on TeMAr were summed up and the map publication at scales of 1:10 M and 5 M has been supported and endorsed.

How to read the tectonic map. On the tectonic map, all areas except those underlain by definitive oceanic crust are subdivided into polygons that designate deformed areas and relatively undeformed sedimentary cover. Deformed areas are colored to reflect the age of their initial tectonic overprint, as shown in the column named "Tectonic events". The age of the first subsequent tectonic overprint is given by diagonal lines from upper right to lower left, colored as above; the age of the second subsequent tectonic overprint is given by diagonal lines from upper left to lower right, colored as above. Polygons are also overprinted by patterns that reflect the tectonic setting of their rock assemblages as shown in the legend. Areas of relatively undeformed sedimentary cover are colored by the age of onset of sedimentation and thickness of basin strata, as shown in the column labelled "Sedimentary Cover". Areas underlain by unambiguous oceanic crust are colored by their crustal age, as shown in the columns under "Oceanic Realms", and the thickness and age of sedimentary cover is ignored. More details are given in the Legend below.

Contents of the tectonic map legend. The symbols are grouped according to their relation to continental or oceanic domains.

Continental Realms embrace cratons and mobile belts of various ages, large igneous provinces and rift systems areas with thinned and extended earlier formed continental crust, as well as epicontinental sedimentary basins, platforms cover and passive Arctic margins of the Eurasian and North American continents. Faults, folds, salt tectonics and other structural elements, typical for the continental crust, are shown separately.

This part of the legend comprises two groups of rock associations, formed in different tectonic regimes (compression and extension) in corresponding tectonic settings.

Cratons and mobile belts. The first group include complexes indicating the crust compression, shortening and thickening ("Accretion-collision-related rock assemblages") and was formed by the processes of the continental crust growth. It comprises volcanic, plutonic, sedimentary and metamorphic complexes of various ages (Fig. 2). These rock assemblages are shown on the map by a colour corresponding to a time of orogenesis and/or cratonization. The age of orogen is determined by a time of subduction-collision processes, structural deformations (folding, faulting etc.), metamorphism, syncollision granitoid intrusive magmatism and molasse accumulation.

Orogenic cycle			Tectonic events	Accretion-collision-related rock assemblages
CENOZOIC (Alpine)	C	C_3	Walakhian } Tectonic events unnamed in the Circum-Arctic (<40 Ma)	**Volcanic assemblages[1]**
		C_2	Shtirian	Basalts and felsic volcanics of ensimatic island arc
		C_1	Eurekan (61–45 Ma), Late Laramian (50–40 Ma), Kamchatkan (50–40 Ma)	Andesites, dacites, rhyolites of ensialic island arc and active continental margin[2]
LATE MESOZOIC	LM	LM_3	Early Laramian (80–50 Ma)	Basalts of oceanic and back-arc basin assemblages
		LM_2	Okhotsk-Chukotka volcanic belt (105–80 Ma)	
		LM_1	Chukotkan (135–105 Ma), Brookian (125–110 Ma)	Undivided volcanic assemblages
EARLY MESOZOIC	EM	EM_3	Late Kimmerian (150–140 Ma), Verkhoyanskian (150–135 Ma), Nevadian (150–140 Ma)	**Sedimentary successions[3]**
		EM_2	Mid-Kimmerian? (200–150 Ma)	Accretional wedge facies
		EM_1	Early Kimmerian (235–190 Ma)	Molasse
LATE PALEOZOIC (Variscan)	LP	LP_3	Uralian (300–250 Ma), Palatinian (260–250 Ma)	**Metamorphic Units[1]**
		LP_2	Late Variscan (310–275 Ma)	Greenschist facies
		LP_1	Early Variscan (340–310 Ma)	Gneiss, amphibolite and migmatites (mainly amphibolite facies)
EARLY PALEOZOIC (Caledonian)	EP	EP_4	Ellesmerian (375–340 Ma)	Gneiss and amphibolite (mainly granulite facies)
		EP_3	Svalbardian (380 Ma), Caledonian (440–410 Ma)	Grey gneiss (TTG) rock assemblage
		EP_2	Taconian (480–430 Ma)	Granulite-gneiss belt rocks
		EP_1	Finnmarkian (510–480 Ma), Early Caledonian (510–470 Ma)	
NEOPROTEROZOIC	P	P_3 P_3^3	Timanian (630–540 Ma), Late Baikalian (600–550 Ma), Avalonian (570 Ma)	a, b – HP blueschist, c – eclogites (a – shown in scale; b, c – small bodies)
		P_3^2	Mid-Baikalian (800–600 Ma)	**Plutonic assemblages**
		P_3^1	Early Baikalian (850–800 Ma)	Subduction granites (M- and I-types)[4]
MESOPROTEROZOIC		P_2 P_2^3	Grenvillian (1,14–0,88 Ga), Sveconorwegian (1,2–0,9 Ga), Dalslandian (1,1–0,9 Ga)	Collision granites (S- and I-type)[4]
		P_2^2	Elsonian (1,4–1,25 Ga)	Zonal confocal mafic massifs of Ural-Alaska type with PGE mineralization (a – shown in scale; b – small body)
		P_2^1	Hallandian (1,47–1,42 Ga), Telemarkian (1,52–1,48 Ga), Danopolonian (1,5–1,4 Ga), Jotnian (1,64–1,42 Ga)	Archean subduction M- and I-type granites[1]
ARCHEAN–PALEOPROTEROZOIC		P_1 P_1^3	Dalarnian (1,72–1,52 Ga)	Archean collision S- and I-type granites[1]
		P_1^2	Svecofennian (2,1–1,75 Ga), Thelonian (1,99–1,91 Ga), Wopmay (1,89–1,84 Ga), Hudsonian (1,85–1,79 Ga), Laplandian (1,94–1,85 Ga)	Archean undivided plutonic assemblages[1]
		P_1^1	Early Karelian (2,5–2,3 Ga)	**Paleooceanic complexes**
	A	A_3	Belomorian (2,7–2,6 Ga), Kenoran (2,72–2,65 Ga)	Ophiolite allochtons (a – shown in scale; b – small body)
		A_2	Kola (3,2–2,8 Ga)	Complexes of paleooceanic crust and sediments, volcanic plateau, ensimatic island arcs and accretionary prisms
		A_1	Belozersk (3,5–3,2 Ga)	Ophiolite sutures and their age established
		A_0	Isua (3,7 Ga), Amitsoq (3,9–3,6 Ga), Acasta (4,0 Ga) (oldest continental crust)	

Baikalian

Structural-thermal reworking

Reworked   Twice reworked

Note. Color stripes portraying of magmatic-metamorphic reworked crust

Notes: 1 – color of polygon corresponds to the age of tectonic event; 2 – undeformed superimposed volcanic belt is shown by color pattern (according the age of volcanism) on white background for the Okhotsk-Chukotka and Cenozoic volcanic belts in North East Russia; 3 – absence of pattern indicates – undivided sedimentary successions; 4 – color of polygon shows the granite type, color of pattern shows the age of rocks
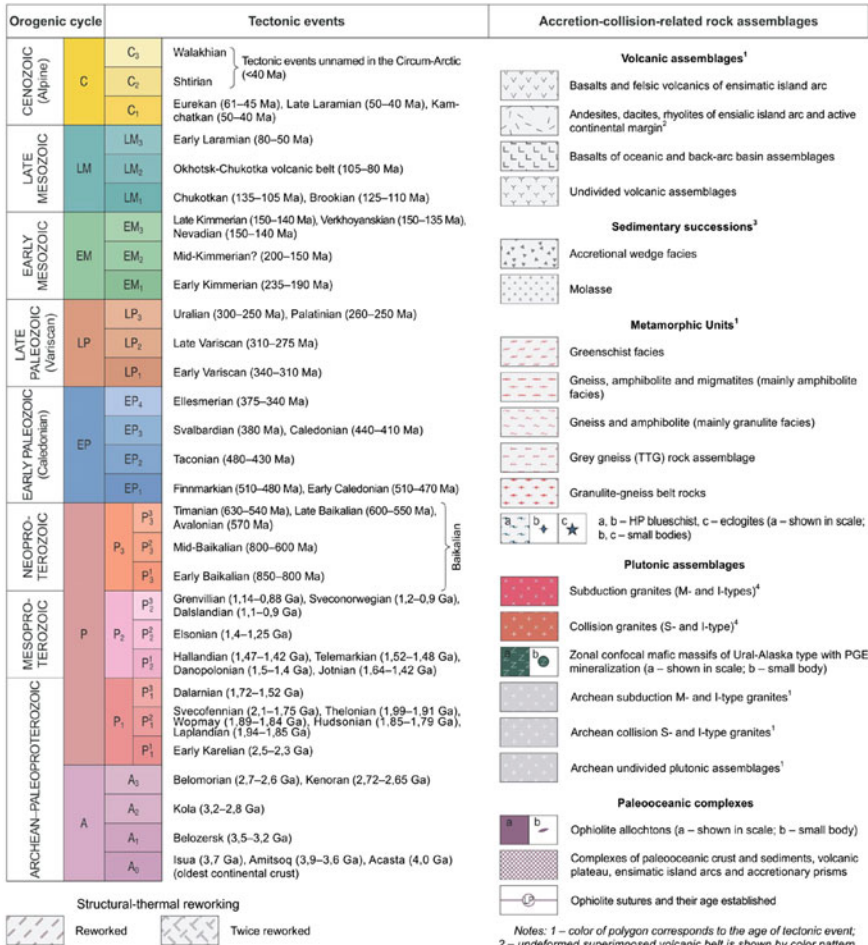
Fig. 2 Legend for cratons and mobile belts

Volcanic formations encompass rock associations of ensimatic island arcs, Andean-type continental margins, and back-arc basins. Related sedimentary rocks are accretion complexes mélange, olistostromes and molasses. This group also includes metamorphic complexes of various facies (greenschist, amphibolite, granulite), Archean TTG complexes and Paleoproterozoic granulite belts (marked with red patterns) along with high-pressure blueschist and eclogite complexes (marked by blue symbols). M- and I-type accretion granitoids, S- and I-type collision granites and zonal mafic intrusions of Ural-Alaska type are also included into this group.

All rock associations of this group (except Paleoproterozoic and younger granitoids as well as ophiolites and mafic rocks) are shown according to the age colour chart (Fig. 2). The Paleoproterozoic and younger granitoids are shown in two shades of red. Crimson colour shows M- and I-type subduction granites, and bright red is used for S- and I-type collisional granites. The age of granitoids, apart from the oldest Archaean granitoids, which are subdivided to I- and S-types, is shown by color patterns in accordance with the tectonic time scale.

Paleooceanic complexes (ophiolite allochthons) are depicted in violet and subdivided into ophiolite mélange and blocks with preserved ophiolite sequence indicating a paleooceanic crust. Extended narrow tectonic zones with ophiolite mélange can be shown by the symbol of ophiolite sutures with age indication.

The Legend permits demonstration of older crust by younger tectonic processes (faulting, folding, granitoids, metamorphism etc.). Superimposed orogenic events are depicted as colour strips superimposed upon a main background colour, allowing display of a general sequence of formation and transformation of tectonic structures.

General succession of geodynamic events can be divided into four turn points (most prominent events) from the assembling to break-up of supercontinents: Kenorland (2500 ± 200 Ma), Nuna (1800 ± 200 Ma), Rodinia (1000 ± 150 Ma) and Pangea (250 ± 10 Ma).

Large igneous provinces, sill-dyke swarms and rift systems. The second group includes magmatic complexes-indicators, typical for crustal extension and thinning regime (Fig. 3). They are correspond with intraplate postorogenic and anorogenic tectonic settings.

A separate time scale is used for this group of magmatic complexes with nine stages of intraplate magmatism and rifting shown by different colours from the Archean-M1 to the Cenozoic-M9. Each stage is exemplified by large igneous provinces, dike complexes and rifts in Greenland, Canada, Alaska, Eastern Russia and Northern Europe. The most prominent magmatic complexes are noted in bold. Most of the examples of large igneous provinces and dike belts are depicted in accordance with recommendations of the International Commission on Large Igneous Provinces.

Greenstone belts are assumed to be Archean protorift structures with komatiite occurrences marked by dot sign. Younger rift areas are outlined by black contour with dots, coloured in accordance with the colour chart (M2 to M9). Colour lines indicate boundaries of volcanic areals and LIP areas. Colour patterns display flood basalts and intraplate gabbrodolerite occurrences in accordance with their ages (M2 to M9). Plutons are shown in different colour according to their compositions: ultramafic-mafic layered bodies are painted blue, gabbro and dolerite—green, rapakivi—pink,

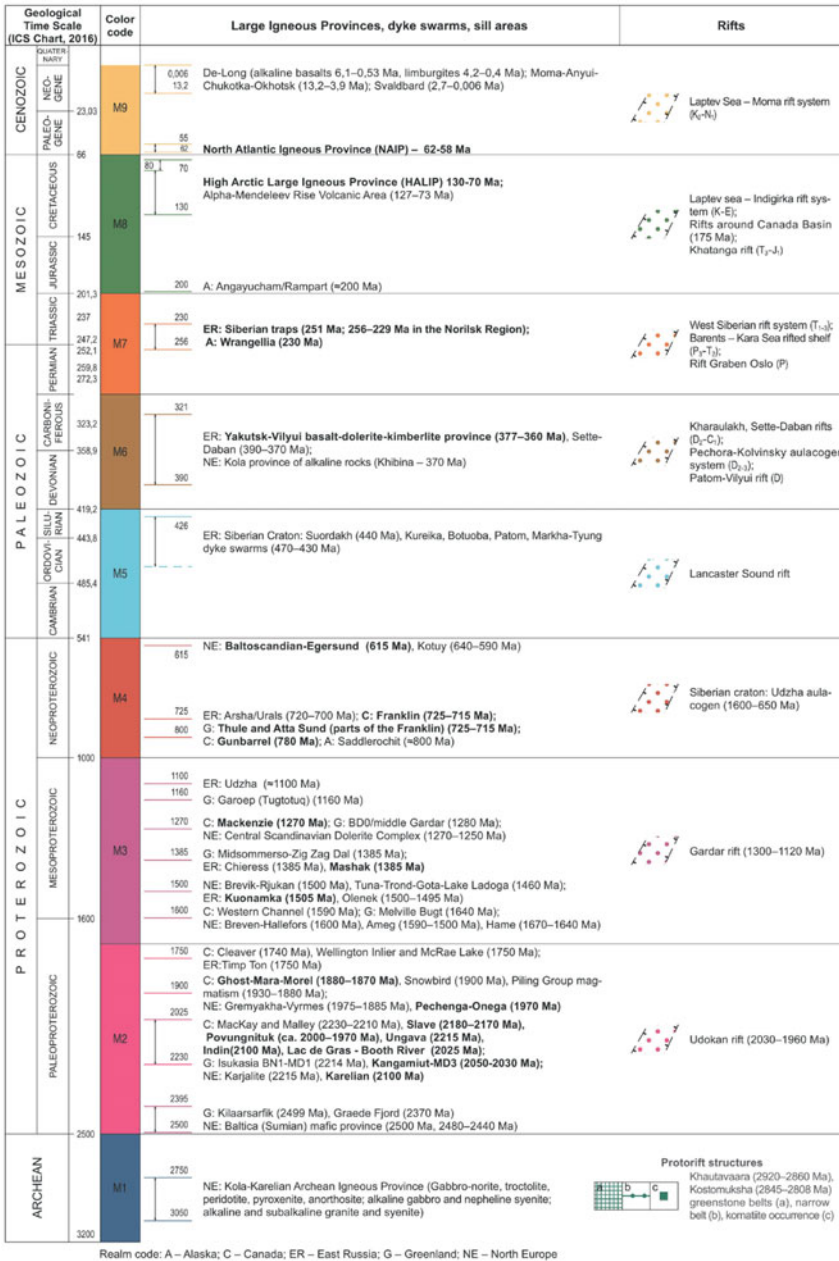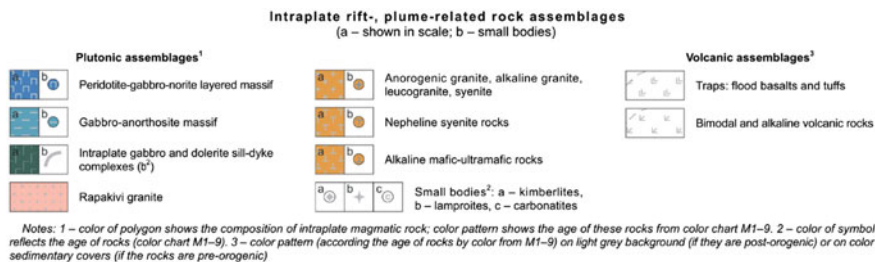## Large Igneous Provinces, Sill-Dyke Swarms and Rift Systems

Geological Time Scale (ICS Chart, 2016)		Color code	Large Igneous Provinces, dyke swarms, sill areas	Rifts
CENOZOIC	QUATERNARY / NEOGENE / PALEOGENE	M9	De-Long (alkaline basalts 6,1–0,53 Ma, limburgites 4,2–0,4 Ma); Moma-Anyui-Chukotka-Okhotsk (13,2–3,9 Ma); Svaldbard (2,7–0,006 Ma) 0,006 / 13,2 / 23,03 / 55 / 62	Laptev Sea – Moma rift system (K₂-N₂)
			North Atlantic Igneous Province (NAIP) – 62-58 Ma	
MESOZOIC	CRETACEOUS / JURASSIC / TRIASSIC	M8	High Arctic Large Igneous Province (HALIP) 130-70 Ma; Alpha-Mendeleev Rise Volcanic Area (127–73 Ma) 80 / 70 / 130	Laptev sea – Indigirka rift system (K-E); Rifts around Canada Basin (175 Ma); Khatanga rift (T₃-J₁)
			A: Angayucham/Rampart (≈200 Ma) 200	
		M7	ER: Siberian traps (251 Ma; 256–229 Ma in the Norilsk Region); A: Wrangellia (230 Ma) 230 / 256	West Siberian rift system (T₁₋₃); Barents – Kara Sea rifted shelf (P₃-T₃); Rift Graben Oslo (P)
PALEOZOIC	CARBONIFEROUS / DEVONIAN	M6	ER: Yakutsk-Vilyui basalt-dolerite-kimberlite province (377–360 Ma), Sette-Daban (390–370 Ma); NE: Kola province of alkaline rocks (Khibina – 370 Ma) 321 / 390	Kharaulakh, Sette-Daban rifts (D₂-C₁); Pechora-Kolvinsky aulacogen system (D₂₋₃); Patom-Vilyui rift (D)
	SILURIAN / ORDOVICIAN / CAMBRIAN	M5	ER: Siberian Craton: Suordakh (440 Ma), Kureika, Botuoba, Patom, Markha-Tyung dyke swarms (470–430 Ma) 426	Lancaster Sound rift
PROTEROZOIC	NEOPROTEROZOIC	M4	NE: Baltoscandian-Egersund (615 Ma), Kotuy (640–590 Ma) 615 / 725 / 800; ER: Arsha/Urals (720–700 Ma); C: Franklin (725–715 Ma); G: Thule and Atta Sund (parts of the Franklin) (725–715 Ma); C: Gunbarrel (780 Ma); A: Saddlerochit (≈800 Ma)	Siberian craton: Udzha aulacogen (1600–650 Ma)
	MESOPROTEROZOIC	M3	ER: Udzha (≈1100 Ma) 1100 / 1160; G: Garoep (Tugtotuq) (1160 Ma); C: Mackenzie (1270 Ma); G: BD0/middle Gardar (1280 Ma); NE: Central Scandinavian Dolerite Complex (1270–1250 Ma) 1270 / 1385; G: Midsommersö-Zig Zag Dal (1385 Ma); ER: Chieress (1385 Ma), Mashak (1385 Ma) 1500; NE: Brevik-Rjukan (1500 Ma), Tuna-Trond-Gota-Lake Ladoga (1460 Ma); ER: Kuonamka (1505 Ma), Olenek (1500–1495 Ma) 1600; C: Western Channel (1590 Ma); G: Melville Bugt (1640 Ma); NE: Breven-Hallefors (1600 Ma), Ameg (1590–1500 Ma), Hame (1670–1640 Ma)	Gardar rift (1300–1120 Ma)
	PALEOPROTEROZOIC	M2	C: Cleaver (1740 Ma), Wellington Inlier and McRae Lake (1750 Ma); ER: Timp Ton (1750 Ma) 1750; C: Ghost-Mara-Morel (1880–1870 Ma), Snowbird (1900 Ma), Piling Group magmatism (1930–1880 Ma); NE: Gremyakha-Vyrmes (1975–1885 Ma), Pechenga-Onega (1970 Ma) 1900 / 2025; C: MacKay and Malley (2230–2210 Ma), Slave (2180–2170 Ma), Povungnituk (ca. 2000–1970 Ma), Ungava (2215 Ma), Indin(2100 Ma), Lac de Gras - Booth River (2025 Ma); G: Isukasia BN1-MD1 (2214 Ma), Kangamiut-MD3 (2050-2030 Ma); NE: Karjalite (2215 Ma), Karelian (2100 Ma) 2230 / 2395 / 2500; G: Kilaarsarfik (2499 Ma), Graede Fjord (2370 Ma); NE: Baltica (Sumian) mafic province (2500 Ma, 2480–2440 Ma)	Udokan rift (2030–1960 Ma)
ARCHEAN		M1	NE: Kola-Karelian Archean Igneous Province (Gabbro-norite, troctolite, peridotite, pyroxenite, anorthosite; alkaline gabbro and nepheline syenite; alkaline and subalkaline granite and syenite) 2750 / 3050	Protorift structures: Khautavaara (2920–2860 Ma), Kostomuksha (2845–2808 Ma) greenstone belts (a), narrow belt (b), komatiite occurrence (c)

Realm code: A – Alaska; C – Canada; ER – East Russia; G – Greenland; NE – North Europe

★ Selected plume centers located by giant radiating dyke swarms coloured in accordance with rock age (M1–9)

Fig. 3 Legend for large igneous provinces (LIPs), sill-dyke swarms and rift systems

Intraplate rift-, plume-related rock assemblages
(a – shown in scale; b – small bodies)

Plutonic assemblages[1]

- Peridotite-gabbro-norite layered massif
- Gabbro-anorthosite massif
- Intraplate gabbro and dolerite sill-dyke complexes (b^2)
- Rapakivi granite

- Anorogenic granite, alkaline granite, leucogranite, syenite
- Nepheline syenite rocks
- Alkaline mafic-ultramafic rocks
- Small bodies[2]: a – kimberlites, b – lamproites, c – carbonatites

Volcanic assemblages[3]

- Traps: flood basalts and tuffs
- Bimodal and alkaline volcanic rocks

Notes: 1 – color of polygon shows the composition of intraplate magmatic rock; color pattern shows the age of these rocks from color chart M1–9. 2 – color of symbol reflects the age of rocks (color chart M1–9). 3 – color pattern (according the age of rocks by color from M1–9) on light grey background (if they are post-orogenic) or on color sedimentary covers (if the rocks are pre-orogenic)

Fig. 4 Legend for large igneous provinces (LIPs), sill-dyke swarms and rift systems (continuation)

and alkaline massifs are orange. Small (nonscale) intrusive bodies are depicted by dot symbols of a relevant age colour. The pattern colour taken from the chart (M1 to M9) indicates an age of magmatic body (Fig. 4). Coloured dot symbols on the map indicate kimberlite pipes, lamproite, carbonatite and occurrence of plume centers. Colours of all tectonic elements of this group correspond to the age of magmatism and/or volcanogenic-sedimentary filling of rifts. Names of the most prominent intrusions and their age (in Ma) are given in the database.

Undeformed and weakly deformed sediments more than 1 km as thick are considered in the legend as *Sedimentary covers* (Fig. 5). Depending on a starting time of a basin's main stage of sagging and formation of its sedimentary cover, they are subdivided into seven generations (B1 to B7), from the late Paleoproterozoic to the Cenozoic, being painted in an appropriate colour. Isopach lines show the total thickness of sediments. A change in a cover thickness is displayed by colour intensity: the thicker sediments—the darker colour. In superposed basins of different age, a total thickness of sediments is displayed by a single isopach system. Boundary of basin buried under sediments off younger basin is shown by double-dash-dot line with dots located at an inner side. Dash lines indicate boundaries of separate sub-basins. Coloured grid indicates a "cold" structural reworking (weak folding) of sedimentary covers. It is best pronounced in the Middle-Paleoproterozoic, Late-Paleoizoic and Cenozoic basins.

The oldest Paleoproterozoic basins (B1) typically have a sedimentary cover that began to fill in the second half of the Paleoproterozoic (2050–1600 Ma). Their relics occur within the Canadian Shield. Formation of the youngest basins (B7) began as the Paleogene-Neogene grabens, usually under rifting regimes. They are confined to the shelf margins of the Canadian Arctic Archipelago and located in the Laptev, East Siberian and Chukchi seas.

In the structure of the Circum-Arctic sedimentary cover forms a peripheral belt of deep marginalshelf depressions (East Barents, North Kara, North Chukchi, Beaufort Sea, McKenzie delta, Lincoln Sea, etc.). The sedimentary cover thickness in these depressions reaches 14–18 km with up to a half of total thickness being composed of the Paleozoic—Early Mesozoic sediments, overlain by the Late Mesozoic—Cenozoic deposits. These depressions are a result of successive two or more tectonic events
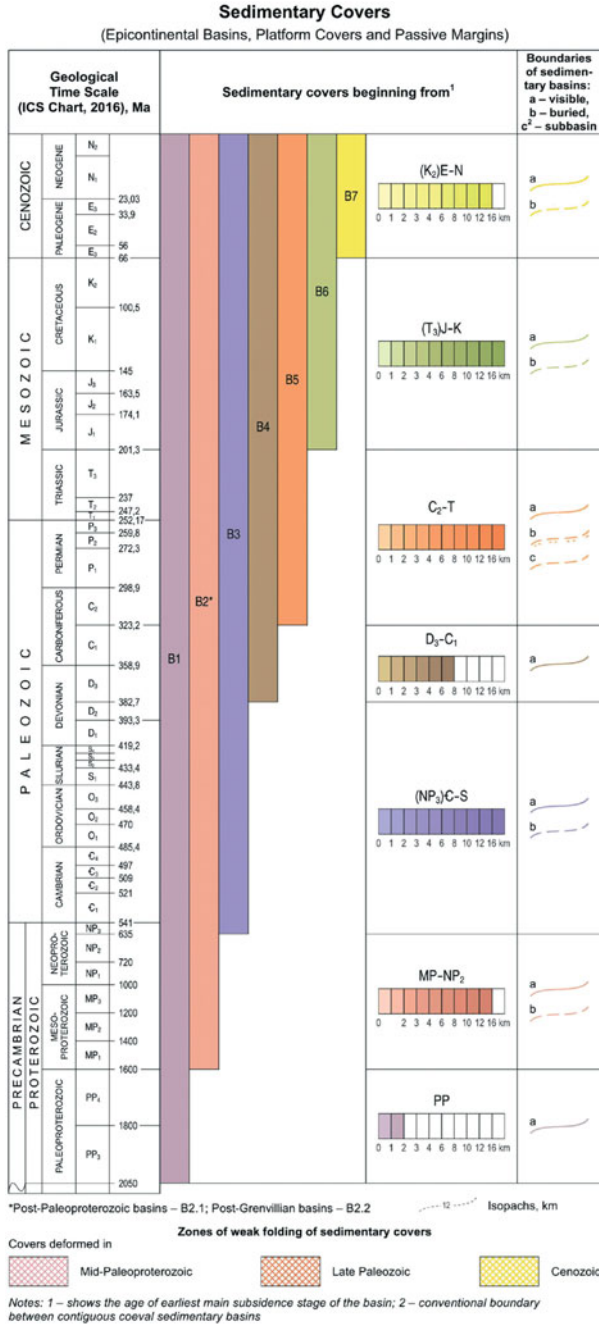
Fig. 5 Legend for epicontinental basins, platform covers and passive margins

Structural Elements

Faults and structural fronts
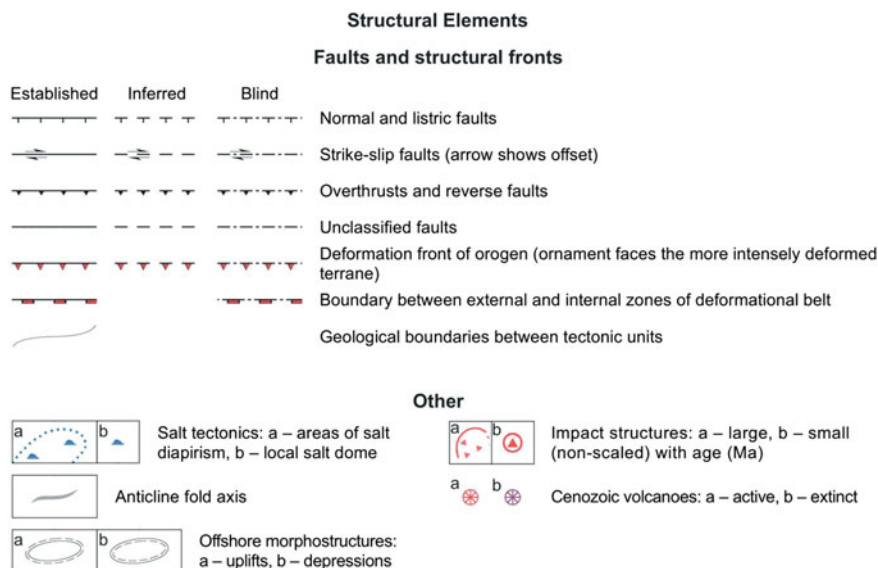
**Fig. 6** Legend for structural elements

of a continental rifting and sedimentation, e.g., the Permian-Triassic and the Late Mesozoic in the North Chukchi Basin and the Hanna Trough.

Structural elements in the continental crust realms are represented by disjunctive dislocations of various kinematics: normal faults and listric faults, strike-slip faults, reverse faults, and thrusts (Fig. 6). Other linear elements show deformation fronts, boundaries between internal and external zones in wide deformation belts and geological boundaries, with exposed, assumed, and buried linear structures depicted by different line types, positive and negative off shore (shelf) morphostructures.

The map demonstrates areas of intensive linear folding, salt tectonics areas and individual salt domes, impact craters, old and active volcanoes.

Oceanic Realms. Domains with oceanic crust in accordance with the recommendations of the Commission for the Geological Map of the World (CGMW) and the practice of compiling of the structural maps of Atlantic and Indian oceans are shown by colour (Fig. 7). The legend contains special colours for the standard thin (5–7 km) mafic crust formed by the Early Cretaceous spreading in the central part of the Canadian Basin, in the Paleocene- Eocene in the Baffin Bay and the Labrador Sea and in the Eocene—Holocene in the North Atlantic and the Eurasian Basin (O1 to O6). Some data for the crust's age of the North Atlantic has been provided from GEUS publication (Tectonostratigraphic Atlas of the North-East Atlantic Region/J. Hopper (et al.). Copenhagen, 2014).

The Iceland-Faroe Ridge and the Iceland Plateau are depicted by a special pattern using for the oceanic plateau an aseismic ridges with these areas over
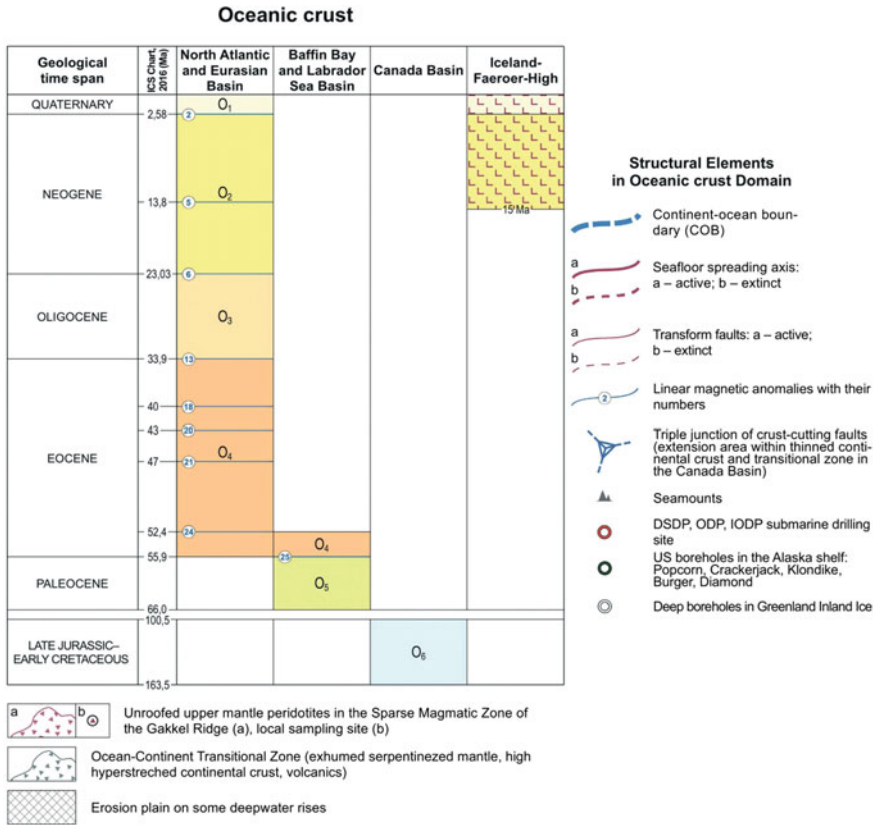
Fig. 7 Legend for the Oceanic realms

thick oceanic crust and intraplate mafic volcanism. Within the Iceland Plateau, the spreading volcanism of the Mid-Atlantic Ridge interacts with intraplate magmatism of ocean plateau type. There the Mid-Ocean Ridge virgates to the Western and the Eastern branches, displaced by transform faults in the northern and southern edges of the plateau. The oceanic crust of the Iceland-Faroe Ridge is split by ages to Pleistocene–Holocene (<2.6 Ma) and Middle Miocene—Pliocene (15–2.6 Ma).

The legend allows display on the map of the key magnetic chrons 2, 5, 6, 13, 18, 20, 21, 24 and 25. They mark heterochronous parts of the oceanic crust, show the most bright and extensional magnetic linear anomalies.

In addition, the legend contains polygonal symbols the Continent-Ocean Transition Zone with cooccurrence of an exhumed serpentinized mantle, peridotites fragments of an extremely stretched continental crust and oceanic volcanic rocks (Iberiantype margin): it is assumed in the central Canada Basin, as well as in the Sparsely Magmatic Zone with numerous mantle peridotite samples dredged from the crest of the ultra-slow spreading Gakkel Ridge (Fig. 7).

Linear symbols mark the continent-ocean boundary (COB), active and extinct spreading axes, active, and extinct transform faults and linear magnetic anomalies with their numbers. Dot symbols show seamount, black cross hatching displays the plain surfaces of the Chukchi Plateau and central Lomonosov Ridge, which apparently have been formed in sub-aerial environments during low stand of sea and active erosion of the ridges by seawater and glaciers.

A triple junction symbol denotes triple-junction fault area revealed in the Moho map in the Canada Basin and Nautilus Basin. It indicates a considerable spatial extension of the continental crust, accompanied by crest-like mantle uplift and controls the location of the Cretaceous volcanic field of HALIP.

The sedimentary cover upon the oceanic crust (Lena and Mackenzie rivers underwater fans) are shown only by isopachs.

The Legend also provides display of well sites of the deep-oceanic drilling, as well as five key parametric wells in the American sector of the Chukchi Sea, and few boreholes, that show the basement rocks under the Inner Ice of Greenland.

2 Tectonic Provinces of the Arctic

The Map of tectonic zoning of the Arctic (Fig. 8) was compiled as a result of work on the tectonic map under the project Atlas of Geological Maps of the Circumpolar Arctic and is based on results of processing geological and geophysical data obtained over recent years during field studies. The tectonic zoning of the Arctic areas was made taking into account crustal types, age of consolidated basement, and characteristics of geological structures of the sedimentary cover. The legend for the map of zoning includes five main groups of elements: continental and oceanic crust, folded platform covers, accretion-collision systems, and provinces of continental basalt cover (Fig. 9). An important feature of the map of tectonic zoning is showing the continental crust in central regions of the Arctic Ocean, the existence of which is assumed from numerous geological data.

It should be noted that suggestions on the existence of continental blocks in the Arctic Ocean were made at the very beginning of studying the tectonic structure of the Arctic. In 1959, first color tectonic map of the Arctic was compiled under the supervision of N.S. Shatsky. It was made in the polar map projection at 1:7 M scale and in 1960 a black and white version was published. It showed outlines of two platforms in the water area of the Arctic: Barents Platform (or Barentsia) in the western part and Hyperborean Platform in the eastern part. The outlines of these two platforms were used again in the Tectonic map of the Arctic at 1:10 M scale (1963) compiled by M. V. Muratov and A. L. Yanshin based on the N. S. Shatsky's map. On this map, the Hyperborean Platform occupies most of the Chukchi and East Siberian seas from the Lomonosov Ridge to Mesozoides of Alaska, Chukotka and Verkhoyansk Range, Variscides of the Canadian Arctic Archipelago. The Barents Platform fully occupied the Barents Sea between Severnaya Zemlya and Novaya Zemlya, Svalbard with the center in the Franz Josef Land Archipelago. In fact, the Northeast and the Canadian
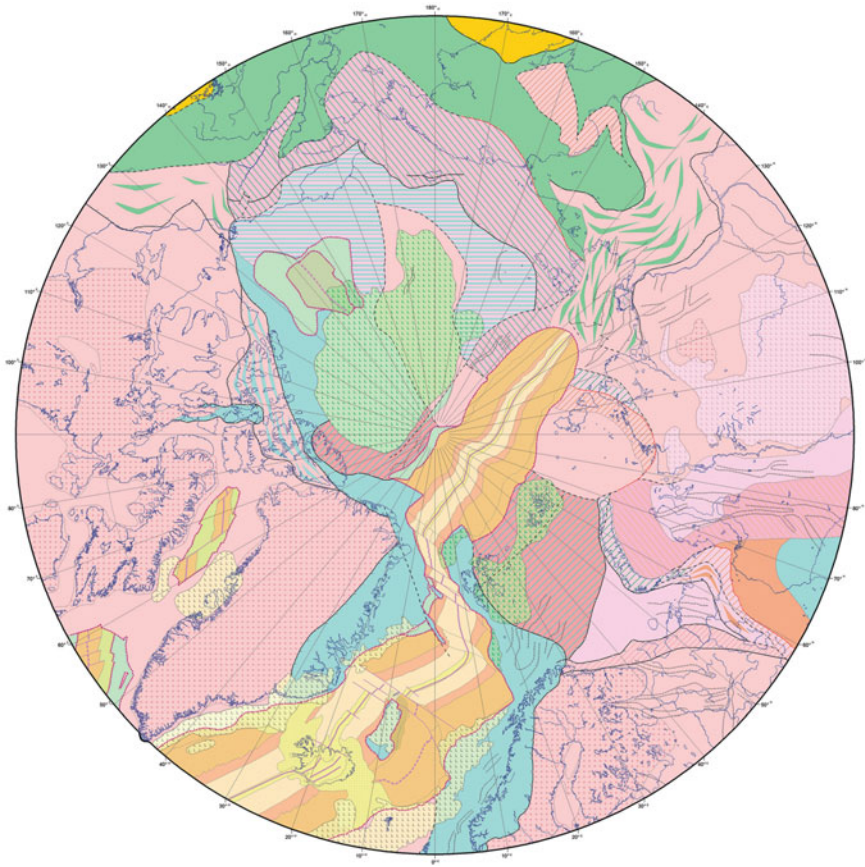
Fig. 8 Map of the Arctic basement tectonic provinces. Materials used: Pease et al. (2014), Harrison et al. (2011), Grantz et al. (2009), Petrov and Smelror (2015), Morozov et al. (2013), Proskurnin et al. (2012), Daragan-Sushchova et al. (2014), Vernikovsky et al. (2013); and other data

Arctic Archipelago were directly connected by the structures of the Eurasian Basin and the Lomonosov Ridge via the Hyperborean Platform.

The Tectonic Map of the Arctic and Subarctic at 1:5 M (1967) prepared under the guidance of I. P. Atlasov, for the first time ever showed the existence of transitional structures between the cratons and folded systems, between continental and oceanic crust. This study suggested much more widespread occurrence of fold belts in the Arctic water area and cast some doubt on the existence of a single large and homogeneous Hyperborean Platform.

The detailed Tectonic Map of the Arctic by B. H. Egiazarov (Egiazarov et al. 1977) reflected the conception of the existence of heterogeneous Arctic Fold Belt formed on the periphery of the Hyperborean Platform with Archaean—Paleoproterozoic and Early-Middle Paleozoic basement.

L E G E N D

CONTINENTAL CRUST

Cratons

+ + + Pre-Mesoproterozoic shields and massifs

Meso-Neoproterozoic-Phanerozoic platform cover

Undivided crystalline complexes and lower cover units:

affected by Latest Neoproterozoic (Timanian) tectonism

reworked in Late Paleozoic

Folded platform covers
Epi-cratonic units, deformed:

in Early Paleozoic

in the Late Paleozoic

in Mesozoic

Post-Timanian units, deformed in the Late Paleozoic

Accretional/collisional fold belts

Meso/Neoproterozoic (~ 1000 Ma), reworked in Early Paleozoic

Collage of Proterozoic-Paleozoic crustal blocks amalgamated in the Late Paleozoic

Collage of Neoproterozoic crustal blocks amalgamated during Paleozoic, with last intense tectono-magmatic reworking in Mesozoic

Timanian:

reworked in the Late Paleozoic
reworked in Mesozoic

Timanian and/or Early Paleozoic, undifferentiated

Early Paleozoic

Late Paleozoic

Mesozoic

Cenozoic

Continental flood basalts

L L L Early Triassic

L L L Cretaceous

L L L Early Tertiary

TRANSITIONAL ZONE

Exhumed serpentinezed mantle, high hyperstreched continental crust, volcanics

OCEANIC CRUST

Late Pliocene /Piacenzian/ – Quaternary

Early Miocene – Early Pliocene

Oligocene – Early Miocene

Eocene

Paleocene

Mesozoic

Overthick oceanic crust of aseismic ridges

Spreading axes

active

extinct

Transform faults

OTHER

Faults:

Overthrusts

Underthrusts

Normal faults and boundaries of rift grabens

Inferred

Continent-ocean boundary

Sutures

Fig. 9 Legend to the map of the Arctic tectonic provinces

Tectonic structure of the Arctic was also discussed by V. E. Hain and his followers (Hain 2001; Filatova and Hain 2007, etc.; Drachev 2011). In the central part of the Arctic Ocean, he identified areas of heterochronic oceanic crust with continental type crust, and intraplate oceanic crust elevations. The possibility of the assignment of the crust in the Makarov and Toll (Podvodnikov) basins to the transitional type is assumed. He classified the Lomonosov, Alpha, Mendeleev structures and the Chukchi Plateau as the continental-type crust.

Currently, the Central Arctic is regarded as a collage of fragments of a Neoproterozoic craton, which underwent destruction during the Paleozoic-Cenozoic evolution and covers almost the entire of the Arctic region exposing along the continental framing of the North Atlantic and Eurasian ocean basins at Novaya Zemlya, Taimyr Peninsula, Kara Massif, New Siberian Islands, De Long Archipelago, Wrangel Island, Seward Peninsula, Canadian Arctic Archipelago and elsewhere (Zonenshain and Natapov 1987; Lawver et al. 2002).

Reliable evidences of the oceanic crust expressed as well-defined structures of the Late Cretaceous—Cenozoic spreading are inherent in the Baffin Bay, Norwegian-Greenland and Eurasian basins. In two small areas located in the center of the southern part of the Canada Basin and in the Makarov Basin, there are indistinct signatures of abandoned spreading, which suggest the presence of enclaves of Mesozoic oceanic crust (Transition O/C Zone).

More than half of the modern distribution area of the continental lithosphere in the Arctic is occupied by the Archaean-Paleoproterozoic continental crust. Its original and/or changed crystalline complexes are preserved in the basement of Precambrian Eastern European, Siberian and North American cratons. Tectonic activation of marginal parts of the cratons adjacent to (Meso?)-Neoproterozoic-Phanerozoic accretion-collision belts caused folded deformations of old platform covers transformed to Ellesmerides of the Franklin Fold Belt and Mesozoides of the Verkhoyansk and South Taimyr fold belts. Archean—Mesoproterozoic convergent processes not only modified peripheral areas of the cratons, but also signifi cantly increased the old continental basement. Grenvillian crust reworked by Early-Middle Paleozoic (Caledonian-Ellesmerian) tectogenesis is identified in the northern part of Ellesmere Island (Pearya Terrane), on the Svalbard and Franz Josef Land archipelagoes and in the basement of the Barents Sea Basin and the near-Greenland segment of the Lomonosov Ridge combined in the pre-spreading reconstruction with the Barents Sea continental margin.

Timanides of the Polar Urals and Pay-Khoy suffered the impact of the Late Paleozoic (Uralian) orogeny that completed the consolidation of the West Siberian and South Kara basins basement. In continuation of the Timan Fold Belt across Novaya Zemlya and Central Taimyr, the strongest reworking of the Late Neoproterozoic crust occurred during the Early Cimmerian orogeny in the Late Triassic–Early Jurassic. Continental crust of Kolyma and south Chukotka increased during the Cretaceous due to the structures of the Okhotsk Volcanic Belt that formed at that time.

Vast "superterrane", which extends from central Alaska to the New Siberian Archipelago across north Chukotka and southern parts of the Chukchi and East

Siberian seas, is interpreted as a collage of Neoproterozoic protoliths, which amalgamated into a single continental block during the Paleozoic. During the Mesozoic collision of this block with Northeastern Asia and south Alaska, it underwent tectono-magmatic reworking to form the compound Late Mesozoic Novosibirsk-Chukotka-Alaska Fold Belt most of which was buried under the Upper Cretaceous-Cenozoic cover in the inland shelf.

Within the outer shelf of the East Siberian and Chukchi seas, Chukchi Borderland, the Beaufort Sea and the North Slope of Alaska, the folded basement is almost entirely hidden under the Middle(?)-Upper Paleozoic—Cenozoic cover reaching in places up to 20 km in thickness. Scarce geological data (observations on De Long northern islands, drilling in the American part of the Chukchi Sea, dredging of bottom rocks of the Chukchi Borderland) suggest mostly Timan-Caledonian formation of the crust, which locally probably also hosts Grenville and older protoliths.

The continental crust, transformed to various degrees by stretching and intensive basaltic magmatism, which led to the HALIP formation, also underlies the Alpha Ridge and Mendeleev Rise and most of negative elements of bottom topography (Poselov et al. 2007; Pease et al. 2014). Seismic data show that the thickness of the continental crust varies widely: from 30–32 km in the Mendeleev Rise to 18–20 km in the Lomonosov Ridge, decreasing to 8–10 km in rift structures of the Makarov Basin due to the reduction of the upper crust layer.

Taking into account the current level of knowledge of the Alpha Ridge and the Mendeleev Rise, the crust of which is armored by volcanic products and modified by deep magmatism, its internal structure cannot be identified and this area is shown on the map of tectonic zoning without subdivision into individual tectonic provinces. The same approach is used for mapping Mendeleev and Chukchi submarine plains and the eastern part of the Podvodnikov Basin wherein the crust that underwent magmatogenic impact is moderately submerged beneath the basement of sedimentary basins, as well as the periphery of the south Canada Basin, where the extremely stretched crust is buried under thick sedimentary cover and almost five kilometers of the water layer.

More detailed descriptions including the justification of the continental crust age are given below for individual morphostructures of the Central Arctic Ocean.

The Arctic Ocean is the smallest and youngest Earth's ocean (Gramberg 2002). It is subdivided into Eurasian and Amerasian Basins that differ in topography and geological and geophysical characteristics of the seafloor.

The **Eurasian Basin** includes abyssal basins (Nansen and Amundsen Basins) separated by the mid-oceanic Gakkel Ridge with axial rift valley (Fig. 10). Along the continent-ocean boundary (COB), it borders the Barents-Kara, Amerasian, and Laptev sea rift passive margins (Jokat and Micksch 2004). The Eurasian Basin has a length of about 2000 km and a width of up to 900 km. To the west, its tectonic boundary corresponds to the Svalbard transform fault system (De Geer Fault), to the east—the Lomonosov Ridge and the Laptev Sea continental margin. The Gakkel Ridge separates the basin into two basins: the Amundsen Basin, adjacent to the Lomonosov Ridge, and the Nansen Basin that emborders the Eurasian shelf.
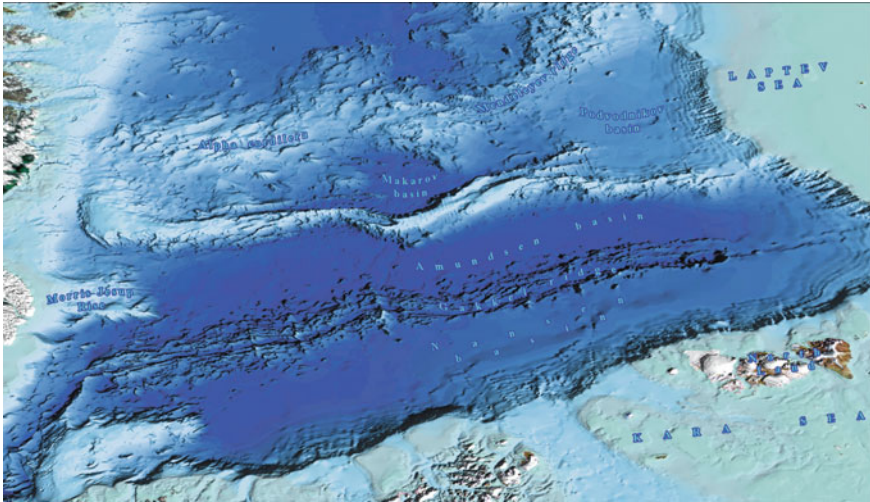
Fig. 10 3D-image of the Eureasian Basin (IBCAO model, version 3.0)

Gakkel Ridge is an extended linear rise with a dissected relief. The ridge is surrounded by abyssal plains along the entire length (1800 km), but close to the Laptev Sea shelf, it gets in contact with an elevation. East of 70 °E, a distinct asymmetry is recorded in the structure of the ridge. In the Nansen Basin part, it is noticeably narrower, and the abyssal plain is almost in contact with the rift valley, and from the Amundsen Basin part, a broad plateau, elevated above the abyssal plain at 200–400 m and complicated by mountains and ridges, is clearly traced in the relief of the ridge. Topography of the rift valley, its depth and other features are impermanent and experience consistent alterations in four blocks of the ridge, which follow one another along the strike. The width in the ridge zone topography is less than 200 km, rift valley depths range from 5000–5200 m near the Laptev Sea shelf to 4300 m in the central and 4500–5000 m in the Greenland part (Naryshkin 1987; Orographic… 1995, etc.).

In the **Nansen and Amundsen Basins**, the bottom is represented by subhorizontal abyssal plains. The greatest depths reach about 4000 m in the Nansen Basin and about 4500 m in the Amundsen. In the Amundsen Basin, maximum depths are concentrated in its axial part, whereas in the Nansen Basin the area with the greatest depths is located in the western part of the basin settings (Orographic… 1995).

The **Amerasian Basin** boundary is located along the base of the western slopes of the Lomonosov Ridge. It is the largest deep-water basin in the Arctic, and issues related to its structure and history of formation are fundamental for reconstructing the history of the evolution of the Earth.

A significant part of the Amerasian Basin is occupied by extensive Central Arctic uplifts (Alpha and Lomonosov Ridges, Mendeleev Rise, Chukchi Borderland). The area of the Central Arctic uplifts "partitions" the central part of the Arctic

Ocean between the Greenland and the Canadian Archipelago shelves on one side and the East Asian one on the other. This area includes not only large positive forms of the seafloor topography, but also dividing extensive depressions (Podvodnikov, Makarov and Nautilus Basins, Mendeleev and Chukchi abyssal plains) and a variety of smaller morphostructures in the intermediate depth interval that complicate first-order features.

The **Makarov Basin** is separated from the Eurasian Basin by the Lomonosov Ridge. According to some last publications (Miller et al. 2017) it is an enclave of the ocean floor, surrounded by continental slopes, namely the outer, tectonically dissected continental slopes (Fig. 11). The slope of the basin, shared with the Lomonosov Ridge, is called the Shmakov Escarpment. It is much steeper and higher than the opposite side of the depression. From the Greenland-Ellesmere shelf, the deep Marvin Spur opens to the Makarov Basin. The abyssal plain in the basin floor is outlined by an isobath of 3800 m. Only in some small areas, the depths in the basin exceed 4000 m. The bottom of the basin is flat, leveled, complicated by an extended asymmetric ridge about 800 m high, which continues westward the Marvin Spur.

Lomonosov Ridge is a rise of the seabed, which extends for almost 1800 km across the Arctic Ocean from the Lincoln Shelf to the East Siberian Shelf. The width of the rise, which has a flat top slightly rounded on the crest, is 45 to 200 km, the height runs up to 4200 m. Seismostratigraphic analysis shows that the formation of the Lomonosov Ridge as a positive structure began in the Cretaceous. During the late Early Cretaceous (Aptian-Albian), the Lomonosov Ridge developed as a sediment-covered rise, which supplies clastic material to the adjacent depressions. This is evidenced by pinching-out of the Lower Cretaceous seismostratigraphic complex towards the dome of the Lomonosov Ridge. Taking into account that Cretaceous
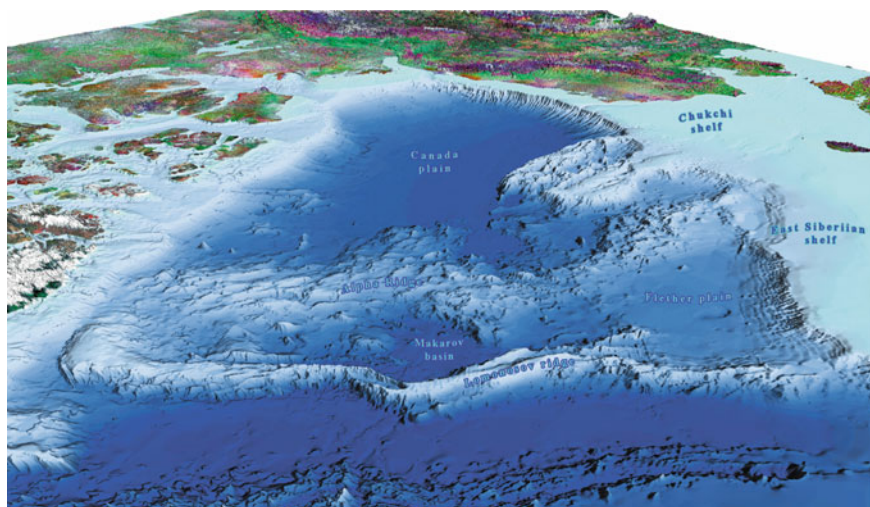
Fig. 11 3D-image of the Lomonosov Ridge and Makarov Basin (IBCAO model, version 3.0)

sediments both in the Lomonosov Ridge (Dove et al. 2010) and the Laptev Sea Shelf are represented by continental and onshore-off shore coal-bearing formations, this rise is interpreted as intracontinental.

Lomonosov Ridge as a morphostructure of the modern Arctic Ocean formed during the Miocene. At that time the shallow-water sediments turned into deep-water ones (Dove et al. 2010). At present, the continental nature of the Lomonosov Ridge uplifting is practically undebatable. The seismostratigraphic analysis showed that structures of the Laptev Sea Shelf continue in the Lomonosov Ridge. The structural-tectonic zoning of the Laptev Sea Shelf with the involvement and partial processing of 35,000 liner km of seismic profiles enabled identification (based on features of the basement and sedimentary cover structure) of two subbasins in the Laptev Sea Shelf: Western and Eastern Laptev Sea. Comparative analysis of composite seismic profiles showed similar features in the structure of the basement and sedimentary cover of the Lomonosov Ridge and the East Laptev Subbasin. In the basement of these structures there is an intermediate complex, which similar to the New Siberian Islands is interpreted as slightly dislocated Paleozoic—Early Mesozoic deposits. Surveys carried out on the New Siberian Islands showed that the East Laptev Subbasin is filled with an assemblage of platform carbonate and terrigenous sediments formed in the Baikalian crystalline basement reprocessed during the Caledonian and Cimmerian phases of tectonogenesis. On the shelf, in the acoustic basement of the continental block, there are fragments of a layered seismic record corresponding to slightly dislocated Paleozoic and Mesozoic strata known on the New Siberian Islands.

Lomonosov Ridge underwent HALIP magmatic manifestations only in local areas. Spreading processes are mainly reflected there in the formation in the upper crust of numerous contrasting horstgraben structures that were not leveled by sedimentation and are well pronounced in the bottom relief. The upper crust is slightly thinned, and between its surface and the acoustic basement there is an almost ubiquitous intermediate seismic layer, conventionally referred to as "metasedimentary" (Poselov et al. 2011a, b; Jackson et al. 2010). This layer is apparently composed of moderately metamorphosed folded complexes of a wide age range silicaclastic rocks (Knudsen et al. 2017; Morozov et al. 2013; Kabankov et al. 2004; Rekant et al. 2012; Vernikovsky et al. 2014a; Grikurov et al. 2014a, b).

Dominant distribution of these rock groups in different segments of the Lomonosov Ridge is shown on the map of zoning on the assumption of an echelon alternation of heterochronic crust blocks correlated with the conjugate Barents-Kara continental margin.

Mendeleev Rise as a denudation area, which has existed at least since the Paleozoic—since the formation of the Post-Ellesmerian North Chukchi Trough. Formation of the eastern flank of the Mendeleev Rise is related to the Early Cretaceous rifting. The Charlie Rift, at that time, separated the Mendeleev Rise from the Chukchi Plateau. The Mendeleev Rise, as a morphostructure of the Arctic Ocean, similar to the Lomonosov Ridge, was formed during the Neogene-Quaternary.

Judging by prevailing Paleozoic carbonate dredged bottom rocks, the Mendeleev Rise, similar to the Chukchi Borderland and Northwind Ridge, is represented by submerged (during the neotectonic phase) fragments of a continental crust block
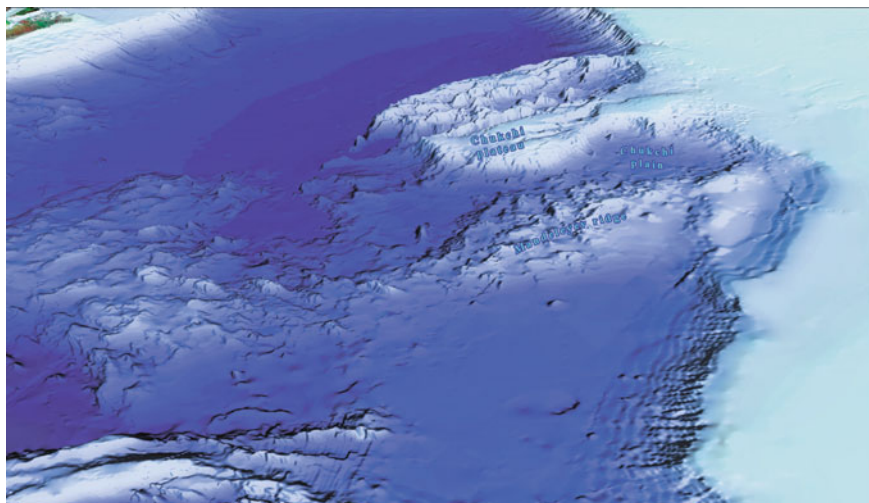
Fig. 12 3D-image of the Mendellev Rise (IBCAO model, version 3.0)

with old Precambrian crystalline basement (Fig. 12). This block includes a Paleozoic platform cover of the continent, known in literature as Hyperborea, Eastern Arctic Platform (Kabankov et al. 2004) or Arctida (Hain et al. 2009). It is quite possible that the Paleozoic cover of the Mendeleev Rise was slightly affected by the Caledonian folding recorded southwards, in the North Chukchi Trough.

As shown by the data obtained during the expedition "Arctic-2012", overwhelming amount of largesize bottom rock material (BRM), dredged from steep submarine scarps is represented by sedimentary littoral and shallow marine carbonate and terrigenous rocks (Morozov et al. 2013). The composition of the sediments and their ages indicate the presence of the platform unmetamorphosed Ordovician-Devonian Carboniferous-Permian sedimentary cover in the Mendeleev Rise.

In 2014 and 2016, the Geological Institute of the Russian Academy of Sciences (GIN RAS) in cooperation with the Geological and Geophysical Survey of the Geological Institute (GEOSLUZHBA GIN) and the Main Directorate for Deepwater Research of the Ministry of Defense of the Russian Federation conducted expeditions in the Alpha-Mendeleev Rise.

Rocks sampled by research submarine manipulators directly from bottom outcrops proved the existence of the Lower Paleozoic mainly carbonate cover on the Mendeleev Rise (Skolotnev et al. 2017, 2019). Among sedimentary rocks exposed in steep slopes of the Mendeleev Rise, three stratigraphic units were identified: the Ordovician-Silurian, Middle-Late Devonian and Early Cretaceous.

On the other hand, seismic data show that in the Mendeleev Rise, the sedimentary cover is represented by Cretaceous and Cenozoic sediments overlying the acoustic basement. To explain this controversy, it should be mentioned that in the Central Arctic Uplifts, primarily in the Alpha-Mendeleev Rise, large intense

magnetic anomaly was recorded (Verba 2006). According to its image, amplitude-frequency characteristics and the scale, this vast region is comparable with the areas of flood basalt large igneous provinces. This assumption was confirmed by the results of seismic interpretation obtained during the cruise of the US icebreaker "Healy" in 2005. Several seismic facies interpreted as sequences of basaltic sheets and sills, intercalating with thick tuff layers and, probably, sedimentary rocks were identified below hemipelagic sediments in the Mendeleev Rise and the north-western part of the Alpha Ridge at the top of the acoustic basement (Bruvoll et al. 2010). Observed cut tops of basement highs are treated as surface erosion of the Mendeleev Rise in a shallow sea, which took place simultaneously with or immediately after its formation. The time of formation of the volcanic rocks in the investigated part of the Alpha Ridge and the Mendeleev Rise is defined as the Aptian-Campanian (112–73 Ma) by Ar/Ar analysis (Mukasa et al. 2015).

The Ar/Ar isotopic analysis of dolerites from Mendeleev Rise obtained in Arctic-2012 expedition shown an Early Paleozoic age. The oldest ages obtained for amphibole reach 471.5 ± 18.1 and 466.9 ± 3.3 Ma, which corresponds to the Early–Middle Ordovician (Vernikovsky et al. 2014b).

Updating of the areas of cretaceous volcanic complexes' distribution is based on the seismostratigraphic analysis of wave fields from seismic profiles. In the Central Arctic Uplifts, anomalies of wave fields were recorded in the sedimentary cover that can be related to magmatic activity in the study area. In the Mendeleev Rise, areal covering volcanics occur over a large area, covering moderately layered weakly folded strata. Their approximate thickness varies greatly, from a few hundred meters in local highs to 1–1.5 km in recent sinking of the basement. Volcanic sheets are exclusively localized in the bottom of the sedimentary cover that allows approximate assessment of the age of acoustic basement from the age of traps, as well as the evaluation of stratigraphic extent of the sedimentary cover. According to sampling results, in the Alpha Ridge, the oldest sediments of the cover and the underlying basalts are Campanian (~82 Ma) (Jokat 2003). This age is much younger than the expected time of the opening of the Canada Basin (~148–128 Ma) and older than the time of the opening of the Eurasian Basin (~56 Ma).

In the Mendeleev Rise, the Russian expedition "Arctic-2012" drilled 3 short (≤ 2 m) wells in two locations. All of them penetrated the acoustic basement composed of Cretaceous basalts and trachybasalts in the south (~102–73 Ma) and late Cretaceous volcanic breccia (73 Ma) in the northern part of the rise (Ar–Ar method). Similar Cretaceous subalkaline and tho leiitic basalts were dredged in the northern spur of the Northwind Ridge (Brumley et al. 2015). Ar–Ar determinations showed later Cretaceous age than U-Pb method (Morozov et al. 2013). Based on available basalt datings, the age of riftogenic movements can be defined as the late Early Cretaceous—Late Cretaceous. Judging by correlated reflectors, next stage of activation of tectonic movements is Paleocene—Oligocene. Formation of the largest seamounts of the Mendeleev Rise is related to them. Wells in the American sector of the Chukchi Sea recorded deep erosion with missing Oligocene and even Miocene sediments that correspond to eustatic minimum of about 33 million years. Since the thickness of Miocene-Holocene sediments on the raised areas of the Mendeleev Rise

is minimal, it is quite possible that the process of uplifting of Paleocene-Oligocene highs has intensified again.

The Mendeleev Rise is the main area of HALIP distribution. In this area, along with intensive basaltic magmatism and block-faulting structures, the spreading is evidenced by significant thinning of the upper crust, which nevertheless retains the "continental" total thickness due to the increase of the lower layer by magmatic underplating. Similar to the Lomonosov Ridge, between the acoustic basement and the upper crust surface, there is an intermediate (metasedimentary) layer, whose seismic transparency is caused by abundant magmatic rocks.

Podvodnikov Basin has a block structure. There are western and eastern blocks separated by the uplift of the Geophysists Spur. Analysis of seismic profiles showed that this separation occurred during the Cretaceous. Despite the fact that the total thickness of sedimentary cover in the basin is almost the same, the eastern and western parts of the basin are characterized by different wave fields. Abundant seismic complexes are recorded in the eastern part. Layer velocities in the basement in the east Podvodnikov Basin reach 5.9–6.3 km/s which is typical of mature basements. Such characteristics of the basement are also observed in the North Chukchi Basin. Unfortunately, there are no reliable velocities in the basement in the western part of the basin, but it is possible that the basement of the Podvodnikov Basin is heterogeneous. By analogy with the North Chukchi Basin, the sedimentation in the east Podvodnikov Basin is assumed to begun in the Late Paleozoic—Early Mesozoic. In the late Early Cretaceous, the basin was divided into eastern and western parts as a result of tectonic movements.

In the western basin during the Cretaceous, relatively thick layer of sediments deposited in the environment of avalanche sedimentation (chaotic seismic record) as a result of drifting from the Lomonosov Ridge and Geophysists Spur. Complete compensation of Cretaceous grabens occurred during the Neogene-Quaternary.

The Laptev Sea Shelf (Fig. 13) is a plain gentle sloping to the north, which is complicated by a few uplifts with islands located in the middle of the shelf, as well as banks and underwater valleys, including those associated with geological features of the seafloor structure. Depths in the area do not exceed 50 m. A trough with depths of up to 40–45 m extends from the Khatanga River mouth along the Taimyr Peninsula coast. The shelf plain is divided into terraces, so the downcutting of underwater valleys is different. In separate segments it reaches 20 m and it does not exceed 5–10 m on flat sections. Submarine valleys continue arterial waterways of the land. The shelf edge is determined from a sharp change in the inclination of the seafloor, which in the Laptev Sea occurs at depths of about 100 m. The orientation of the shelf edge varies from northwestern in the west to sublatitudinal in the central part of the Laptev Sea and to northeastern in the eastern part of the sea.

Specific features of the continental margins in the Laptev Sea are its location at the junction with the underwater Gakkel Ridge, the northernmost segment of the world system of mid-oceanic ridges, and the extremely smooth flattening of the continental slope with depth. It is due to the presence of a thick plume of sediments from the shelf. Over the recent years, VSEGEI focused its activity on the Russian part of the Eastern Arctic where new detailed geological and geophysical data were obtained.
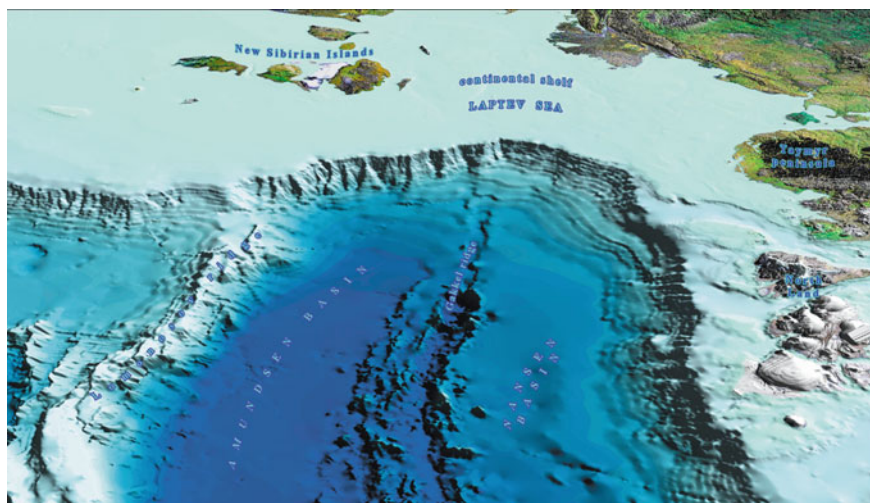
Fig. 13 3D-image of the Laptev Sea continental margin (IBCAO model, version 3.0)

These data became the basis for the creation of the modern tectonic model of the Arctic.

References

Brumley K, Miller EL, Konstantinou A, Grovel M, Meisling KE, Mayer L (2015) First bedrock samples dredged from submarine outcrops in the Chukchi Borderland Arctic Ocean. Geosphere 11(1):76–92

Bruvoll V, Kristoffersen Y, Coakley BJ, Hopper JR (2010) Hemipelagic deposits on the Mendeleev and northwestern Alpha submarine ridges in the Arctic Ocean: Acoustic stratigraphy, depositional environment and an inter-ridge correlation calibrated by the ACEX results. Mar Geophys Res 31:171. https://doi.org/10.1007/s11001-010-9094-9

Daragan-Sushchova LA, Sobolev NN, Petrov EO, Grinko LR, Petrovskaya NA, Daragan-Sushchov YuI (2014) On substituation of stratigraphic control of reference seismic horizons in the East Arctic Shelf and in Central Arctic Uplifts. Reg Geol Metallogeny 58:5–21 (in Russian)

Dove D, Coakley B, Hopper J, Kristoffersen Y, HLY0503 Geophysics Team (2010) Bathymetry, controlled source seismic and gravity observations of the Mendeleev ridge; implications for ridge structure, origin, and regional tectonics. Geophys J Int. https://doi.org/10.1111/j.1365-246X.2010.04746.x

Drachev SS (2011) Tectonic setting, structure and petroleum geology of the Siberian Arctic offshore sedimentary basins. In: Spencer AM, Embry AF, Gautier DL, Stoupakova AV, Sørensen K (eds) Arctic petroleum geology, vol 35. Geol. Soc., London, Mem. pp 369–394

Egiazarov BX, Ermakov BV, Anikeeva LI, Romanovich BS, Pol'kin YaI, Atlasov IP, Demenitskaya RM, Grachev AF, Karasik AM, Kiselev YuG, Andreev SI, Kos'ko MK (1977) An explanatory note to a tectonic map of the northern polar area, scale 1:5,000,000. Leningrad, NIIGA, p 190

Filatova NI, Hain VE (2007) East Arctic tectonics. Geotectonics 3:3–29

Gramberg IS (2002) Comparative geology and mineralogeny of the oceans and their continental margins from the perspective of the staged development of the oceans. Russian Arctic: geological history, mineralogy, geoecology; SPb.: VNIIOkeangeologiya, pp 17–35 (in Russian)

Grantz A, Scott RA, Drachev SS, Moore TE (2009) Maps showing the sedimentary successions of the Arctic Region (58–64 to 90 degrees N) that may be prospective for hydrocarbons. American Association of Petroleum Geologists GIS-UDRIL Open-File Spatial Library. http://gisudril.aapg.org/gisdemo/

Grikurov G, Petrov O, Shokalsky S, Recant P, Krylov A, Laiba A, Belyatsky B, Rozinov M, Sergeev S (2014a) Zircon geochronology of bottom rocks in the central Arctic Ocean: analitical results and some geological implications. Proceedings of the international conference on arctic margins VI, Fairbanks, Alaska, May 2011. Press VSEGEI, St. Petersburg, pp 211–232

Grikurov G, Petrov O, Shokalsky S, Recant P, Krylov A, Laiba A, Belyatsky B, Rozinov M, Sergeev S (2014b) Zircon geochronology of bottom rocks in the central Arctic Ocean: analitical results and some geological implications. ICAM VI: Proceedings of the international conference on arctic margins VI, Fairbanks, Alaska, May 2011. SPb.: Press VSEGEI, pp 211–232

Hain VE (2001) Tectonics of continents and oceans. Scientific world. Moscow, p 606

Hain VE, Filatova NI, Polyakova DI (2009) Tectonics, geodynamics and petroleum potential of Eastern Arctic seas and their continental framing. Proceedings of the geological institute, vol 601. Nauka, Moscow, p 227

Harrison JC, St-Onge MR, Petrov OV, Strelnikov SI, Lopatin B, Wilson F, Tella S, Paul D, Lynds T, Shokalsky S, Hults C, Bergman S, Jepsen HF, Solli A (2008) Geological map of the Arctic, 1:5 million. Geological survey of Canada, open file report, p 5816. http://geogratis.gc.ca/api/en/nrcanrncan/ess-sst/44e20e9d-bd46-5098-9222-4d653382f2c5.html

Harrison JC, St-Onge MR, Petrov OV, Strelnikov SI, Lopatin B, Wilson F, Tella S, Paul D, Lynds T, Shokalsky S, Hults C, Bergman S, Solli A, Jepsen HF (2009) A new geological map of the Arctic: geological survey of Canada open file 5816. Frontiers + innovation—2009 CSPG CSEG CWLS Convention, pp 750–752

Harrison JC, St-Onge MR, Petrov OV, Strelnikov SI, Lopatin B, Wilson F, Tella S, Paul D, Lynds T, Shokalsky S, Hults C, Bergman S, Solli A, Jepsen HF (2011) Geological map of the Arctic. Geol Surv Canada, Ottawa 9

Jackson HR, Dahl-Jensen T, the LORITA working group (2010) Sedimentary and crustal structure from the Ellesmere Island and Greenland continental shelves onto the Lomonosov Ridge, Arctic Ocean. Geophys J Int 182:11–35

Jokat W (2003) Seismic investigations along the western sector of Alpha Ridge, Central Arctic Ocean. Geophys J Int 152(1):185–201. https://doi.org/10.1046/j.1365-246X.2003.01839.x

Jokat W, Micksch U (2004) Sedimentary structure of the Nansen and Amundsen basins, Arctic Ocean. Geophys Res Lett 31:L02603

Kabankov VYa, Andreeva IA, Ivanov VI, Petrova VI (2004) About geotectonic nature of the system of Central Arctic morphostructures and geological significance of bottom sediments in its definition. Geotectonics 6:33–48 (in Russian)

Kenyon S, Forsberg R, Coakley B (2008) New gravity field for the Arctic. EOS Trans AGU 89(32):1–2. https://doi.org/10.1029/2008EO320002

Knudsen C, Hopper JR, Bierman PR, Bjerage M, Funck T, Green PF, Ineson JR, Japsen P, Marcussen C, Sherlock SC, Thomsen B (2017) In: Samples from the Lomonosov Ridge place new constraintson the geological evolution of the Arctic Ocean. Geological Society London Special Publications, p 460. https://doi.org/10.1144/SP460.17

Lawver LA, Grantz A, Gahagan LM (2002) Plate kinematic evolution of the present Arctic region since the Ordovician. In: Miller EL, Grantz A, Klemperer SL (eds) Tectonic evolution of the bering shelf—Chukchi Sea—Arctic Margin and adjacent land masses. Special papers, vol 360. Geological Society of America, Boulder, Colorado, pp 333–358

Miller EL, Meisling KE, Anikin VV et al (2017) Circum-Arctic liotsphere evolution (CALE) transect C: displacement of the Arctic Alaska-Chutkotka microplate towards the Pacific during the opening

of the Amerasia Basin in the Arctic. In: Pease V, Coakley B (eds) Circum-Arctic Litosphere Evolution. Geol Soc London, Spec Publ, vol 460. https://doi.org/10.1144/sp460.9

Morozov AF, Petrov OV, Shokalsky SP, Kashubin SN, Kremenetsky AA, Shkatov MYu, Kaminsky VD, Gusev EA, Grikurov GE, Rekant PV, Shevchenko SS, Sergeev SA, Shatov VV (2013) New geological evidence grounding the continental nature of the Central Arctic Uplifts. Reg Geol Metallogeny 53:34–56 (in Russian)

Mukasa SB, Mayer LA, Aviado K, Bryce J, Andronikov A, Brumley K, Blichert-Toft J, Petrov OV, Shokalsky SP (2015) Alpha/Mendeleev Ridge and Chukchi Borderland 40Ar/39Ar geochronology and geochemistry: character of the first submarine intraplate lavas recovered from the Arctic Ocean. Geophys Res Abs 17, EGU2015-8291-2

Naryshkin GD (1987) The middle ridge of the Eurasian basin of the Arctic Ocean. Nauka, Moscow, 72 p. (in Russian)

Nordahl B, Harrison CJ, Jarna A, Solli A (2016) Metal and mineral deposits of the Arctic, scale 1:10 M. Geological survey of Norway

Orographic map of the Arctic basin [map] (1995) Gramberg IS, Naryshkin GD, Scale 1:5,000,000. Helsinki, Karttakeskus, p 1 (in Russian)

Pease VL, Kuzmichev AV, Danukalova MK (2014) The new Siberian Islands and evidence for the continuation of the Uralides, Arctic Russia. J Geol Soc 172

Petrov OV, Smelror M (2015) Uniting the Arctic frontiers—international cooperation on Circum-Arctic geological and geophysical maps. Polar Rec 51(5):530–535. http://dx.doi.org/10.1017/S0032247414000667

Petrov OV, Shokalsky SP, Kashubin SN, Morozov AF, Sobolev NN, Pospelov II, Box S, Brekke H, Ernst R, Faleide Y, Gaedicke C, Gaina C, Gernigon L, Glumov IF, Grantz A, Grikurov GE, Guarnieri P, Harrison JC, Kaminsky VD, Kazmin YuB, Labrousse L, Lemonnier N, Leonov YuG, Malyshev NA, Milshtein ED, Moore T, Orndorff R, Petrov EO, Piepjohn К, Poselov VA, Pubellier M, Puchkov VN, Smelror M, Sokolov SD, Stephens M, St-Onge MR, Tolmacheva TYu, Verba ML, Vernikovsky VA (2019) Tectonic map of the Arctic, scale 1:10,000,000

Poselov VA, Verba VV, Zholondz SM (2007) Crust typification in the central arctic uplifts, the Arctic Ocean. Geotectonics 4:48–59

Poselov V, Butsenko V, Chernykh A, Glebovsky V, Jackson HR, Potter DP, Oakey G, Shimeld J, Marcussen C (2011a) The structural integrity of the Lomonosov Ridge with the North American and Siberian continental margins. In: Proceedings of the international conference on arctic margins VI, Fairbanks, Alaska, pp 233–258. http://www2.gi.alaska.edu/icam6/proceedings/web/

Poselov VA, Avetisov GP, Kaminsky VD et al (2011b) Russian arctic geotraverses. VNIIOkeangeologia, St. Petersburg, p 172

Proskurnin VF, Petrov OV, Sobolev NN, Remizov DN, Vinogradova NP, Yudin SV (2012) First data on the manifestation of Oligocene-Lower Cretaceous continental magmatism in the Belkovsky Island (New Siberian Islands). Reg Geol Metallogeny 52:49–58 (in Russian)

Rekant PV, Pyatkova MN, Nikolaev ID, Taldenkova EE (2012) Bottom-rock material from the Geofizikov Spur as a basement petrotype for the southern part of the Lomonosov Ridge (the Arctic Ocean). Geol Environ Geol Eurasia Cont Margins 4:29–40

Skolotnev SG, Fedonkin MA, Korniychuk AV (2017) New data concerning the geological structure of the South-West part Mendeleev Rise (Arctic Ocean). Doklady RAS 476(2):190–196

Skolotnev S, Aleksandrova G, Isakova T, Tolmacheva T, Kurilenko A, Raevskaya E, Rozhnov S, Petrov E, Korniychuk A (2019) Fossils from seabed bedrocks: Implications for the nature of the acoustic basement of the Mendeleev Rise (Arctic Ocean). Mar Geol 407:148–163

Verba VV (2006) Nature of the anomalous magnetic field in the central arctic uplifts province in the Amerasian Basin of the Arctic Ocean. Geophys J Kiev 28(5):95–103

Vernikovsky VA, Metelkin DV, Tolmacheva TYu, Malyshev NA, Petrov OV, Sobolev NN, Matushkin NYu (2013) On the problem of paleotectonic reconstructions in the Arctic and the tectonic unity of the New Siberian Islands terrane: New paleomagnetic and paleontological data. In: Proceedings of the Russian Academy of sciences, vol 451(4), pp 423–429 (in Russian)

Vernikovsky VA, Metelkin DV, Vernikovskaya AE, Matushkin NYu, Lobkovsky E, Shipilov V (2014a) Early evolution stages of the arctic margins (Neoproterozoic-Paleozoic) and plate reconstructions. In: Stone DB et al (eds) Proceedings of the international conference on arctic margins VI, Fairbanks, Alaska. Press VSEGEI, St. Petersburg, pp 265–285

Vernikovsky VV, Morozov AF, Petrov OV et al (2014b) New data on the age of dolerite and basalt in the Mendeleev Rise: on the problem of the continental crust in the Arctic Ocean. Proc Russ Acad Sci 454(4):431–435

Zonenshain LP, Natapov LM (1987) Tectonic history of the Arctic. Current problems of the tectonics of oceans and continents. Nauka, Moscow, pp 31–57

Deep Structures of the Circumpolar Arctic

S. N. Kashubin, O. V. Petrov, V. A. Poselov, S. P. Shokalsky, E. D. Milshtein, and T. P. Litvinova

Abstract The deep model of the Earth's crust and upper mantle of the Arctic basin is represented by a series of velocity sections along the DSS profiles and a set of maps showing the thickness of the sedimentary cover, the thickness of the Earth's crust as a whole and the distribution of the continental and oceanic types of the Earth's crust in the Circumpolar Arctic. Crustal Thickness Map is based on results of deep seismic studies and gravity field anomalies in the Circumpolar Arctic. Over 300 profiles of total length of about 140,000 km and equations of correlation, which link the depth of the Moho discontinuity occurrence with Bouguer anomalies and the topography, were used for the map compilation. Correlation sketch map of crustal types, which differ in velocity and density parameters, structure, and total crust thickness, has been compiled based on the data of deep seismic studies on continents and in oceans. The sketch map of crustal types distribution, which was compiled based on seismic profiles in the Arctic, demonstrates the position of the oceanic and continental crust in the structures of the Circumpolar Arctic. Summary geotransect is composed of DSS seismic line fragments and supplemented with density modelling. The geotransect demonstrates structure of the Earth's crust and upper mantle along the line 7600 km long, which crosses the continental crust of the East European Platform, Barents-Kara shelf seas, Eurasian Basin oceanic crust, reduced crust of the Central Arctic Submarine Elevations, shelf seas of Eurasia passive margin, and crust of the Chukotka-Kolyma folded area.

S. N. Kashubin (✉) · O. V. Petrov · S. P. Shokalsky · E. D. Milshtein · T. P. Litvinova
Russian Geological Research Institute (VSEGEI), 74 Sredny Prospect, St. Petersburg 199106, Russia
e-mail: sergey_kashubin@vsegei.ru

V. A. Poselov
Russia Research Institute for Geology and Mineral Resources of the Ocean (VNIIOKEANGEOLOGIA), 1 Angliyskiy av., St. Petersburg 199106, Russia

1 Gravity and Magnetic Anomaly Maps

Compilations of the magnetic and gravimetric maps was coordinated by the Geological Survey of Norway and Carmen Gaina was chosen as the leader of the «Circum-Arctic Mapping Project-Gravity and Magnetic Maps» (CAMP-GM) working group. In August 2008 the geophysical maps were displayed at the 33rd International Geological Congress in Oslo (Saltus and Gaina 2007; Gaina et al. 2007, 2008, 2011). In 2009, the final report from the CAMP-GM working group was published as an open file in the Geological Survey of Norway report series (NGU Report 2009.010) (Gaina 2009; Gaina et al. 2010). In 2011, the gravity and magnetic anomaly maps were published at the CAMP-GM web-site (Figs. 1 and 2) (Gaina et al. 2011).

The maps were compiled in the Polar Stereographic projection (datum: WGS 84) and compose gridded data that were provided from Polar Regions by Russia, Canada and USA. As the "master grid" the Alaska USGS aeromagnetic compilation was used. The original projections are listed in NGU Report 2009.010 (Gaina 2009). Preliminary the MF4 and MF5 models were used CAMPGM-M compilation, but for the compilation of the final version of CAMPGM-M magnetic anomaly model MF6l was used (e.g. Hemant et al. 2007; Maus et al. 2007, 2008).

For the compilation of the gravity map a polar-stereographic projection as well as the IBCAO bathymetry was used. The digital gridded data for it was presented in a grid-cell size of 10 km by 10 km (Gaina 2009). The final product included one map of the Free Air gravity anomaly and one map of combined Free Air and Bouguer) in a 1:5,000,000 scale, both at 10×10 km grid resolution. A new grid of the Free Air gravity anomaly was produced under the lead of René Forsberg (DNSC) (Kenyon and Forsberg 2000; Kenyon et al. 2008).

Taking into account the lack of direct geological data in Arctic both of these maps we actively used in tectonic compilations.

2 Earth's Crust Velocity Models by Wide-Angle Seismics

At present, data from more than 35,000 km of refraction and wide-angle reflection (deep seismic sounding—DSS) lines have been acquired in the Arctic Ocean, including over 12,000 km done in course of Russian high-latitude expeditions. The sketch-map (Fig. 3) shows main Russian DSS lines in the central and eastern Arctic studied in 1989–2014.

Main technologies for refraction and wide-angle reflection seismic surveys in the Arctic are: (1) observations with ocean bottom seismometers using high-power air-guns and (2) ice-based observations using TNT blasts. With both technologies, seismic waves are recorded at offsets up to 250–300 km, which allows recording all the main reference phases containing information on the crustal structure and velocity parameters through the whole crustal and uppermost mantle. The most informative are detailed seismic soundings with 3-component ocean bottom seismometers.
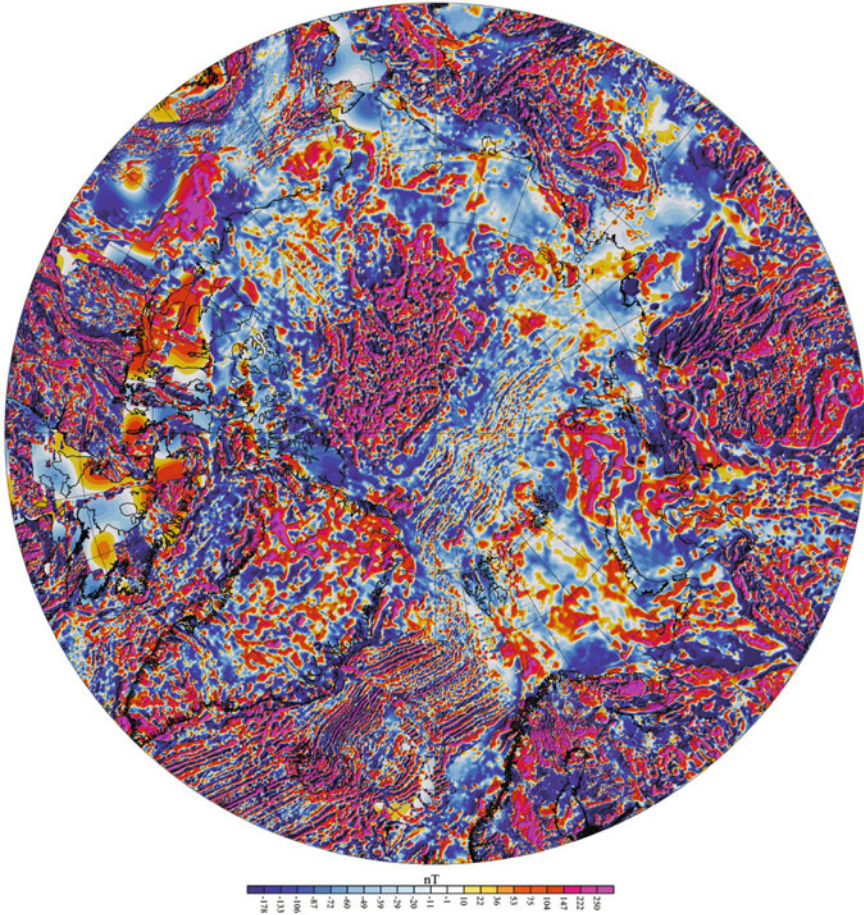
Fig. 1 CAMPGM-M magnetic anomaly compilation of gridded data (to 60 °N) based on ground/airborne regional compilations and global model of lithospheric field, based on satellite data (MF6) (Gaina et al. 2011) (http://www.geodynamics.no/Web/Content/Projects/CIRCUM-ARC TIC%20MAPPING%20PROJECT)

However, in areas with the perennial ice cover, where ocean bottom observations are impossible, ice-based seismic surveys with pure Z-component recording also provide recording of main target P-waves.

In 1989–1992, ice-based DSS surveys were performed using airborne method, i.e. using air delivery of seismic recording equipment to receiver points on ice surface. Later, in 2000–2007, research vessels were used. TNT explosive charges of 0.2 to 1.2 tons were used to excite seismic energy. Seismic signal was recorded by autonomous low-channel "land" seismometer equipped with vertical seismic receivers (Z). Shot point spacing varied from 35 to 70 km, receiver point spacing varied from 3 to 15 km.
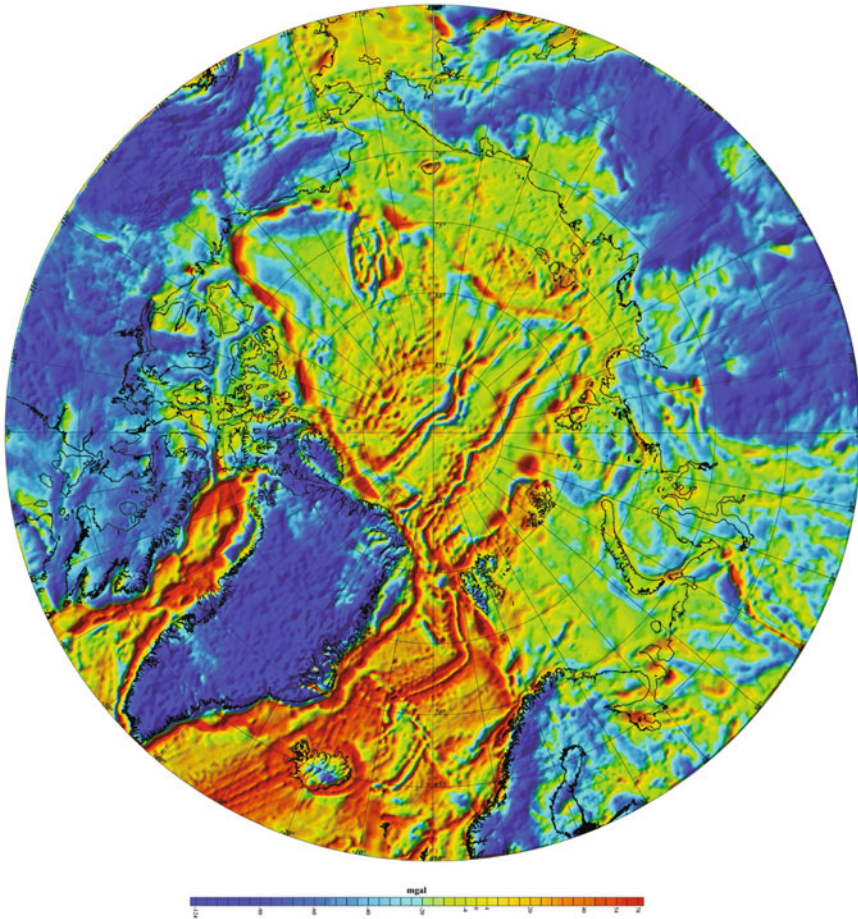
Fig. 2 Gravity map of the Circum-Arctic, with Bouguer gravity anomaly data onshore and Free Air gravity anomaly data offshore, at a grid resolution of 10 × 10 km in a polar stereographic projection (Gaina et al. 2011) (http://www.geodynamics.мno/Web/Content/Projects/CIRCUM-ARCTIC%20MAPPING%20PROJECT)

DSS observations with ocean bottom seismometers were carried out "in open water" in 2008–2014. Powerful air-guns with the chamber volume of 80–120 L (4880–7320 in.^{3}) with a working pressure of up to 150 atm were used. Seismic signal was recorded by autonomous ocean bottom seismometers equipped with a hydrophone (H) and 3-component geophones (X, Y, Z). Observations were made with receiver spacing of 10 to 20 km and shot point spacing of 250 to 315 m.

TransArctic-89-91 (Podvodnikov Basin) (Fig. 4). S-N geotransect Transarctic-89-91 extending for 1500 km from the shelf of the De Long islands in the East Siberian Sea across the Podvodnikov and Makarov basins to the circumpolar part of the
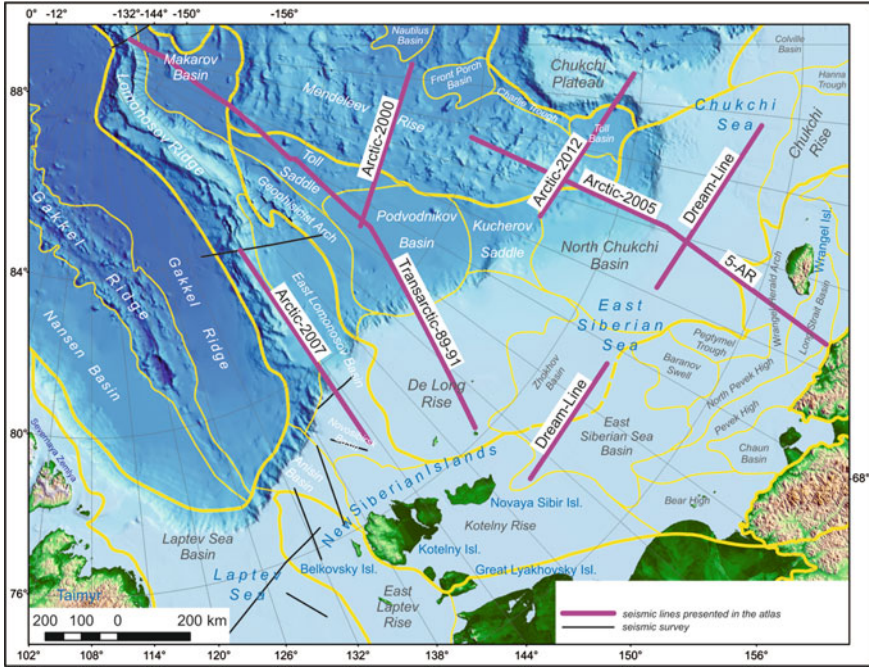
Fig. 3 DSS-profiles in the Eastern Arctic
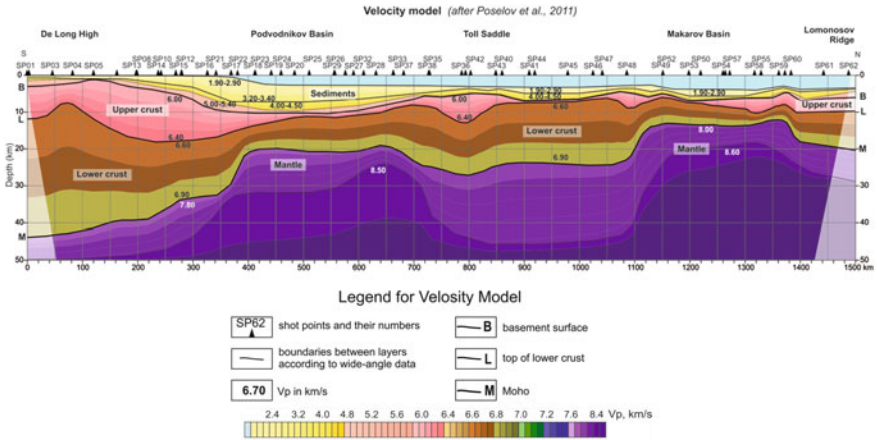
Fig. 4 Velocity model along TransArctic-89-91 profile (Poselov et al. 2011a). Profile position is shown in Fig. 3. Numeric designations of the Vp in km/s. B—basement surface; L—top of lower crust; M—Moho

Arctic Ocean was shot by airborne method from drifting ice bases. The set of studies included DSS and reflection seismic surveys, ice-based airborne gravimetric surveys, and aeromagnetic surveys.

The crustal velocity model along the line made it possible to trace: (1) sedimentary cover with Vp of 1.9 to 4.5 km/s and thickness from 7 km in the Vilkitsky Trough to 2–4 km in the Makarov Basin; (2) intermediate sequence with Vp from 5.0 to 5.4 km/s and thickness from several hundred meters in the Makarov Basin to 2–2.5 km under the continental slope; (3) the upper crust (Vp of 6.0–6.4 km/s) with greatly varying thickness from 15 km in the De Long Rise to 1–2 km in the Makarov Basin; (4) the lower crust (Vp of 6.6–6.9 km/s) with 9 km thickness in the Makarov Basin to 25–35 km thickness in the De Long Rise; (5) the upper mantle (Vp of 7.8–8.0 km/s). The crustal thickness changes rather sharply from 44 km under the De Long Rise to 20–21 km under the Podvodnikov Basin and to 13–14 km under the Makarov Basin. Thus, stratified sedimentary sequences, the intermediate sequence, and the crystalline two-layer crust are traced from the outer shelf of the East Siberian Sea to the Podvodnikov and Makarov Basins, which corresponds to the model of the thinned continental crust.

Arctic-2000 (Mendeleev Rise) (Fig. 5). The 485-km-long W-E profile Arctic-2000 extending from the Podvodnikov to the Mendeleev Basin across the submarine Mendeleev Rise was shot using the airborne method from the research vessel Akademik Fedorov. The set of geophysical studies included DSS and single channel seismic (SCS) reflection observations (with ~5 km station spacing), ice-based gravimetric measurements. Geophysical explorations were supplemented with bottom geological sampling.

The crustal and upper mantle velocity model demonstrates: (1) the sedimentary cover (Vp of 1.7–3.5 km/s) reaching up to 3.5 km in thickness in the Podvodnikov Basin; (2) the intermediate sequence with Vp of 5.0 to 5.4 km/s and the thickness
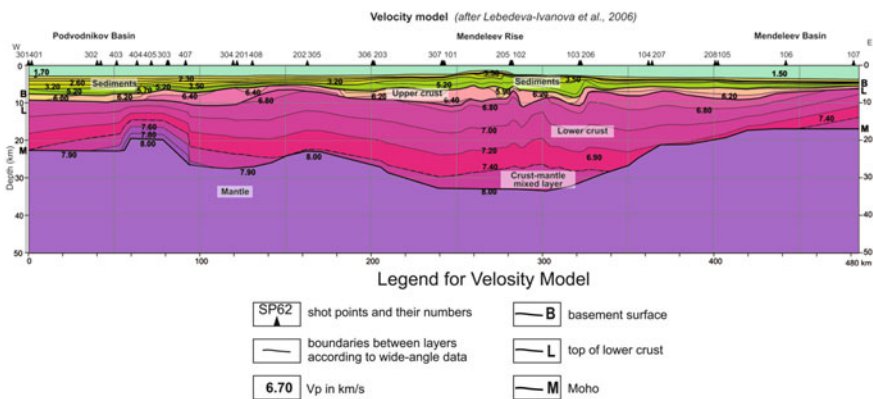
Fig. 5 Velocity model along Arctic-2000 profile (Lebedeva-Ivanova et al. 2006). Profile position is shown in Fig. 3. The basic notation is the same as in Fig. 4
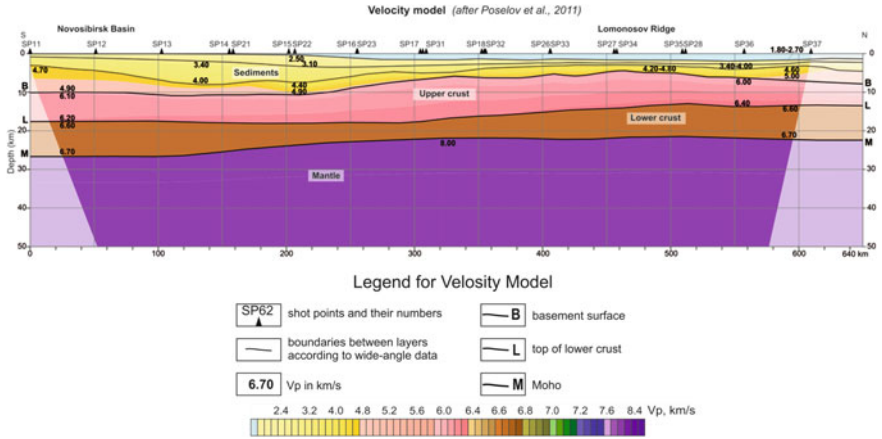
Fig. 6 Velocity model along Arctic-2007 profile (Poselov et al. 2011a). Profile position is shown in Fig. 3. The basic notation is the same as in Fig. 4

of up to 4 km in the Lomonosov Ridge; (3) the upper crust (Vp of 5.9–6.5 km/s) varying from 2 to 4 km in thickness; (4) the lower crust (Vp of 6.7 to 7.3 km/s) having the thickness of 10 km under troughs to 20 km under the Lomonosov Ridge; (5) presumably crust-mantle mixture (Vp of 7.4 to 7.6 km/s); (6) upper mantle (Vp of 7.9 to 8.0 km/s). The crustal thickness varies from 13 km under the Mendeleev Basin to 32 km under the Lomonosov Ridge. According to existing conceptions, such velocity model is typical of the continental crust.

Arctic-2007 (Lomonosov Ridge) (Fig. 6). The 650-km-long S-N DSS line Arctic 2007 stretching along axial zone of the Lomonosov Ridge towards the zone of its junction with the Laptev and the East Siberian shelves was shot using the airborne method from the Rossiya nuclear icebreaker.

In the same year, another survey was made along the line using multi-channel seismic (MCS) reflection technique with a 8100-m-long streamer and shot point spacing of 37.5 m. The northern end of the Arctic-2007 line adjoins the Transarctic-92; similar sequences have been traced along both of them (see earlier). The southern end of Arctic-2007 goes towards the shelf near the New Siberian Islands. As can be seen from the above cross-section, all the main sequences typical of the continental crust with insignificant variations in thickness and velocity are continuously traced from the shelf to the Lomonosov Ridge. Currently, the continental nature of the Lomonosov Ridge and its relationship with the shelf of Northern Eurasia are recognized by most Arctic researchers.

Composite line 5-AR—Arctic-2005 (East Siberian Shelf, Mendeleev Rise) (Fig. 7). The 650-km-long DSS line Arctic-2005 along the crest of the submarine Mendeleev Rise was shot using the airborne method from the research vessel Akademik Fedorov in 2005. In 2008, DSS seismic survey was carried out with ocean bottom seismometers along the 550 km line 5-AR directly adjacent to the line Arctic 2005 in the south.
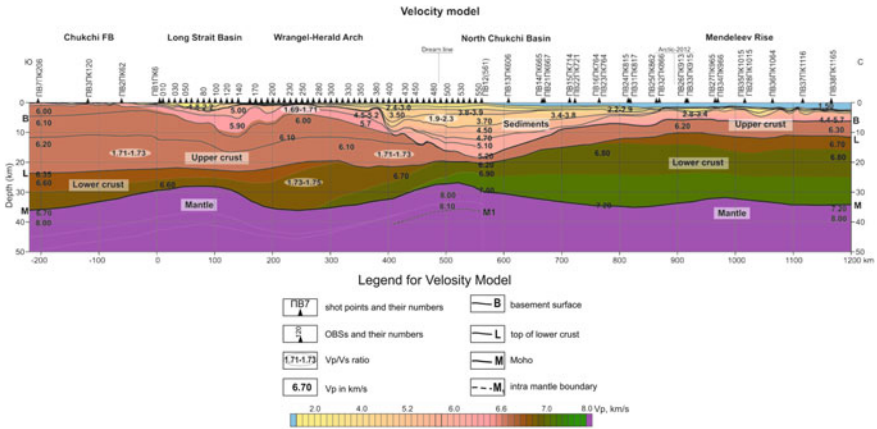
Fig. 7 Velocity model along Composite line 5-AR—Arctic-2005 (Kashubin et al. 2018b). Profile position is shown in Fig. 3. The basic notation is the same as in Fig. 4. The numbers in the circles correspond to the Vp/Vs ratio

It was supplemented by onshore-offshore surveys along the 220 km segment of the ground line 2-DV. In addition, MCS survey with a towed streamer of 8100 m length and shot point spacing of 50 m was carried out along 5-AR, and in 2012, near the line Arctic 2005, MCS survey was carried out using the 600-m-long towed streamer and shot point spacing of 50 m. Thus, based on results of all these seismic surveys, it was possible to construct the composite crustal and upper mantle velocity model along the 1400-km-long line extending from the continental land in the south to the submarine Mendeleev Rise in the north.

All major seismic sequences were traced along the profile based on the crustal velocity model: stratified sedimentary sequences, the intermediate sequence, and crystalline crust sequences. The change in the crust type is also clearly visible in the transition from the continental shelf through the thick sedimentary basin to the submarine Mendeleev Rise. The typical continental crust having the thickness of 32–35 km with the thick upper part (thickness of the "granite gneiss" layer is 15–20 km and more) is observed on the land and in the shelf part. Within the Mendeleev Rise, the crustal thickness practically does not change, but the thickness of the upper crust significantly decreases. This type of the crust (with typical or somewhat reduced thickness but significantly increased thickness of the lower crust) is rare on continents, but is common for the most Central Arctic Elevations.

Dream-line (North Chukchi Basin) (Fig. 8). Deep seismic soundings with ocean bottom seismometers along the 925 km Dream-line profile in the East Siberian and the Chukchi Seas were carried out by order of the BP PLC in 2009.

The data of these studies and the MSC data obtained from studying the Russian lines RU2-1350, OGT-2, and ARS10Z01 located not far from the DSS Dream-line resulted in the development of the Vp and Vp/Vs crustal and upper mantle velocity models of the North Chukchi Trough.
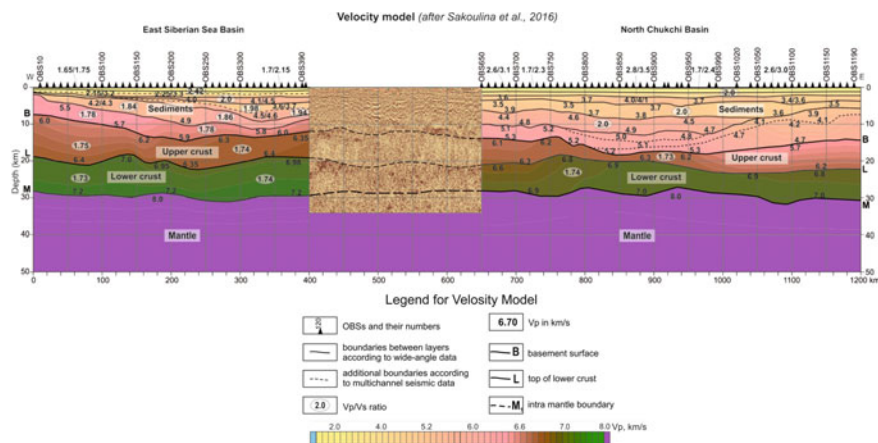
Fig. 8 Velocity model along Dream-line profile (Sakoulina et al. 2016). Profile position is shown in Fig. 3. The basic notation is the same as in Fig. 4. The numbers in the circles correspond to the Vp/Vs ratio

In the crust section, there are: (1) the sedimentary cover (Vp from 1.6–1.9 km/s in the upper part to 4.8–5.6 km/s on its bottom, Vp/Vs from 1.9 to 2.4); (2) the intermediate (meta-sedimentary) sequence (Vp of 4.6–6.0 km/s, Vp/Vs, 1.8–1.9); (3) the upper crystalline crust (Vp of 6.0–6.4 km/s, Vp/Vs, 1.73–1.75); (4) the lower crystalline crust (Vp of 6.6–7.2 km/s, Vp/Vs, 1.73–1.74); (5) the upper mantle (Vp of 8.0 km/s).

The average crust thickness along the Dream-line is 28–30 km. The greater part of the crust (7 to 16 km) corresponds to the sedimentary cover. Such velocity parameters and thickness of the Earth's crust in the North Chukchi Trough are typical of the crust of continental deep depressions.

Arctic-2012 (Mendeleev Rise) (Fig. 9). The 740-km-long DSS profile Arctic 2012 crosses the Mendeleev Rise approximately at the latitude of N77°. Integrated MCS and DSS seismic surveys were carried out along the line. DSS surveys were done with the use of ocean bottom seismometers deployed with 10–20 km spacing. A powerful 120-l (7320 in.³) air-gun was used. Vp and Vp/Vs crustal and upper mantle velocity models were developed.

In the crustal section, there are: (1) the sedimentary cover (Vp of 1.6–1.9 km/s in the upper part to 4.8–5.6 km/s in the bottom, Vp/Vs from 1.9 to 2.8); (2) the intermediate (meta-sedimentary) sequence (Vp of 4.6 to 6.0 km/s; Vp/Vs, 1.9–2.0); (3) the upper crystalline crust (Vp of 6.0–6.3 km/s in the upper part to 6.7 km/s in the bottom, Vp/Vs, 1.70–1.73); (4) the lower crystalline crust (Vp of 6.8 to 7.3 km/s, Vp/Vs, 1.74–1.78); (5) the upper mantle (Vp of 7.8–8.0 km/s).

The crustal thickness in the Mendeleev Rise is about 32 km, 20 km being the lower crust. In general, the velocity parameters and crustal thickness in the Mendeleev Rise are typical of the continental crust. The increased thickness of the lower crust
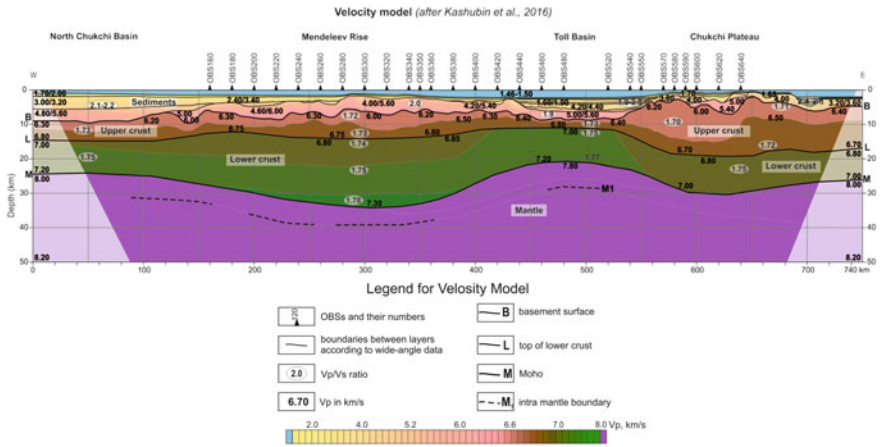
Fig. 9 Velocity model along Arctic-2012 profile (Kashubin et al. 2016, 2018a; Kashubin and Petrov 2019). Profile position is shown in Fig. 3. The basic notation is the same as in Fig. 4. The numbers in the circles correspond to the Vp/Vs ratio

is probably due to magmatic underplating, which in its turn led to intraplate basic volcanism and the High Arctic large igneous province (HALIP) formation in this part of the Arctic.

3 Set of Deep Structure Maps

Gravity and magnetic domains of the Arctic. Anomalous potential field zoning makes it possible to delineate blocks with different types of crust and reveal similarities in the nature of potential field and tectonic structures (Fig. 10).

Maps of the anomalous magnetic field (AMF) and the anomalous gravity field (AGF) of the Arctic at 1:5 M scale are basic elements in the zoning. The Russian part of the maps has been supplemented with data obtained during modern medium-scale surveys. The maps are supplied with matrices of the magnetic and gravity fields with the size of the cell of 5×5 km and 10×10 km respectively (Litvinova et al. 2012a, b).

Transformations of potential fields and a set of specialized maps (geological, topography and bathymetry, sedimentary cover and crustal thickness) were used as auxiliary materials for the delineation of the units shown on the scheme (Petrov and Smelror 2015a, b, Petrov et al. 2016). The delineation was carried out in an iterative mode directly on the computer screen using GIS ESRI ArcMap v.9.3.

The analysis is based on principles of tectonic zoning proposed by Kosygin (1975), which fully correspond to the concept of comprehensive zoning of potential fields. In compliance with principles, the zoning was considered as a set of methods of space
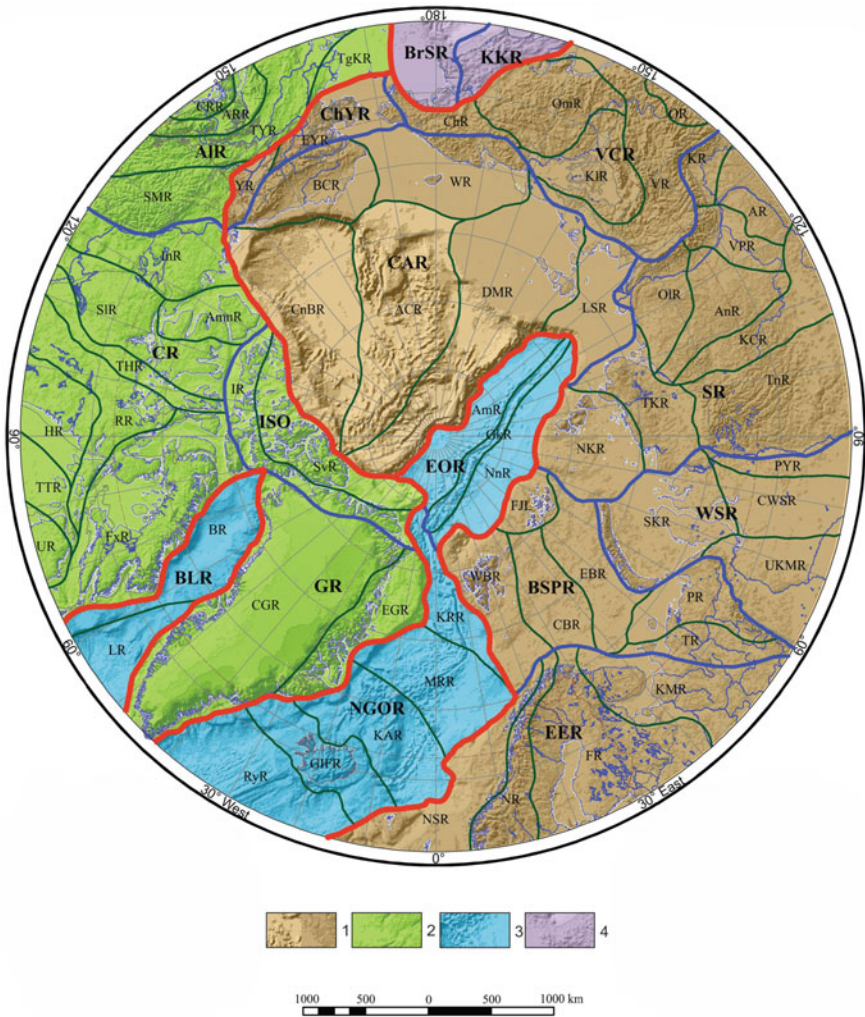
Fig. 10 Circumpolar Arctic zoning map based on the character of potential fields. Color indicates provinces: 1—Eurasian (lighter tone corresponds to areas submerged to bathyal depths), 2—North American, 3—Mid-oceanic ridges, 4—Pacific. Blue lines indicate boundaries of regions (bold); green lines show borders of areas. Digital encoding of potential field types and corresponding tectonic units are shown in Table 1. At the bottom: gravity anomalies map (**a**) and anomalous magnetic field map (**b**)

division (including the 3D version) according to the selected systematics of the bodies (ranks), following the rules of complete space division with no remainder, no border crossing, and the identity of characteristics of distinguished elements (Voronin 2007).

When delineating the areas, the following ranking system was used (in descending order): anomalous province, anomalous district, and anomalous area. Morphostructural features (including zonality) of potential fields were adopted as a main criterion in zoning. The distinguishing of taxa of the first (anomalous province) and second (anomalous district) orders was to a great extent based on the assessment of crustal alterations and mean values of the crustal thickness (Kashubin et al. 2011, 2014).

Morphostructure of the fields, intensity and the sign of anomalies are taken as a basis for the characterization of these structures.

The research resulted in a comprehensive map of potential fields zoning of the Circumpolar Arctic (Fig. 10; Table 1), which was used as the basis for compilation of a base map of crustal types and tectonic zoning sketch-map.

The compiled map of complex zoning makes it possible to demonstrate rather specific similarities in the character of the potential field and tectonic structures in the Arctic basin and its continental margins. Figure 10 shows an example of distinguishing on the maps of potential fields large magmatic provinces corresponding to the region of the Mendeleev-Alpha rises within the Arctic Basin and the Tunguska Block in the Siberian platform.

Map of thickness of undeformed sedimentary cover in the Arctic. By sedimentary cover is meant a sequence of sedimentary, slightly dislocated, and usually unmetamorphosed rocks characterized by gentle dipping that form the upper part of the Earth's crust. On continents, as a rule, on continents the sedimentary cover lies on consolidated crust and in oceans—on the second oceanic layer. However, in some sedimentary basins, between the sedimentary cover and crystalline basement, there are intermediate complexes represented by metamorphosed and sediments dislocated to a varying degree. Sometimes, these sediments are included in the sedimentary layer (Gramberg et al. 2001), but more often they are treated as formations of the so-called intermediate structural stage (Poselov et al. 2011a, b, 2012). In geological mapping, the thickness of sediments lying on heterochronic basements is shown by isopach lines.

As a rule, the sedimentary cover is confidently identified in seismic cross-sections by the nature of seismic record and values of elastic wave velocities, so seismic methods play a key role in the study of the sedimentary cover. In CDP time cross-sections, the base of the sedimentary cover is usually recorded from the sharp change of extended and subhorizontally oriented lineups to dashed variously oriented field of reflectors or complete cessation of regular seismic record. This horizon, indexed in CDP cross-sections as AB (acoustic basement), usually coincides with the first-order velocity boundary identified when observing with P-wave method, DSS, and corresponding to sharp increase in P-wave velocity values from less than 3.5–4.0 km/s to 5.0 km/s and higher. As a rule, the base of the sedimentary cover is constructed from seismic data using these features.

The thickness map of the Circumpolar Arctic sedimentary cover shown in Fig. 11 was compiled as a part of the international project on the compilation of the Atlas of geological maps of the Circumpolar Arctic carried out under the auspices of the Commission for the Geological Map of the World (Petrov et al. 2016). The map

Table 1 Matching of letter symbols (indices) on the zoning map (Fig. 10) to the units identified

Index on the map	Potential fields' zoning (units names)	Tectonic zoning
Eurasian province		
EER	**East Europe Realm**	**East European Platform**
NSR	Norwegian Sea Region	Norwegian Shelf (Voring Plateau etc.)
NR	Norwegian Region	Scandinavian Caledonides
FR	Fennoscandian Region	Fennoscandian Shield
KMR	Kola-Mezen Region	Kola-White Sea and Mezen' blocks
BSPR	**Barents Sea—Pechora Realm**	**Timan-Pechora and Barents Sea Shelf**
WBR	West Barents Region	Svalbard and structural elements of the West Barents Sea Shelf
CBR	Central Barents Region	Central Barents Rises
EBR	East Barents Region	East Barents Trough
FJL	Franz Josef Land Region	Franz Josef Land Uplift
TR	Timan Region	Timan-Varanger dislocation zone
PR	Pechora Region	Pechora Sea Block
WSR	**West Siberia Realm**	**East Uralian Fold Belt, West Siberian Basin**
SKR	South Kara Region	South Kara Block
UKMR	Uralian Khanty-Mansi Region	East Ural Fold Belt, Uvat-Khanty-Mansi Block
CWSR	Central-West Siberian Region	Central-West Siberian Fold System
PYR	Pre-Yenisei Region	Pre-Yenisei Fold-Thrust Zone
SR	**Siberian Realm**	**Siberian Platform**
NKR	North Kara Region	North Kara Block
TKR	Taimyr-Khatanga Region	Taimyr Fold Belt, Khatanga Trough
TnR	Tunguska Region	Tunguska Block
KCR	Kotui-Chon Region	Magan Block
AnR	Anabar Region	Anabar Shield
OlR	Olenek Region	Olenek Block
AR	Aldan Region	Aldan Shield
KR	Khandyga Region	Pre-Verkhoyansk Foredeep
VPR	Vilyuy-Patom Region	Patom-Vilyuy Aulacogen
VCR	**Verkhoyansk-Chukotka Realm**	**Verkhoyansk-Chukotka Fold-Thrust area**
VR	Verkhoynask Region	Verkhoyansk-Chukotka Fold-Thrust System
OR	Okhotsk Region	Okhotsk Block

(continued)

Table 1 (continued)

Index on the map	Potential fields' zoning (units names)	Tectonic zoning
KlR	Kolyma Region	Kolyma Loop
OmR	Omolon Region	Omolon Block
ChR	Chukchi Region	Chukchi Fold-Thrust System
ChYR	**Chukotka-Yukon Realm**	**Eastern Chukchi-Seward Fold-Thrust Belt**
EYR	East Yukon Region	Seward Peninsula Block, Yukon-Koyukuk Basin
YR	Yukon Region	Ruby and Central Alaskan Terranes
CAR	**Central Arctic Realm**	**Amerasian Basin**
LSR	Laptev Sea Region	Laptev Sea Shelf
DMR	De Long-Makarov Region	De Long High, Lomonosov Ridge, Podvodnikov Basin, Makarov Basin
ACR	Alpha-Chukchi Region	Chukchi Plateau, Mendeleev-Alpha Rise
CnBR	Canada Basin Region	Canada Basin
BCR	Brooks-Colville Region	Brooks Fold-Thrust Belt, Colville Basin, Alaska North Slope
WR	Wrangel Region	Wrangel-Herald Fold-Thrust Arch
North America province		
ISR	**Innuitian-Sverdrup Realm**	**Innuitian Orogen, Sverdrup Basin**
SvR	Sverdrup Region	Sverdrup Basin
IR	Innuitian Region	Innuitian Orogen
AlR	**Alaska Realm**	**Alaska Superterrane**
TgKR	Togiak-Koyukuk Region	Togiak-Koyukuk Terrane
TYR	Tanana-Yukon Region	Yukon Terrane
ARR	Alaska Range Region	Alaska Range
CRR	Coast Range Region	Coast Range
SMR	Selwyn-Mackenzie Region	Selwyn-Mackenzie Fold Belt
CR	**Canada Realm**	**North America Craton**
InR	Interior Region	Interior Platform
SlR	Slave Region	Slave Block
AmnR	Amundsen Region	Amundsen Block
THR	Trans-Hudson Region	Trans-Hudson Fold Belt
RR	Rae Region	Rae Block
HR	Hearne Region	Hearne Block
UR	Ungava Region	Ungava Block
TTR	Teltson-Thelon Region	Teltson-Thelon Fold Belt

(continued)

Table 1 (continued)

Index on the map	Potential fields' zoning (units names)	Tectonic zoning
FxR	Fox Region	Fox Block
GR	**Greenland Realm**	**Greenland Shield, East Greenland Caledonides**
CGR	Central Greenland Region	Greenland Shield
EGR	East Greenland Region	East Greenland Fold-Thrust Belt
Province of mid-oceanic ridges		
BLR	**Baffin-Labrador Realm**	**Baffin-Labrador Oceanic Basin**
LR	Labrador Region	Labrador Sea Basin
BR	Baffi n Region	Baffi n Bay Basin
NGOR	Norway-Greenland Oceanic Realm	Norway-Greenland Oceanic Basin
RyR	Reykjanes Region	Icelandic Basin, Reykjanes Ridge, Irminger Basin
GIFR	Greenland-Iceland-Faroe Region	Greenland-Iceland Ridge, Iceland-Faroe Ridge, Iceland Plateau
KAR	Kolbeinsey-Aegir Region	Greenland Basin, Kolbeinsey Ridge, Norwegian Basin, Aegir Ridge
MRR	Mohns Ridge Region	Mohns Ridge
KRR	Knipovich Ridge Region	Knipovich Ridge
EOR	**Eurasian Oceanic Realm**	**Eurasian Oceanic Basin**
NnR	Nansen Region	Nansen Basin
GkR	Gakkel Region	Gakkel Ridge
AmR	Amundsen Region	Amundsen Basin
Pacific Ocean province		
BrSR	**Bering Sea Realm**	**Bering Sea Basin**
KKR	**Koryak-Kamchatka Realm**	**Koryak-Kamchatka Fold Area**

was compiled on the basis of all available recent maps showing the structure of the sedimentary cover and seismic cross-sections (Gramberg et al. 2001; Smelror et al. 2009; Grantz et al. 2011a, b; Drachev et al. 2010; Divins 2008; Laske and Masters 2010; Poselov et al. 2011a, b, 2012; Artemieva and Thybo 2013, etc.). All available data on the thickness of the sedimentary cover collected from various sources were converted into a single coordinate system and presented in a unified grid with a cell size of 5 × 5 km. In overlapping areas of original maps, priority was given to more detailed studies. Areas with no seismic data were filled by means of sediment thickness interpolation using the global model CRUST1.0 built on a grid of 1 × 1 degree (Laske et al. 2010).

In its present form, the map can serve as a factual basis for the distribution of sediments' thickness in the Arctic region for the analysis of the geological structure and tectonic evolution of the Arctic. The structure of the sedimentary cover reflects
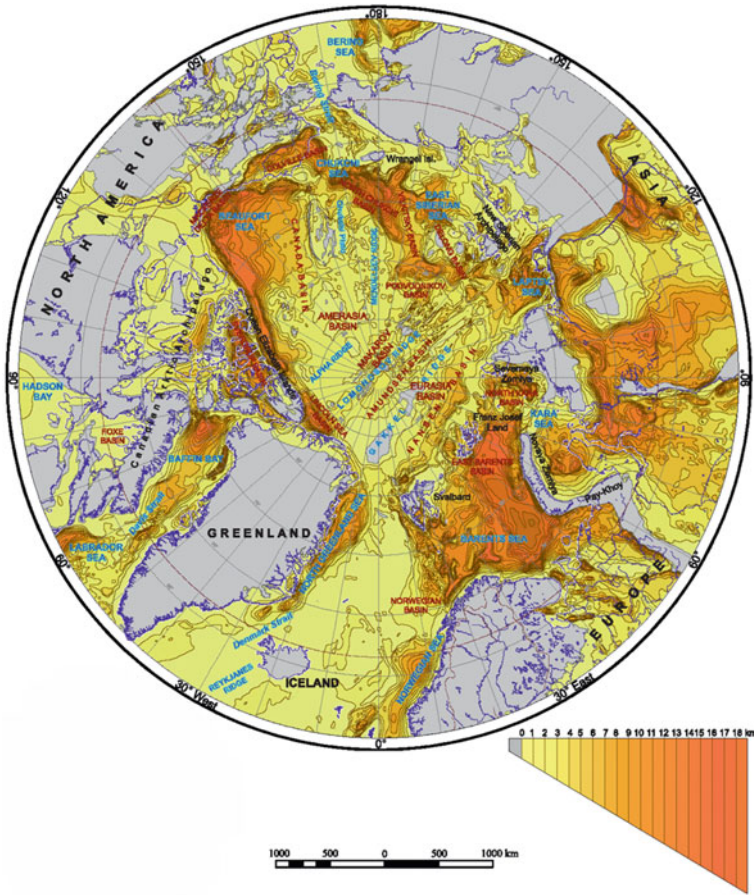
Fig. 11 Thickness map of circumpolar Arctic sedimentary cover (Petrov et al. 2016; Petrov and Smelror 2019). Index map of authors' layouts: 1—Erinchek et al. (2002) (unpublished material). Relief map of the basement of various ages of the East European Platform and the Timan-Pechora Province; 2—Divins (2003) (unpublished material). NGDC Total Sediment Thickness of the World's Oceans and Marginal Seas; 3—Grantz et al. (2009). Map showing the sedimentary successions of the Arctic Region that may be prospective for hydrocarbons; 4—Laske and Masters (2010). Global Digital map of Sediment Thickness; 5—Sakoulina et al. (2011). Sedimentary basins of the Sea of Okhotsk region; 6—Shokalsky et al. (2010) (unpublished material). Schematic thickness map of the sedimentary cover of the Urals, Siberia and the Far East; 7—Sakoulina et al. (2011). Thickness map of the Barents-Kara sedimentary cover; 8—Poselov et al. (2012). Thickness map of the Arctic Ocean sedimentary cover; 9—Stavrov et al. (2011) (unpublished material). Thickness map of sedimentary cover at 1:5 M; 10—Kumar et al. (2010) (unpublished material). Tectonic and Stratigraphic Interpretation of a New Regional Deep-seismic Reflection Survey off shore Banks Island; 11—Mosher et al. (2012) (unpublished material). Sediment Distribution in Canada Basin; 12—Petrovskaya et al. (2008) (unpublished material). Main features of the geological structure of the Russian Chukchi Sea; 13—Vinokurov et al. (2013) (unpublished material). Sedimentary cover thickness from seismic profiles of the expedition Arctic-2012

the location of rift systems in continental margins, orogenic belts, and also allows identifying borders of sedimentary basins.

The sedimentary cover of the Arctic, which includes the total thickness of unde-formed rock sequences lying on the tectonic basement, reveals a belt of deepwater shelf and marginal shelf basins (East Barents Basin–North Kara Syncline, Vilk-itsky Trough–North Chukchi Basin; Colville Trough; Beaufort Sea–Mackenzie River delta; Sverdrup Basin and Lincoln Sea Basin, etc.). In these basins, the sedimentary cover reaches 18–20 km.

System of submeridional (NS) deep-sea basins (Eurasia—Laptev Sea, Makarov Basin—Podvodnikov Basin—De Long Basin and others) with sedimentary cover of 6–10 km, is apparently a younger system superimposed on Paleozoic–Mesozoic marginal shelf basins and troughs.

Sedimentary cover thickness decreases to 1 km and less on the ridges separating the basins (Lomonosov—New Siberian, Alpha—Mendeleev—Wrangel), where the basement with different age of formation and folding is outcropped. Among positive structures, the Gakkel Ridge should be noted as one of the youngest oceanic spreading systems with outcrops of Cenozoic oceanic basement, which is formed in the axial part of the Eurasian sedimentary basin.

The map of sedimentary cover thickness of the Arctic is of extraordinary impor-tance for evaluation of oil and gas resources. It is shown by the map of sedimentary successions prospective for hydrocarbons compiled by A. Grantz in 2009 (Grantz et al. 2009) and maps for the the oil and gas resource potential for the Arctic produces by the US Geological Survey (USGS) (Gautier et al. 2011).

Crustal thickness map of the Arctic. The Earth's crust is commonly seen as an external hard sialic shell located above the Moho. Information about crustal thickness plays an important role in studying the deep structure of the Earth. In seismic and global geophysical constructions, knowledge of crustal thickness is necessary for the calculation of appropriate corrections, and in geological interpreting, it is important to know crustal thickness both for structural and geodynamic constructions. While studying areas of transition from continents to oceans, changes in crustal thickness are often a determining criterion for the identification of continental and oceanic crustal types.

Determination of crustal thickness is primarily carried out by seismic methods. The generally accepted method is the determination by means of deep seismic sounding (DSS) when the sole of the crust is identified with the Moho (M), deter-mined from data of refracted and overcritically reflected waves (Mooney 2007). Sometimes the base of crust is determined in seismic sections obtained by reflected waves (RW-CDP) (Suleimanov et al. 2007) and remote earthquake converted wave (ECW) methods (Zolotov et al. 1998). In the absence of seismic data, the crustal thickness is estimated using the correlation relationship between the M-discontinuity depth, topography, and Bouguer anomalies (Demenitskaya 1967; Kunin et al. 1987).

The crustal thickness map shown in Fig. 12 was been compiled as part of the international project for compiling the Atlas of geological maps of the Circumpolar Arctic under the auspices of the Commission for the Geological Map of the World.
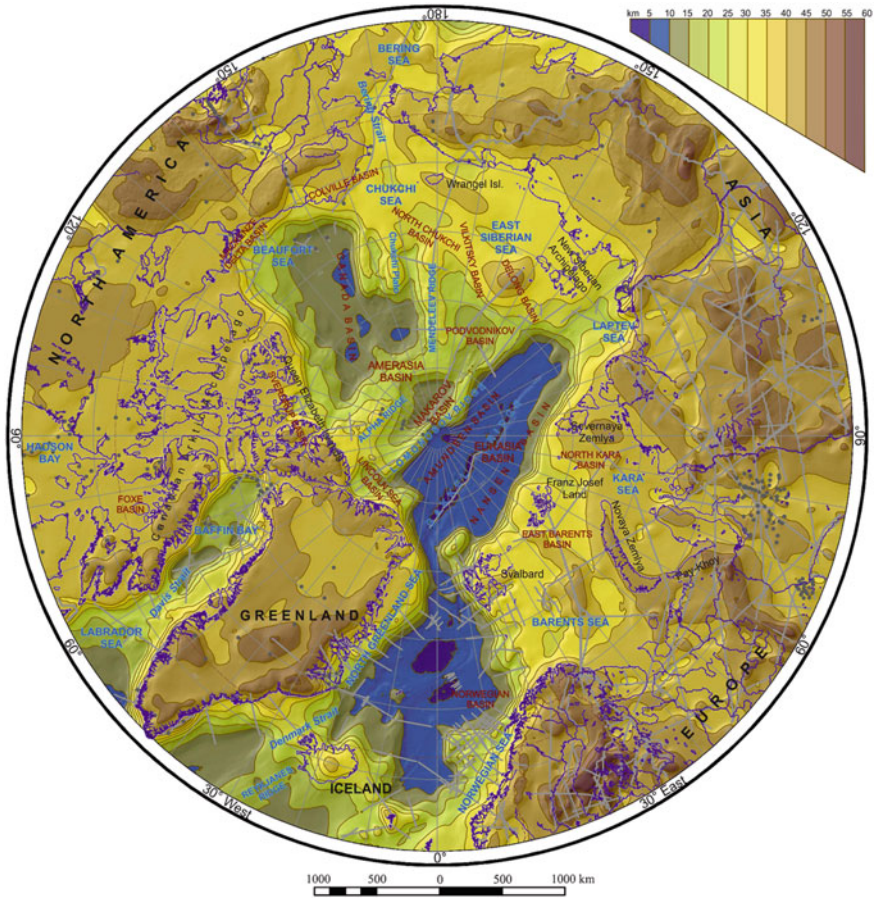
Fig. 12 Circumpolar Arctic crust thickness Map (Kashubin et al. 2011, 2014). Gray lines indicate main seismic lines and grey dots show seismic stations which materials were used for map compilation

For this purpose, all available deep seismic sections north of 60 °N (see list of publications of major seismic sections shown at the end of this section) were used. This array of information includes more than 300 seismic sections with total length of over 140,000 km. Approximately 75% of the sections are results of studies performed by means of DSS, and the rest is represented by deep seismic sections using CDP and RF methods.

The Map of crustal thickness was built in several steps (Kashubin et al. 2011, 2014). First, the depth values to the M discontinuity obtained from seismic cross-sections with a 25-km interval of were plotted on the physical and geological maps. Totally, 5500 Zm (Moho depth) values within the Circumpolar Arctic were plotted on the map based on seismic and seismological data. Digital layouts of the anomalous

gravity field map (Gaina 2009) and maps of surface relief and depths of the ocean floor (IBCAO ver 2.23) were used to show the depth values to the M discontinuity in the space between the profiles and vast areas where seismic data were lacking. Zm values were calculated separately for the continental and marine parts of the area following the network of 10×10 km based on Bouguer anomaly values and relief data averaged within a radius of 100 km using correlation equations (Kashubin et al. 2011). The resulting digital arrays were integrated into one database along the coastline border with subsequent correlation of isolines in the area of their intersections. On the basis of adjusted data, the calculation of the new digital array was made, which was integrated with pre-existing digital maps of M discontinuity depths (Ritzmann et al. 2006; Grad et al. 2007; Erinchek et al. 2007; Artemieva and Thybo 2013). The final map is presented in the form of a Zm digital model with the cell size of 10×10 km for the entire study area. In the course of recalculation of Zm values to uniform values, the interpolation error was estimated by comparing interpolated and initial values in 3600 spots, in which depth values were plotted using seismic data. Mean-square deviation between the interpolated and initial values was ± 1.7 km, and the area between the isolines in the resulting map was taken as 5 km. After subtracting the depths of the ocean and the introduction of corrections for the height of the observation on land, the map of depth values to the M discontinuity was transformed into the Circumpolar Arctic crustal thickness Map (Fig. 12).

The compiled crustal thickness Map of the Circumpolar Arctic differs from the global model CRUST2.0 available for this area (Laske et al. 2000) greatly because, first, significantly more new seismic data were used for its compilation, and, second, global data averaging was not used in this work. As can be seen from the figure, the crustal thickness in the Circumpolar Arctic changes quite significantly: from 5 to 10 km within the Norwegian-Greenland and the Eurasian ocean basins to 55–60 km in Scandinavia and in the Urals. Areas with oceanic and continental crust are identified on the map of crustal thickness rather confidently and the size and configuration of individual lateral variations of the thickness are quite comparable to the size of the regional geological structures. So, the new map is not only suitable for the introduction of corrections during seismological and planetary geophysical constructions, but it can also be used for tectonic constructions in the Arctic basin.

The map of Arctic basin crustal thickness generally shows the structure of the area of the Central Arctic uplifts including the Lomonosov Ridge, the system of Mendeleev-Alpha rises, and separating them Podvodnikov-Makarova basins, Chukchi Borderland, and the Northwind Ridge. Results of the most recent Russian and foreign deep seismic surveys ("Transarctic-1989–92", "Arctic-2000", "Arctic-2005", "Arctic-2007", "Lorita-2006", "Arta-2008", "Arctic-2012") (Jackson et al. 2010; Funck et al. 2011; Lebedeva-Ivanova et al. 2006, 2011; Poselov et al. 2011a; Kashubin et al. 2016, 2018a) were used for the map of crustal thickness of the Central Arctic uplifts and areas of their intersection with structures of the Eurasian and North American continental margins.

Seismic data indicate that the area of the Central Arctic uplifts has the lowest degree of destructive transformations of the continental crust. What we see is its thinning caused by rifting continental crust transformations while preserving vertical

layering. Thus, in the Lomonosov Ridge, the crustal thickness is 17–19 km with an equal ratio of the upper and lower crust. In the Podvodnikov-Makarov Basin, the crustal thickness varies widely: from 19 to 21 km in the southern part of the Podvodnikov Basin to 7–8 km in the northern part of the Makarov Basin. In the Mendeleev Rise, the total thickness of the crust is 31–34 km with upper crust varying in the range of 4–7 km. The available geological and geophysical data (Grantz et al. 2011a, b; Kabankov et al. 2004) indicate that the Northwind Ridge and the Chukchi Borderland are relatively shallow submerged ledge of the continental crust.

Thus, the area of the Central Arctic uplifts and the Eurasian and North American continental margins represent an ensemble of continental geologic structures with the common history of geological evolution. Subdivision of the ensemble into shelf and deepwater parts is a result of neotectonic submergence of the central Arctic Basin. With the present level of knowledge of the Arctic Basin, there are no relevant data concerning the structural isolation of the Central Arctic uplifts area from the adjacent continental margins.

Map of crustal types in the Arctic. Through the lens of current views, based primarily on geophysical data, oceanic and continental crust naturally differ in their basic physical properties including density, thickness, age, and chemical composition. The continental crust is characterized by average thickness of about 40 km, density of 2.84 g/cm^3, and the average age of 1500 Ma, whereas the oceanic crust's average thickness is 5–7 km, density is about 3 g/cm^3 and it is younger than 200 Ma all over the Arctic area. There is a common view that oceanic crust consists mainly of tholeiitic basalts formed from quickly cooling magma, whereas the continental crust, which has a long history of development, is characterized by more felsic composition (Blyuman 2011).

Deep seismic studies conducted in different regions of the world, continents and oceans make it possible to identify the main patterns in the velocity model of the crust and their variability depending on tectonic setting and history of development of the Arctic region. Typical features of velocity models of the crust, their relation to the tectonic structure and history of development of various geological structures have been widely discussed (Belousov and Pavlenkova 1989; Meissner 1986; Mueller 1977; Mooney 2007; McNutt and Caress 2007, etc.). Some of the researchers made attempts to distinguish main types of crust. They were based on crustal thickness data and seismic wave velocities in the crust. According to these parameters, typical features of the continental crust are: great thickness (usually over 25–30 km) and the presence in the consolidated crust of thick (up to 10 km or more) upper layer with the P-wave velocity of 5.8–6.4 km/s. This layer is often referred to as "granite gneiss". The oceanic crust is thin (typically less than 8–10 km); the granite gneiss layer is lacking in it, and it is almost entirely represented by rocks with seismic wave velocities of more than 6.5 km/s.

Detailed seismic surveys covering active and passive continental margins and oceanic uplifts have shown that in addition to typical continental and oceanic crust, the crust with intermediate parameters is also common. It is characterized by the thickness of 10 to 30 km and the "granite-gneiss" layer in it is significantly reduced
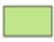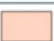
or completely absent. The assignment of this crust to the oceanic or continental type is often ambiguous, so some researchers have even suggested that this crust should be defined as a separate type—interim or transitional crust (Belousov and Pavlenkova 1989), but most researchers suggest using in tectonic constructions two main genetic types of the Earth's crust—continental and oceanic.

Differences in the composition of the oceanic and continental crust are most evident when comparing their velocity models constructed from data of multi-wave seismic surveys. It turns out that the oceanic and continental crust differ greatly in ratios of P-waves and S-waves (Vp/Vs) (Hyndman 1979). In the consolidated continental crust, the Vp/Vs rarely exceeds 1.75, while in the second and third oceanic layers, Vp/Vs is 1.85–1.90. At the same time, in the sediment layer and in the oceanic and continental crusts, Vp/Vs varies widely, generally exceeding values of 1.9–2.0. These data are confirmed by numerous DSS studies in oceans performed by bottom stations providing registration of S-waves and converted waves (Breivik et al. 2005; Ljones et al. 2004; Mooney 2007, etc.). Taking into account the relation between the total content of silica in crystalline rocks and the Vp/Vs ratio (Aleinikov et al. 1991), these differences seem quite natural and evidence different basicity of the oceanic and continental crust. Thus, the generalized data on the structure and velocity parameters of the oceanic and continental crust can be represented as follows (Table 2).

As can be seen from the table, in contrast to the continental crust, the oceanic crust lacks upper (felsic) crust that is recorded most reliably from Vp/Vs ratio. It is more difficult to distinguish the oceanic crust from the continental crust based on absolute P-wave velocity values because of significant overlap of P-wave velocity values in the second oceanic layer and in the upper part of the consolidated continental crust. However, velocities in the second oceanic layer rarely reach values of more than 6.0 km/s, so this problem can be partly solved without information about Vp/Vs.

Table 2 Generalized model of the structure and velocity parameters of the oceanic and continental crusts (Kashubin et al. 2013, 2018b)

Generalized model of the structure and velocity parameters of the oceanic and continental crusts (Kashubin et. al., 2013)

Oceanic crust			Vp, km/s	Continental crust		
Main layers		Vp/Vs		Vp/Vs		Main layers
Water		–	1.45–1.50	–		Water
Sediments		2.1–2.5	2.0–4.5	2.1–2.5		Sediments
Second layer of oceanic crust		1.8–2.2	4.2–6.0	1.8–2.2		Basalts, interbedded with sediments / folded meta-morphic layer
–		–	5.8–6.4	1.69–1.73		Upper crust
–		–	6.3–6.7	1.73–1.75		Mid crust
Third layer of oceanic crust		1.81–1.87	6.6–7.2	1.75–1.77		Lower crust
Crust-mantle layer		1.78–1.84	7.2–7.6	1.78–1.84		Crust-mantle layer

Following the generally accepted characteristics of seismic velocity for the oceanic and continental crust (Table 2), following types of the Earth's crust can be distinguished in the Circumpolar Arctic (Fig. 13; Table 3) (Kashubin et al. 2013; Petrov et al. 2016).

Normal oceanic crust (type 1, Fig. 13), which includes normal oceanic crust of spreading basins (less then 10 km thick) and thickened crust of oceanic plateaus and
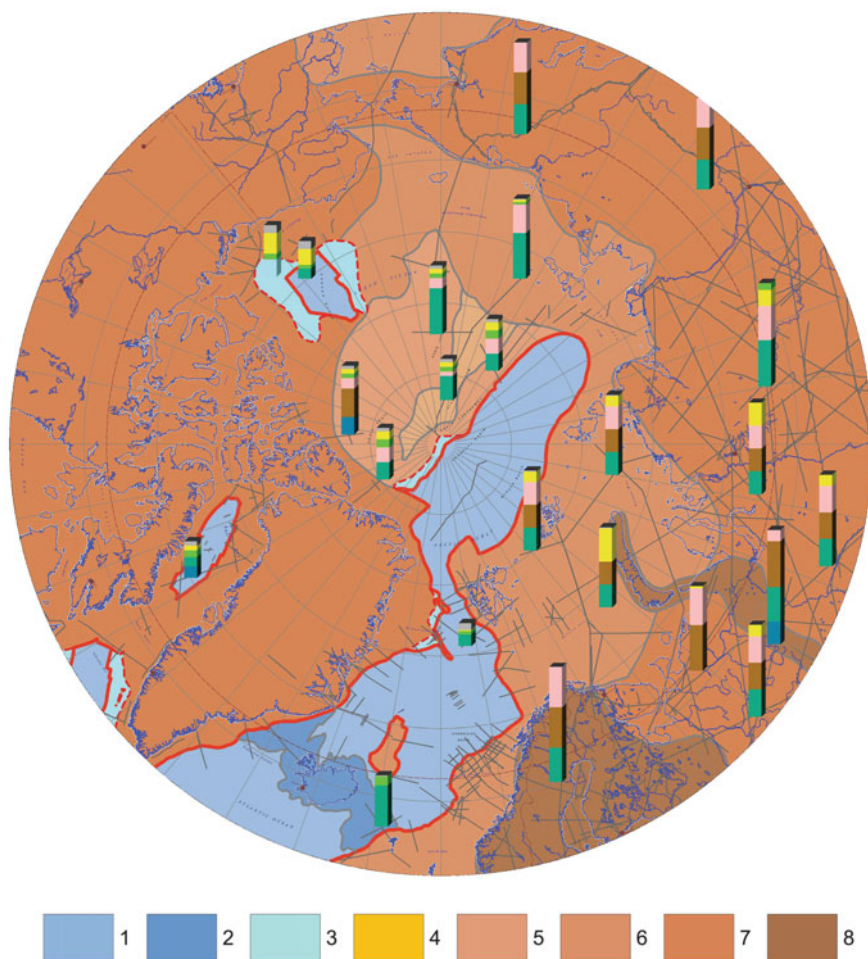
Fig. 13 Map of crust types in the circumpolar Arctic (Kashubin et al. 2013; Petrov and Pubellier 2019). 1–2—oceanic crust: 1—normal crust of spreading basins, 2—thickened crust of oceanic plateaus and hot spots; 3—reduced (transitional to oceanic) crust of deep depressions; 4–8—continental crust: 4—thinned crust of submarine rifts and basins, 5—thinned crust of submarine ridges and rises, 6—thin crust of shelf seas, 7—normal crust of platforms and fold systems, 8—thick crust of shields and collision areas. Gray lines show seismic-refraction and DSS profiles; type columns of the crust from seismic data are the same as in Table 3

Table 3 Type columns of the crust of circumpolar Arctic structures based on seismic profiles in accordance with generalized velocity parameters given in Kashubin et al. (2013), Petrov and Pubellier (2019)
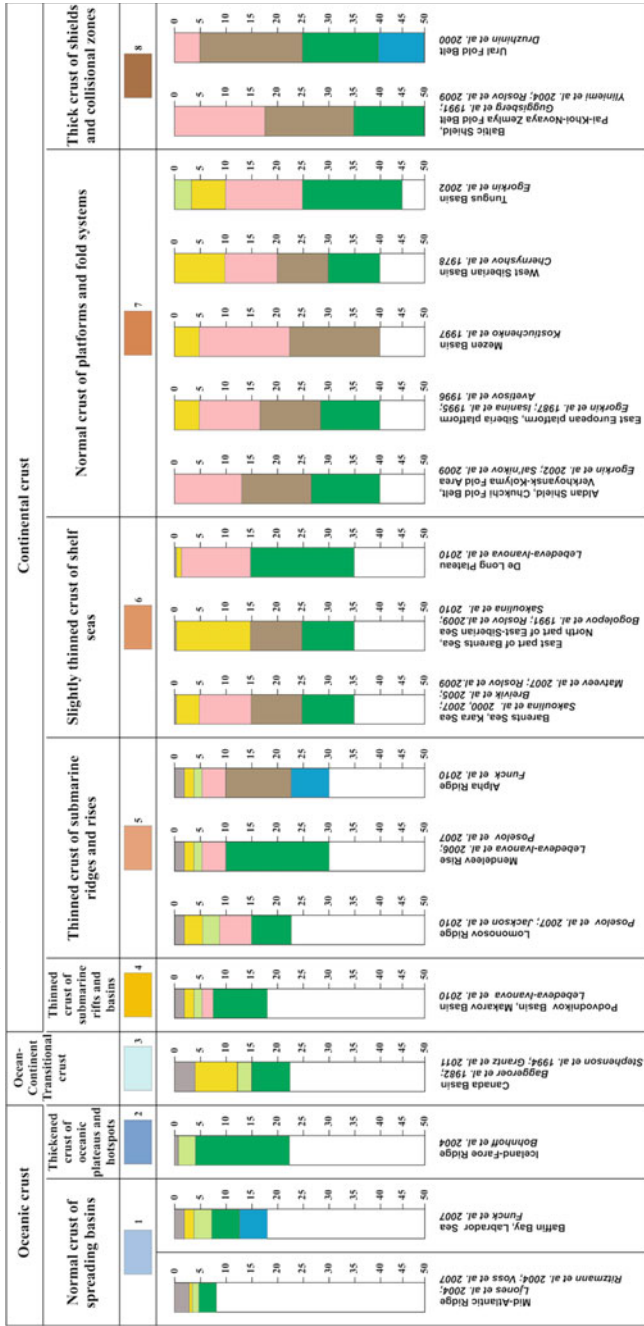
hot zones (about 15–30 km thick, type 2), is common in the Circumpolar Arctic, in the Norwegian-Greenland, Eurasian, and Baffin-Labrador ocean basins (Bohnhoff and Makris 2004; Ljones et al. 2004; Funck et al. 2007). It includes two oceanic layers overlain by thin sediments (Ljones et al. 2004, etc.). In the Baffin-Labrador ocean basin, the crust thickens to 15–17 km mainly due to magmatic underplating in the lower crust (Thybo and Artemieva 2013), where P-wave velocity reaches 7.4–7.6 km/s (Funck et al. 2007). Thick (more than 20 km) crust of oceanic plateaus and hot zones also forms the Greenland-Iceland-Faroe Ridge (Bohnhoff and Makris 2004; Ljones et al. 2004), which apparently continues to the west of the southern Greenland via the Baffin Bay and forms a single zone of thickened crust—the Baffin Island-Greenland-Iceland-Faroe Islands Ridge (Artemieva and Thybo 2013). Main increase in the thickness is a result of the third oceanic layer, whose thickness reaches more than 15 km thick.

Transitional crust. Nature of the thinned crust of deep rift basins (type 3, Fig. 13) is a question under discussion. E.g., the crust thickness in the Canada Basin is more than 10–15 km, and the single-layer crystalline crust with the thickness of less than 10 km and Vp of 6.8–7.2 km/s is typical of the third oceanic layer (Mair and Lyons 1981; Baggeroer and Falconer 1982; Stephenson et al. 1994). Based on the seismic velocity structure, it is traditionally believed that the Canada Basin was formed on the oceanic crust (e.g., Mooney 2007; Grantz et al. 2011a).

Nevertheless, the comparison of velocity models in the crust of the Canada Basin and the South Barents Basin (Faleide et al. 2008), as well as the Caspian Basin (Volvovsky and Volvovsky 1988) shows that the depth-velocity models are very similar whereas the nature of the crystalline crust (oceanic and continental) is viewed differently by different researchers. One viewpoint is that these depressions have oceanic crust, which forms so-called "oceanic crust windows" on the shelf and continents (Mooney 2007; Grantz et al. 2011). An alternative interpretation (Volvovsky and Volvovsky 1988) suggests that thick sedimentary strata in these depressions cover the reduced (thinned) continental crust that lacks the upper (or intermediate) layer. In our approach, we do not take any side in the dispute (continental or oceanic origin), but, instead, we consider the crust of the Canada Basin transitional. It should be noted that the P-wave velocity models are not enough to understand the nature of the crystalline crust in deep rift basins. Further studies using data from S-waves and deep drilling will provide substantial arguments in favor of a particular interpretation.

Marine continental crust. In contrast to the oceanic crust, continental crust in the Circumpolar Arctic is studied based on a large number of deep seismic sounding(DSS) profiles (for regional reviews see Faleide et al. 2008; Drachev et al. 2010; Artemieva and Thybo 2013; Cherepanova et al. 2013, and in the publications that are referred to in these papers; Russian publications: Volvovsky and Volvovsky 1975; Druzhinin 1983; Druzhinin et al. 2000; Druzhinin and Karmanov 1985; Egorkin 1991; Egorkin et al. 1980, 1988, 2002; Isanina et al. 1995; Poselov et al. 2007, 2010, 2011a, b; Roslov et al. 2009; Sharov et al. 2010; Ivanova et al. 2006, etc.).

These studies resulted in the identification of the thin crust of *submarine rifts and basins* as a separate type of continental crust (type 4, Fig. 13). An example of this type of the crust is the Podvodnikov-Makarova Basin. According to the interpretation of the DSS profiles obtained during expeditions Transarctic-89–91, Transarctic-92, Arctic-2000 (Poselov et al. 2011a, b; Lebedeva-Ivanova et al. 2011), seismic records of Pg-waves are typical of the crustal complex with Vp = 6.1–6.3 km/s at the top of the consolidated crust, which is typical of the continental crust. Therefore, in spite of low thickness typical of the oceanic crust (12–15 km), the crust in this basin is interpreted as thinned continental crust.

Thinned crust is typical of *submarine ridges and rises*: the Lomonosov Ridge and the Alpha-Mendeleev Rise (type 5, Fig. 13), as it can be seen from interpretations of Russian seismic profiles Arctic-2000, Arctic-2005, Arctic-2007 and Arctic-2012 in the Lomonosov and Mendeleev structures (Lebedeva-Ivanova et al. 2006; Poselov et al. 2011a, b; Kashubin et al. 2016, 2018a), seismic experiment LORITA in the Lomonosov Ridge (Jackson et al. 2010), and the seismic profile obtained by seismic refraction in the Alpha Ridge (Funck et al. 2011). According to these interpretations, the crustal thickness of the ridges varies greatly from 15–17 km to 30–35 km (Artyushkov 2010). The crystalline crust is represented by slightly thinned upper crust as compared to the normal continental crust and the thick lower crust; thick crust-mantle complex was recorded under the Alpha Ridge where the normal lower crust is apparently lacking (Funck et al. 2011).

The continental nature of the crust in the Lomonosov Ridge has been recognized by most researchers of the Arctic, while the nature of the crust in the Alpha-Mendeleev Ridge has long been a subject of debate. In particular, Funck et al. (2011) proposed to classify the Alpha Ridge crust as volcanic crust similar to hot zone crust such as that of the Greenland-Iceland-Faroe Ridge. However, the results of Russian studies (Lebedeva-Ivanova et al. 2006; Poselov et al. 2011a, b; Kashubin et al. 2016, 2018a) show that main stratified sedimentary complexes, the intermediate complex, and crystalline complexes of the Earth's crust are traced to the Mendeleev Rise from the shelf of the East Siberian Sea. Thus, Mendeleev Rise should be considered as the continuation of the Eurasian continent (type 5, Fig. 13). Although the relationship between the crustal structures of the Alpha and Mendeleev ridges is still not clear. Similarities between the Vp velocity models and depth models suggest that the crust both of the Lomonosov Ridge and the Alpha-Mendeleev Ridge is thinned continental crust. It should be noted that the general thinning of the Alpha Ridge crust is somewhat veiled due to the presence of thickened lower crust and may result from intraplate magmatism related to LIP (magmatic underplating) (Thybo and Artemieva 2013).

Shelf seas' crust (type 6, Fig. 13) occupies almost all shallow-water areas of the Arctic Ocean; it is somewhat thinned continental crust characterized by very similar thickness (about 35 km) but highly variable structure. Sedimentary cover thickness varies widely from a few meters near islands up to 15 km or more in the East Barents and North Chukchi troughs. The crystalline crust structure on the shelf is usually three-layered as in most of the Barents and Kara seas (Breivik et al. 2005); however, two-layer structure was recorded in the East Barents Basin and the northern part of the East Siberian Sea (Roslov et al. 2009; Sakoulina et al. 2000; Ivanova et al. 2006)

where the upper crust is apparently lacking, and in the De Long plateau where the intermediate crust is lacking on the graphs of seismic velocities (Lebedeva-Ivanova et al. 2011).

Normal continental crust of platforms and fold systems (types 7 and 8, Fig. 13) occupies most of the Circumpolar Arctic covering almost the entire land area. Thickness, internal structure and composition of the crust vary considerably, which reflects its complex tectonic evolution. Detailed information on the crust structure and tectonic evolution of the European continent, Greenland, Iceland, the North Atlantic region, the West Siberian Basin and the Siberian Platform can be found in recent reviews published by Artemieva and Thybo (2013) and Cherepanova et al. (2013).

Thus, different types of the Circumpolar Arctic crust form a global structure, one of the centers of which is the area of Central Arctic Uplifts including the Lomonosov Ridge and the system of Alpha-Mendeleev rises with separating them Podvodnikov-Makarov Basin. The zone of volume strain, areas of intraplate basic magmatism (Cretaceous HALIP Province) (Filatova and Hain 2009; Mukasa et al. 2015), and submergences of shallow-water volcanic structures to bathyal (up to 3.5 km) depths (Brumley 2009) in the absence of pronounced spreading structures with typical linear magnetic anomalies do not allow structures of the Central Arctic Uplifts to be assigned to the oceanic type. It is assumed that this type of the crust could be formed by processes of basification and eclogitization of the normal continental crust (Petrov et al. 2016).

4 Geotransect Across the Circumpolar Arctic

The 7600-km geotransect across the Circumpolar Arctic has been created along the line, which unites following DSS seismic geotraverses: 1-EB-1-AR—"Transarctica-89-92"—"Arctic-2000"—"Arctic-2005"—5-AR-2-DV (5400 km) from Petrozavodsk in the west to Magadan in the east (Berzin et al. 1998; Kashubin et al. 2018c; Sakoulina et al. 2011, 2016; Salnikov 2007; Lebedeva-Ivanova et al. 2006, 2011) (Figs. 14 and 15). It includes velocity and density models and geological and geophysical sections. The sedimentary cover bottom (B), the upper crust bottom, the upper crust roof, the Earth's crust bottom—Moho discontinuity are shown in the geotransect. For the determination of boundaries, velocity parameters (Vp) are indicated: sedimentary cover, 2.0–4.5 km/s; upper crust, 5.8–6.4 km/s; intermediate crust, 6.3–6.7 km/s; lower crust, 6.6–7.2 km/s; upper mantle, 7.8–8.4 km/s. The geological-geophysical section crosses the Eurasian oceanic basin with the Eocene, Oligocene-Early Miocene and Late Miocene—Quaternary oceanic crust (less than 10 km thick), the Baltic Shield and fold areas of northeastern Russia.

Passive continental margins of the Eurasian oceanic basin (Barents-Kara Basin, Laptev Rift and the submerged Amerasian Basin with the Lomonosov Ridge and the Alpha-Mendeleev Rise) have thin crust. The rise is thought of as a block of a three-layer Early Precambrian crust up to 30 km thick with Late Precambrian and Paleozoic
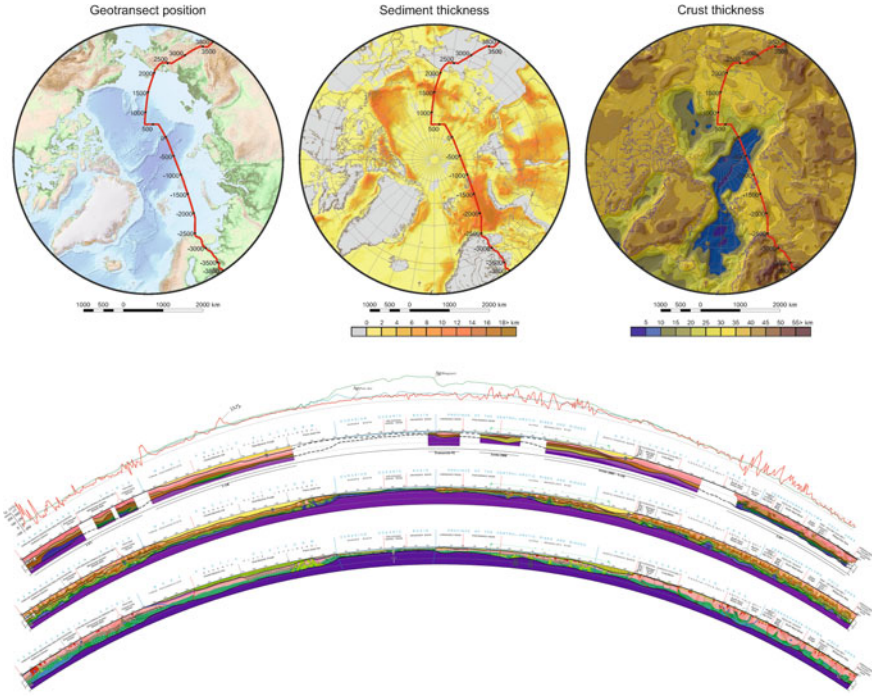
Fig. 14 Geotransect across the circumpolar Arctic
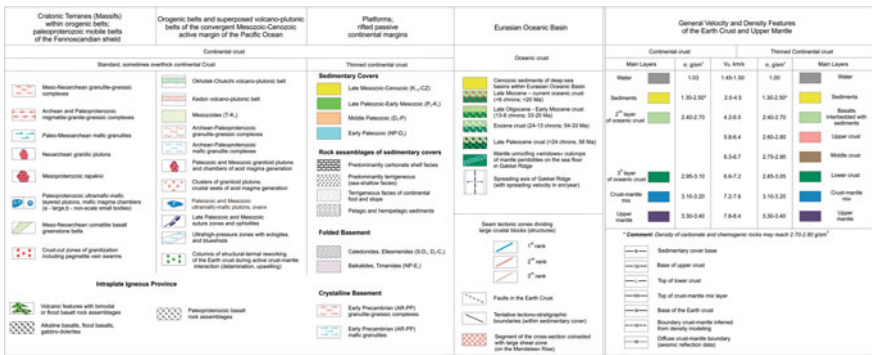
Fig. 15 Legend for the combined geological and geophysical section in Fig. 14

sedimentary cover under Late Mesozoic and Cenozoic sediments and basalts of the HALIP. Limits and deep structure of the Anyui-Chukotka and Verkhoyansk-Kolyma regions are indicated within the limits of cross-sections. The Karelian granite-diabase region has thick (up to 45 km) three-layer crust and crust-mantle lenses of high density and velocity indicative of underplating and mafic-ultramafic magmatism.

The Alpha-Mendeleev Rise has speed and density parameters, which suggest that this is a tectonic block with a three-layer crust 30 km thick. The crust thickness is maximum for the Central Arctic uplifts area. At the bottom of the lower crust, there are local areas of high speed and high density, similar to the crust-mantle complex. This suggests the occurrence of mafic magma chambers beneath the vast HALIP basaltic areal, interpreted from the typical magnetic field.

Alpha Rise basalts north of the geotransect date back to the Cretaceous (82 Ma). It is believed that the supracrustal complex of Late Precambrian and Paleozoic sediments occurs in the acoustic basement of the Mendeleev Rise. The North Chukchi Basin is located within the Anyui-Chukchi fold area.

Gneiss granite fragments raised from the seabed using a piston sampler (sampling of the Geophysicists Spur slope) also showed the age (1139 ± 15, 688 ± 5, 48.7 ± 4, 407.5 ± 5.1 Ma) younger than granite samples on the Mendeleev Rise.

Structural similarity of the Alpha-Mendeleev Rise crust and the Karelian granite-diabase area suggests the presence of Early Precambrian tectonic blocks in the rise basement. This assumption is confirmed by isotopic dating of the seabed rock samples obtained during the Arctic-2000 and Arctic-2005 expeditions. The granite-gneiss fragments taken out and raised by box or piston samplers from the Mendeleev Rise, showed the age of 2.7, 2.6, 2.3 and 1.9 Ga; gabbro-dolerite fragments showed the age of 790 ± 20 Ma and 2650 Ma (from allogenic zircon grains). Paleozoic sandstone and quartzite (430–300 Ma) from the Mendeleev Rise also contain Archean (3.1 Ga) detrital zircons indicating the participation of Early Precambrian sources.

The Laptev Sea part of the Lomonosov Ridge, crossed by the geotransect, is characterized by two-layer structure and thinner (about 25 km) crust. The velocity and density of the lower crust is noticeably lower than that of the Mendeleev Rise. Main parameters of the consolidated crust of the Lomonosov Ridge are similar to the thin crust of orogenic belts in northeastern Russia.

References

Aleinikov AL, Nemzorov NI, Kashubin SN (1991) Rock type determination from seismic data. Author's certificate No 1642416 A1 cl. G 01 V1/30 (in Russian)

Artemieva IM, Thybo H (2013) EUNAseis: A seismic model for Moho and crustal structure in Europe, Greenland, and the North Atlantic region. Tectonophysics 609:97–153. https://doi.org/10.1016/j.tecto.2013.08.004

Artyushkov EV (2010) Continental crust in the Lomonosov Ridge, Mendeleev Ridge, and the Makarov basin. The formation of deep-water basins in the Neogene. Russ Geol Geophys 51(11):1179–1191. https://doi.org/10.1016/j.rgg.2010.10.003 (in Russian)

Baggeroer AB, Falconer R (1982) Array refraction profiles and crustal models of the Canada Basin. J Geophys Res 87:5461–5476

Belousov VV, Pavlenkova NI (1989) Types of the Earth's crust of Europe and North Atlantic. Geotectonics 3:3–14 (in Russian)

Berzin RG, Zamozhnaya NG, Kulakov SI et al (1998) Seismological model of the Earth's crust along the northern part of the I-EB profile. In: Mitrofanov FP, Shary NV (eds) Seismological model of the lithosphere of Northern Europe; Apatity: KSC RAS, Part 1, pp 93–109 (in Russian)

Blyuman BA (2011) Earth's crust of oceans. Based on data of international programs for deep-water drilling in the World Ocean. VSEGEI Publishing House, St. Petersburg, p 344 (in Russian)

Bohnhoff M, Makris J (2004) Crustal structure of the southeastern Iceland-Faeroe Ridge (IFR) from wide aperture seismic data. J Geodyn 37:233–252

Breivik AJ, Mjelde R, Grogan P, Shimamura H, Murai Y, Nishimura Y (2005) Caledonide development off shore-onshore Svalbard based on ocean bottom seismometer, conventional seismic and potential field data. Tectonophysics 401:79–117

Brumley K (2009) Tectonic geomorphology of the Chukchi Borderland: constraint for tectonic reconstruction models. Thesis for the degree of master of science, University of Alaska, Fairbanks, p 116

Cherepanova Yu, Artemieva IM, Thybo H, Chemia Z (2013) Crustal structure of the Siberian Craton and the West Siberian Basin: an appraisal of existing seismic data. Tectonophysics 609:154–183

Demenitskaya RM (1967) The Earth's crust and mantle. Moscow, Nedra, p 280 (in Russian)

Divins DL (2008) NGDC total sediment thickness of the World's oceans and marginal seas. http://www.ngdc.noaa.gov/mgg/sedthick/sedthick.html

Drachev SS, Malyshev NA, Nikishin AM (2010) Tectonic history and petroleum geology of the Russian Arctic Shelves: an overview. In: Vining BA, Pickering SC (eds) Petroleum geology: from mature basins to new frontiers. In: Proceedings of the 7th petroleum geology conference geology social, vol 7. London, pp 591–619

Druzhinin VS (1983) Deep structure characteristic of the West Siberian Plate along the DSS Khanty-Mansiysk profile. Geol Geophys 4:3–9 (in Russian)

Druzhinin VS, Karmanov AB (1985) Study of the crustal structure in the North-Western part of the West Siberian Plate. Sov Geol 9:39–48 (in Russian)

Druzhinin VS, Karetin YS, Kashubin SN (2000) Deep geological mapping of the Ural region from DSS data. Reg Geol Metallogeny 10:152–161 (in Russian)

Egorkin AV (1991) Crustal structure from seismic geotraveses. In Belousov VV, Pavlenkova NI (eds) Deep structure of the USSR. Nauka, Moscow, pp 118–135 (in Russian)

Egorkin AV, Chernyshov NM, Danilov EG et al (1980) Regional cross section across the north of the Asian continent, the Vorkuta-Tiksi profile. Seismic Models of the Lithosphere of Main Geological Structures in the USSR. Nauka, Moscow, pp 61–67 (in Russian)

Egorkin AV, Zyuganov SK, Pavlenkova NA, Chernyshev NM (1988) Results of lithospheric structure investigations along profiles in Siberia. Geol Geophys 5:120–128 (in Russian)

Egorkin AV, Akinshina LV, Artemenko LS et al (2002) Crystalline crust structure in Siberia along the Khanty-Mansiysk—Lena Line. Explor Prot Mineral Res 2:33–35 (in Russian)

Erinchek YuM, Milstein ED, Egorkin AV, Verba VV (2007) Moho structure in Russia and adjacent water areas. Models of the Earth's crust and upper mantle from results of deep seismic profiling. In: Proceedings of the international scientific and practical seminar. VSEGEI, St. Petersburg, pp 241–244 (in Russian)

Faleide JI, Filippos T, Asbjorn JB, Mjelde R, Ritzmann O, Engen O, Wilson J, Eldholm O (2008) Structure and evolution of the continental margin off Norway and the Barents sea. Episodes 31:82–91

Filatova NI, Hain VE (2009) Structures of the Central Arctic and their relationship with the Mesozoic Arctic plume. Geotectonics 6:24–51 (in Russian)

Funck T, Jackson HR, Louden KE, Klingelhofer F (2007) Seismic study of the transform-rifted margin in Davis Strait between Baffin Island (Canada) and Greenland: what happens when a plume meets a transform. J Geophys Res 112:B04402

Funck T, Jackson HR, Shimeld J (2011) The crustal structure of the Alpha Ridge at the transition to the Canadian Polar Margin: results from a seismic refraction experiment. J Geophys Res 116:B12101. https://doi.org/10.1029/2011JB008411

Gaina C, CAMP-GM group (2007) Circum-Arctic mapping project: new magnetic and gravity anomaly maps of the Arctic. ICAM V, Tromsø, Norway

Gaina C, Saltus R, Harrison C, St-Onge M, Alvey A, Kusznir N (2008) Circum-Arctic mapping project: new magnetic anomaly map linked to the geology of the Arctic. Eos Trans AGU 89(53), Fall Meet. Suppl., Abstract GP53B-04

Gaina C, CAMP-GM working group (2009) Gravity anomaly map of the Arctic. Geological Survey of Norway

Gaina C, Werner SC, the CAMP-GM Group (2010) Circum-Arctic mapping project—gravity and magnetic maps (CAMP-GM). NGU rapport 2009.010.(http://www.ngu.no/upload/Publikasjoner/Rapporter/2009/2009_010.pdf)

Gaina C, Werner SC, Saltus R, Maus S, the Camp-GM GROUP (2011) Circum-Arctic mapping project: new magnetic and gravity anomaly maps of the Arctic. Arctic petroleum geology. Geological Society, vol 35. London, Memoirs, pp 39–48

Gautier DL, Bird KJ, Charpentier RR, Grantz A, Houseknecht DW, Klett TR, Moore TE, Pitman JK, Schenk CJ, Schuenemeyer JH, Sörensen K, Tennyson ME, Valin ZC, Wandrey CJ (2011) Chapter 9. Oil and gas resource potential north of the Arctic Circle. Arctic petroleum geology, vol 35. Geol Soc, London, Mem, pp 151–161

Grad M, Tiira T, working group (2007) The Moho depth of the European plate. http://www.seismo.helsinki.fi/mohomap, http://www.igf.fuw.edu.pl/mohomap2007

Gramberg IS, Verba VV, Verba ML, Kos'ko MK (2001) Sedimentary cover thickness map—sedimentary basins in the Arctic, vol 69. Polarforschung, pp 243–249

Grantz A, Hart PE, Childers VA (2011a) Geology and tectonic development of the Amerasia and Canada Basins, Arctic Ocean. In: Spencer AM, Embry AF, Gautier DL, Stoupakova AV, Sörensen K (eds) Arctic petroleum geology, vol 35. Geol. Soc., London, Mem, pp 771–799

Grantz A, Scott RA, Drachev SS, Moore TE, Valin ZC (2011b) Sedimentary successions of the Arctic Region (58–64 to 90 degrees N) that may be prospective for hydrocarbons. Arctic Petrol Geol Geol Soc London Mem 35:17–37

Hemant K, Thebault E, Mandea RD, Maus S (2007) Magnetic anomaly map of the world: merging satellite, airborne, marine and ground-based magnetic data sets, Earth Planet. Sci Lett 260:56–71

Hyndman RD (1979) Poisson's ratio in the oceanic crust—a review. Tectonophysics 59:321–333

Isanina EV, Sharov NV et al (1995) Atlas of regional seismic profiles of the European North of Russia. Rosgeofizika, St. Petersburg (in Russian)

Ivanova NM, Sakoulina TS, Roslov YuV (2006) Deep seismic investigation across the Barents-Kara region and Novozemelskiy Fold belt (Arctic Shelf). Tectonophysics 420:123–140

Jackson HR, Dahl-Jensen T, the LORITA working group (2010) Sedimentary and crustal structure from the Ellesmere Island and Greenland continental shelves onto the Lomonosov Ridge, Arctic Ocean. Geophys J Int 182:11–35

Kabankov VY, Andreeva IA, Ivanov VI, Petrova VI (2004) About geotectonic nature of the system of Central Arctic morphostructures and geological significance of bottom sediments in its definition, vol 6. Geotectonics, pp 33–48 (in Russian)

Kashubin SN, Petrov OV, Androsov EA, Morozov AF, Kaminsky VD, Poselov VA (2011) Map of crustal thickness in the circumpolar Arctic. Reg Geol Metallogeny 46(2011):5–13 (in Russian)

Kashubin SN, Pavlenkova NI, Petrov OV, Milshtein ED, Shokalsky SP, Erinchek YuM (2013) Crust types in the circumpolar Arctic. Reg Geol Metallogeny 55:5–20 (in Russian)

Kashubin SN, Petrov OV, Androsov EA, Morozov AF, Kaminsky VD, Poselov VA (2014) Crustal thickness in the circum Arctic. In: ICAM VI: proceedings of the international conference, pp 1–17

Kashubin SN, Petrov OV, Artemeva IM, Morozov AF, Vyatkina DV, Golysheva YuS, Kashubina TV, Milshtein ED, Rybalka AV, Erinchek YuM, Sakoulina TS, Krupnova NA (2016) Deep structure of crust and the upper mantle of the Mendeleev Rise on the Arktic-2012 DSS profile. Reg Geol Metallogeny 65(2016):16–35 (in Russian)

Kashubin SN, Petrov OV, Artemieva IM, Morozov AF, Vyatkina DV, Golysheva YuS, Kashubina TV, Milshtein ED, Rybalka AV, Erinchek YuM, Sakoulina TS, Krupnova NA, Shulgin AA (2018a) Crustal structure of the Mendeleev rise and the Chukchi Plateau (Arctic Ocean) along the Russian

wide-angle and multichannel seismic reflection experiment "Arctic-2012". J Geodyn 119:107–122

Kashubin SN, Petrov OV, Milshtein ED, Androsov EA, Vinokurov IYu, Shokalsky SP (2018b) Crustal types of Central and Northeast Asia, Far Eastern and Arctic continent–ocean transition areas. Reg Geol Metallogeny 73:6–18 (in Russian)

Kashubin SN, Petrov OV, Milshtein ED, Vinokurov IYu, Androsov EA, Golysheva YuS, Efimova NN, Yavarova TM, Morozov AF (2018c) The structure of the Earth's crust of the junction zone of the Mendeleev Rise with the Eurasian continent (according to geophysical data). Reg Geol Metallogeny 74:5–18 (in Russian)

Kashubin SN, Petrov OV (eds) (2019) Shear and converted waves in marine deep seismic studies. In: Kashubin SN, Petrov OV (eds) VSEGEI Proceedings. New series, vol 360. VSEGEI, St. Petersburg, 155 p (in Russian)

Kenyon S, Forsberg R (2000) Gravity, geoid and geodynamics 2000, vol 123. International Association of Geodesy Symposia, pp 391–395

Kenyon S, Forsberg R, Coakley B (2008) New gravity field for the Arctic. EOS Trans AGU 89(32):1–2. https://doi.org/10.1029/2008EO320002

Kosygin YA (1975) Fundamentals of tectonic zoning: principles of Tectonic Zoning. Vladivostok. Far Eastern Scientific Center, Academy of Sciences of the USSR, pp 8–24 (in Russian)

Kunin NYa, Goncharova NV, Semenova GI et al (1987) Map of the mantle surface topography in Eurasia [map]. IPE Ac. Sci. USSR, Moscow, Ministry of Geology of the RSFSR (in Russian)

Laske G, Masters G (2010) A global digital map of sediment thickness. EOS Transactions American Geo pfisical Union, vol 78. F 483. http://igppweb.ucsd.edu/~gabi/sediment.html

Laske G, Masters G, Reif C (2000) CRUST 2.0: a new global crustal model at 2×2 degrees. http://igppweb.ucsd.edu/~gabi/rem.html

Lebedeva-Ivanova NN, Zamansky Yu Ya, Langnen AE, Sorokin MYu (2006) Seismic profiling across the Mendeleev Ridge at 82 °N evidence of continental crust. Geophys J Int 165:527–544

Lebedeva-Ivanova NN, Gee DG, Sergeyev MB (2011) Chapter 26 crustal structure of the East Siberian continental margin, Podvodnikov and Makarov basins, based on refraction seismic data (TransArctic 1989–1991). In: Spencer, Embry, Gautier, Stoupakova and Sørensen (eds) Arctic petroleum geology, vol 35. Geological Society of London, pp 395–411

Litvinova TM, Kashubin SN, Petrov OV (2012a) Zoning of the circumpolar region after the potential fields character. Geophys Res Abstr. EGU2012–4436, EGU General Assembly, p 14

Litvinova TM, Petrov OV, Kashubin SN, Erinchek YM, Milshteyn ED, Shokalsky SP, Glebovsky VYu, Chernykh AA (2012b) Arctic tectonic provinces from gravity and magnetic data. In: 34th international geological congress (abstracts), 5–10 August 2012. Brisbane, Australia, pp 16–19

Ljones F, Kuwano A, Mjelde R, Breivik A, Shimamurac H, Murai Y, Nishimura Y (2004) Crustal transect from the North Atlantic Knipovich Ridge to the Svalbard Margin west of Hornsund. Tectonophysics 378:17–41

Mair JA, Lyons JA (1981) Crustal structure and velocity anisotropy beneath the Beaufort sea. Can J Earth Sci 18:724–741

Maus S, Luehr H, Martin R, Hemant K, Balasis G, Ritter P, Claudia S (2007) Fifth-generation lithospheric magnetic field model from CHAMP satellite measurements. Geochem Geophys Geosyst 8:Q05013. https://doi.org/10.1029/2006GC001521

Maus S, Yin F, Luhr H, Manoj C, Rother M, Rauberg J, Michaelis I, Stolle C, Muller RD (2008) Resolution of direction of oceanic magnetic lineations by the sixth-generation lithospheric magnetic field model from CHAMP satellite magnetic measurements. Geochem Geophys Geosyst 9

McNutt M, Caress DW (2007) Crust and lithospheric structure—hot spots and hot-spot swells. In: Romanowicz B, Dziewonski A (eds) Treatise on geophysics, vol 1. Elsevier, pp 445–478

Meissner R (1986) The continental crust, a geophysical approach. International Geophys Series, vol 34. Academic Press, INC, Orlando, p 426

Mooney WD (2007) Crust and lithospheric structure—global crustal structure. In: Romanowicz B, Dziewonski A (eds Treatise on geophysics: seismology and structure of the earth, vol 1. Elsevier, pp 361–417

Mueller S (1977) A new model of the continental crust. Am Geophys Un Mon 20:289–317

Mukasa SB, Mayer LA, Aviado K, Bryce J, Andronikov A, Brumley K, Blichert-Toft J, Petrov OV, Shokalsky SP (2015) Alpha/Mendeleev Ridge and Chukchi Borderland 40Ar/39Ar geochronology and geochemistry: character of the first submarine intraplate lavas recovered from the Arctic Ocean. Geophys Res Abst 17, EGU2015–8291-2

Petrov OV, Pubellier M (eds) (2019) Scientific contributions to the Tectonic Map of the Arctic. (VSEGEI/CGMW). Paris: CGMW, 64 p

Petrov OV, Smelror M (eds) (2019) Tectonostratigraphic Atlas of the Arctic (eastern Russia and adjacent areas). Petrov OV, Smelror M (editor-in-chief), Kiselev EA, Morozov AF, Kazmin YuB, Kaminsky VD, Fedonkin MA (editorial board) SPb.: VSEGEI Publishing House, 136 p

Petrov OV, Smelror M (2015a) Cooperation of geological surveys of Arctic states to study the Arctic. Arctic J 1(13):22–28

Petrov OV, Smelror M (2015b) Uniting the Arctic frontiers—international cooperation on circum-Arctic geological and geophysical maps. Polar Rec 51(5):530–535. http://dx.doi.org/10.1017/S0032247414000667

Petrov OV, Smelror M, Morozov AF, Shokalsky SP, Kashubin SN, Artemieva IM, Sobolev NN, Petrov EO, Ernst RE, Sergeev SA (2016) Crustal structure and tectonic model of the Arctic region. Earth Sci Rev 154:29–71

Poselov VA, Avetisov GP, Kaminsky VD et al (2011a) Russian Arctic geotraverses. FGUP I.S. Gramberg VNIIOkeangeologia, St. Petersburg, 172 p (in Russian)

Poselov V, Butsenko V, Chernykh A, Glebovsky V, Jackson HR, Potter DP, Oakey G, Shimeld J, Marcussen C (2011b) The structural integrity of the Lomonosov ridge with the North American and Siberian continental margins. In: Proceedings of the international conference on arctic margins VI, Fairbanks, Alaska, May 2011, pp 233–258. http://www2.gi.alaska.edu/icam6/proceedings/web/

Poselov VA, Verba VV, Zholondz SM (2007) Crust typification in the Central Arctic uplifts, the Arctic Ocean. Geotectonics 4:48–59 (in Russian)

Poselov VA, Kaminsky VD, Ivanov VL, Avetisov GP, Butsenko VV, Trukhalev AI, Palamarchuk VK, Zholondz SM (2010) Crustal structure and evolution in the junction area of the Amerasian Subbasin uplifts and the East Arctic Shelf. Structure and history of the lithosphere evolution. Paulsen, Moscow, pp 599–637 (in Russian)

Poselov VA, Zholondz SM, Trukhalev AI et al (2012) Map of sedimentary cover thickness in the Arctic Ocean. In: Geological and geophysical characteristics of the lithosphere of the Arctic region. VNIIOkeangeologia, St. Petersburg, pp 8–14 (in Russian)

Ritzmann O, Maercklin N, Faleide JI, Bungum H, Mooney WD, Detweiler ST (2006) A 3D-geophysical model of the crust in the Barents sea region: model construction and basement characterization. 28th Seismic research review: ground-based nuclear explosion monitoring technologies, pp 229–237

Roslov YuV, Sakoulina TS, Pavlenkova NI (2009) Deep seismic investigations in the Barents and Kara Seas. Tectonophysics 472:301–308

Sakoulina TS, Telegin AN, Tikhonova IM, Verba ML, Matveev YuI, Vinnick AA, Kopylova AV, Dvornikov LG (2000) The results of deep seismic investigations on Geotraverse in the Barents Sea from Kola peninsula to Franz-Joseph land. Tectonophysics 329(1–4):319–331

Sakoulina TS, Verba ML, Kashubina TV, Krupnova NA, Tabyrtsa SN, Ivanov GI (2011) Comprehensive geological and geophysical studies along the reference profile 5-AR in the East Siberian Sea. Explor Preserv Miner Res 10:17–23 (in Russian)

Sakoulina TS, Kashubin SN, Petrov OV, Morozov AF, Krupnova NA, Dergunov NT, Razmatova AV, Tabyrtca SN, Kashubina TV, Yavarova TM (2016) Deep structure of the Earth's crust and the upper mantle of the North Chukchi basin of the DSS dream-line profile. Reg Geol Metallogeny 68(2016):52–65 (in Russian)

Salnikov AS (ed) (2007) The structure of the Earth's crust of the Magadan sector of Russia according to geological and geophysical data. Sat. scientific tr. Nauka, Novosibirsk, 173 p (in Russian)

Saltus RW, Gaina C (2007) Circum-Arctic map compilation in the international polar year. EOS 88:227

Sharov NV, Kulikov VS, Kulikova VV, Isanina EV, Krupnova NA (2010) Seismogeological characteristic of the Earth's crust in the south-eastern part of the Fennoscandian Shield (Russia). Geophys J 32:3–17

Smelror M, Petrov O, Larssen GB, Werner S (eds) (2009) Atlas—geological history of the Barents Sea. Geological survey of Norway, Trondheim, p 35

Stephenson RA, Coflin KC, Lane LS, Dietrich JR (1994) Crustal structure and tectonics of the southeastern Beaufort Sea continental margin. Tectonics 13:389–400

Suleimanov AK, Zamozhnyaya NG, Andryushchenko YuN, Lipilin AV (2007) Deep seismic studies based on reflected waves. In: Salnikov AS (Ex ed) Crustal structure of the Magadan sector of Russia from geological and geophysical data: collection of scientific papers. Nauka, Novosibirsk, pp 22–26 (in Russian)

Thybo H, Artemieva IM (2013) Moho and magmatic underplating in continental lithosphere. Tectonophysics 609:605–619

Volvovsky IS, Volvovsky BS (1975) Sections of the Earth's crust in the USSR from deep seismic sounding. Soviet radio, Moscow, p 258 (in Russian)

Volvovsky BS, Volvovsky IS (1988) Structures of continents with "granite-free" crust type. Problems of deep geology in the USSR. Moscow, pp 169–187 (in Russian)

Voronin AY (2007) Zoning of areas on the basis of artificial intelligence and image identification in nature management objectives. Abstract of thesis for the degree of doctor of technical sciences, Moscow, p 44 (in Russian)

Zolotov EE, Kostyuchenko SL, Rakitov VA (1998) Tomographic sections of the lithosphere Eastern European Platform. In: Mitrofanov FP, Sharov NV (eds) Seismological model of the lithosphere of Northern Europe: the Barents Region, vol 1. KSC RAS, Apatity, pp 71–79 (in Russian)

Arctic Sedimentary Cover Structure and Eastern Arctic Structure Maps

L. A. Daragan-Sushchova, E. O. Petrov, O. V. Petrov, and N. N. Sobolev

Abstract The section presents the FGUP VSEGEI seismic knowledge base in the form of a map. It contains data on regional seismic surveys (CDP, seismic refraction, DSS and many others). All the survey data were selected from open access and include activities from 1957 to the present. Data obtained by Russian companies (OAO MAGE, AO Sevmorgeo, OAO DMNG, etc.) and foreign expeditions (AWI, Healy, USGS, etc.) are shown. The correlation chart of the stratigraphic reference of reflecting horizons demonstrates an approach to substantiating the reflected horizon (RH) ages and the opinion of other major researchers and organizations in the region on this issue. A set of composite seismic lines (6 lines) intersecting major geological structures of the northeastern part of the Arctic is shown with a complete seismo-geological interpretation: correlation of reflected seismic horizons (RH) with all seismic recording disturbances (faults) and reservoir velocities observed in the wavefield. Based on seismo-geological lines, conclusions are drawn concerning the structure, age of the basement and sedimentary cover complexes in different geological structures. The inheritance of sedimentary basins from shelves to the deepwater part of the Arctic Ocean is shown. There are three structural maps in the section: the acoustic basement of different ages, the Cretaceous deposit roof (RH pCU) and the Eocene deposit roof (RH UB). Zoning was made for each map, the basement and sedimentary cover structures were identified and characterized.

1 Sedimentary Cover Structure

1.1 Map of Seismic Knowledge

The VSEGEI marine seismic database stores metadata as well as selected digital seismic sections based on regional seismic surveys (multichannel seismic (MCS)

L. A. Daragan-Sushchova (✉) · E. O. Petrov · O. V. Petrov · N. N. Sobolev
Russian Geological Research Institute (VSEGEI), 74 Sredny Prospect, St. Petersburg 199106, Russia
e-mail: ldaragan@vsegei.ru

data, sonobuoy sounding data, refraction and wide-angle reflection data and many others). The database catalogue contains information on each line: the line name; survey technique; year of survey; the country that performed the survey; the company that performed the survey. All the data on the surveys were collected from open access and include works from 1957 till the present day. Surveys of Russian companies (OAO MAGE, AO Sevmorgeo, OAO DMNG, etc.) and foreign expeditions (AWI, Healy, USGS, etc.) are also included.

The chart-map shows the framework of multichannel seismic reflection profiles included in the ATLAS, locations of sonobuoy soundings, geological and geophysical crosssections of the Russian Arctic water areas (Fig. 1).

The grey (seismic surveys up to 2000) and violet (seismic surveys after 2000) colours indicate the lines available in the VSEGEI seismic database.
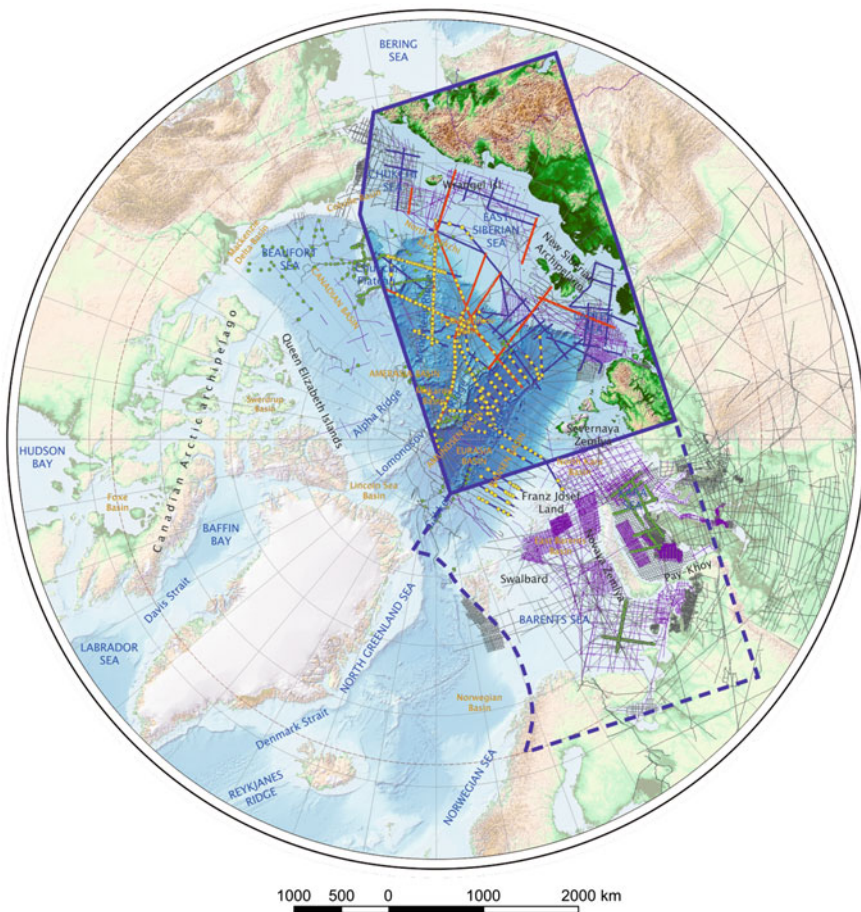
Fig. 1 Scheme of location of CDP seismic profiles and geological–geophysical sections of the Sub-Polar Zone of Russia and adjacent seas depicted in the ATLAS

The blue colour shows lines included in the set of correlated lines. This seismic framework consists of 77 CDP SRM profiles with a total length of about 30,000 km. A unified stratigraphic model was created to link the profiles included in this framework. Geological data on the Arctic islands and wells on the Alaskan shelf and the North Pole were used as the basis for the stratigraphic correlation of seismic horizons.

The red lines are composite geological and geophysical sections presented in the atlas. There are six profiles that intersect all geological structures of eastern Russian part of the Arctic Ocean areas. The profiles clearly demonstrate the structural features of the sedimentary cover of this region.

The map also shows the location of the 201 sonobuoys (yellow dots) that were used to interpret the lines included in the framework. Other sonobuoys available in the seismic database are shown as green circles.

1.2 Correlation Chart Showing Stratigraphic Tie of Reflectors

The basic approach to the stratigraphic tie of reflecting horizons in the sedimentary cover of the Arctic Ocean in this study is based on the characterization of wave fields and reflectors tracking (Fig. 2). In addition, the authors used results of deep-sea drilling in the cis-polar part of the Lomonosov Ridge (well ACEX-302), deep wells drilled in the Alaskan shelf in the Chukchi Sea and geological studies on the Arctic islands and the mainland. Additional characteristics taken into account while correlating seismic units (quasi-synchronous seismic sequences) include the distribution of layer velocities in the seismic section, which cannot be attributes of the stratigraphy itself, although they contain important information on physical properties of the studied environment. The correlation chart showing stratigraphic correlation of reflectors demonstrates views of various authors.

Age correlation of reflectors in the junction zone of the Lomonosov Ridge with the shelf was made from indirect data, since there are no wells in the area. In the sedimentary cover of Line A7, a number of seismic sequences and reflectors have been identified. Two seismic horizons are most striking: the acoustic basement and the RU regional unconformity. The thickness of the sediments above the unconformity gradually increases from the shelf to the continental slope leading to the formation of a progradational prism. Northward, it decreases again to 0.5–1.0 km on the crest of the ridge. The thickness of the sedimentary layer between the acoustic basement and the regional unconformity varies more significantly: it increases sharply to 8–10 km in local depressions and troughs of the shelf and decreases to 0.5–2.0 km on shelf elevations and below the Lomonosov Ridge. It can be assumed that the age of the RU regional unconformity is Late Eocene–Early Miocene. Correspondence of the paleostructural plan of Miocene and Pliocene-Quaternary strata of the Laptev Sea continental margin to its modern structural plan also evidences in favor
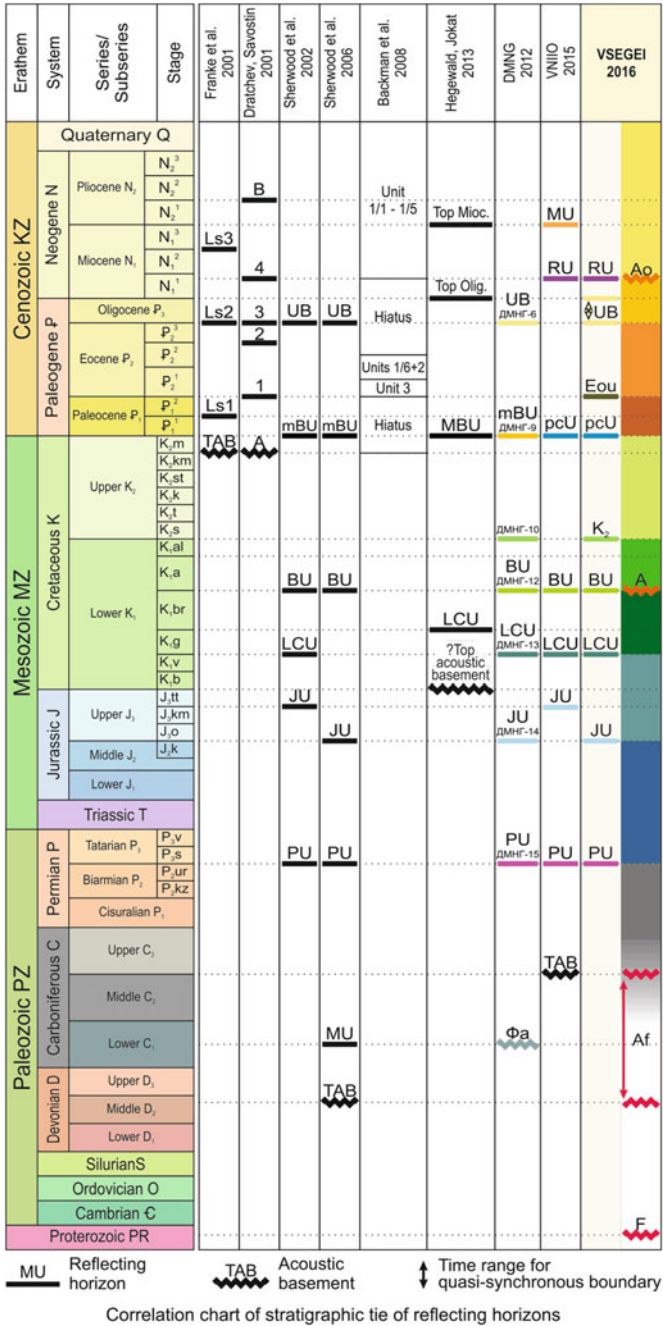
Fig. 2 Correlation chart of stratigraphic tie of reflecting horizons

of the Miocene age of the unconformity (Daragan-Sushchov et al. 2002). The activation of the movements came to its end by the end of the Miocene. The Laptev Sea basin experienced uplifting and erosion followed by lowering in the early Pliocene (Daragan-Sushchova et al. 2010). Thus, the shelf, continental slope and deep-water depression of the Eurasian Basin of the Arctic Ocean emerged in the Miocene (especially from the Pliocene) as evidenced from the wave field pattern and the ratio of thicknesses of the upper seismic sequence on lines A7 (Daragan-Sushchova et al. 2014, 2015a, b), AR1401, AR1403 and some others.

To correlate the age of reflectors in the east and northeast, we relied on the correlation of wave fields and US seismic line D84-33, which in its turn was stratified from Burgers and Popcorn-1 wells. Line D84-33 is located 3.7 km from the Burger well and 0.5 km from the Popcorn-1 well (Sherwood, 2006; Petrovskaya and Savishkina, 2014; Petrovskaya et al., 2008; Daragan-Sushchova et al. 2014, 2015a, b). Kinematic characteristics of the section give additional information on reflectors' stratigraphic tie and correlation (oral communication of Kirk W. Sherwood) (Daragan-Sushchova and Kopylova 1990).

In the correlation chart, in the column "VSEGEI, 2016", there are four types of basement. The North Kara region has sequence geology. The age of the basement there varies from the Upper Proterozoic, Baikalian (F) to the Upper Devonian, Carboniferous (Af) (Malyshev et al. 2012; Daragan-Sushchova et al. 2014). In part of the shelf of the Chukchi and East Siberian seas (in the North Chukchi depression, the Eastern trough of the Podvodnikov basin—Vilkitsky trough), Af is Ellesmerian or Late Caledonian. In the Western trough of the Podvodnikov basin, in the Lomonosov Ridge, and in the Makarov basin, A is Cimmerian. The youngest basement in the Eurasian Basin is found the Gakkel Ridge; A0 ranges from the middle Miocene to the Recent. The correlation chart has been refined based on lines in the Chukchi Sea. The figure shows an example of the wave field with the change of the uneven-aged basement and erosional truncation at the boundary of the major geological reconstruction between Mesozoic and Cenozoic deposits (pCU reflector).

On the seismic line south of point 30 (Fig. 3), there is a chaotic seismic record character, which is typical of a folded basement. Most likely, it is a young Cimmerian basement, which is observed in the south of the Chukchi Sea. There, the young basement is exposed on the surface of the seafloor and somewhat overthrusted onto the sedimentary cover of the section located northwards.

Further on the line, the thickness of the sedimentary cover sharply increases to 6.8–7.3 s that corresponds to 15 km.

According to the character of the dynamic recording, major unconformity of the pCU reflector divides the wave field of the sedimentary cover into 2 parts. The upper part has four sub-horizontally layered seismic units with minor disturbances of seismic record. Thicknesses of the sequences sharply increase towards the North Chukchi trough. The lower part of the section is composed of six seismic units severely broken by faults. The thickness in the sequences changes insignificantly and with no obvious tendencies. The structure of the wave field of the lower part of the section (occurrence of six sequences and relatively old basement, their dynamic and
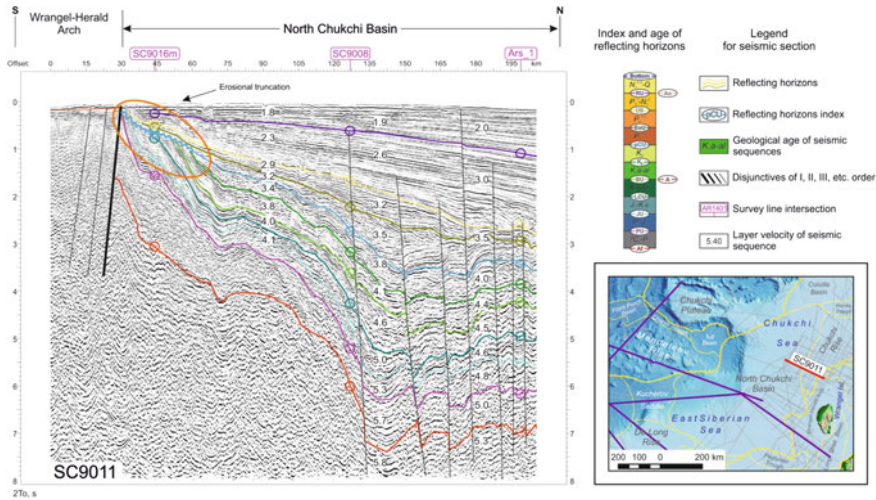
Fig. 3 Wavefield parameters in the suture zone of basements having different ages along Line SC9011 on the northeastern shelf of the Russian Arctic

kinematic characteristics) suggests that the sequences are related to the Paleozoic-Mesozoic section penetrated in US wells. Based on this reflector, constraining seismic units were given the same indices as the reflectors in the US sector.

1.3 Set of Composite Seismic Profiles Across Major Geological Structures of the Northeastern Arctic

Complete correlation of key reflecting horizons with all disturbances of seismic record (faults) observed in the wave field (over 100 profiles, about 30,000 km of total length) was made in the Arctic Ocean and adjacent water areas of the Laptev Sea, the East Siberian and the Chukchi seas. All refraction-reflection sonobuoy soundings (totally 201) were processed, tied to seismic stacked sections and interpreted. On the lines where no sounding was performed, the velocities were calculated using the CMP data. All the lines were presented in a unified manner: the wave field without reflectors' correlation, with correlation in time sections, and complete interpretation of seismogeological data in the depth section.

To illustrate changes in seismogeological characteristics in different geological structures of the northeastern and Arctic Ocean shelves, composite seismogeological sections were compiled for the following lines:

Seismogeological section of composite line A4–A7 (Figs. 4 and 5) consists of two seismic lines made by OAO MAGE in 2009–2010 using unified field and processing techniques. During the MCS observations, the researchers used the Sercel Seal
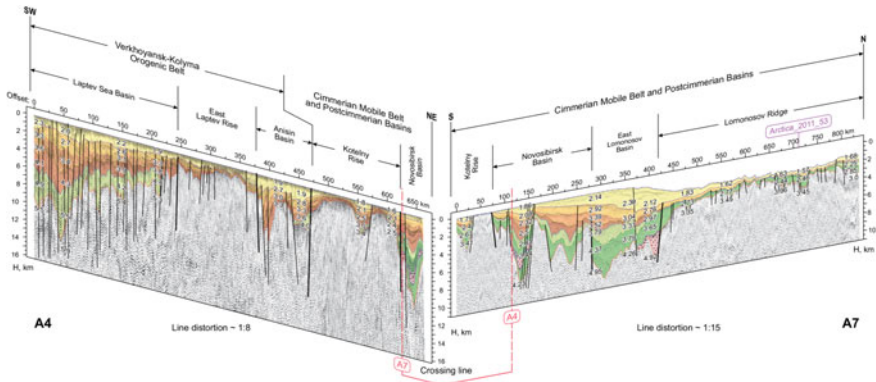
Fig. 4 Seismogeological section of composite line A4 (637.358 km)–A7 (832.4 km)

seismic station, Bolt air guns (total volume of 1500 in.[3]), Sercel seismic streamer with the working part length of 8100 m and the record length of 12 s. The line underwent the conventional processing flow.

E-W line A4 crosses almost the entire Laptev Sea basin. The figure shows the eastern part of the section at the intersection with Line A7 and the sub-meridian section of Line A7 extending from the Kotelny Island to the continental slope and along the Lomonosov Ridge with the correlation with the ACEX well. Names and ranking of main structures are given above the composite section. Changes in time, depth thicknesses and layer velocities are listed in a composite line. The line underwent the conventional processing flow.

Water depth on the shelf does not exceed the first tens of meters; on the continental slope it reaches 450 m; maximum values of 1.8 km are observed over the submerged parts of the Lomonosov Ridge. The multiple event on the shelf has a short time delay, therefore, its influence does not lead to a change in the recording format and the appearance of independent lineups. Starting from stake 300 (line A7) and further onto the continental slope, when the bottom is submerged, multiple event reflections are observed in the tracing region of marker reflectors. Gradually they cross all reflectors on the border of the Western basin of the Podvodnikov Basin and the Lomonosov Ridge, but do not bring any significant distortion. The intensity of reflectors remains higher than that of the multiple event.

The basement is commonly broken by faults, has an unstable form of seismic record with layer velocity ranging from 3.0 to 5.2 km/s. In the Laptev shelf to the continental slope (stake 400), higher velocities (3.8–5.2 km/s) and residual bedding in the basement are recorded. This may indicate that formerly terrigenous sequences (residual stratigraphic tie) underwent slight folding without metamorphism (spread of velocities). Higher velocities (up to 5.2 km/s) may indicate possible subsidence of the basement strata to considerable depths. The Lomonosov Ridge is characterized by lower velocities and their spread (3.0 to 4.0 km/s). The character of reflector A is unstable; it is often correlated at the interface by layered and unstructured seismic
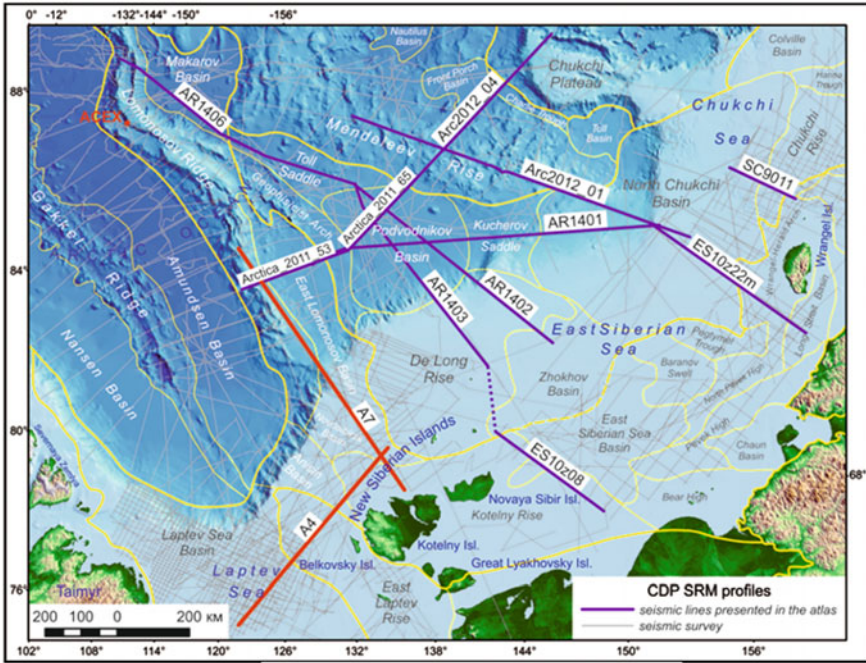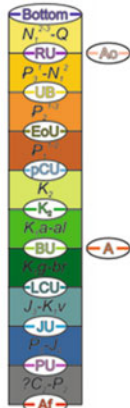
Fig. 5 Scheme of location and legend for CDP seismic profile and geological–geophysical section of the line A4 (637.358 km)–A7 (832.4 km)

record. These characteristics indicate a relatively young folding (Cimmerian) without metamorphism.

The sedimentary cover on the composite line is represented by the Cenozoic sediments—deposits to reflector pCU (4 quasi-synchronous seismic sequences 'QSSS') and deposits of the Cretaceous Period. Thickness of the Cenozoic sequences varies

depending on the structures. They reach their greatest values in depressions in the Laptev Sea Basin (stake 45, line A4), where the Cenozoic sediments are more than 8 km thick. On the highs, there is not only a decrease in the thickness of mapped QSSS, but also a loss in completeness of the stratigraphic framework. On the East Laptev and Kotelny uplifts, it is not always possible to map reflectors pCU, EoU, UB, since the sediments corresponding to these time intervals are insignificant and their thickness is below the resolution; in addition, due to the elevation of these areas, possibly no sedimentation conditions occurred nor washing out took place during uplifting. The Lomonosov Ridge is characterized by relatively thin sedimentary cover in general and its Cenozoic component in particular, as well as the lack of the Eocene base tracing (reflector EoU). Reservoir velocities increase in depressions to 4.3 km/s (stake 50, line A4); they take the minimum values in the youngest sediments, about 1.6 km/s.

The pre-Cenozoic part of the sequence on composite line A4–A7 is not present everywhere; it is absent in the East Laptev Uplift and in the west of the neighbouring Anisinsky Basin (stake 2240, line A4); in addition, sediments of this age are almost lacking on the Kotelny Uplift, stake 5475, where a slight immersion of the entire sedimentary strata is observed. The maximum thickness of the pre-Cenozoic deposits reaching 5.7 km is found in the Laptev Sea Basin (line A4), Novosibirsky Basin (lines A4 and A7), and the Western Podvodnikov Basin (line A7). Reservoir velocity indices start at 2.3 km/s in the northern part of the Lomonosov Ridge, although velocity measurement is less reliable here due to the low thickness and strong disruption of the layers. Velocity increases to 5.5 km/s near stake 50 on line A4.

Two lower seismic units (quasi-synchronous seismic sequences), the basement (A)–K2 and K2–pCU, are characterized by varying thicknesses (0 to 2.7 km). The velocities are determined more reliably in the shelf zone, including the continental slope: from bottom to top 3.4–4.4 km/s and 2.7–4.0 km/s respectively. In the Lomonosov Ridge, determination of velocities is less reliable due to the low thickness and severely broken layers, so their values are not discussed. Reflector pCU is the main seismic horizon. Below, on part of the line, an unconformity of erosional surface type is recorded, and above, there is an overlap.

Reflectors pCU-EoU, EoU-UB, UB-RU are very common on the shelf. Their velocities and thickness generally decrease towards the continental slope and in the Lomonosov Ridge. In the Ridge (stake 420–839), it is possible to trace an undifferentiated section between reflectors pCU-RU.

Seismic units bounded by the reflector RU and seafloor, as a rule, have a "seismically transparent" record with low-amplitude wave patterns typical of pelagic sediments and low velocities of 1.7 km/s on average. Thickness in this sequence is, in general, rather small (0.3–0.4 km/s), but it increases sharply in the continental slope reaching up to 2.4 km/s and in the Laptev shelf in the immediate vicinity of source areas (stake 390–480) up to 1.1–1.5 km/s.

Wave field parameters suggest that main disturbances of the seismic record, which were constantly rejuvenated, occurred during the formation of the basement A. Active rejuvenation of the disturbances occurred at the Mesozoic-Cenozoic boundary

(reflector pCU), in the Middle Miocene (reflector RU), and in the Cenozoic (reflectors EoU, UB); in recent times it was less active.
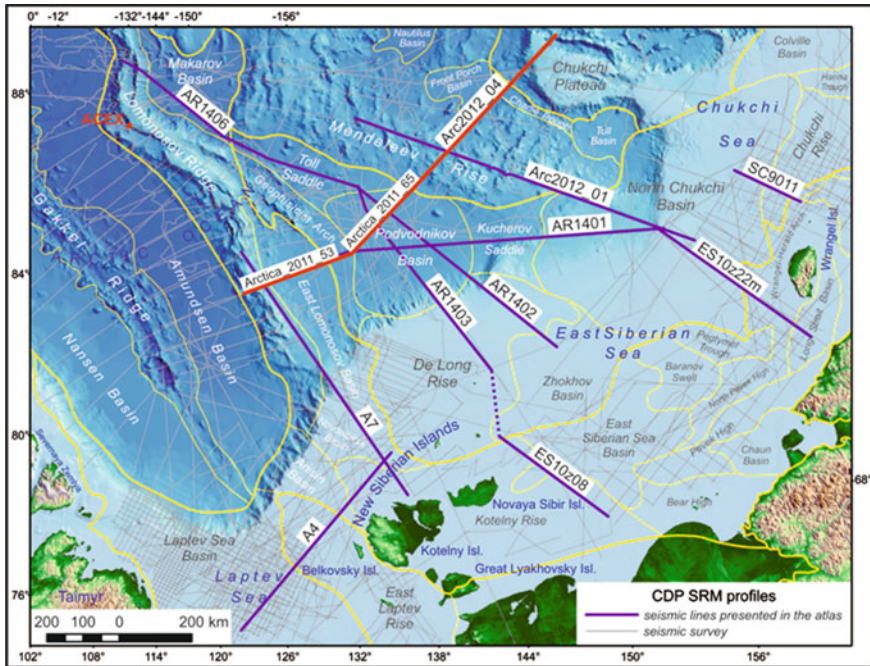
Seismogeological section of composite line Arctica 2011 28-65–Arc2012 04 (Figs. 6 and 7) consists of two seismic lines Arctica_2011_053_065, built by GNINGI in 2011 using unified field and processing techniques. During the observation using the CDP seismic reflection method, the DigiSTREAMER seismic station, BoltAPG air guns (total volume of 1025 in.^{3}), DigiSTREAMER seismic streamer with the working part length of 600 m and the record length of 15 s were used as a recording device. The line underwent the conventional processing flow. FGUP Sevmorgeo built line Arc2012_04 in 2012. During the observation with CDP seismic reflection method, the DigiSTREAMER seismic station, BoltAPG 8500 air guns (total volume of 1025/2050 in.^{3}), DigiSTREAMER seismic streamer with the working part length of 600 m and the record length of 12 s were used as a recording device. The line underwent the conventional processing graph.

In the Arctic Ocean, composite latitudinal seismogeological section crosses main structures from the Lomonosov Ridge to the Chukchi Plateau (all of them are indicated above the section).

The upper Cenozoic (Kz) part of the section (from recent sediments to reflector pCU—4 seismic units) occurs almost everywhere. The thicknesses are rather variable, while the velocities vary to a lesser extent; the stratigraphic volume is almost not changed. As a rule, thicknesses and layer velocities decrease in uplifts (sometimes totally disappear) and increase sharply in depressions. The wave field of the upper seismic unit is typical of pelagic sediments. In the sequence limited by reflector RU-UB, sedimentation occurred mainly under marine conditions. Depths of sedimentation in the seismic unit UB (Lower Oligocene unconformity)–EoU (strata from the Upper Eocene top to the Lower Eocene base) varied from offshore to onshore-offshore. Onshore-offshore sedimentation is predicted in the sequence limited by
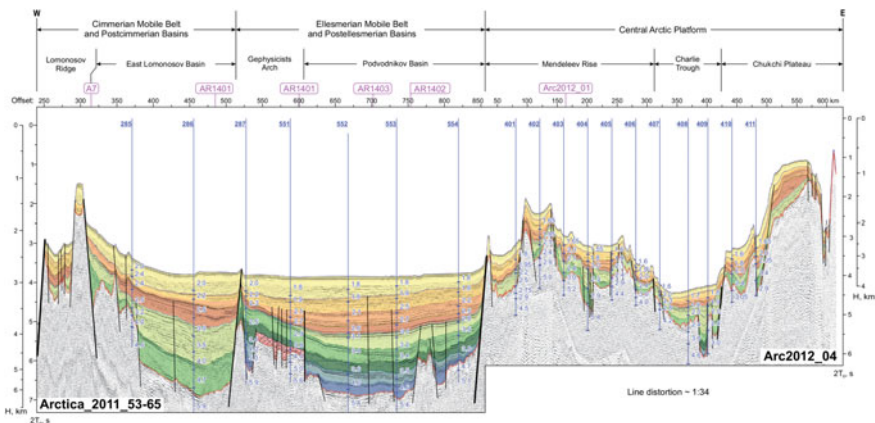
Fig. 6 Seismogeological section of composite line Arctica 2011 28-65–Arc2012 04

Fig. 7 Scheme of location of CDP seismic profile and geological–geophysical section of the line Arctica 2011 28-65–Arc2012 04

reflectors EoU (Lower Eocene unconformity)–pCU (strata from the Lower Eocene base to the Lower Paleogene base, possibly to the top of the Upper Cretaceous).

The lower part (pre-Cenozoic) occurs in different stratigraphic volumes and thicknesses, considerably varying depending on the structural position. The Geofizikov Spur is the interface between two types of the section in the lower part (up to Kz) of the sedimentary cover.

West of the spur, there are two sequences with unstructured form of record. Such a record is characteristic either of the acoustic basement or the strata formed in course of avalanche sedimentation, for example, molasses resulted from intensive destruction of neighboring orogens. Reflections that separate these sequences indicate the presence of lower and upper molasses that is particularly evident in the Western Podvodnikov Basin where both sequences are present in considerable volumes.

The lower sequence (K2—Aptian-Albian Lower Cretaceous sediments to A—acoustic basement surface) is more seismically transparent; in the junction zone with the Lomonosov Ridge, it is recorded only in grabens. On the ridge, this sequence is lacking. There is an inherent alluvial fan on the western slope of the Podvodnikov Basin. It evidences that at that time the Lomonosov Ridge was intensively eroded to form coarse molasses in neighboring depressions, which means that it was an orogen. Its thickness reaches 1.4 km, velocities range from 3.2 to 4.7 km/s.

During the formation of the upper sequence (reflector pCU—post-Campanian unconformity to K2—Upper Cretaceous), the Lomonosov Ridge orogen was apparently partially eroded, as indicated by the discontinuous layered record of the sequence, and hence one can assume thinner molass. The layer velocity in the Western Podvodnikov Basin varies from 2.5 to 3.5 km/s. The thickness ranges from 0.3 km in uplifts to 1.7 km in depressions.

The basement in the western part of the section is dynamically flat in wave fields. The basement relief in the Lomonosov Ridge, and the western slope of the Podvodnikov Basin is sharply dissected, but in the Western Podvodnikov Basin, it is smooth and in some areas dynamically pronounced. Such instability of dynamic record indicates a relatively young age of the basement. The layer velocity in the basement ranges from 4.0 to 5.9 km/s.

East of the Geofizikov Spur (including the spur itself), in the lower part of the cover section, one can observe a larger number of seismic units with more extended, high-amplitude, dynamically pronounced reflections, which are rather thin. This indicates an earlier development of the sedimentary basin in this part of the line and clearly shelf-stable sedimentation conditions.

The wave field of the acoustic basement surface (Af) corresponds to a 3–4-phase boundary, which is smooth, stable and broken near fault zones (basement uplifts). The layer velocity ranges from 4.4–5.9 km/s dropping in the area of fault zones. Dynamic features of the wave field are typical of the longstanding basement, which is older than the one in the Western Podvodnikov Basin. Judging by the stratigraphic volume of the cover, it is an Ellesmerian folded basement.

In the Eastern Podvodnikov Basin, there are five seismic sequences in the lower part of the cover section, which, in accordance with the proposed interpretation model, are limited by certain reflectors and correspond to:

1. JU (Middle Jurassic unconformity)–Af (acoustic basement surface), strata from the Middle Jurassic top to the acoustic basement. The wave field is characterized by obvious extended reflections, but towards the acoustic basement, the reflections diminish, their amplitude decreases that indicates an increase of content of marine sediments up the section. Layer velocity (3.8–5.0 km/s) are typical of terrigenous rocks. Thickness varies from 0.3 to 1.0 km.
2. LCU (Late Cretaceous unconformity)–JU, strata from the bottom of Hauterivian Lower Cretaceous deposits to the Upper Jurassic bottom. The wave field is characterized by long elongated obvious reflectors with high amplitude values. Layer velocity varies from 3.4 to 4.6 km/s. The thickness ranges from 0.2 to 0.6 km, decreasing towards the Mendeleev Rise.
3. BU (Brookian unconformity)–LCU, strata from the top of Barremian sediments to the bottom of Hauterivian Lower Cretaceous deposits. The wave field is characterized by extended, weakly pronounced phases; in the area of the Geophysicists Rise, the record becomes even less pronounced. Layer velocity ranges from 2.5 to 3.8 km/s. The thickness is stable and smooth, 0.5 km on average.

4. K2 (Aptian-Albian Lower Cretaceous deposits)–BU, strata from the top of Albian sediments to the bottom of Aptian deposits. The wave field is characterized by long, extended obvious reflections with high amplitude values. Layer velocity varies from 3.4 to 3.8 km/s. The thickness of the strata is constant (about 0.6 km).

5. pCU (post-Campanian unconformity)–K2, Upper Cretaceous strata. The wave field is characterized by long, extended obvious reflections with high amplitude values. Closer to K2 horizon, the obvious character of the reflections is weakened. Layer velocity ranges from 3.2 to 3.5 km/s. The thickness varies from 0.7 km to complete erosion on the Geophysicists Rise.

Similar differences in the sedimentary cover structure of the western and eastern parts of the Podvodnikov Basin are recorded on lines located to the north and south of the section described. It is possible that the western part of the Podvodnikov Basin was a Cretaceous rift on the Cimmerian base. At the time, the Geofizikov Spur corresponded to the eastern slope of the Cretaceous rift, whereas the Lomonosov Ridge corresponded to the western slope. This explains the unstructured nature of the record in the wave fields of Cretaceous deposits in the western part of the Podvodnikov Basin and the sharp reduction of coeval deposits in the Geofizikov Spur and the Lomonosov Ridge.

In the Central Arctic Platform, as it can be seen from this section, the stratigraphic volume of the cover roughly corresponds to the cover volume in the eastern part of the Podvodnikov Basin, at least in deep troughs (Charlie Trough). In the Mendeleev Rise and Chukchi Plateau, the stratigraphic volume is reduced and only one or two upper Cretaceous sequences are recorded. This is most likely due to erosion. Although this conclusion based on this section is disputable. Some velocities in the basement (2.4–2.9 km/s) of the uplifts are typical of sedimentary rocks; it is confirmed by results of dredging.

The character of the wave fields suggests that main constantly rejuvenating disturbances in the seismic record occurred during the basement formation. Active rejuvenation of the disturbances took place at the Mesozoic- Cenozoic boundary (reflector pCU), in the Middle Miocene reflector RU) and in recent times; in the Cenozoic (reflectors EoU, UB) it was less active.

Sheetlike character of Kz sequences' distribution over the whole area suggests that modern morphostructures were formed recently after the accumulation of N-Q sediments. Another important point: by the beginning of accumulation of Kz sediments, the entire territory was peneplenized. Otherwise, Kz would be absent in modern uplifts. Recent tectonic movements inherited the ancient structural plan, as evidenced by the through development of tectonic dislocations on the boundaries of morphostructures.

Seismogeological section of composite line ES10z22m–AR1401 (Figs. 8 and 9) consists of two seismic lines. ES10z22m was made by Dalmorneftegeofizika in 2010. In the MCS survey, the following devices were used: the Seal as a recording device, the Sercel seismic streamer with the working part length of 7950 m, Bolt 1900
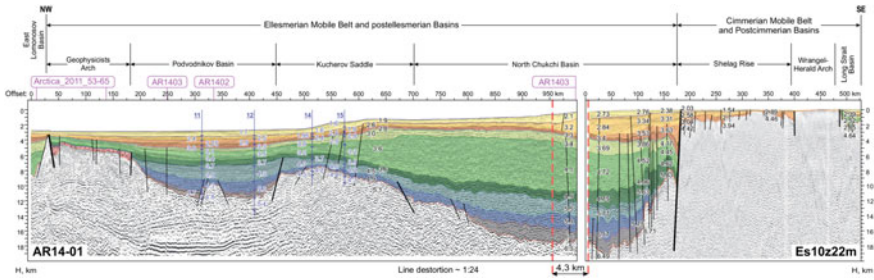
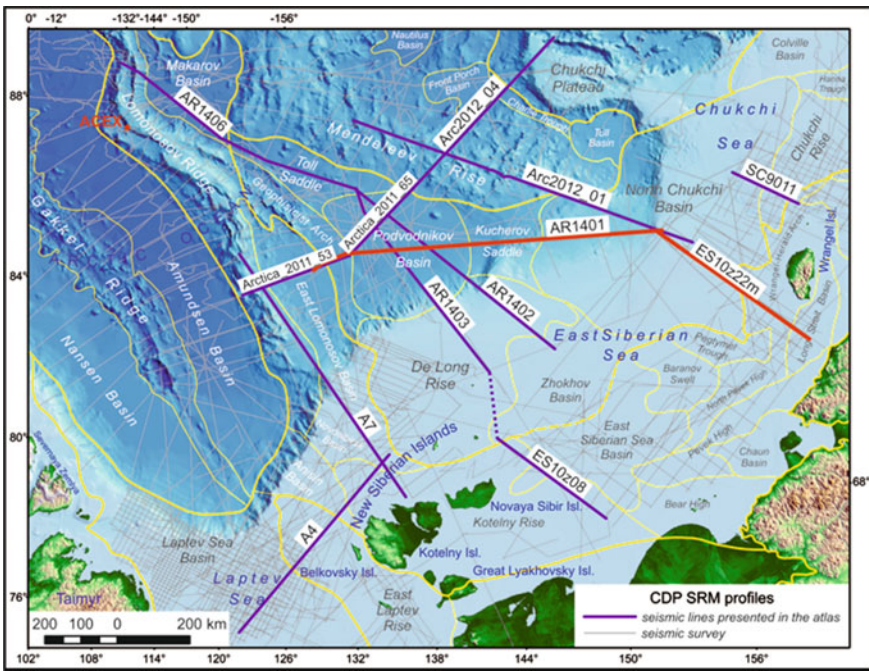**Fig. 8** Seismogeological section of composite line ES10z22m–AR 1401

Fig. 9 Scheme of location of CDP seismic profile and geological–geophysical section of the line ES10z22m–AR 1401

air guns (total volume of 4000 in.^{3}), the record length was 12 s. The line underwent the conventional processing flow.

AR 1401 was performed by OAO MAGE in 2014. In the MCS survey, the Sercel SEAL System was used as a seismic recording station, ver. 5.1, the seismic streamer Sercel SEAL Fluid, 24 bit, with the streamer length of 4500 m; APG BOLT-8500 air guns (total volume of 1300 in.^{3}), the record length was 12 s. The line underwent the conventional processing flow.

Composite line ES10z22m–AR1401 is an excellent example of a seismic unit being continuously traced from the shelf to the Podvodnikov Basin. Minimum amount of sediments (0–3.0 km) is recorded in the southeast, along Line ES10z22m to stake 180. In the area of this stake, a major disturbance of the seismic record is observed. The basement in the southern block at shallow depths is broken into blocks; it does not have consistent reflection (reflector) from the surface, and velocities in it are relatively low (4.1 to 4.5 km/s). All these features are typical of the young Cimmerian basement. North of stake 180, there is a sharp increase in the amount of seismic units (by 5) and the amount of sediments (up to 19 km). The same structure of the record is inherited in the Arctic Ocean along Line AR 1401 up to stake 700.

Wave fields of reflector Af associated with the basement are practically identical: high-amplitude 3–4-phase waves are quite consistent, particularly in the deepest downwarps of the North Chukchi Basin (NChB). The amount of sequences remains unchanged with some variations in their thickness, depth of occurrence and characteristic features of the wave field. The velocities in the basement there range from 5.4 to 6.6 km/s.

In the lower seismic unit (reflector Af-PU), we find high-amplitude extended reflectors with high layer velocity ~5.9–6.2 km/s, which is common for the terrigenous-carbonate complex. In it and overlapping it seismic unit (reflector PU-JU), there are two structures: North Chukchi Basin (NChB) and the eastern part of the Podvodnikov Basin (EpPB), formerly known as the Vilkitsky Trough. At that time, they are separated by the typical (in structure) Kucherov saddle (Ks). The basement on the saddle is broken by numerous faults and, apparently, due to this fact, has a lower layer velocity (4.5–5.17 km/s) and a dissected relief. Judging by the wave field (discontinuous and less-amplitude reflectors, layer velocity is 5.5–4.9 km/s), seismic unit (reflector PU-JU) is composed of terrigenous rocks, in which the content of marine sediments (extended smooth reflectors) slightly increases northwestwards. The total maximum thicknesses in this part of the section vary within 4.0 km in NChB, 0.5 km in Ks, and 2.2 km in EpPB.

Sequences between reflectors JU-LCU and LCU-BU inherit the behavior of the underlying seismic unit in the separation of the trough by a saddle, but in a softer form—as if flowing along and leveling it. The content of marine sediments in the lower sequence increases northwestwards and in the upper one—southeastwards. The total maximum thicknesses in this part of the section vary within 4.0 km in NChB, 2 km in Ks and about 3 km in EpPB. The layer velocity of the lower sequence varies from 5.8 to 4.2 km/s, that of the upper one varies from 4.9 to 4.0 km/s.

The seismic unit between reflectors BU and K2 in the shelf and the Arctic Ocean to stake 625 (with high-amplitude cross-bedded layers) is a marker sequence. Its top in the Burger well and in NChB was compared to the Late Aptian shelf cross-bedded layers. When advancing northwestward, cross-bedded character of the sediments is observed upwards the section, capturing younger sediments of the Albian and, possibly, partly Upper Cretaceous age, therefore, reflector K2 can not be taken as the reference horizon and it would be more precise to consider two seismic units (reflector BU-K2 and reflector K2-pCU) together. Apparently, at that time there was a very intensive migration of sediments from the south, southeast. Cross bedding in the

seismic unit is observed in the NChB to the middle of Ks (stake 625). Further north-westward, these sequences sharply become much thinner (from 8.0–3.0 km in the south, 3.4–2.2 km in the saddle, 1.8–1.6 km in the EpPB to 0.6 km at the Geofizikov Spur, where the upper seismic unit reflector K2 pCU is completely eroded). Reflectors in the sequences become extended, more high-amplitude. The layer velocity in the lower seismic unit varies within 4.2–3.6 km/s in the south, 3.4–3.2 km/s in the saddle, and 3.4–3.7 km/s in EpPB. The layer velocity in the upper seismic unit varies within 3.8–2.8 km/s in the south, 3.1–2.9 km/s in the saddle, and 3.5–3.1 km/s in EpPB. Such patterns (extended lineups and relatively high velocities) can indicate relatively deep (dominated by clay fractions) sedimentation regime at that time in EpPB.

The upper part of the 4th section (from recent sediments to pCU) occurs in its entirety only in the southern NChB and in EpPB. In these tectonic structures, thickness varies, but the stratigraphic framework is almost unchanged and consists of the following sequences:

1. Bottom–RU (regional Miocene unconformity). It is characterized by low discontinuous extended lineups with layer velocity of 1.6–1.9 km/s. Thickness varies from 0.1 to 0.3 km in uplifts to 1.1 km in depressions. Similar wave fields, as a rule, are observed in pelagic sediments.

2. RU–UB (stratum from the Middle Miocene to the Lower Oligocene base). The wave field is characterized by long, extended reflections, approximately of similar frequency and amplitude. In NChB, particularly in its southern part, there are various cross-bedded facies that indicates intensive drifting from the south, southeast and a constant rise in sea level. Layer velocity of 2.0–2.5 km/s, in some cases, up to 3.2 km/s indicates a predominantly sandy composition. Thickness varies from 0.2 to 0.4 km in uplifts to 2.4 km in the south of NChB. Sedimentation occurred mainly under offshore or onshore-offshore conditions.

3. UB (Lower Oligocene unconformity)–EoU (strata from the Upper Eocene top to the Lower Eocene base), the wave field is characterized by discontinuous weakly expressed reflections. Layer velocity ranges from 3.3 to 2.3 km/s. Thickness varies from 0.2 to 0.7 km. Depth of sedimentation is offshore to onshore-offshore.

4. EoU (Lower Eocene unconformity)–pCU (strata from the Lower Eocene base to the Lower Paleogene base, possibly the very tops of the Upper Cretaceous). EoU is one of the most pronounced unconformities with high-amplitude reflections. Layer velocity ranges from 3.7 to 2.5 km/s. Thickness varies from 0.8 km in southern N-ChT to 0.2–0.4 km in EtPB. Conditions of sedimentation are offshore to onshore-offshore.

Two lower sequences either become thinner or are completely lacking in uplifts (in the Cimmerian Mobile Belt and Postcimmerian Basins, the Geofizikov Spur, in northern NChB and Ks). The thickness and layer velocities tend to decrease in the uplifts and sharply increase in troughs.

Nature of the wave fields suggests that main disturbances of the seismic record occurred during the basement formation, which underwent constant rejuvenation.

The active rejuvenation of disturbances occurred at the Mesozoic-Cenozoic boundary (reflector pCU), in the Middle Miocene (reflector RU), and the most recent time; it was less active in the Cenozoic (reflector EoU, UB).

The composite seismic line Es10z22m–Arc2012 01 (Figs. 10 and 11) consists of two seismic lines that have no intersection points, but the distance between them is rather small (5 km). Composite line, starting on the East Siberian Sea shelf (ES10z22),
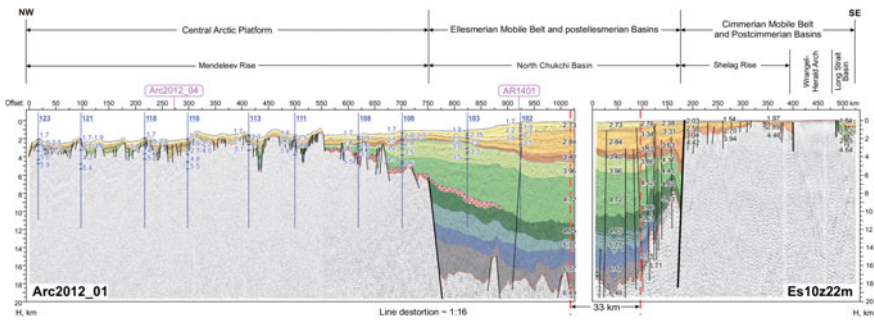
Fig. 10 Seismogeological section of composite line Es10z22m (515 km)–Arc2012 01
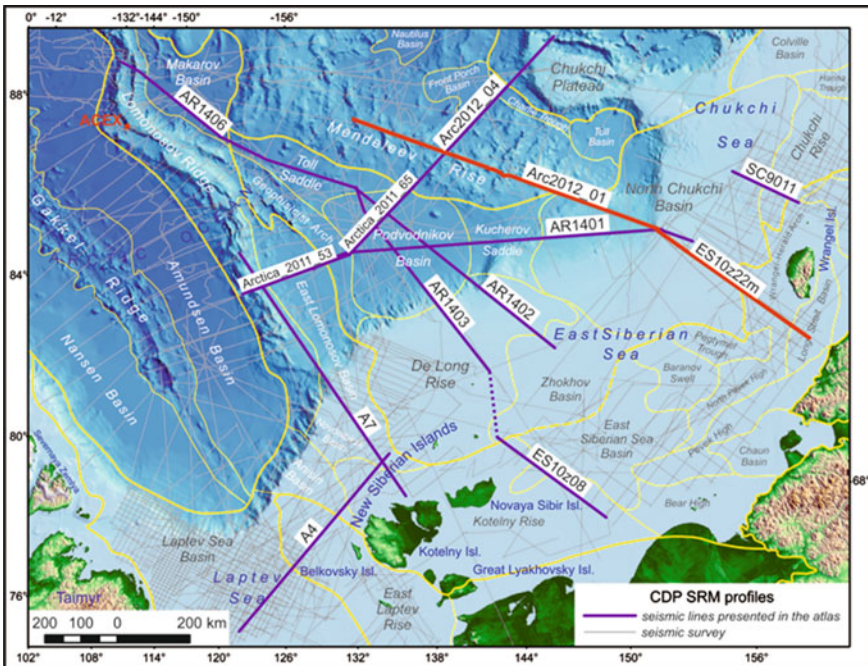
Fig. 11 Scheme of location of CDP seismic profile and geological–geophysical section of the line Es10z22m (515 km)–Arc2012 01

crosses such structures as the Wrangel-Herald foldedblock uplift, the Shelagh Uplift, and finally passes into the North Chukchi Basin. The northwestern part of the section along Line Arc2012_01 shows the Mendeleev Rise structure. More detailed ranking of the structures are given above the seismogeological line. The water depth varies from tens of meters on the shelf to ~2 km in most submerged areas.

Line Es10z22m was made by OAO DMNG in 2010. The work procedure with 2D MCS profiling included the use of a 636-channel 7.9-km-long tow streamer. The record length was 12 s. The line passed the conventional processing flow.

Line Arc2012_01 was made by FGUNPP Sevmorgeo in 2012 as part of the work entitled "Follow-up comprehensive geological and geophysical surveys in the central part of the Arctic Basin to substantiate the nature of the Central Arctic Elevations, adjacent depressions, and to determine the location of the Russian Federation outer limit of the continental shelf". The work procedure with 2D CDP seismic reflection method included using a 48-channel 600-m-long tow streamer. The distance between sources (Bolt APG 8500) was 50 m, the group interval was 12.5 m. The line passed the conventional processing flow.

First multiple events from the East Siberian Sea shelf bottom can be traced practically behind the waves from the bottom, forming a single **Composite seismic line Es10z22m (515 п.км)–Arc2012_01 (1020 п.км)** reflected train. In the NChB, in cases when the floor is submerged up to the northern boundary of the NChB (stake 930), they fall into the tracing region of marker reflectors, gradually crossing, but not substantially distorting all marker reflectors. On the Mendeleev Rise (stakes 0-675), multiple events from the bottom are mainly traced in the region below the correlated reflected waves (below reflector Af).

Upper sedimentary horizons are reliably traced along Line Arc2012_01: RU, UB, and pCU, and the correlation of lower horizons is compatible with the existing wave field and velocity characteristics along lines ES10z23m, ES10z22m, ES10z02_1, 5-AP, Arc12-03.

Line Es10z22, due to more favorable geographical position in terms of fieldwork conditions, was worked out using better technique that significantly improved the quality of the recording. All major unconformities, which are typical for the region, are confidently mapped on this line.

Wave fields within this basin along lines ES10z22m and Arc2012_01 are rather similar, particularly those that are related to the basement. They are consistent high-amplitude 3-4-phase waves mainly located in the most submerged parts of the depression. When transferring the correlation from the shelf to the ocean, the thickness of the mapped sequences is inherited, which fully corresponds to the parameters of the wave field, but the thickness of the Cenozoic sediments decreases sharply when approaching the northern slope of the basin. The velocities are mainly typical of terrigenous rocks, which, when submerged, increase their values. More detailed description of the seismic unit velocities and thickness is given in composite seismic line Es10z22m–Arc2012_01.

In the wavefield of the geo-seismic section along composite line ES-10z22m–Arc2012_01, the Cenozoic sediments can be found almost everywhere. Partially, their lower complexes are absent (line ES10z22m, stakes 180–527) in the region of the

Belt of Cimmerian displacements and epi-Cimmerian troughs and at the maximum peaks of the Mendeleev Rise (line Arc2012_01) or grow thinner (in the north of the NChB and on the Mendeleev Rise). In general, seismic complexes vary in thickness, but the stratigraphic framework on the biggest part of the geo-seismic section mostly remains unchanged and is presented by 4 QSSS, similar to those distinguished in other sections. As a rule, thickness and reservoir velocities decrease on highs and increase in depressions.

On geo-seismic section ES10z22m–Arc2012_01, QSSS can be continuously traced from the shelf to the Arctic Ocean. Two basements of different age are distinguished here. One is in the southeast of line ES10z22m to stake 180, where a minimum amount of sediments (0-3.0 km) is observed. In the area of this stake, a major failure in seismic record was revealed, apparently associated with a large fault zone. The basement in the southern block occurs at shallow depths; it is divided into blocks, does not have a stable reflection from the surface and its velocities are relatively low (4.1–4.5 km/s). All these signs are characteristic of young, in this case, **Cimmerian** basement. North of stake 180 on line ES10z22m the situation is different; there is a sharp increase in the number of the pre-Cenozoic QSSS (to 6) and the volume of all sediments (to 19 km). Reflectors associated with the basement form quite stable intense 3-4-phase waves, especially in the most sagged parts of the NChB. Further to the northwest along line Arc2012_01 to stake 750 wave fields of reflectors Af, PU, JU, LCU, BU, K2, connected with the basement and the pre-Cenozoic sequence, can be traced conditionally, being guided by the positions of reflectors, crossing them lines ES10z22m, ES10z02_1, AR1401, AR 1411. Practically the same number of complexes is retained in depressions, with some variation in their thickness, occurrence depth, and characteristic features of the wave field. The velocities in the basement (Af) here range from 5.4 to 6.4 km/s. The dynamic features of the wave field are typical of a stable, more ancient basement. Judging by the stratigraphic framework of the cover, it is the **Ellesmerian** folded basement. On the northeast edge of the Kucherov Saddle and Mendeleev Rise (stakes 0-750), the basement is broken into blocks by numerous displacements. The wave field of the reflectors from the basement is not stable. Judging by the nature of failures (displacement and, in some cases, "tearing up" of the cover horizons upsection), the blocks finally formed during the Cenozoic. In some blocks above the basement, a train of intense low-frequency reflections is observed, which, together with magnetic data, could be interpreted as reflections from basaltic "covers". However, there are also depressions (stakes 509–520 and 429–441), in which such "covers" are absent, and then up to 5 seismic complexes can be traced in the wave field in the pre-Cenozoic sequence, similar to those observed in the NChB, but thinner and with lower velocities. These facts give us a reason to assume the presence of the Paleozoic-Mesozoic rocks on the Mendeleev Rise, which are possibly slightly folded in most blocks, broken by faults or overlapped by basalts. The presence of depressions (stakes 509–520 and 429–441) with a complete unbroken sedimentary pre-Cenozoic cover and low Vp below the acoustic basement on the highs (2.8–4.1 km/s) give us grounds to predict here the same basement as in the NChB, i.e. Ellesmerian. At the same time, the acoustic basement in the Mendeleev Rise is uneven-aged. It is traced either along

the base of the alleged "basaltic covers" in the Cretaceous sediments, or in depressions (stakes 501–522 and 429–441), along the base of the Paleozoic-Mesozoic strata and correlates with the Ellesmerides.

Agreeably with the basement behaviour, lower Carboniferous-Lower Permian QSSS (reflectors Af-PU), Upper Permian-Middle Jurassic QSSS (reflectors PU-JU) are assumed only in the NChB. Complexes between reflectors Af-U (Upper Permian–Middle Jurassic), JULCU (from the bottom of the Upper Jurassic to the bottom of the Hauterivian) and reflectors LCU-BU (from the bottom of the Hauterivian to the roof of the Barremian Lower Cretaceous deposits), except for the Northern Chukchi Basin, are observed in depressions on the Mendeleev Rise (stakes 501–522 and 429–441).

According to the character of the seismic record, major disturbances occurred during the formation of basement A. The disturbances were constantly rejuvenated. Active rejuvenation of the disturbances took place at the Mesozoic-Cenozoic boundary (reflector pCU), in the Middle Miocene (reflector RU), and in the Cenozoic (reflectors EoU, UB).

Composite seismic line AR1402–AR1406 (Figs. 12 and 13). The section consists of seismic lines that do not have an actual intersection point, but the distance between them is so small that, with the scale used, it is possible to neglect this fact.

Both AR1402 and AR1406 lines were shot by OAO MAGE in 2014 from the R/V "Akademik Fedorov". CDP-reflection technique included APG BOLT-8500 sources; operating volume, 1300 in.[3], Sercel SEAL Fluid towed streamer of 24 bit, 600 m long for AR14-06 line and 4500 m for AR1402 line. The distance between the sources was 50 m, the group interval, 12.5 m. The line underwent the standard processing graph.

The composite line starts in the north of the East Siberian Sea (AR1402), crosses the De Long Uplift, the eastern part of the Podvodnikov Basin, the Toll Saddle, the Makarov Basin and the Lomonosov Ridge. More detailed ranking of the structures
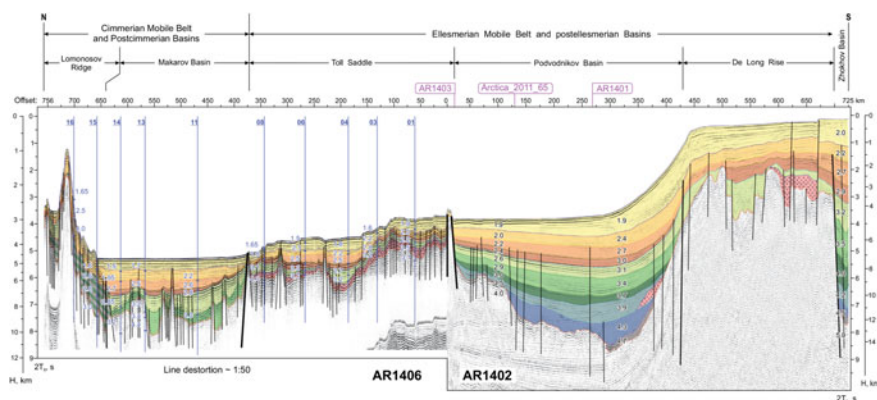
Fig. 12 Seismogeological section of composite line AR1402 (728 km)–AR1406 (765 km)
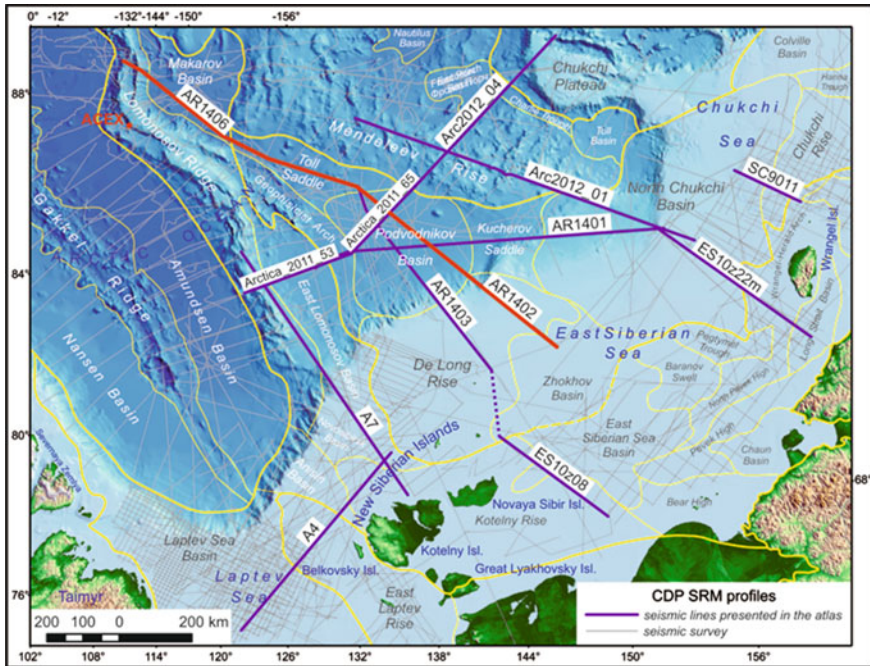
Fig. 13 Scheme of location of CDP seismic profile and geological–geophysical section of the line AR1402 (728 km)–AR1406 (765 km)

is given over the seismogeological line. The water depth varies from tens of meters on the shelf to ~4.5 km in the most submerged areas.

The multiple event on the shelf interferes with the reflection from the bottom; its influence leads to a change in the recording format and the appearance of independent lineups that prevent the dynamic image of the record in the upper QSSS from being observed. On the De Long Uplift slope and further, when the bottom is submerged, starting from stake 280 (AR1402), multiple event reflections are observed in the tracing region of marker reflectors. Gradually they cross all the reflectors in the south of the eastern part of the Podvodnikov Basin. Reflector intensity, apart from reflectors JU and PU, remains higher than that of the multiple event, so the multiple event introduces significant distortion into the dynamics of only 2, 3 lower QSSS. Probably, its influence does not enable us to confidently follow reflectors PU and JU here. Nevertheless, the strata between reflectors Af-JU give us this possibility, and we distinguish the lowest QSSS between reflectors Af-PU. Near stake 580, the multiple event goes beyond the correlated sedimentary cover and can be traced below reflector Af at ~7.5 s.

The section along AR1402 and AR1406 lines gives an idea of the structure and characteristics of the sedimentary cover in the transition from the East Siberian Sea shelf to the Arctic Ocean.

The sedimentary cover, composed of the Carboniferous, Middle Permian, Upper Permian-Middle Jurassic, Upper Jurassic-Valanginian, Lower Cretaceous (Hauterivian-Barremian), Upper Cretaceous and Cenozoic seismic complexes, unconformably overlaps the heterogeneous basement top.

The stratigraphic framework of the Pre-Cenozoic part undergoes significant changes: the greatest thicknesses are quite naturally recorded within the Zhokhov Basin and the eastern part of the Podvodnikov Basin (up to 7–8 km). The oldest rock sequence composed of Carboniferous-Middle Permian sediments is enclosed between the basement and the PU unconformity. It is mapped only within pickets of 700–725 km in the north of the East Siberian Sea. According to calculations, the layer velocity is not high: 4.5 km/sec, but the existence of serious fault tectonics, large depths of occurrence, and inconsistency of parallelism in sequence boundaries could affect the velocity determination.

Composite line AR1406–AR1402, based on the sequence completeness, illustrates the existence of two basement types: A and Af. On the Lomonosov Ridge and in the Makarov Basin, younger basement is traced—A. The basement topography is rugged unstably; velocities in this type of basement range from 2.9 to 4.4 km/s. Based on the stratigraphic framework of the sedimentary cover (2 Cretaceous QSSS), it is the Cimmerian folded basement. Basement Af is confidently mapped in troughs—the eastern part of the Podvodnikov and Zhokhov basins—and poorly on the Toll Saddle and in the De Long Uplift region. It is characterized by brighter lineups, consistent nature of the record, from which one may conclude that it is ancient. This conclusion is supported by the computation of kinematic characteristics: velocity in the basement reaches 5.0 km/s and more. Judging by the stratigraphic framework of the sedimentary cover, it is the Ellesmerian folded basement. On the Toll Saddle, a train of intense low-frequency reflections is observed at the base of the Upper Cretaceous QSSS, which, together with the magnetic data, can be associated with basaltic covers, acting as screens for tracing underlying slightly folded sedimentary rocks. This assumption confirms the single value of reservoir velocity observed below this train, 4.0 km/s (probe 1406_08), which is not typical of the basement. Weak folding with strong fault tectonics hinders tracing of the basement on the De Long Uplift as well. On the Lomonosov Ridge, below the young Cimmerian basement, strong low-frequency reflections can be traced sporadically, which could be associated with a more ancient basement. This fact may indicate that the Cimmerian folding on the Lomonosov Ridge becomes weaker in the north, near the pole.

The thickness of the Upper Permian-Cretaceous sequences is characterized by velocity variability, but velocity differences are stable for each QSSS: Upper Permian-Middle Jurassic (top-JU reflector) is about 4.3 km/sec, Upper Jurassic-Valanginian (top-reflector LCU) is 3.5–4.2 km/sec, Lower Cretaceous (top-reflector BU) is 3.0–4.0 km/sec, Upper Cretaceous (top-reflector pCU) is 2.6–3.5 km/sec.

The Cenozoic part of the sedimentary cover (deposits to reflector pCU) on composite line AR1402–AR1406 is usually conventionally presented by 4 QSSS. Thickness of these complexes varies in different structures; the stratigraphic framework remains consistent almost throughout the studied line, except for individual sections in the continental slope area (stakes 400–500, line AR1402), Toll Saddle

(stakes 60–135, line AR1406) and the Lomonosov Ridge (stakes 645–756, line AR1406). There are failures in record due to major tectonic movements. Reservoir velocities and thickness regularly increase in depressions.

Cenozoic rocks are widespread almost everywhere, their thickness reaches 4 km, as compared to the underlying complexes. They are practically unaffected by serious fault tectonics, whose activity in the Cenozoic faded out. The lowest velocities are recorded in the QSSS, limited by the RU reflector and the sea floor, their values do not exceed 2.0 km/sec, the wave field of the sequence is essentially seismically transparent that is typical of pelagic sediments. Velocities in the Paleocene-Lower Miocene part of the section retain their values in the interval from 2.0 to 3.0 km/sec.

Within the Mendeleev Rise, above the acoustic basement, there is a group of clear low-frequency reflections, which are supposedly related to effusives, i.e., a basaltic formation. Its presence there can create a sort of a screen for mapping underlying layers, which allows one to assume older deposits in the section. Therefore, the boundary between the older (Af) and younger (A) basements, most likely, passes to the area of Picket 375 on AR1406 line.

Composite seismic line ES10z08-AR1403 (Figs. 14 and 15). The composite section consists of two seismic lines located at a distance of 191 km; on the sketch map, this interval is shown in pecked lines. The line takes its beginning in the southwest of the East Siberian Sea shelf (ES10z08) and crosses it strictly northwards. Further, the section characterizes the De-Long Uplift area, the Eastern Podvodnikov Basin, and a small part of the Mendeleev Rise. More detailed ranking of the structures is shown above the section. The water depth varies from tens of meters on the shelf to more than 2 km within the basin.

ES10z08 line was shot by OAO DMNG in 2010. During the CDP-reflection studies, the following tools were used: SEAL recorder, Sercel seismic towed streamer with a working part length of 7950 m, Bolt 1900 airguns (total volume of 4000 in.^{3}), the record length was 12 s; the achieved record fold was 106. The line underwent standard processing graph.
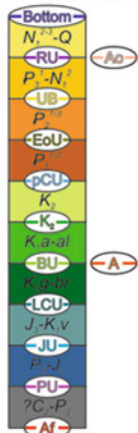
AR1403 line was shot by OAO MAGE in 2014 from the R/V "Akademik Fedorov". The CDP-reflector technique included APG BOLT-8500 sources; operating volume of 1300 in.^{3}, Sercel SEAL Fluid towed streamers of 24 bit and 4500 m long; the
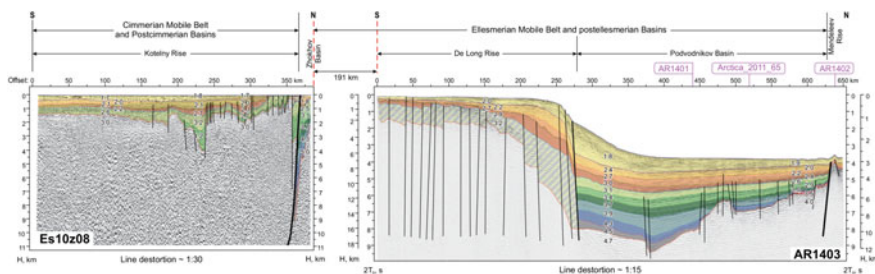
Fig. 14 Seismogeological section of composite line ES10z08 (375 km)–AR1403 (642 km)
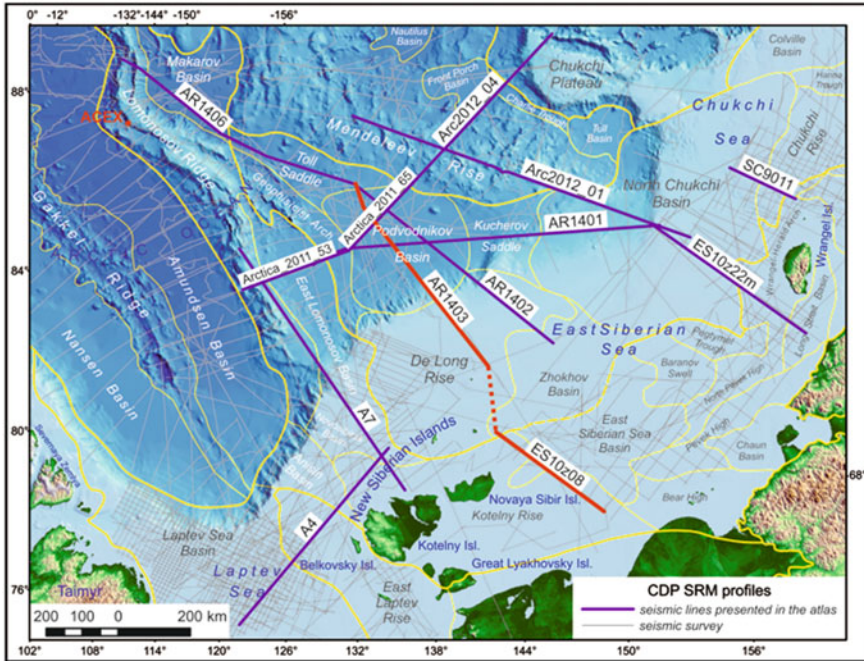
Fig. 15 Scheme of location and legend for CDP seismic profile and geological–geophysical section of the line ES10z08 (375 km)–AR1403 (642 km)

distance between the sources was 50 m, the group interval was 12.5 m. The line underwent standard processing graph.

The composite section along Es10z08 and AR1403 lines illustrates the structure of and variations in individual intervals of the sedimentary cover on the East Siberian Sea shelf and in the zone of its juncture with the Arctic Ocean. The sedimentary cover, composed of seismic sequences of different age, unconformably breaks out the heterogeneous basement top.

The water depth on the shelf does not exceed the first tens of meters; on the De Long Uplift it reaches 150 m; maximum values of 2–2.7 km are observed in the submerged part of the Podvodnikov Basin. The multiple event on the shelf has a short time delay, so its influence does not lead to any changes in the recording format and the appearance of independent lineups. On the De Long Uplift and further when the bottom is submerged, starting from stake 210 (AR14-03), multiple event reflections are observed in the tracing region of marker reflectors. Gradually they cross all the reflectors in the south of the Eastern Podvodnikov Basin, however, they do not bring significant distortion. Reflectors intensity remains higher than that of the multiple event. Near stake 450, the multiple event travels beyond the correlated sedimentary cover (below reflector Af) and goes down at 7.5 s.

The line can be conditionally divided into 4 main areas: a shelf area (Es10z08), where a young basement is observed and the Cenozoic and Upper Cretaceous sediments are present; an area of the Zhokhov Basin or the thrust region, where the basement is more ancient and judging by the amount of sediments (from the Carboniferous-Middle Permian to the Cenozoic inclusive)—Ellesmerian; the De Long Rise has an ancient basement with the pre-Cenozoic non-dismembered cover; the Podvodnikov Basin with the Ellesmerian basement and complete stratigraphic framework of sediments. On Es10z08 line in the area of stake 300, a transition from the younger folding to an older one is recorded. This transition is characterized by a change in the reflection from the basement: more stable reflection replaces the inexpressive reflection, which was often identified from changing the seismic record. In addition, kinematic properties also change: at stakes from 0 to 300, the basement rocks velocities vary within 3.6–4.8 km/sec, whereas in the north of the line, velocities increase to 5.6–5.8 km/sec. This allows concluding that the rocks underwent substantial reworking under increased pressure and temperature. To the south of the line, the consistent thickness of Upper Cretaceous-Cenozoic rock sequences is recorded.

The wave field of AR1403 line demonstrates structures of the De Long Uplift and the Eastern Podvodnikov Basin. The total thickness of the sediments in the Eastern Podvodnikov Basin reaches 9 km; and in the section, all QSSS are typical of the region: from the Carboniferous, Permian to the Cenozoic. On the De Long Uplift, the number of identified sequences does not exceed five; the greatest thickness is typical of sediments (below the reflector pCU), which can presumably be dated to a sufficiently large time interval from the Carboniferous to the Upper Cretaceous. They cannot be differentiated to sequences because of complex seismogeological settings.

In general, the Cenozoic part of the sedimentary cover (sediments to reflector pCU) on composite line **ES10z08-AR1403** is conventionally presented by 4 QSSS. The thickness of these complexes varies in different structures; the stratigraphic volume remains consistent almost throughout the studied line.

The Pre-Cenozoic part of the sequence on composite line ES10z08-AR1403 is not present everywhere. A bulk of these sediments is observed to the north, after the transition from the relatively young folding to the more ancient one (stake 360, line Es10z08). The thickness and stratigraphic framework both on line Es10z08 and on line AR1403, are variable and depend on the structural setting. The pre-Cenozoic deposits reach their maximum thickness in the Zhokhov Basin (Es10z08) and in the Eastern Podvodnikov Basin (AR1403), they are 8 and 7 km, respectively. Reservoir velocities start at 2.9 km/s and naturally increase with depth, reaching 5.6 km/s.

According to the seismic record, major faults emerged during the basement formation, then the tectonic movements renovated (at the boundary between Mesozoic and Cenozoic deposits, in the mid-Miocene and, in some cases, in recent time).
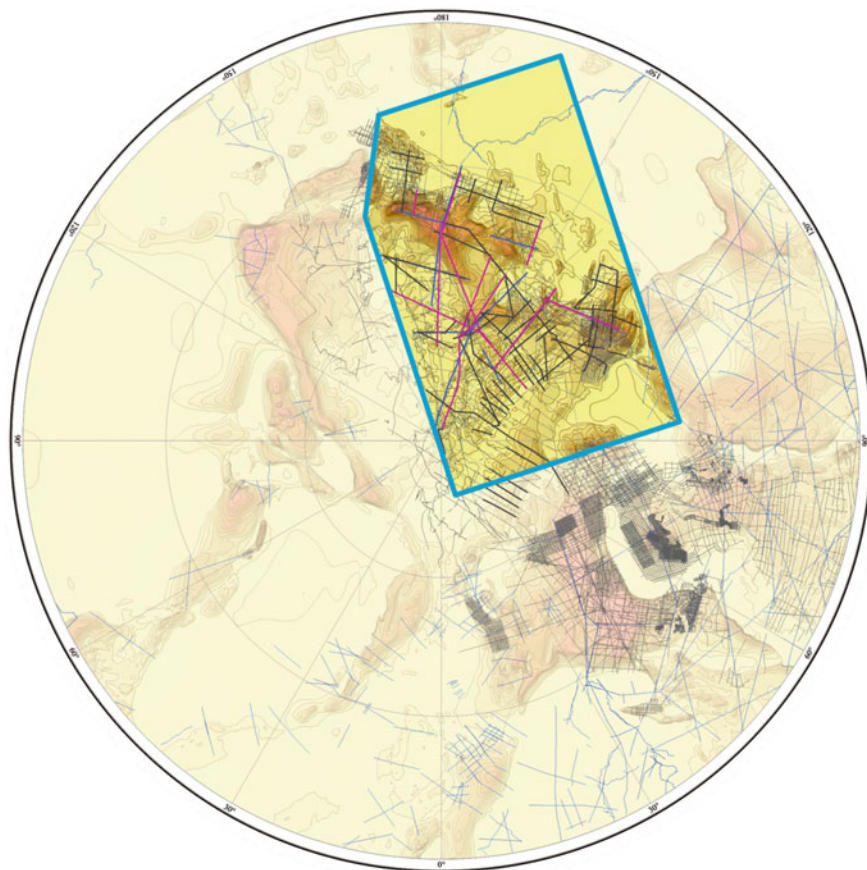
2   Structural Maps of the Eastern Arctic

Structural maps of the Arctic northeast of the Russian Federation were constructed on the basis of the framework of the seismic profiles of the CDP seismic reflection method, created on a single stratigraphic model covering the entire region (Fig. 16). At the first stage, temporary maps were constructed, which were then transformed into depth maps using a velocity model obtained by analysing the sensing data (201 sondes) and velocity profiles recently constructed using modern field and processing techniques. When constructing the velocity model, a number of discrepancies in the velocity values between the sensing data and the CDP section data were detected, which were eliminated in a detailed velocity analysis, revealing the most common patterns. According to the similarity of the average dependencies of Vrms and Vint on depth and time, the sedimentary basins of the North Arctic Ocean can be divided into 2 groups.

The first of these includes the Eurasian and East Lomonosov basins, the basin of the Makarov, and, in part, the Lomonosov ridge. The upper, Cenozoic, part of the section in these basins has lower velocities. On the lower part of the section and the basement in the Makarov Basin, as well as on the Lomonosov ridge, V int is less than in similar quasi-synchronous depositional seismic zone of this group.

The second group combines the basins of the North Chukchi and Podvodnikov, Charlie's trough and the Chukchi Plateau. In these elements, the thickness and depths of the QSSS, respectively, vary greatly, but in general, have higher V int values than in the sedimentary basins of the first group. Nevertheless, from the analysis of the velocity characteristics of the sedimentary basins of the Arctic Ocean, it follows that, with small-scale constructions, only one averaged V curve for the studied structures can be used to calculate the depths (Daragan-Suschova et al. 2017).

Fig. 16 Seismic profiles of the CDP seismic reflection method that was used for construction of structural maps of the Arctic

2.1 Acoustic Basement Structure Map

At the regional scale, the relief of the acoustic basement surface allows clear recognition of a number of large deep-sunken basins and extensive relatively raised massifs (Fig. 17).

The Laptev Sea sedimentary basin, which occurs on a heterogeneous, mainly Late Cimmerian basement, consists of three parts: Offshore Taimyr Rise, East Laptev Rise and the Central Laptev belt of relatively narrow depressions separated by horsts, disrupted by numerous tectonic dislocations of submeridional or north-western strike. Within the rises, the basement occurs at a depth of 1 to 3–4 km. In the Central Laptev belt, the basement depth reaches 10–13 km; in adjacent uplifts, the depth may be reduced by a factor of two–three. This creates a distinctly contrasting relief of the
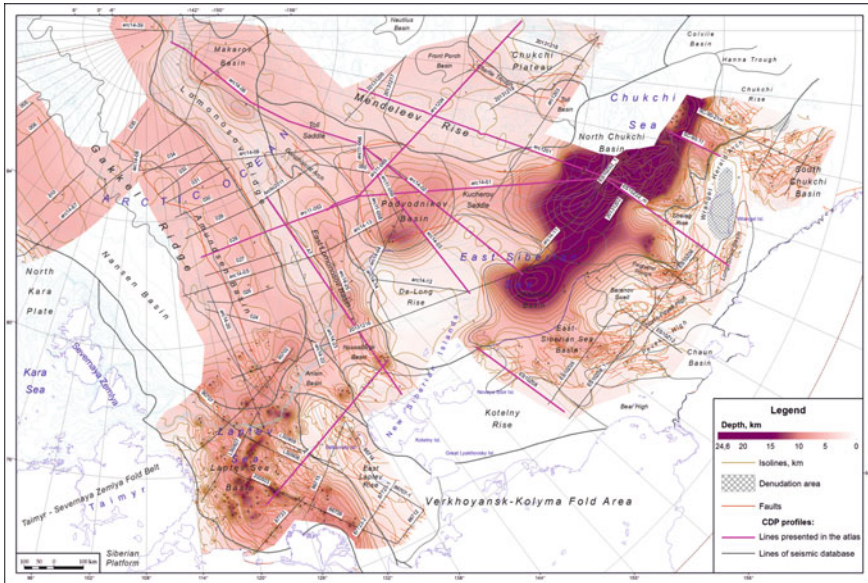
Fig. 17 Acoustic basement structure map

acoustic basement surface. Any sufficient reasons to suggest that structural elements of the named belt were formed by the processes of rifting are so far absent.

The Eurasian sedimentary basin occurs on a predominantly oceanic basement. At the basement's roof level, the boundary with the Laptev Sea Basin is conditional. The Eurasian Basin is subdivided into two basins: Nansen and Amundsen, separated by the Gakkel Ridge. The Nansen Basin is more submerged (down to 10 km or even more). At the centriclinal closure of the Eurasian Basin, an extensive belt of depressions is located: there the basement roof's depth often reaches 9–10 km. The continuation of the Amundsen Basin onto the land is the Anisin Depression. On the Gakkel Ridge, the basement roof occurs close to the sea bottom surface, only in places plunging to a depth of 1–1.5 km.

The East Lomonosov Basin comprises a structure elongated in the NNW direction, traceable from the island of New Siberia to 84 °N and laid over a Cimmerian basement. It consists of three troughs from 6 to 8 km in depth, separated by saddles. It is separated from the Amundsen subbasin by the folded-block Lomonosov uplift (ridge), which is clearly expressed in the relief of the basement, since its plunge depth is 4–5 km shorter than in adjacent negative structures. The Lomonosov Ridge is connected to the Kotelnichesky uplift through the bridge (saddle).

The Western Podvodnikov sedimentary Basin is a NNE stretched structure. It can be traced from the New Siberia Island up to 84 °N, occurring on the Cimmerian basement. The Basin comprises three depressions with depths ranging from 6 to 11 km and separated by saddles. It is separated From the Amundsen Basin by the

Lomonosov Ridge, clearly pronounced in the basement relief: its depth here is by 5–8 km lesser than in adjoining. The Lomonosov Ridge is connected with the Kotelny Rise through the saddle.

The Eastern Podvodnikov sedimentary Basin is as deep as the Western, but its shape is close to isometric or slightly elongated northwestwards. The Geophysicists Spur and the De Long Rise separate the basin from the mentioned depressions. In the central part of the De Long Rise, the basement occurs at absolute altitude of 1 km or less.

The Makarov sedimentary basin is located in the subpolar part of the territory. Its deepest part (5–8 km) is bounded by, most likely, typical faults. Southwards, through a complexly structured saddle, it neighbors with the above mentioned Basin.

The North Chukchi sedimentary Basin is the most extensive and deepest in the Eastern Arctic. It is surrounded almost entirely by well pronounced rises: Mendeleev and Chukchi—in the north, De Long—in the west, Kotelny, Baranov and Wrangel-Herald—in the south. It is separated from the Eastern Podvodnikov Basin by a broad, weakly marked Kucherov saddle. It occurs upon the Late Caledonian (Ellesmerian) basement, whose depth reaches 20 km in the eastern half, while in the west it does not exceed 15 km.

In the southeastern part of the territory, a number of rift-like depressions have been revealed: the basement's roof depth in those varies from 1–4 km (South Chukotka Depression) to 7–9 km (Denbar Depression). The basement's age in all these structures is Late Cimmerian (pre-Albian).

2.2 Top Cretaceous Structure Map (Reflector pCU)

The general structure of the region along the Cretaceous sediments roof (reflector pCU) remains approximately the same as that along the acoustic basement roof (Fig. 18).

The extent area of the reflecting horizon pCU is mainly increased due to the emergence of thick Late Cretaceous strata in the west Laptev Shelf and almost ubiquitous appearance of the Upper Cretaceous in the area of the Recent Mendeleev Rise and Lomonosov Ridge. Eurasian and Makarov basins and the western part of the Laptev Sea are the most submerged and contrasting structures. By the beginning of the Cenozoic, the Lomonosov Ridge and Mendeleev Rise were not so contrasting structures, although the large Amundsen, Podvodnikov and Makarov sedimentary basins, which separated them, already existed.

In large sag structures, the greatest absolute depth of subsidence of the basement typically occurs in the Laptev Sea sedimentary basin, often reaching 6–8, sometimes up to 9–10 km, especially in its northern part, where it neighbours the Eurasian Basin. The junctures of its central part with the surrounding in the east and west are the most contrasting: within those uplifts, an erosive surface of the reflecting horizon pCU is often cropped out.
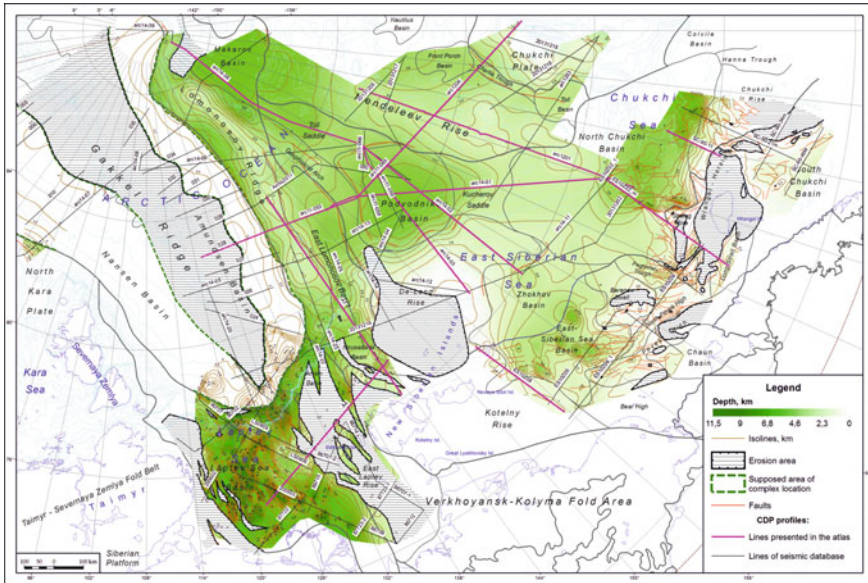
Fig. 18 Top cretaceous structure map (reflector pCU)

The junctures are expressed by tectonic benches, the amplitude of which can reach 2.5–3 km. The structural plan of the pCU surface is complicated and is associated with NNW blocks and with structures crossing them. There are no reliably traceable long structures that could be classified as riftogenic.

Within the Eurasian Basin, the centriclinal belt of depressions and troughs is even more distinct: their depth often reaches 8–10 km. Absolute marks of the acoustic basement in the Nansen and Amundsen sub-basins are significantly different, but the same marks for the surface of the reflector pCU are substantially leveled (Line AR1407). In the Makarov Basin, the depth of the reflecting horizon pCU is also significant down to 6–7 km.

The Lomonosov Ridge is characterized by high position of the reflecting horizon pCU usually not deeper than 2–2.5 km in the most elevated blocks, which is 2–4 times shallower than in the adjacent depression structures (Amundsen Basin and the Western Podvodnikov Basin).

There are 4 or 5 large elevated blocks, divided by saddles pronounced to a different degree.

Basins in the eastern part of the region are characterized by a much shallower depth of sagging of the Cretaceous deposits roof than in the west. E.g. in the North Chukchi Trough, it is commonly 3–4 km. Almost the same depth is recorded in the western part of the Podvodnikov Basin and, on average, somewhat larger depth is typical of the eastern part of the same basin. The North Chukchi sedimentary basin gradually passes to the East Siberian (Melville) Basin. Within the latter, there are several linear rift-type negative structures (Denbarsky, Pentymelsky troughs, etc.), where

the depth of the reflector pCU reaches 3.5–4 km. As with the acoustic basement, the submeridional Charley Basin divides the Mendeleev and Chukchi Rises. Elevated blocks, in particular, the De Long and Wrangel-Herald Rises are more pronounced in the structure of the eastern part of the region.

2.3 Eocene Structure Map (Reflector UB)

The structure of the region recognized along the reflecting horizon UB is largely similar to that for the reflecting horizon pCU (Fig. 19).

The Oligocene base has not been recorded in the Lomonosov Ridge, Geofizikov Spur, the De Long, East Laptev and Wrangel-Herald rises. The greatest depths of the reflecting horizon UB have been recorded in the Amundsen and Nansen basins, in the Makarov Basin and at the outer limit of the Laptev Shelf. The area of the sedimentary basin of the Laptev Shelf is significantly reduced. Moderate depths of the reflecting horizon have been identified in the Podvodnikov, North Chukchi and Front Porch basins. On most of the shelves of the East Siberian and Chukchi Seas and in the South Chukchi Basin, the depths do not exceed first hundreds of meters. There has been a clear tendency for the submergence of the reflecting horizon UB towards the center of the Arctic Ocean.

Main tectonic elements remain in the former position and often retain their size and configuration.
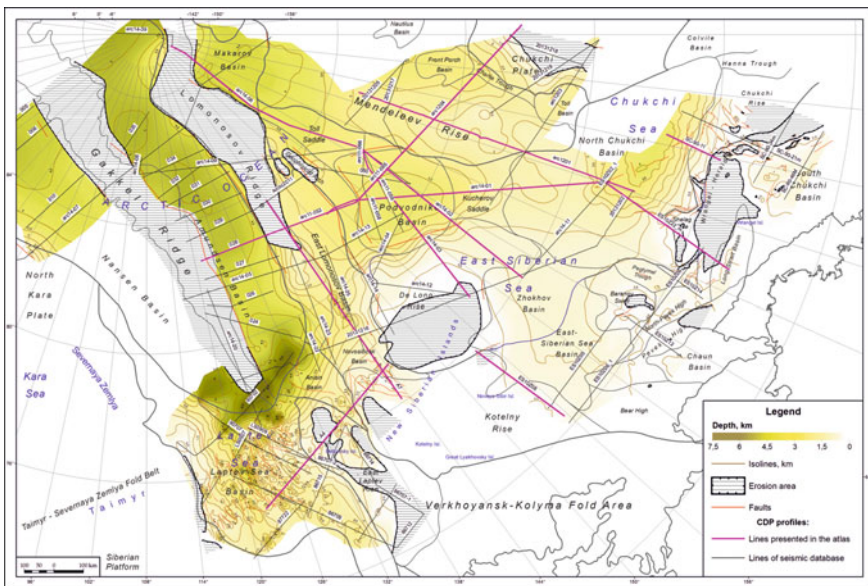

Fig. 19 Eocene structure map (reflector UB)

In the southwestern part, the moderately submerged (2–4 km) Laptev Sea Basin occurs with an expected noticeable increase in the depth directly behind the present day edge of the continental shelf.

A belt of centriliclinal negative structures of the Eurasian Basin is clearly seen; the isolated depressions of this belt generally retain their position in relation to the structural plan of the reflecting horizon pCU. Within the limits of the basin, the greatest sagging of the roof of the Eocene sediments is still observed in the subpolar regions of the Amundsen Basin, as well as in the Nansen Basin north of 82 °N (Profile AR1407). There, the UB reflector sagging reaches 5.5–6 km. In the Makarov Basin, the Eocene sediments roof occurs around the same depths.

Approximately at the same hypsometric level, the Eocene sediments are located in the Western and Eastern Podvodnikov Basins. The Geophysicists Spur, a long positive structure that divides them, loses its expressiveness, especially in the southern part, which is connected with the De Long Rise; there, the Western and Eastern Podvodnikov Basins merge into one.

The reflecting horizon UB in the North Chukchi Basin, though significantly submerged (down to 3.7 km), is expressed to a lesser degree in its western part, where it joins the East Siberian (Melville) Basin. In the latter, there are still both negative and positive structural elements: Denbarsky, Pegtymelsky Grabens, Baranovsky Rise and others.

The systems of De Long and Wrangel-Herald rises are sharply defined. Within their limits, the thickness of the Upper Cenozoic sedimentary cover often does not exceed the first hundreds of meters, and in large areas, the reflector UB is not traced, as it is cut by erosion (Lines AR1412, Arc2012_16, ES10Z23_m, etc.).

References

Daragan-Sushchova LA, Kopylova AV (1990) Empirical dependences of reservoir velocities on the depth of subsidence of seams from the data of borehole studies and marine seismic survey. Geophysical methods of studying the shelf and the continental slope. Leningrad, pp 28–31 (in Russian)

Daragan-Sushchov YuI, Daragan-Sushchova LA, Poselov VA (2002) Problems of sedimentary cover stratigraphy of the Eurasian basin, the Arctic Ocean. Geol Geophys Characteristics Arctic Lithosphere 4:103–113 (in Russian)

Daragan-Sushchova LA, Petrov OV, Daragan-Sushchov YuI, Rukavishnikova DD (2010) New insight into Laptev Sea sedimentary cover geology. Reg. Geol.Metallogeny 41:5–16 (in Russian)

Daragan-Sushchova LA, Sobolev NN, Petrov EO, Grinko LR, Petrovskaya NA, Daragan-Sushchov YuI (2014) On substitution of stratigraphic control of reference seismic horizons in the East Arctic Shelf and in Central Arctic Uplifts. Reg. Geol. Metallogeny 58:5–21 (in Russian)

Daragan-Sushchova LA, Petrov OV, Sobolev NN, Daragan-Sushchov YuI, Grin'ko LR, Petrovskaya NA (2015a) Geology and tectonics of the northeast of the Russian Arctic (according to seismic data). Geotektonika 6:3–20 (in Russian)

Daragan-Sushchova L, Grinko L, Petrovskaya N, Daragan-Sushchov Yu (2015b) On the problem of stratigraphic assignment of the key seismic horizons on the East-Arctic shelf and in the area of Central Arctic uplifts. Am J Geosci 5(1):1–11. https://doi.org/10.3844/ajgsp.2015.1.11

Daragan-Suschova LA, Chitailo DM, Zimovsky AV (2017) High-speed analysis of sedimentary basins of the Arctic Ocean. Reg. Geol. Metallogeny 71:67–74 (in Russian)

Malyshev NA, Nikishin VA, Nikishin AM (2012) New model of geological structure and history of formation of the North-Kara sedimentary basin. Doklady Earth Sci 445(1):50–54

Petrovskaya NA, Savishkina MA (2014) Comparison of seismic complexes and major disagreements in the sedimentary cover of the shelf of the Eastern Arctic. Neftegazovaya Geol Theor Pract 9(3):1–26 (in Russian)

Petrovskaya NA, Trishkina SV, Savishkina MA (2008) Main features of the geological structure of the Russian sector of the Chukchi Sea. Geologija nefti i gaza. 6:20–28 (in Russian)

Sherwood KW (2006) Structure of Hanna trough and facies of Ellesmerian sequence, U.S. Chukchi Shelf Alaska. Geol Soc Am 38:85–85. http://eurekamag.com/research/020/134/020134529

Geological and Paleogeographic Map of the Eastern Arctic

O. V. Petrov, E. O. Petrov, N. N. Sobolev, D. I. Leontiev, and V. N. Zinchenko

Abstract The Atlas summarizes geological and geophysical data acquired in recent years while preparing the 1:1 M State Geological Map of the Russian Federation and the implementation of the international project *Atlas of Geological Maps of the Arctic*. A set of tectono-stratigraphic charts has been produced for Arctic islands (Severnaya Zemlya Archipelago, New Siberian Islands, Wrangel Island) and the continental land (Taimyr Peninsula, Northeast Eurasia). Results of the latest studies, including international ones, on the determination of main stages of tectonic evolution in Arctic regions, specification of petrological composition and age of sedimentary and igneous complexes, as well as paleogeographic and geodynamic setting of their formation for each tectonic stage have been taken into account. A set of maps including the 1:5 M Geological Map, Tectonic Map, Paleogeographic maps for age levels was prepared based on a comprehensive analysis of seismic data and geological studies for the North-East of the Russian Federation and adjacent water areas. The general pattern in geology of the studied area has been identified; it is reflected in the gradual change of the Cretaceous fold area to the Baikalian and *Elesmerian* fold areas in the northern direction. On the Mendeleev Rise, Precambrian consolidation block is reconstructed from results of bottom stone sampling. Main tectonic structures of the East Siberian shelf are traced to the deepwater part of the Arctic Ocean. Cretaceous movements were most pronounced in the junction zone of the Canada Basin and the Wrangel-Geraldine Block, where a thick thrust zone and the North Chukchi Foredeep are formed. To the west, on the De Long Islands and Kotelny Island, the Cretaceous dislocations are much less pronounced; here, the structural geometry that formed in the Late Paleozoic is preserved.

O. V. Petrov (✉) · E. O. Petrov · N. N. Sobolev · D. I. Leontiev · V. N. Zinchenko
Russian Geological Research Institute (VSEGEI), 74 Sredny Prospect, St. Petersburg 199106, Russia
e-mail: vsgdir@vsegei.ru

1 Eastern Arctic Geological Map at Scale 1:5 M

The geological map of the eastern Russian Arctic (Figs. 1 and 2) was compiled based on the 1:1 M seamless geological map. In addition to the materials of the sheet-by-sheet State Geological Map-1000, it also includes results obtained during international expeditions to the Arctic islands in 2011 and 2013, as well as data stored in the first database on seismic lines built using CDP seismic reflection method and DSS.

The geological map is based on the geological legend, which contains correlated stratified mapped units on land and seismic units in water areas of the northeastern seas. The fact that the compiled integrated digital model contains all available geological and geophysical information on the area made it possible to proceed to the compilation of the 3D interactive geological map of the eastern Russian Arctic.

The geological map of the eastern regions of the Russian Arctic incorporates two areas—water and continental (together with island land)—which have been unequally covered and studied. The water region was relatively poorly studied in comparison with the continental area; basic information on the geological structure of this area was obtained from the analysis of wave fields of seismic lines and the study of bottom rock material. Practically no drilling took place in the water area, except for the shallow ACEX well on the Lomonosov Ridge near the North Pole.
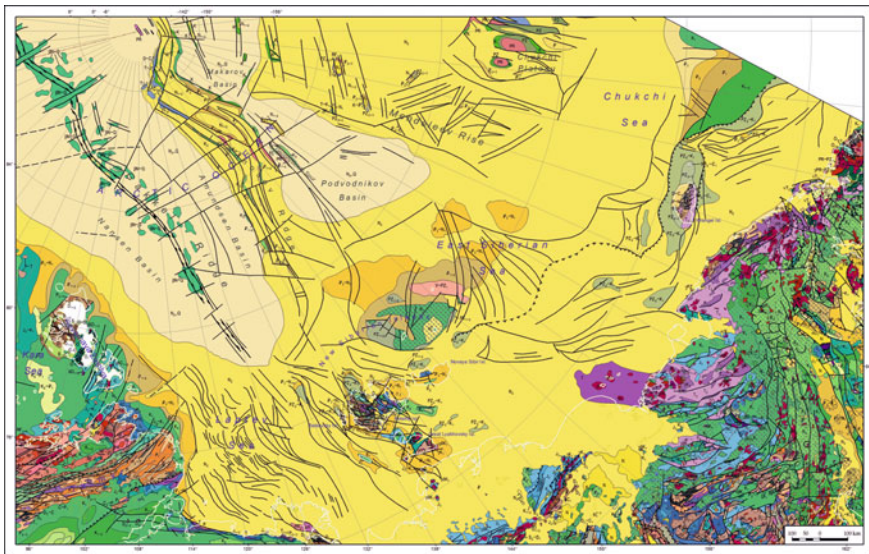

Fig. 1 Geological map at 1:5 M scale

Fig. 2 Legend of geological map at 1:5 M scale

The nearest offshore wells, which ground the stratigraphic correlation of seismic reflectors, are found on the Arctic shelf of Alaska.

The water area is subdivided into the abyssal zone of the Arctic Basin and the shelf zone of the Eurasian continent. According to the bottom sampling, the Archean granites and Proterozoic altered rocks are the most ancient formations in the Central Arctic Submarine Elevations region, on the Lomonosov Ridge, Geofizikov Spur, Alpha-Mendeleev Rise, and Chukchi Plateau. Upsection, the Middle-Upper Paleozoic carbonates and sandstones are noted among the sedimentary rocks, as well as the Mesozoic and Cenozoic mainly terrigenous sediments. The Eurasian and Amerasian basins are almost universally covered by pelagic sediments of Eocene-Quaternary age. In the central part of the Eurasian Basin, in the Gakkel Ridge region, volcanic formations, represented by N–Q basalt lavas, are mapped.

Shelf regions incorporate sedimentary basins of the Laptev, East Siberian, and Chukchi seas. Most of this area lies in the Late Mesozoic folding region, associated with the South Anuyi Ocean closure, subsequent orogenesis and rift-related
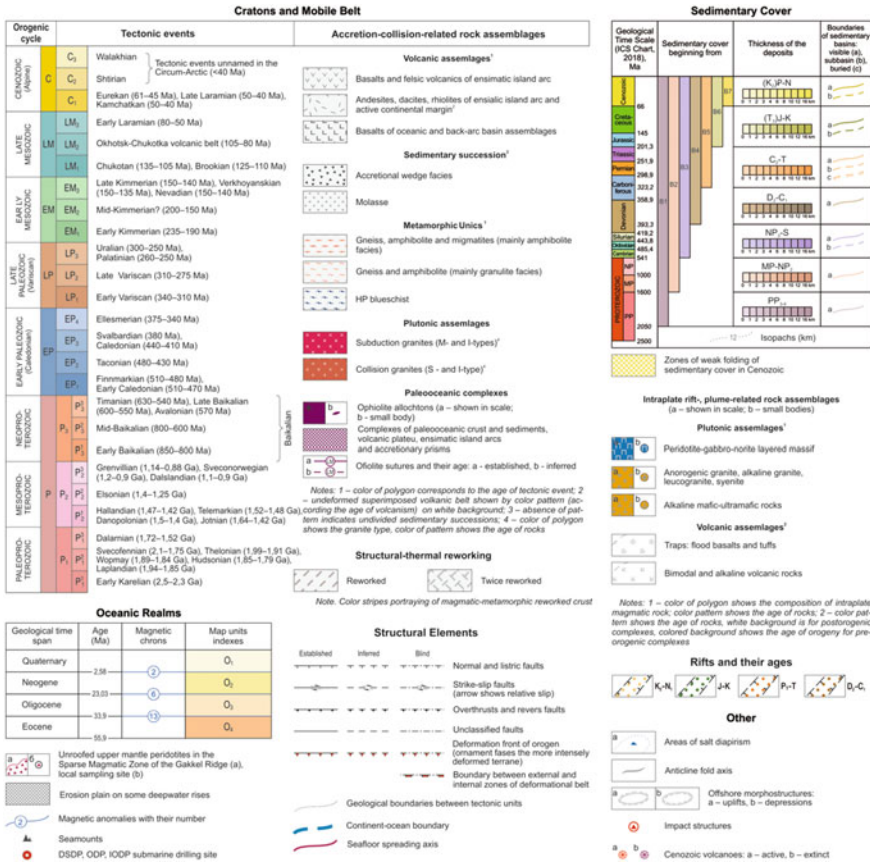
processes. More ancient sedimentary complexes, which emerge to the day surface of the New Siberian Islands, Wrangel Island etc. are disturbed to one degree or another. The structure of the Laptev Sea Basin is determined by rift-based processes of predominantly Cenozoic age; the earliest rift grabens presumably formed in the Late Cretaceous. These processes are probably genetically related to the Eurasian Basin opening.

2 Eastern Arctic Structural Geological Map

The tectonic map of the Eastern Arctic regions of the Russia and adjacent territories (Figs. 3 and 4) is based on the tectonic map of the Arctic (Petrov and Pubellier 2018).

The contemporary understanding of the tectonic structure and classification of the Eastern Arctic region is based on the extensive empirical material collected as a result of expeditionary and analytical studies conducted in recent years in Russia, including the active participation of VSEGEI, as well as the results of regional generalisations of retrospective data.

By virtue of the new seismic data, it was possible to significantly clarify the structure of the sedimentary basins and the structure of the earth's crust in the aquatorial region. Data from recent geological expeditions (including international ones) made it possible to substantiate the tectonic structure of the shelf areas of the Eurasian continental margin with the archipelagoes of the Arctic islands and the correlation with the structures of the continent and the deep-sea areas of the Arctic Ocean.

Fig. 3 Eastern Arctic structural geological map

Fig. 4 Legend for Eastern Arctic structural geological map

The structural-geological map shows hetero-chronous tectonic elements, including the modem Eurasian oceanic basin, mobile (folded) belts, cratons, modern and ancient sedimentary basins. The map also shows the material composition of tectonic subdivisions, namely rocks associations, appearing for indicators of geodynamic settings (accretionary, collisional, rift induced, metamorphic, plumes and related settings and complexes, as well as complexes of sedimentary covers).

In general, the following tectonic elements are allocated on the project area from the south-west to the north-east: the North-Asian Craton as a part of a fragment of the Siberian Platform and the Verkhoyansk fold and thrust belt; the vast mosaic mesozoid area covering the northern part of continental landmass, the shelf and the deep-water part of the Arctic Ocean, which presents a collage of terranes of different geodynamic types; the Caledonid (Elsmyrid) belt; and the Precambrian Mendeleev craton. The Late Mesozoic fold area within the project area includes the structures of the Verkhoyansk cover overthrust complex, the Verkhoyansk-Kolyma acrection

folded belt, the Chukotka-Novosibirsk folded area, the Okhotsk-Chukotka pluton volcanic belt and the northern part of the Koryak-Kamchatka folded area.

At the same time, structures of the last two areas are not observed on the shelf and in the deep-sea part of the Arctic Ocean. The sedimentary basins include geo-depressions performed by an undisturbed sedimentary cover having a thickness of 500–1000 m. The colour of the sedimentary basin reflects the beginning of the formation of the sedimentary cover, while the isopachites reflect the total thickness of the sediments.

3 Map of Tectonic Zoning of the Eastern Arctic Basement

The map of the basement subdivision displays areas of: (1) Mesozoic Late Cimmerian orogeny; (2) areas of Baikalide, which suffered tectonic reworking at the end of the Early Cretaceous; (3) areas of Late Caledonide (Ellesmeride) and (4) Precambrian Arctida Massif (Fig. 5). According to seismic data, the Baikalide structures are traced from the Kotelny Uplift to the southern part of the Lomonosov Ridge. It is for the first time that the Late Caledonides have been revealed in the De Long Archipelago: they can be traced northwards to the Geofizikov Spur and are also presumed in the North Chukchi Trough basement. Precambrian age of the Mendeleev Rise basement is supported by the analytical results of dredged bottom rock material.

Within the territory under consideration, the Precambrian continental Arctida Massif comprises the Mendeleev Rise and the western part of the Chukchi Plateau:

Fig. 5 Map of tectonic zoning of the eastern Arctic basement

these two are separated by the Charlie Trough of the Cretaceous–Cenozoic age. The boundaries of the Arctide Massif were refined using seismic data obtained by the expeditions Arctic-11 and Arctic-12. The study revealed that in the south and south-west this block is bounded by the epi-Ellesmerian North Chukchi Trough. The seismic data (profile Arc12-01) poorly show the southern boundary of the Mendeleev Rise. In the south-west, the Mendeleev Rise adjoins the North Chukchi Trough through a series of faults formed at the terminal Early—Late Cretaceous. The North Chukchi Through opens into the eastern part of the Podvodnikov Basin, separating the Mendeleev Rise from the Geofizikov Spur.

The Kotelny and Wrangel-Herald continental blocks are believed to be a part of the Chukchi-Novosibirsk fold belt. They are separated by depressions of the Cretaceous–Cenozoic age. First paleomagnetic studies (Vernikovsky et al. 2013) provided an important data for clarifying the continental Kotelny block boundaries, as well as studies of mantle xenoliths from the Cenozoic Zhokhov Island basalts. These studies allowed clarifying the northern boundary of the Kotelny block. The obtained results also suggest that the De Long Archipelago southern islands (Bennett and Zhokhov Islands) are constituents of the block, and its basement age is probably Neoproterozoic.

The boundaries of the continental Wrangel-Herald block have been refined applying results of regional seismic studies. At a regional scale, the continental Wrangel-Herald block is a part of the Wrangel-Herald-Brooks thrust-and-fold belt. According to the seismic data, this continental block includes the Wrangel and Tigar rises, and Herald Ridge. In the north it is separated from the North Chukchi Through by the Wrangel Fault, in the east—from the Chukchi Plateau, in the south and south-west by a series of normal faults—from the Aptian—Cenozoic basins: Pegtymel, Billins and Schmidt.

The location of the Chukchi-Novosibirsk fold belt southern boundary raises no questions: it lies along the South Anui Suture, which is pronouncedly expressed in anomalous magnetic field. However, the western boundary is debatable. Studies on the Belkovsky and Stolbovoy islands (Novosibirsk Islands Archipelago), which were carried out in 2011–2012, revealed that the Laptev Sea basement encompasses sediments similar to those of the Verkhoyansk fold-thrust belt. According to our data, a boundary between the Neoproterozoic Kotelny block and the Late Cimmerian Verkhoyansk belt lies between the Belkovsky and Stolbov Islands in the west and the Kotelny Island in the east. Study of sedimentary sections on the Belkovsky and Stolbovoy Islands proves that the Mesozoic structures of the Northeast continue to the Laptev Sea shelf.

4 Paleogeographic Maps of the Eastern Arctic

Paleogeographic reconstructions have been implemented for pre-oceanic and oceanic evolution stages of the Eastern Arctic and the adjacent basins. The paleogeographic maps are based upon the following body of information:

- results of regional seismic profiles;
- structural maps of main reflecting horizons and thickness maps charted for the Mesozoic and Cenozoic seismic complexes;
- lithology and facies studies carried out in the New Siberian Islands Archipelago and Wrangel Island;
- study of rocks dredged on the Arctic Ocean bottom rises;
- isotope geochronological study of sedimentary and magmatic rock complexes exposed on the Arctic islands, as well as dredged rocks and pelagic Arctic Ocean silt.

Reconstructions have been made for time intervals, corresponding to significant tectonic changes in the region (Fig. 6).

4.1 Late Jurassic Paleogeographic Map (−145 Ma)

The Late Jurassic—the beginning of the Early Cretaceous era (Figs. 7, 8 and 9). In the Amerasian sector of the Arctic Ocean, J_3-K_1 deposits in non-folded basins are revealed between reflecting horizons JU and BU. Here this complex is composed of clayey and sandy-clayey layers, sometimes with an admixture or individual thin layers of pyroclastics.

This complex occurs widely in the North Chukchi Basin, where its thickness exceeds, according to geophysical data, 4.5 km in the eastern part of the basin (profiles SC-90-11, SC-90-21M, etc.).

The complex is formed in a depression of foreland type: towards the folded region of the Wrangel-Herald Rise, the thickness of the complex rapidly decreases down to 1 km or less. Northwards, towards more rigid structures of the Chukchi Rise, it decreases more smoothly, reaching 1.5–2 km at the profiles ends. In the western part of the North Chukchi Basin (profile ES10z23m), the structures of the foreland trough are poorly pronounced. In the South Chukchi Basin, the J_3-K_1 complex makes a part of the acoustic (folded) basement.

According to geophysical data, presence of the considered complex is possible in deep grabens on the Mendeleev and Chukchi Rises (profiles Arc-01—south of the picket 24,000, Arc-03—stations 27,000–28,000, etc.) and in the eastern part of the Podvodnikov Basin (profiles 053-14, 065-14), where their thickness does not exceed the first hundred meters.

4.2 Early Cretaceous (Aptian-Albian) Paleogeographic Map (−112 Ma)

The Early Cretaceous, the Aptian and Albian Stages (Figs. 10, 11 and 12). During that time, the destruction of the Okhotsk-Chukotka Volcanic Belt rear part led to the
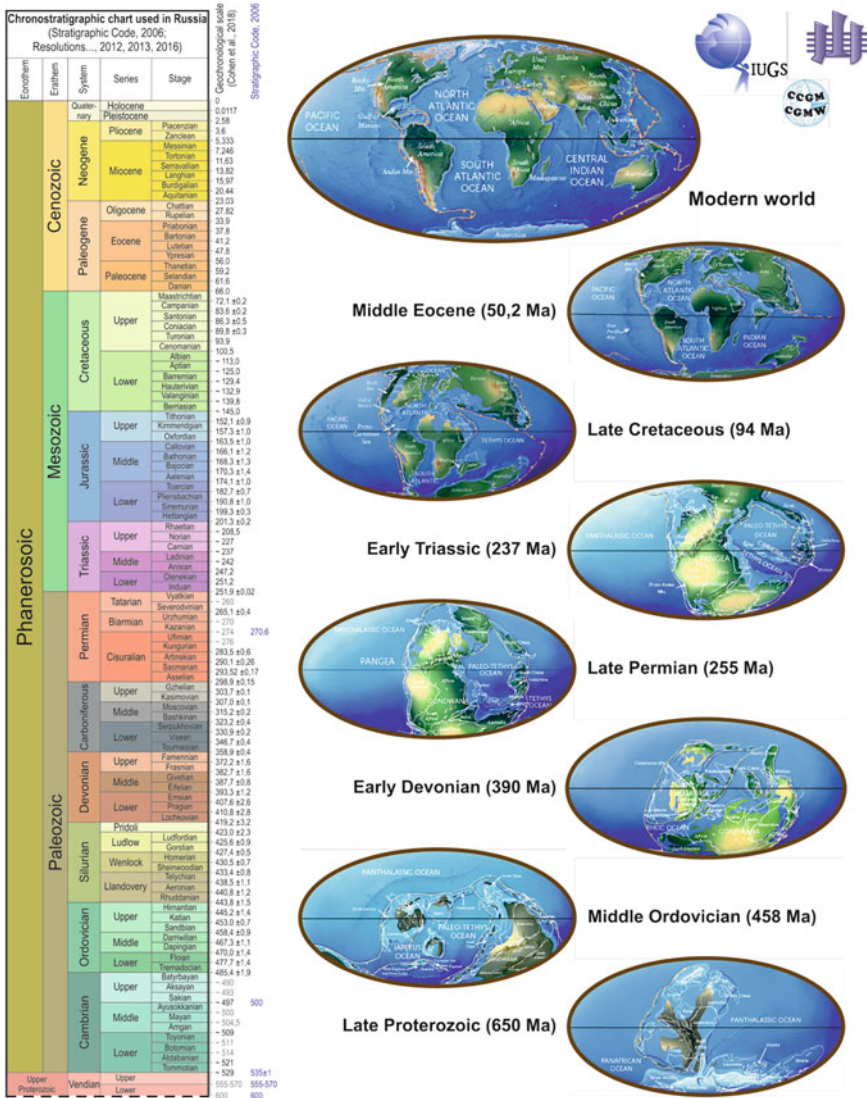
Fig. 6 Chronostratigraphic chart used in Russia and plate tectonic development of the ocean basins and continents of Ch.R. Scotese PALEOMAP project (http://www.scotese.com/earth.htm)

formation of deep-water depressions in place of previously existing seas and land areas, to which the North Chukchi Basin belongs. The following subdivision of the considered Basin into two parts is proposed. In the Aptian time, its southern part was dominated by shelf environments of clastic sedimentation, while in the north there was a deep-water basin. Compensation of this basin occurred with rapid sediments progradation from the south to north. The progradation wedges (clinoform complex)
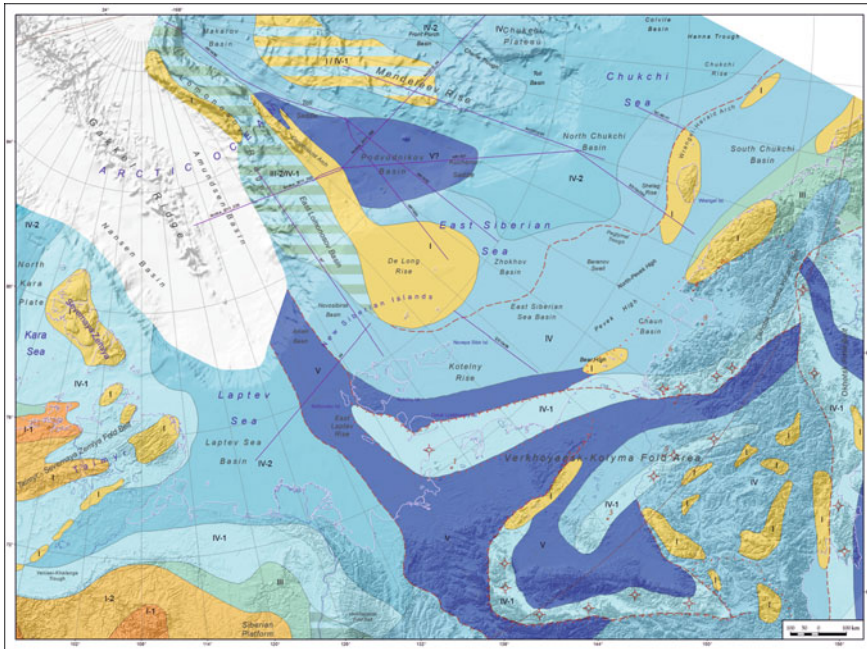
Fig. 7 Late Jurassic paleogeographic map (−145 Ma)

are distinctly seen in profile ES-10z23m. Approximate calculations show that the northward migration of the shelf edge occurred at an average rate of 7.0–7.5 m/Kyr. According to our assumptions, by the end of the Aptian Stage, the deep-water part of the North Chukchi Basin was largely compensated by sediments; in the Albian Period, a shallow water environment prevailed in almost all of its territory. The Aptian paleoshelf edge occurred more than 100 km northwards. The depths of the pseudo-abyssal basin can be estimated from the difference of altitudes of undaform and fondoform of the clinoforms; it reached about 1000 m, but could be even deeper. The Aptian–Albian deposits total thickness in the North Chukchi Basin reaches 3000 m. The presence of a discontinuous cover of thin Albian deposits in the Lomonosov Ridge is possible (seismic complex LR1-LR2, according to Kim and Glezer 2007); The Aptian sediments, most likely, did not accumulate. Over a significant part of the Mendeleev Rise and the adjacent Chukchi Plateau, the Albian and Aptian sediments are preserved in narrow graben-like structures. The Aptian Period was dominated by possibly hemipelagic sedimentation: mainly siliciclastic silts of various grain sizes, as well as siliceous–clastic and biogenic silts. Near the continental slope, the occurrence of sandy and silty "tongues" is quite possible. During the Albian Period here over the whole territory sedimentation occurred in sublittoral and moderately deep-water environments. The thickness of these deposits varies from the first to several hundred meters.

Fig. 8 Legend for Late Jurassic paleogeographic map

Legend for paleogeographic map

Environments

| I | Denudation relief |

| I-1 | High-mountain relief |

| I-2 | Low-mountain relief |

| III | Costal plains and shallow-water |

| III-2 | Costal and tidal plains, lagoons |

| III-3 | High salinity lagoons |

| IV | Shelf |

| IV-1 | Upper sublittoral (inner shelf, depth 80-100 m) |

| IV-2 | Lower sublittoral (outer shelf, depth 80-200) m |

| IV-3 | Deep water shelf (depth >200 m, average depth 500-700 m) |

| V | Deep water oceanic realm |

Other symbols

Synsedimentary faults

Environment boundaries

Volcanic deposits boundaries

A7 Seismic lines

Island arc volcanic complexes

3 Key sections
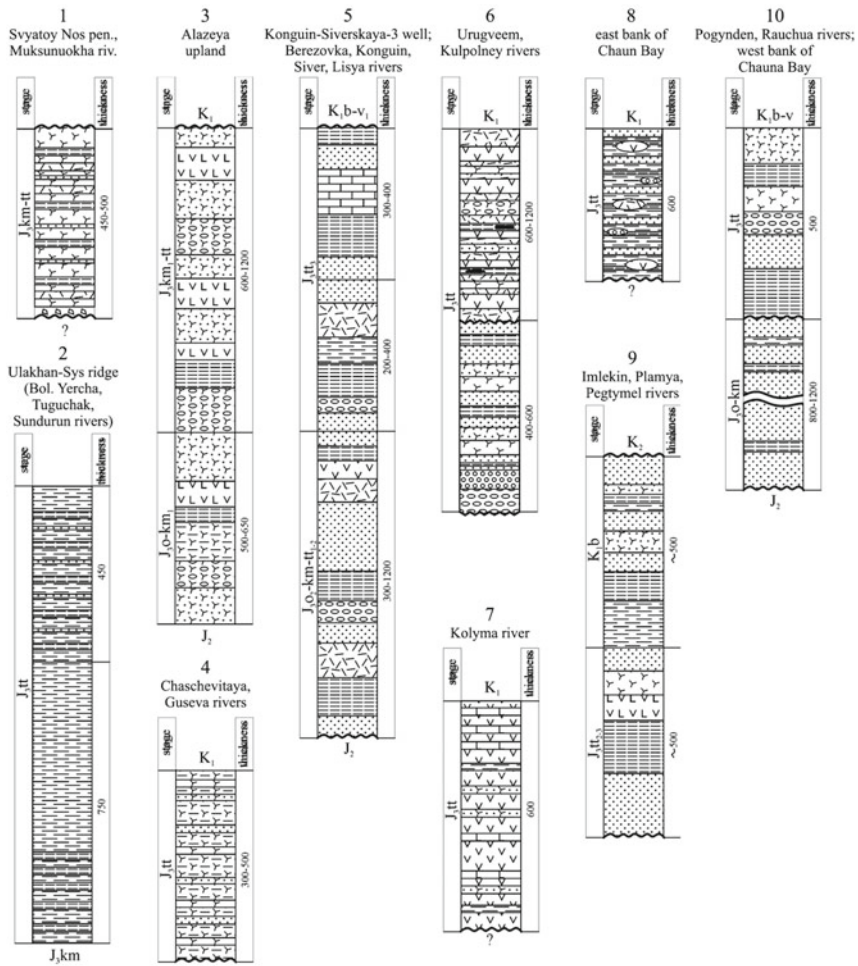
Lithological logs
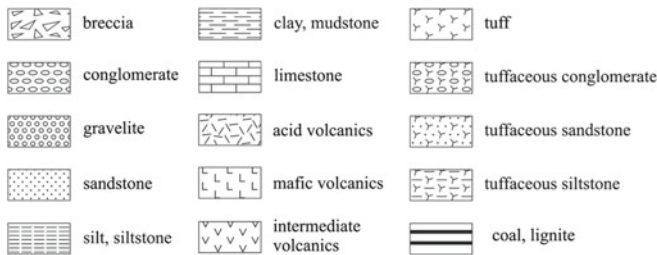
Fig. 9 Lithological logs
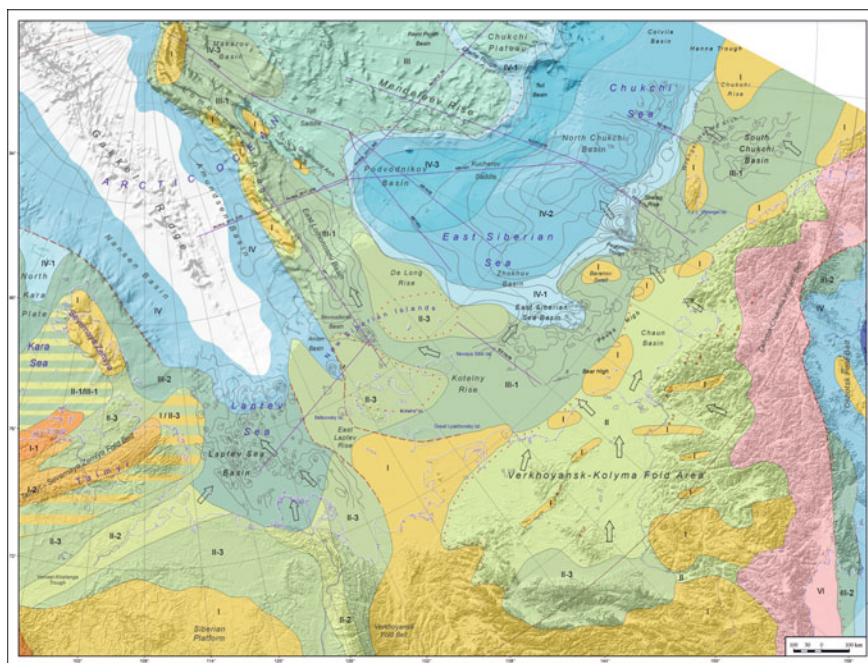
Fig. 10 Early Cretaceous (Aptian-Albian) paleogeographic map (−112 Ma)

The more complete sequences, judging from preliminary geophysical profiles correlation, are common in the Podvodnikov Basin, where the thickness of the complex in question may exceed 1 km (western end of Arc-03 profile and a part of the profile 053_14 between pickets 20,000 and 40,000). Accumulation of them in shelf and moderately deep-water sedimentation environments is assumed.

4.3 Paleogene (Eocene) Paleogeographic Map (−35 Ma)

The Paleogene Period, the Eocene (Figs. 13, 14 and 15). In the Late Eocene, appeared the first clear signs of the deepwater basin presence in the offshore area of the Arctic Ocean. Here the nepheloid type of accumulation prevailed, while near the continental slope, another type with gravitational flows of debris of different density probably dominated. The sediments are typically fine-grained, characteristic even in elevated areas of the region (e.g. the Lomonosov Ridge), as evidenced by the drilling data. In the transition zone shelf → slope → continental foot on the CDP profiles, a vast occurrence of clinoform units has been revealed, indicating an abrupt step of depths of the marine basin. Judging by the height of the clinoforms, this depth difference can be estimated to be within 1500–1700 m, in some areas it reaches up to 2000 m.

Legend for paleogeographic map

Environments

|	
I	Denudation relief
I-1	High-mountain relief
I-2	Low-mountain relief
II	Accumulative lowlands
II-1	Intermontane plains
II-2	Alluvial plains
II-3	Lacustrine and alluvial plains
III	Costal plains and shallow-water
III-2	Costal and tidal plains, lagoons
III-3	High salinity lagoons
IV	Shelf
IV-1	Upper sublittoral (inner shelf, depth 80-100 m)
IV-2	Lower sublittoral (outer shelf, depth 80-200) m
IV-3	Deep water shelf (depth >200 m, average depth 500-700 m)
V	Deep water oceanic realm
VI	Continental volcanic belts

Other symbols

Environment boundaries	Directions of transportation of clastic sediments
Seismic lines	Island arc volcanic complexes
Isopachs	Key sections

Fig. 11 Legend for early cretaceous (Aptian-Albian) paleogeographic map
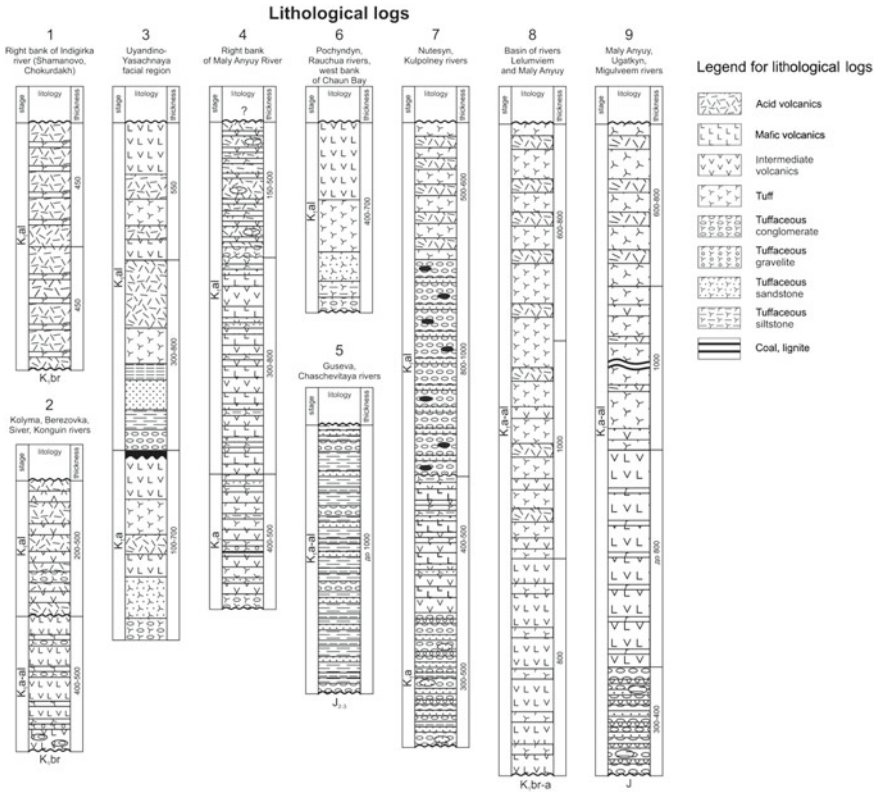
Fig. 12 Lithological logs

In some geophysical profiles, signs of a brief but very high-amplitude pre-Late Miocene in sea level drop and an equally rapid rise of it was clearly identified (profile ES10z23m between the picket 11,896 and the northern end of the profile, time interval from c. 1.25 to 2.25 s). This event reflected in most of present day dry land sections, being pronounced as a hiatus of different time amplitudes, as well as at the rises of the Amerasian Basin (Bruvoll et al. 2010a, b; Rekant et al. 2015, etc.). According to geophysical data, the sea by that time had retreated not only from the paleoshelf, but even fallen below its edge. In this case, abundant sand sediments may appear in sedimentary LST (low sea level tracts) lenses.
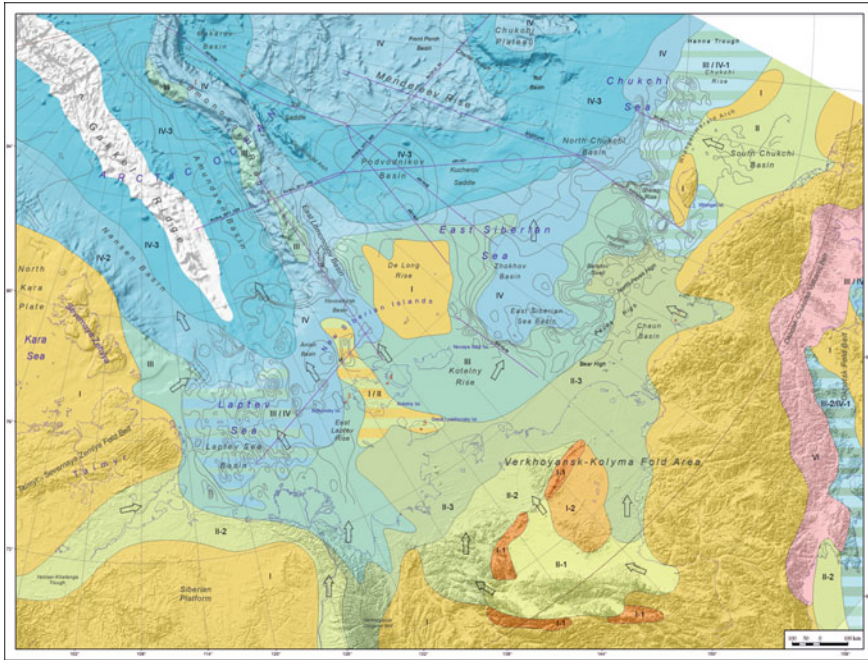
Fig. 13 Paleogene (Eocene) paleogeographic map (−35 Ma)

4.4 Neogene (Miocene) Paleogeographic Map (−10 Ma)

The Neogene period, the Miocene (Figs. 16, 17 and 18). Over the dry land, the Miocene deposit sequences are most complete on the Jana-Kolyma interflow coastal plains.
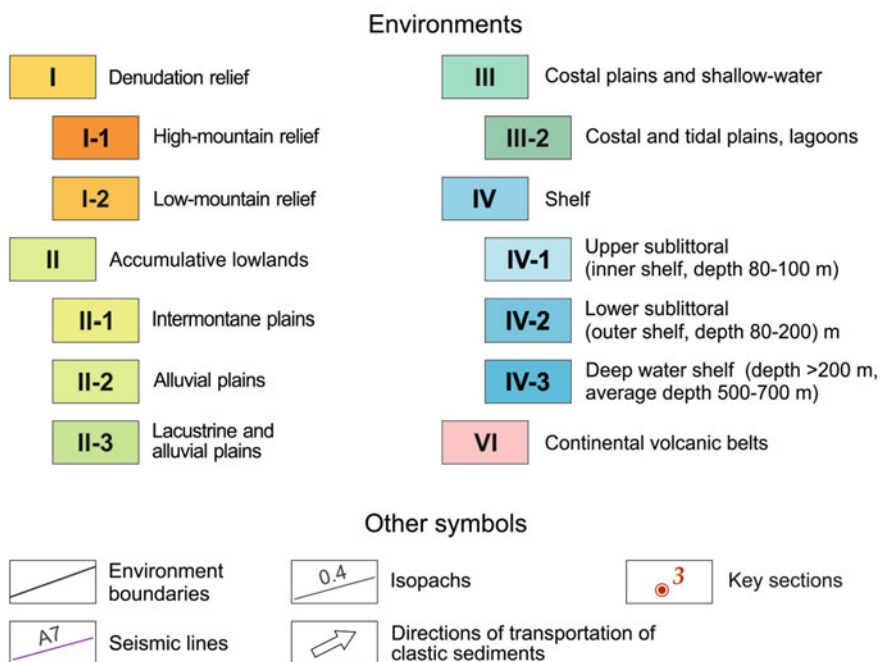
In the Lower Miocene Omoloy Basin, sediments comprise continental cross-bedded sands, clays and clayey silts with lignite beds. In the rest of the territory, sandy and sandy-pebble fluvial deposits sharply prevail: they are often cross-bedded with fragments of wood; siltstone and clay from occasional layers.

Eastwards of the Yana River delta and to the lower reaches of the Kolyma River, the Miocene sediments form an almost continuous cover with a thickness of 10–60 m, but are lacking in some parts of this territory (Kondakovo Plateau). Those are continental polygenetic sands of different granularity and pebble with rare interlayers and thin packs of silt, clay, peat or lignite. In the northernmost sections (Cape Svyatoi Nos, Vankina Guba), layers with marine diatom algae occur. The Miocene unit as a whole is distinguished by the lateral variability of proportion of different clastic rock types. Almost the entire Middle Miocene corresponds to cessation of sedimentation.

In the lower reaches of the Kolyma River, the Neogene deposits conformably to or upon a weakly eroded surface rest on the Paleogene sediments. The Lower-Middle Miocene sequence consists of silt, clay, sand and contains layers of lignite. The

Legend for paleogeographic map

Environments

I	Denudation relief		**III**	Costal plains and shallow-water
I-1	High-mountain relief		**III-2**	Costal and tidal plains, lagoons
I-2	Low-mountain relief		**IV**	Shelf
II	Accumulative lowlands		**IV-1**	Upper sublittoral (inner shelf, depth 80-100 m)
II-1	Intermontane plains		**IV-2**	Lower sublittoral (outer shelf, depth 80-200) m
II-2	Alluvial plains		**IV-3**	Deep water shelf (depth >200 m, average depth 500-700 m)
II-3	Lacustrine and alluvial plains		**VI**	Continental volcanic belts

Other symbols

	Environment boundaries	0.4	Isopachs	•³	Key sections
A⁷	Seismic lines	↗	Directions of transportation of clastic sediments		

Fig. 14 Legend for Paleogene (Eocene) paleogeographic map

Neogene landscapes here were typically marshy plains with large lakes covered with broad-leaved forest. North- and northwestwards, they passed into a coastal plain, occasionally flooded by the sea. The Upper Miocene base is an intensely eroded surface underlain by deposits of a coarser-grained composition. The landscapes were lake-alluvial plains with coniferous-deciduous forests and an admixture of broad-leaved species (climatic pessimum).

In the depressions of the Chukchi Sea coast, the Miocene deposits with a hiatus or erosion rest on the Paleogene sequences or the basement rocks. They are predominantly continental clastic sediments with a thickness of 20 to 210 m: silts, clays, lignite and sands of marsh-lake plains and lagoons. In the Chauna Trough and the Valkarai Depression, the Miocene sediments contain horizons with marine faunas. The sediments lithological composition and spore spectra, suggest that the Chukotka coastal plains were limited from the south by rises with a medium- and low-mountainous landscape.

On the New Siberian Islands and adjacent sections of the shelf, the Miocene sediments are of continental and coastal-marine type as well as lagoon-lagoon and deltaic deposits. The alluvial facies are formed by cross-bedded sands, silts and clays, while the lacustrine one comprise finely interbedded gray-colored sandy clays and silt with layered accumulations of floral detritus. The coastal-marine (littoral)
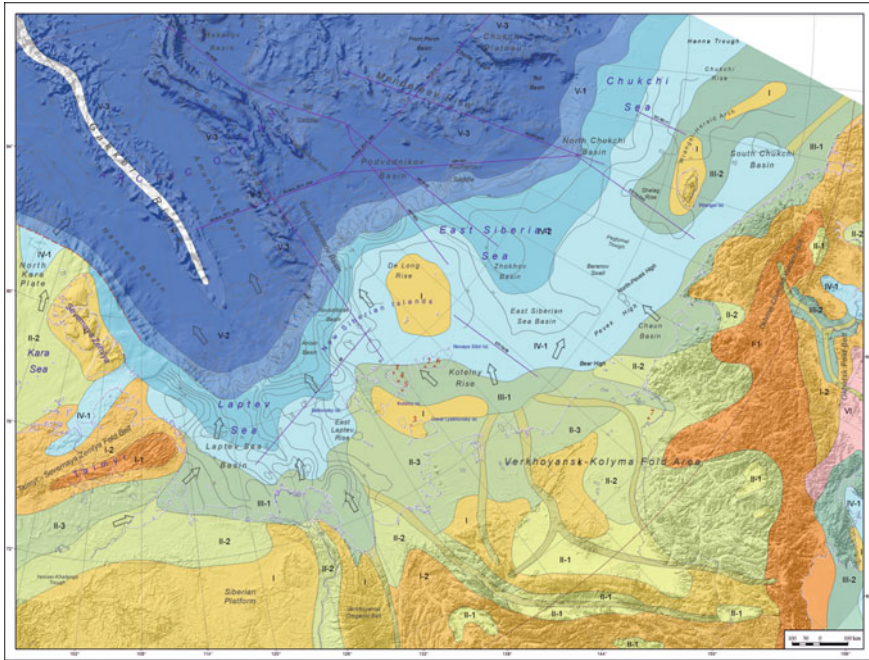
Lithological logs

Fig. 15 Lithological logs

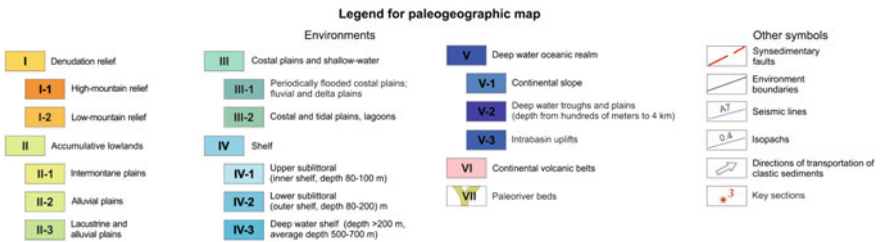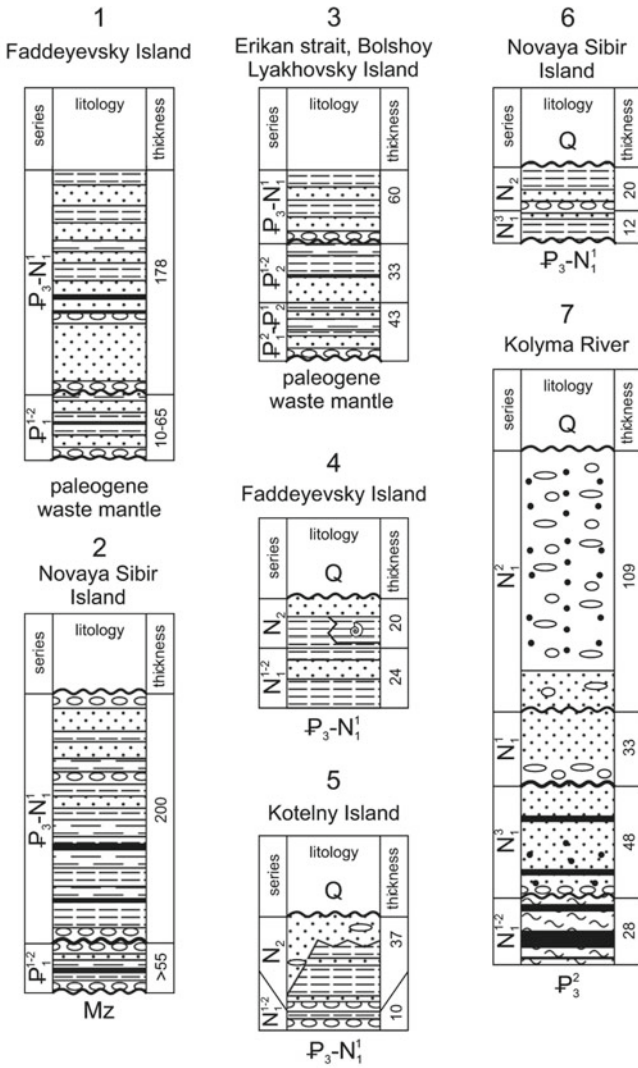**Fig. 16** Neogene (Miocene) paleogeographic map (−10 Ma)

Fig. 17 Legend for Neogene (Miocene) paleogeographic map

sediments are gray and greenish-gray sandy clays and clayey silts with muddy sand layers. They contain some organic remains: diatoms, fragments of marine mollusks shells and vegetative detritus. The sediments thickness reaches 100 m. Probably, the same deposits occur over the Novosibirsk-Wrangel paleo-shelf.

Lithological logs

Legend or lithological logs

Conglomerate   Sandstone   Clay, mudstone   Shale

Pebble, gravel   Silt, siltstone   Coal, lignite
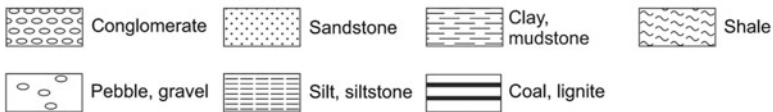
Fig. 18 Lithological logs

References

Bruvoll V, Kristoffersen Y, Coakley BJ, Hopper JR, Planke S, Kandilarov A (2010a) The nature of acoustic basement on Mendeleev and northwestern Alpha ridges, Arctic Ocean. Tectonophysics 514–517, 123–145

Bruvoll V, Kristoffersen Y, Coakley BJ, Hopper JR (2010b) Hemipelagic deposits on the Mendeleev and northwestern Alpha submarine ridges in the Arctic ocean: acoustic stratigraphy, depositional environment and an inter-ridge correlation calibrated by the ACEX results. Mar Geophys Res 31:149–171. https://doi.org/10.1007/s11001-010-9094-9

Kim BI, Glezer ZI (2007) Lomonosov ridge sedimentary cover (stratigraphy, geological history of sediments, structure and datings). Stratigrafiya Geologicheskaya korrelyatsiya 15(4):63–83 (in Russian)

Petrov OV, Pubellier M (2018) Tectonic map of the Arctic. SPb., Publishing House, 60 p

Rekant PV, Petrov OV, Kashubin SN, Rybalka AV, Shokalsky SP, Petrov EO, Vinokurov IYu, Gusev EA (2015) The history of sedimentary cover formation in the Arctic basin. Multichannel seismic approach. Reg Geol Metallogeny 64:11–27 (in Russian)

Vernikovsky VA, Metelkin DV, Tolmacheva TYu, Malyshev NA, Petrov OV, Sobolev NN, Matushkin NYu (2013) On the problem of paleotectonic reconstructions in the arctic and the tectonic unity of the New Siberian Islands terrane: New paleomagnetic and paleontological data. Proceedings of the Russian Academy of Sciences. 451(4):423–429

Study of the Arctic Seabed Rocks

O. V. Petrov, S. P. Shokalsky, T. Yu. Tolmacheva, O. L. Kossovaya, and S. A. Sergeev

Abstract The chapter presents results of studying the seabed rocks from scarps of steep mountainsides of the Mendeleev Rise collected during the Arctic-2012 expedition. The seabed collection consists of five thousand samples dominated by sedimentary rocks of shallow shelf facies. Carbonates are dominated by massive dolomites and limestones, which contain Devonian to Permian fauna. Terrigenous rocks are mainly represented by quartz sandstone and siltstone. Judging by the composition and age, the sedimentary rocks of the Mendeleev Rise belonged to the platform cover of the Early Precambrian cratonic block, which forms the crystalline basement of the uplifts in the Central Arctic. Basalt and gabbro-dolerite occupy no more than 10–20% of the raised seabed rocks. The basalt of the Mendeleev Rise belongs to the intraplate moderately alkaline Permian-Triassic basalt of the trap formation of Siberia and the Jurassic-Cretaceous basalt of the High Arctic Province (HALIP).

## 1   Study of the Arctic Basin Bottom-Rock Material

Geological sampling of the seafloor of underwater ridges and uplifts outcropped in the Central Arctic gives direct geological data on the structure and age of the rocks composing the seafloor morphostructures. Along with the geophysical data, it allows to reconstruct the formation history of these structures.

Over the past 10 years, a number of high-latitude expeditions took place, during which, sampling of modern loose hemipelagic sediments as well as geological sampling of seafloor hard rocks was carried out (Figs. 1 and 2) In the course of the latest field research works supplemented by photo and video recording, in many cases the stones a priori identified as "drop-stones" (the products of long-distance transfer by old ice or icebergs and exogenous scattering) in fact turned out to be of local origin and feature the underwater uplifts in which they were discovered. In numerous escarpments of the Lomonosov Ridge, Alpha-Mendeleev, and Chukchi

O. V. Petrov (✉) · S. P. Shokalsky · T. Yu. Tolmacheva · O. L. Kossovaya · S. A. Sergeev
Russian Geological Research Institute (VSEGEI), 74 Sredny Prospect, St. Petersburg 199106, Russia
e-mail: vsgdir@vsegei.ru
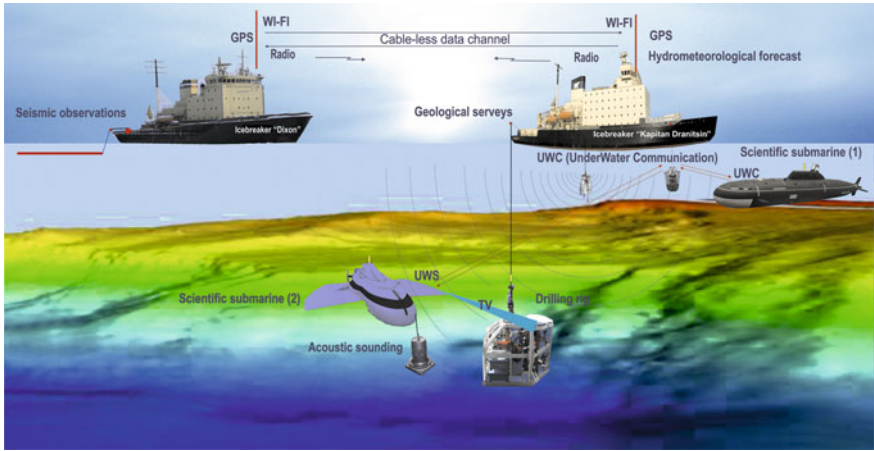
Fig. 1 The sketch-map of bottom sampling stations (dredging, deep-sea drilling and sampling from the research submarine—NIPL) in the Central Arctic underwater uplifts and the adjacent shallow shelf distributed by Russian and foreign high-latitude expeditions, mainly in accordance with the programmes: OLCS (Russia) and ECS (Denmark, Canada, USA) until 2016 and the concepts in the submissions of the Arctic states
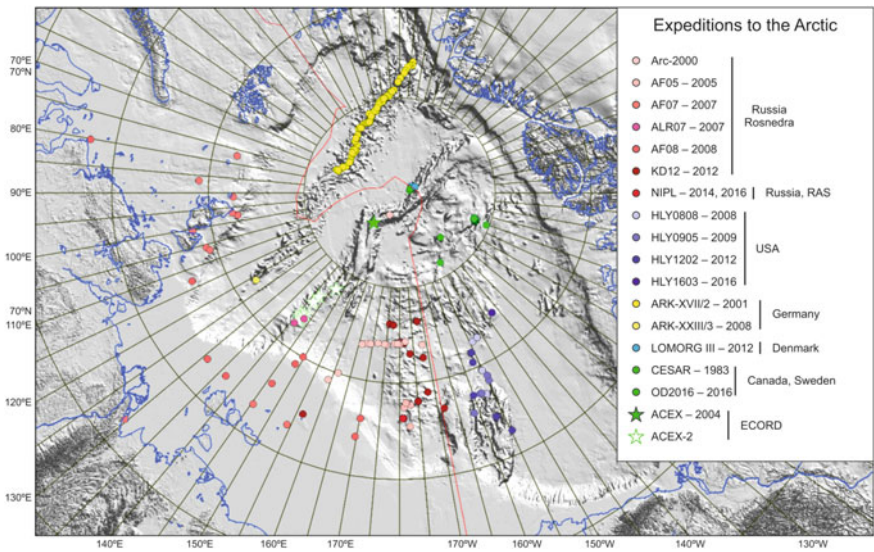
Fig. 2 Geological sampling of the seabed deposits in the Arctic Basin for different expeditions

Rises and their spurs at a depth of 1.5–3.5 km, there is a large number of exposures and outcrops of bedrock onto the surface of the seafloor, which are to be explored to benefit geological argumentation of the geological concepts in the submissions of the Arctic states.

The "Arctic 2012" expedition findings convincingly demonstrated outcrops of bedrock in the Mendeleev Rise (Fig. 3). The research submarine manipulator, a dredge and a grab lifted at least 100 rock fragments larger than 10 cm (Fig. 4). Complex studies of the bottom-rock samples as well as the rock samples from the Arctic islands and coastland were carried out (Fig. 5).

Steep slopes of 10 seafloor sites were sampled in the Mendeleev Rise in the course of the expeditions "Arctic 2000, -2005 and -2012" organized by Rosnedra and the Ministry of Natural Resources and Environment of the Russian Federation (Sevmorgeo and VNIIOkeangeologia, with the participation of VSEGEI).

Sites 5, 6 and 8 are located in the southwestern extremity of the Alpha Rise (in the Trukshin and Rogotsky underwater elevations).

Four sites (1, 2, 9, 10) are located in the northern Mendeleev Rise (in the Shamshura elevation and to the southeast of it). Three sites (0, 3 and TO) are located in the central Mendeleev Rise.

Three wells 2 m deep each were drilled in two sites. The first well was drilled in the SW Alpha Rise (site 6). The other two wells were drilled in the central Mendeleev Rise (site 0).

In accordance with the video recording made during the "Arctic-2012" seafloor sampling expedition, there are only sporadic, usually small (gravel and rarely pebble) hard rock fragments, apparently ice-breaking products, on the flat tops of table mountains. In such places, recent seafloor mud hardly contains accessory mature continental crust minerals—zircon, monazite, garnet.

The abundant accumulation of rock fragments, usually poorly rounded or angular, happened to be confined to steep slopes and footsteps of horst uplifts and escarpments, below bedrock exposures. In bottom sediments at the foot of underwater uplifts, for example, the Lomonosov Ridge and the Mendeleev Rise, detrital zircon accumulates, forming weight contents in mud.

Sedimentary rocks. Video recording made from the submarine and a core drill showed two types of bedrock in the sea floor escarpments. Some outcrops (of sinter type) resemble volcanic covers of basalt com position; the others are typical of practically unreformed platy-layered sedimentary rocks.

Bottom sampling in the Mendeleev Rise, the Chukchi Borderland and other structures showed that widespread Paleozoic sedimentary bedrocks in the acoustic basement outcrops on the surface of underwater elevations can actually account for the sedimentary rocks dominance in the composition of coarse detrital bottom-rock material.

Devonian Carboniferous-Lower Permian bioclastic (with fossils) limestone and secondary dolomite were identified among the sedimentary rock samples. Middle Late Paleozoic (and younger-Triassic-Jurassic) quartz sandstone was identified in the same bottom samples with U-Pb dating of detrital zircon (Fig. 6).
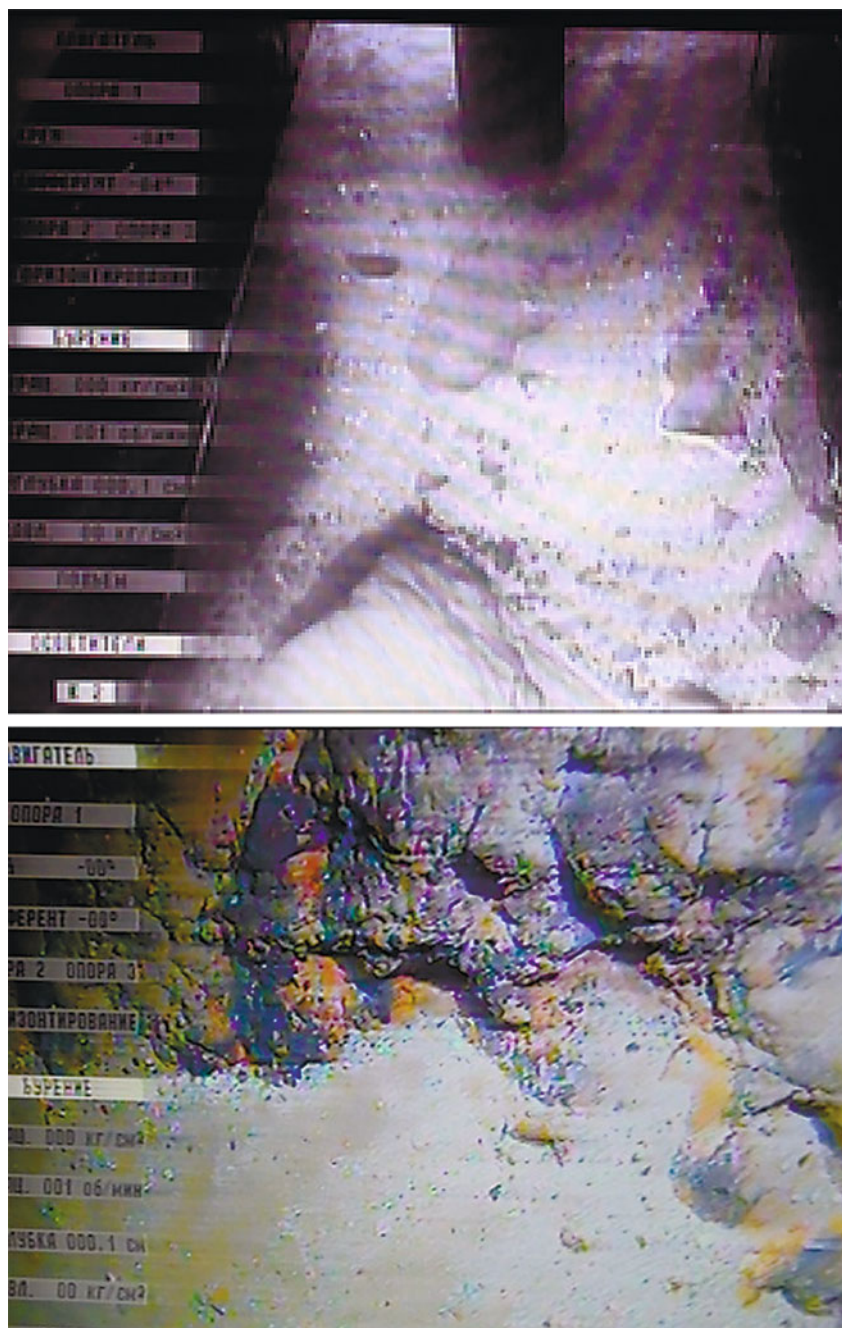
Fig. 3 View of the sea bottom of the Mendeleev Rise (photo of Arctica-2012)

Fig. 4 Rock samples from the Mendeleev Rise

Cenozoic hard carbonate crusts and flattened concretions were found in the samples (lifted from 2.3–3.5 km depth) from four escarpments of the Mendeleev Rise and no fewer than one site in the Chukchi Border land in addition to typically Paleozoic or older sedimentary rocks. They are composed of quartz-calcite or quartz-dolomite-calcite matrix, which contains abundant gruss and coarse dolomite sand, sandstone, dolerite and other rocks, usually coated in black ferromanganese, as well as small shell fragments. Numerous Cenozoic planktonic foraminifera were found in large quantities in carbonate crusts.

As a result of geochronological studies of subalkaline basalts and variegated volcanoclastic rocks of trachyandesite composition obtained from the wells in the central Mendeleev Rise, with U-Pb zircon dating in the CIR (Centre for Isotope
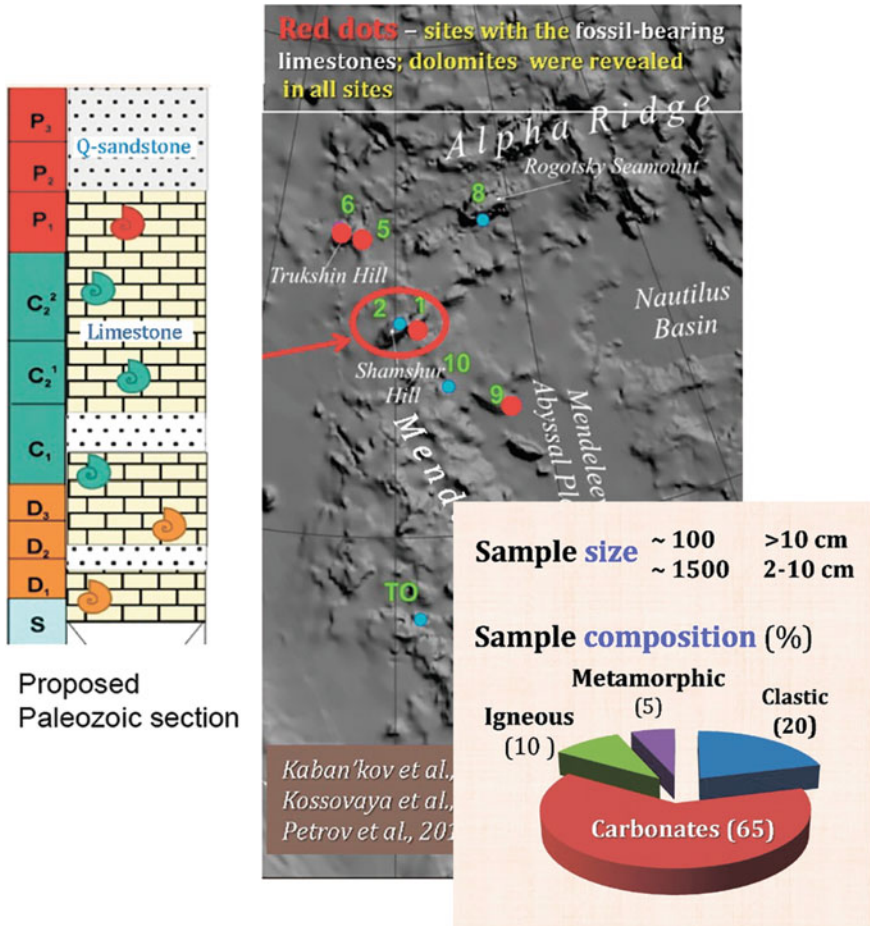
Fig. 5 Location of sampled fossiliferous carbonates on Alfa-Mendeleev Rise quantitative ratio of rock types collected during the expedition Arctica-2012 and proposed geological section of the Mendeleev Rise acoustic fundament

Research) VSEGEI and 40Ar/39Ar dating at the Laboratory of New Hampshire University (the USA) the basalts were identified as Cretaceous.

Based on obtained isotope-geochemical data, Russian and foreign experts discovered that the composition of these rocks is similar to the plateau basalt and volcanic formations of continental rifts. In accordance with the contour of the positive magnetic anomaly in the Central Arctic Elevations, Cretaceous basalt should be widespread over the roof of the acoustic basement not only in the Alpha-Mendeleev Rise, but also far beyond it—within the High Arctic large igneous province. Yet basalt and tuff is extremely rare in the seafloor rock fragments, which is a kind of geological enigma.

Fig. 6 Lower Devonian microfauna from sample KD-12-09-12d-85: *1* ostracod (Palaeoco-pamorpha); *2* Inarticulate brachiopod; *3* scolecodont; *4*, *9–11* conodonts [*4 Panderodus* sp., *9–11 Zieglerodina*? *remscheidensis* (Ziegler, 1960)]; *5–7* dacryoconarids (*Nowakia* cf. *zlicho-nensis* Bouček amd Prant); *8* sponge spicule

In the course of the "Arctic 2012" expedition, apart from Cretaceous volcanic rocks of the High Arctic large igneous province (HALIP), scarce but found in almost all the samplings and blocks, dredged up with the research submarine manipulator, gabbro-dolerite with intraplate petrogeochemical characteristics was dredged up as well. Its composition was studied and it was U-Pb zircon, Rb-Sr and Sm-Nd dated as Late Precambrian, Early and Middle Paleozoic. Such rocks usually occur at different levels of craton platform mantle in the form of silo-dike complexes.

The research works carried out by Rosnedra organizations in 2000–2012 resulted in the accumulation of over 500 rocks that were comprehensively studied; 400 of them come from deep-sea uplifts, including gabbro-dolerite (70), granitoid and meta-morphic rocks (50), quartzite sandstone (80), sandstone and siltstone, dolomite and limestone (over 100), and in addition, 50 samples of bottom sediments from ground cores (Sergeev et al. 2014; Kabankov et al. 2004, 2008a, b, 2012; Grikurov et al. 2014; Morozov et al. 2013; Vernikovsky et al. 2013; Petrov et al. 2016, etc.)

VSEGEI built up a Depository to store and to carry out follow-up studies of the rock samples from the "Arctic 2012" expedition, as well as the samples from the Arctic islands that were accumulated in the course of the international Arctic expeditions to Novaya Zemlya, Anzhu and De Long Islands in 2011–2013. Following the same procedure, they were later analyzed together with the samples from the high-latitude expedition "Arctic 2012" in the VSEGEI CIR (Centre for Isotope Research) and CL (Central Laboratory). They were also compared and the findings were used to prove the relationship between the Central Arctic deep-sea Elevations and the shallow Eastern Russia Arctic shelf structures.

2   Geochemical and Isotope-Geochronological Knowledge of the Eastern Arctic

Up-to-date isotope-geochemical and isotope-geochronological analytical techniques were used to study the sedimentary and magmatic rocks from the Eastern Arctic (Fig. 7) The study was carried out in the Center for Isotope Researches of the FSBV "VSEGEI", and employed various techniques, including ID-TIMS (whole-rock and minerals), ICP-MS-(MC) coupled with laser ablation, noble gases isotope ratios measurements and SIMS local analyses.

Between 2012 and 2015, a total of 530 samples, collected from the islands of the Eastern Arctic, dredged from the Arctic Ocean and sampled in its continental surroundings were analyzed. The samples encompass a wide range of compositions including magmatic, metamorphic and sedimentary rocks, as well as deep-water silt:

4530 local SIMS (SHRIMP-II) U-Pb analyses of zircon and baddeleyite in 348 rock samples;

2319 local LA-ICP-MS U-Pb zircon analyses in 164 samples;

35 ID-TIMS Rb-Sr datings;

31 ID-TIMS Sm-Nd age determinations;

10 Ar-Ar age determinations;

6 isotope analyses of He-Ar systematic;

342 chemical analysis by XRD, ICP-MS and ICP-AES;

108 isotope analyses of O, C and Sr in carbonates;

61 isotope analysis of the Re-Os systematics;

231 isotopic analyses of Nd system of bulk rocks;

240 isotope whole-rocks analyses of Sr;

69 isotope whole-rocks analyses of Pb;

1193 local LA-ICP-MC-MS analyses of the Lu-Hf systematics in zircon from 61 samples.

The following results were obtained:

The Baikalian and Caledonian age of granitoid fragments, dredged from the Ceno-zoic sediments of the Geophysicists Spur was determined. The acid igneous rocks
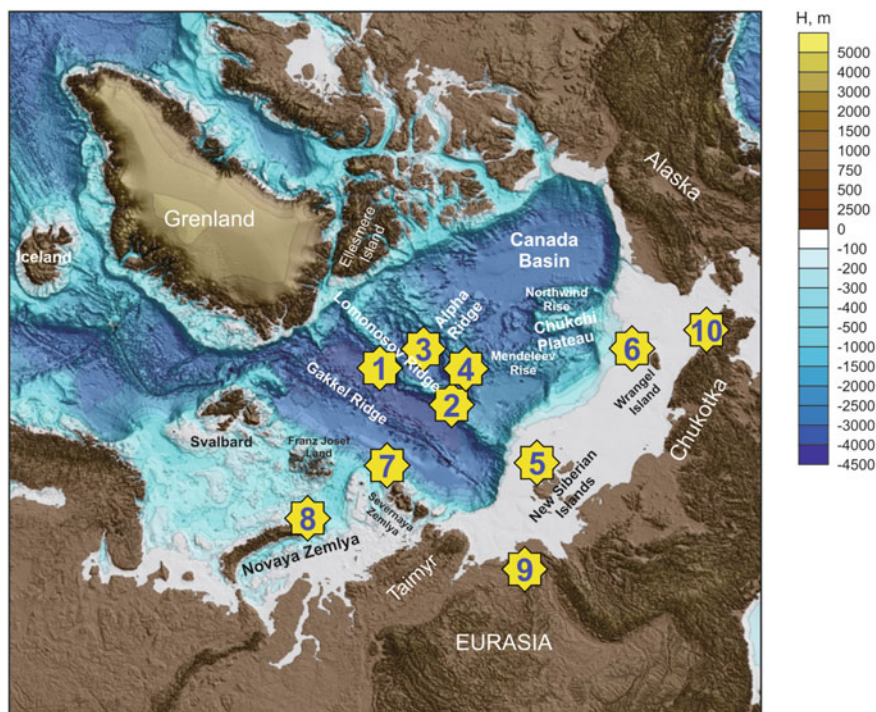
Fig. 7 Sampled localities: 1—Lomonosov Ridge (the Pole); 2—Lomonosov Ridge (Geophysicists Spur); 3—Alpha Ridge; 4—Mendeleev Rise; 5—Islands of De Long, Anjou and Lyakhovskie; 6—Wrangel Island; 7—Schmidt Island (Severnaya Zemlya); 8—Novaya Zemlya Islands; 9—Siberian Craton; Verkhoyansk-Kolyma and Anyi-Chjukchi fold-and thrust belts

dredged on the Mendeleev Rise proved to be gneiss granites of the Archaean and Palaeoproterozoic ages.

The distribution of the zircon ages in the Lomonosov Ridge and Mendeleev Rise bottom sediments is very close to that of the Asian continent, but differs sharply from the North American Continent and Europe (Grenvillian ages of c. 1100 Ma are absent). The pelagic silts contain a noticeable amounts of zircon, monazite, and garnet, which is not typical for the areas of the oceanic crust (Fig. 8). At least 25 provenance sources of detritus—Late and Early Cretaceous, Jurassic, Triassic, Permian and others, up to the Archaean were identified. The pelagic silts from the Lomonosov Ridge and Mendeleev Rise are of various origins, since differences of Re/Os ratios between these two sediment groups are quite large, hence they could not be derived from a single source.

The dating of the samples from the Mendeleev Rise implies existence of uneven-aged (Cretaceous, Ediacaran and Cryogenian) magmatic domains.
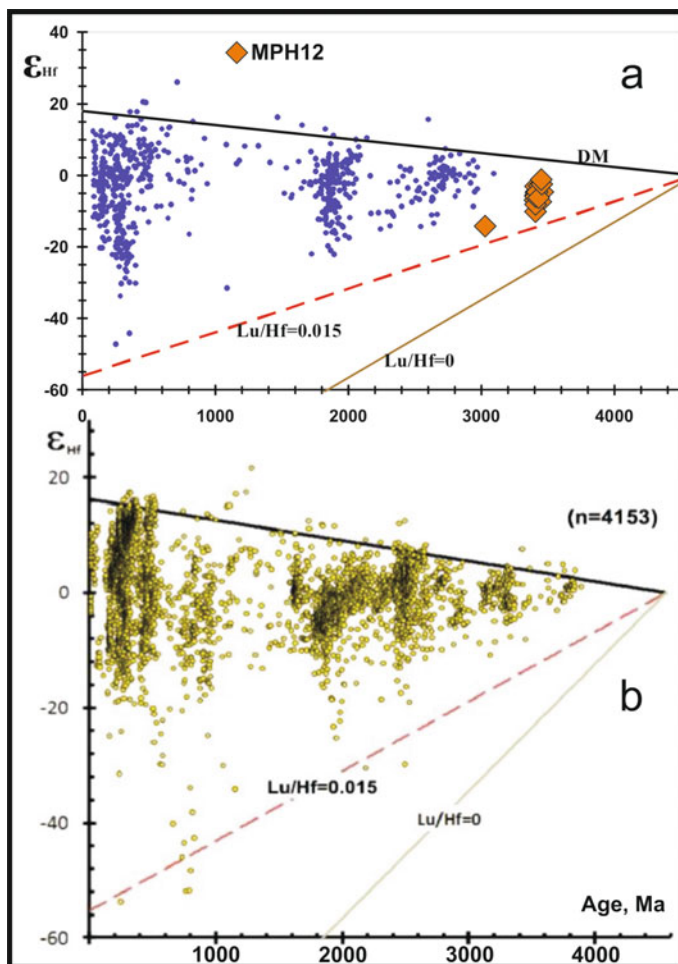
Fig. 8 Hf-isotope composition of detrital zircons from: A—hemipelagic deep-water deposits of Alpha-Mendeleev Rise. B—Asian sedimentary rocks. Plot U-Pb detrital zircon age vs ?Hf demonstrates that the main detritus portion of the deep-water muds and that of the present-day sediments with ages not exceeding 1.8 Ga is the result of river drift from the Asian continent of crustal matter of predominantly Caledonian age. The oldest 3450 Ma zircon from a meta-sandstone (MPN12) is shown as diamond

In the Mendeleev Rise, the age of dolerites was determined. The time of their intrusion from a moderately enriched or moderately depleted source (subcontinental lithospheric mantle) is estimated to 660 Ma.

Presence in basalts and dolerites of typical magmatic zircons with ages of 120, 180 and 260 Ma indicates existence of several magmatic complexes in the Eastern Arctic. The basic rocks themselves resemble those derived from plumes of the Jurassic-Cretaceous-Cenozoic (HALIP) and Early Triassic (Siberian trap formation) age. The

studies showed that the basalts from the Mendeleev Rise are geochemically distinct from the rocks in the mid-oceanic ridges but similar to Arctic intraplate moderately alkaline Cretaceous basalts (HALIP) and Cretaceous continental traps of the Deccan Plateau.

Ages of detrital zircons from sandstones, dredged in the Mendeleev Rise were determined. The northwest of the Rise is dominated by the Devonian-Silurian and the Riphean-Paleoproterozoic ages with a subordinate amount of the Vendian and Neoarchaean detritus. The central part is dominated, by material of the Triassic age with minor Devonian-Silurian and other sources. In the south, bi-component sandstones were dredged: detrital zircons from those yielded Palaeoproterozoic and Archaean ages.

Geochemistry and geochronology of the Eastern Arctic Probability density plots U-Pb of detrital zircons ages from meta-sandstones (Fig. 9). Two chronologic levels may be distinguished: Proterozoic and Mesozoic-Cenozoic, corresponding to the structures of the Precambrian basement and continental cover, respectively. The figure shows a typical zircon composition of one of the meta-sandstone sample (MPN12) and the results of the local U-Pb SIMS analyses of its oldest component (see the Concordia plot).

Arctic intraplate moderately alkaline Cretaceous basalts (HALIP) and Cretaceous continental traps of the Deccan Plateau.

Ages of detrital zircons from sandstones, dredged at the Mendeleev Ridge have been determined. The northwest of the Ridge is dominated by the Devonian-Silurian and the Riphean-Paleoproterozoic ages with a subordinate amount of the Vendian and Neoarchaean detritus.

The central part is dominated, by material of the Triassic age with minor Devonian-Silurian and other sources. In the south, bi-component sandstones have been dredged: detrital zircons from those yielded Palaeoproterozoic and Archaean ages.

3 Geological Section of the Acoustic Basement of the Alpha-Mendeleev Rise

In 2014 and 2016, the Geological Institute of the Russian Academy of Sciences (GIN RAS) in cooperation with the Geological and Geophysical Survey of the Geological Institute (GEOSLUZHBA GIN) and the Main Directorate for Deepwater Research of the Ministry of Defense of the Russian Federation organized expeditions in area of the Alpha-Mendeleev Rise to collect data in order to study the geological section of the Rise. The work was carried out using research submarine technical equipment at three test sites confined to the bottom areas, where acoustic basement rocks protrude from the sedimentary cover in the southwestern and central parts of the Mendeleev Rise and in Trukshin seamount (Alpha Ridge). When choosing sampling sites, 2D CDP reflection data obtained during expeditions "Arctic 2011" and "Arctic 2012", were analyzed. Rocks were sampled by research submarine manipulators directly

Fig. 9 Probability density plots U-Pb of detrital zircons ages from meta-sandstones. Two chronologic levels may be distinguished: Proterozoic and Mesozoic-Cenozoic, corresponding to the structures of the Precambrian basement and continental cover, respectively. The figure shows a typical zircon composition of one of the meta-sandstone sample (MPN12) and the results of the local U-Pb SIMS analyses of its oldest component (see the Concordia plot)
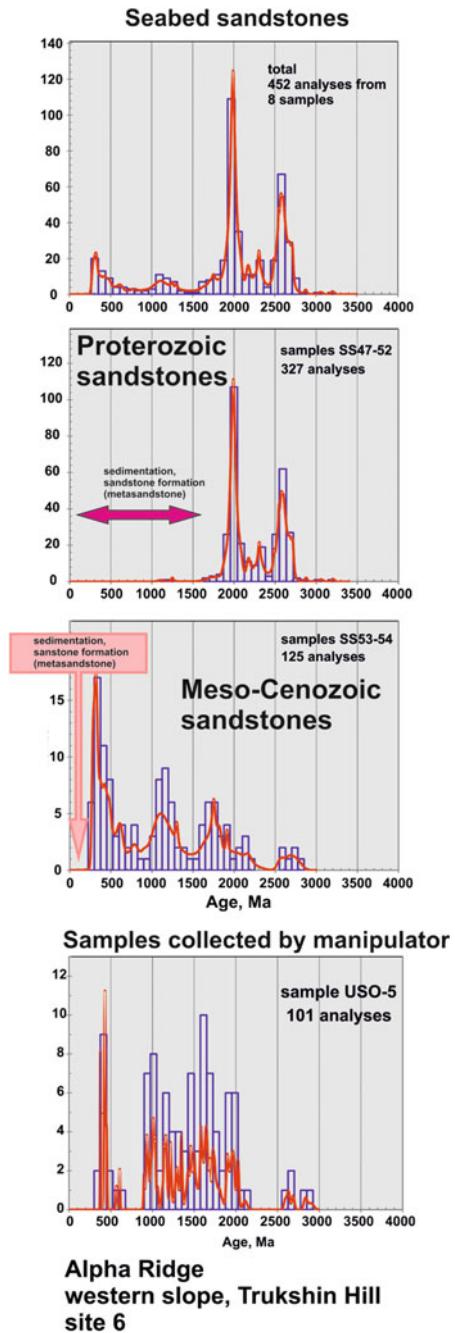
Fig. 10 Seabed exposures on the Mendeleev Rise sampled by research submarine manipulators (photo by GINRAS and GEOSLUZHBA GIN in Arctic-2014 expedition)

from cliffs, ledges, elevations, as well as from debris beneath them and loose rocks formed on their terraces and peaks resulted from bedrock destruction (Fig. 10). The rock collection is dominated by dolomite (37%), quartzite sandstone (20%), volcanic rocks (16%), limestone (10%), sandstone (6%), tuff (6%), microgabbro (3%) and dolerite (2%).

By now, the materials of the expedition 2014, obtained in the southwestern part of the Mendeleev Rise, have been analyzed. Twenty nine samples were studied, which are evenly distributed over the test site. Petrographic study of rocks was carried out, their chemical and mineral compositions were determined, and concentrations of impurity elements were measured. To determine the age of sedimentary rocks, their palyno-spectra were analyzed.

As a result of the studies, a visible geological section of the acoustic basement was reconstructed. In the lower part of the visible section, there is a lower rock sequence of apparent thickness of 230 m, composed of steeply bedded (30–40) dolomite and quartzite sandstone (Skolotnev et al. 2017a, b). Its outcrops are confined to the steepest lower part of the slope with a depth interval of 1500–1275 m. In the palynological collection of one of dolomite samples, there are abundant chorate forms—acritarchs such as *Baltisphaeridium* sp. ex gr. *B. varium* Volkova; Late Ordovician—Silurian acanthomorphic acritarchs such as *Micrhystridium* were also recorded (Fig. 11).

The *lower rock sequence* is overlapped with stratigraphic and angular unconformity by the *upper rock sequence* of about 40–50 m in thickness, composed of limestone and sandstone. Layers of the *upper rock sequence* of 5–10 cm in thickness show less steep bedding (15°–20°) than the *lower rock sequence*. The rock sequence forms the upper gently dipping part of the slope in the depth interval 1275 to 1230 m and, in accordance with seismic data, is directly overlain by the Mesozoic-Cenozoic sedimentary cover of oceanic origin. In the limestone, the palynospectrum is represented by a variety of myospores, the set of which makes it possible to refer it to the Contagisporites optivus—Spelaeotriletes krestovnikovii palynozone, characterizing Early Frasnian deposits of the Late Devonian. It should be noted that in the limestone,
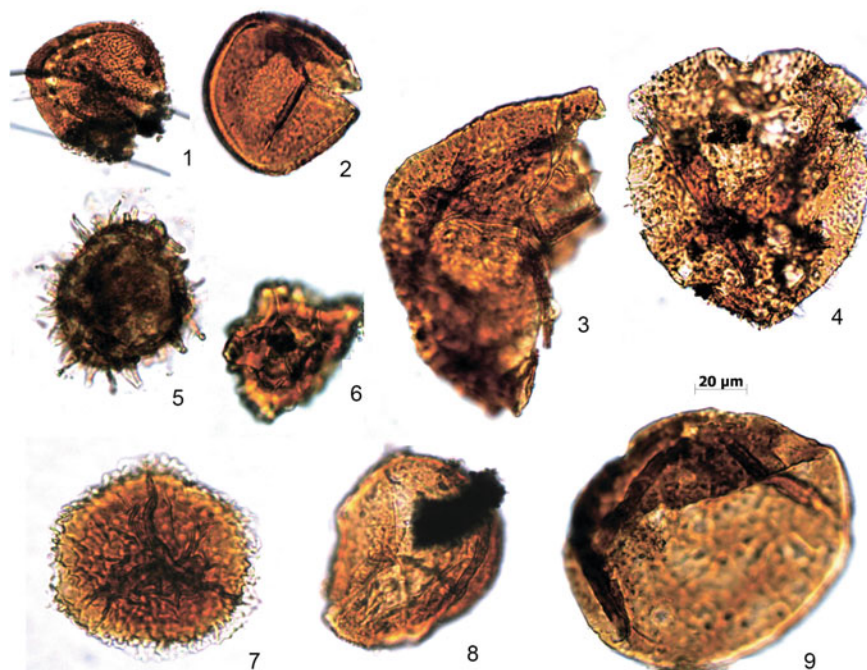
Fig. 11 Organic microfossils (spores and acritarchs) form the Lower Paleozoic carbonates sampled from seabed exposures (Skolotnev et al. 2019): 1—Geminospora micromanifesta (Naumova); 2—Geminospora lemurata Balme emend. Playford; 3—Contagisporites optivus (Tschibrikova) Owens; 4—Apiculatisporis adavalensis (de Jersey) Grey; 5—Baltisphaeridium sp. ex gr. B. varium Volkova; 6—Archaeozonotriletes timanicus Naumova; 7—cf. Acinosporites acanthomammillatus Richardson; 8—Cymbosporites sp.; 9—Inderites devonicus (Naumova) Telnova. ×500

the proportion of fragments of sandy and small-gravel size, composed of dolomite, quartzite sandstone and volcanic rock, is rather large (about 20%).

The *lower rock sequence* neighbours a tuff sequence of visible thickness of 50 m, consisting of layers of very loose clay rocks 10–20 cm thick, dipping at an angle of about 20°, which are easily broken off by the manipulator. Petrographic studies revealed relic structures of vitroclastic tuff in these rocks. The rock sequence makes up a terrace, formed at the foot of the slope. Judging by the nature of the sequence occurrence, it is a product of erosion and redeposition of tuff deposits accumulated in the upper part of the slope. According to seismic data (Jokat et al. 2003), tuff and lava horizons having a thickness of first hundreds of meters are located in lower parts of the Mesozoic-Cenozoic sedimentary cover overlapping the Alpha-Mendeleev Rise. The age of the tuffs has not yet been determined. Geochemically, they are close to volcanic rocks that form the Cretaceous magmatic HALIP province in the Arctic region (Estrada et al. 2016). Therefore, and also taking into account the above seismic data, it can be assumed that the *tuff sequence* has a Cretaceous age.

The *lower rock sequence* is cut by a *subvolcanic complex* of trachyandesite and trachybasalt, the formation time of which has not been identified. Probably, part of volcanic rocks of this complex is of Cretaceous age.

Intermediate results of the materials obtained in 2016 indicate that the geological structure of the Alpha-Mendeleev Rise in the area of two other above-mentioned test sites does not fundamentally differ from that in the southwestern part of the rise. This is indicated by close sets of selected rocks, and the discovery of late Devonian foraminifera in one of the limestones (Isakova et al. 2017).

As a result of the work performed, unambiguous evidence has been obtained that this rise has a continental-type crust, since the studied sedimentary rocks are widespread in the craton platform covers to form the lower Paleozoic parts of their sections.

In the Early Paleozoic (Late Ordovician-Silurian), thick carbonate and sandstone sequence formed under platform conditions in coastal, multifacies settings of the shallow sea (probably rift regime accompanied by volcanism) (Fig. 12). The warm climate contributed to the formation of deep weathering profiles on land and diagenetic dolomitization of silty mud under stagnant marine conditions. Caledonian orogenesis led to the rise of the area, which resulted in the dislocation of Early Paleozoic sediments; subsequently they were considerably eroded. The new land subsidence below sea level began in the Late Devonian. Sedimentation occurred during the subsidence under shallow-sea conditions complicated by islands, and probably continued until the late Paleozoic. During the Jurassic and Triassic, apparently most of the area was the land. During this period, the Late Paleozoic sediments were also dislocated and partially eroded. New submergence of the area, continuing to the present, started after the opening of the oceanic Canada basin in the Cretaceous. The beginning of the submergence coincided with the volcanic activity that led to the formation of the magmatic HALIP province, covering the Arctic region from Spitsbergen to the Chukchi Plateau, the origin of which is associated with the rise of the deep mantle plume (Estrada et al. 2016).
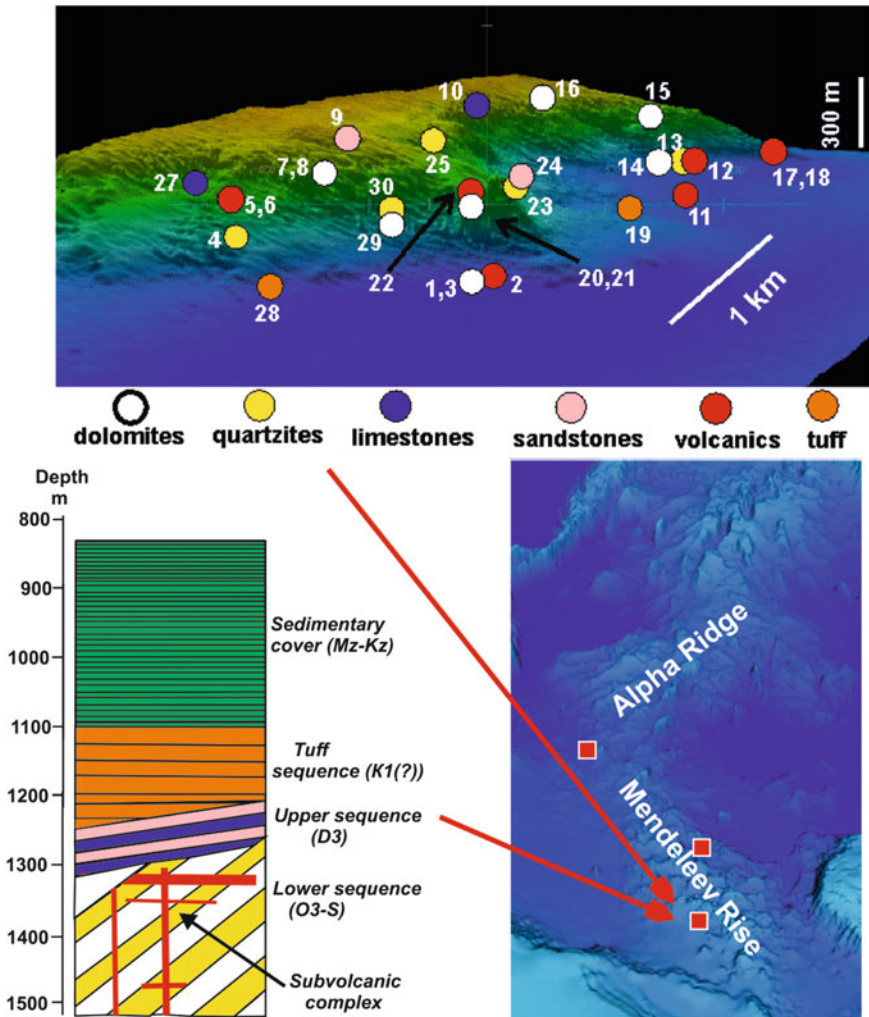
Fig. 12 Schematic geological section of the Mendeleev Rise revealed by Skolotnev et al. (2019) in a result of direct sampling of seabed exposures

References

Estrada S, Damaske D, Henjes-Kunst F, Schreckenberger B, Oakey GN, Piepjohn K, Eckelmann K, Linnemannn U (2016) Multistage cretaceous magmatism in the northern coastal region of Ellesmere Island and its relation to the formation of Alpha Ridge—evidence from aeromagnetic, geochemical and geochronological data. Norw J Geol 96(2). http://dx.doi.org/10.17850/njg96-2-03/

Grikurov G, Petrov O, Shokalsky S, Recant P, Krylov A, Laiba A, Belyatsky B, Rozinov M, Sergeev S (2014) Zircon geochronology of bottom rocks in the central Arctic Ocean: analitical results

and some geological implications. In: ICAM VI: Proceedings of the international conference on Arctic Margins VI, Fairbanks, Alaska, May 2011. SPb.: Press VSEGEI, pp 211–232

Isakova TN, Skolotnev SG, Kosovaya OL (2017) Paleozoic foraminifera of the Mendeleev Rise (Arctic Ocean, Eastern Arctic). Stratigraphic meeting, (in press) (in Russian)

Jokat W, Ritzmann O, Schmidt-Aursch MC, Drachev S, Gauger S, Snow J (2003) Geophysical evidence for reduced melt production on the Arctic ultraslow Gakkel mid-ocean ridge. Nature 423:962–965

Kabankov VY, Andreeva IA, Ivanov VI, Petrova VI (2004) About geotectonic nature of the system of Central Arctic morphostructures and geological significance of bottom sediments in its definition. Geotectonics 6:33–48 (in Russian)

Kabankov VY, Andreeva IA, Kaminskii DV, Razuvaeva EI, Krupskaya VV (2008a) New data on the composition and origin of bottom sediments in the southern Mendeleev Ridge Arctic Ocean. Dokl Earth Sci 419(2):403–405

Kabankov VY, Sobolevskaya RF, Lazarenko NP et al (2008b) On the problem of stratification of the Late Precambrian Early Paleozoic sediments of Central Taimyr. Novosibirsk: SNIIGGiMS, 169 p (in Russian)

Kabankov VYa, Andreeva IA, Lopatin BG (2012) Geology of the Amerasian subbassine. In: Geological and geophysical characteristics of the lithosphere of the Arctic region. Works VNIIOkeangeologiya, pp 30–40 (in Russian)

Morozov AF, Petrov OV, Shokalsky SP, Kashubin SN, Kremenetsky AA, Shkatov MYu, Kaminsky VD, Gusev EA, Grikurov GE, Recant PV, Shevchenko SS, Sergeev SA, Shatov VV (2013) New geological data substantiating the continental nature of the Central Arctic Uplifts area. Reg Geol Metallogeny 53:34–55 (in Russian)

Petrov OV, Morozov A, Shokalsky S, Kashubin S et al (2016) Crustal structure and tectonic model of the Arctic region. Earth-Sci Rev 154:29–71

Sergeev S, Petrov O, Belyatsky B, Sobolev N, Shokalsky S, Shevchenko S, Krymsky R, Petrov E (2014) Age (U-Pb zircon) and isotope-geochemical characteristics of bedrocks from New Siberian islands and its tectonic implications. Geophys Res Abs 16:EGU2014-10984

Skolotnev SG, Fedonkin MA, Korniychuk AV (2017a) New data concerning the geological structure of the South-West part Mendeleev Rise (Arctic Ocean). Doklady RAS 476(2):190–196 (in Russian)

Skolotnev SG, Fedonkin MA, Aleksandrova GN (2017b) Geological section of the acoustic foundation of the southwestern part of the Mendeleev Rise (Arctic Ocean). XLIX Tectonic collection of materials: "Tectonics of modern and ancient oceans and their suburbs"/M.: GEOS, pp 196–200 (in Russian)

Skolotnev S, Aleksandrova G, Isakova T, Tolmacheva T, Kurilenko A, Raevskaya E, Rozhnov S, Petrov E, Korniychuk A (2019) Fossils from seabed bedrocks: Implications for the nature of the acoustic basement of the Mendeleev Rise (Arctic Ocean) Marine Geology 407: 148–163

Vernikovsky VA, Metelkin DV, Tolmacheva TYu, Malyshev NA, Petrov OV, Sobolev NN, Matushkin NYu (2013) On the problem of paleotectonic reconstructions in the Arctic and the tectonic unity of the New Siberian Islands terrane: new paleomagnetic and paleontological data. Proc Russ Acad Sci 451(4):423–429 (in Russian)

Geology of the Eastern Arctic Islands and Continental Fridge of the Arctic Seas

O. V. Petrov, N. N. Sobolev, S. D. Sokolov, A. V. Prokopiev, V. F. Proskurnin, E. O. Petrov, and T. Yu. Tolmacheva

Abstract Expeditions carried out in the Arctic in recent years resulted in the accumulation of a significant amount of new information, which allowed better understanding the geology of the islands and coastal areas of the Arctic Ocean. Overviews on geology and evolution for the Severnaya Zemlya archipelago, the Taimyr Peninsula, the New Siberian Islands, the Wrangel Island and the areas of the Verkhoyansk Fold-thrust Belt adjacent to the Arctic Ocean, the Kolyma-Omolon Superterrane and the Chukchi-New Siberian Fold Belt include tectonic-stratigraphic maps showing petrographic composition, paleogeographic and lithogeodynamic conditions for the formation of sedimentary complexes, the phasing of tectonic and magmatic events.

The study of geology and tectonic evolution of the structures of the Arctic Basin bottom is complicated by severe polar conditions. The main sources of information here are remote geophysical data. The direct geological observations in this region are possible only on the islands and on the coastal areas of the Arctic Basin (Fig. 1). Therefore, these are the key territories to understanding the geological history and structure of the entire northeast of the Russian Arctic.

In recent years, a considerable quantity of empirical material has been assembled as a result of the various expeditions carried out in the region. These data substantially refined the knowledge of the geological structure of the islands and coastal of the Arctic Basin.

O. V. Petrov (✉) · N. N. Sobolev · V. F. Proskurnin · E. O. Petrov · T. Yu. Tolmacheva
Russian Geological Research Institute (VSEGEI), 74 Sredny Prospect, St. Petersburg 199106, Russia
e-mail: vsgdir@vsegei.ru

S. D. Sokolov
Geological Institute, Russian Academy of Sciences (GIN RAS), 7 Pyzhevksy per., Moscow 119017, Russia

A. V. Prokopiev
Diamond and Precious Metal Geology Institute, Russian Academy of Sciences, 39 Lenina st., Yakutsk 677007, Russia

Fig. 1 Map of the Eastern Arctic islands and continental fridge of the Arctic seas

In order to summarize the available new data, general settings of the geological structure and development have been compiled for a number of regions of insular and continental land of the eastern Arctic regions of Russia. Extensive retrospective material, including published scientific works, state geological maps and unpublished reports, was also used.

The description is based on a fomnational approach, considering the geodynamic settings, tectonics and magmatism characteristic of individual eras in the history of the development of each region. The result and illustration of this work are tectonic-stratigraphic schemes, compiled for the Severnaya Zemlya archipelago, Taimyr Peninsula, New Siberian archipelago, Wrangel Island, as well as the Verkhoyansk folded and thrust belt adjacent to the North Arctic Ocean areas, the Kolyma-Omolon superterrane and Chukotka-Novosibirsk folded system.

The schemes reflect the formational composition, paleogeographic and lithogeodynamic conditions for the formation of the tectonostrati-graphic complexes, as well as the phasing of tectonic and magmatic events.

1 Severnaya Zemlya Archipelago

The Severnaya Zemlya archipelago is an integral part of the Middle Mesozoic–Cenozoic North Kara Basin (Fig. 2). In the present-day structural plan, the archipelago forms an orogenic rise, which divides the sedimentary basins: the shelf South Kara and the oceanic Eurasian.

Tectonic conditions of formation of the pre-Jurassic–Cretaceous rocks were thought in various ways. During the early studies, these rocks were ascribed either to the geosyncline folded formations of the Kara platform with the Archaean–Palaeoproterozoic basement (Ravitch 1954; Vakar et al. 1958; Zabiyaka 1971), or to the Kara Hercynian—Early Cimmerian dome-plutonic epi-platformal rise with the Grenville

Fig. 2 Geological map of the Severnaya Zemlya Archipelago. *1* glacers; *2–10* epicontinental, mainly terrigenous deposits of the Cenozoic, Mesozoic, and Upper Paleozoic; *11–15* terrigenous-carbonate, carbonate, sulphate-bearing complexes of the Upper Ordovician Devonian gently folded in Variscan time; *16–20* terrigenous-carbonate, volcanogenic, and flysch complexes of the Cambrian—Middle Ordovician folded in Caledonian time; *21–22* Variscan and Caledonian granitoids; *23* tectonic boundaries; *24* geological boundaries

basement (Pogrebitsky 1976; Daragan-Sushcheva et al. 2009). At present, the pre-Jurassic rocks are tectonically attributed to the Kara Microcontinent, a part of the ancient Arctida (Zonenshain et al. 1990a, b; Uflyand et al. 1991; Vernikovsky 1996; Kuznetsov 2008) and/or North Kara Massif of Hercynian age with epi-platformal deposits on the Timanide (Late Baikalian) basement (Gee 2002; Proskurnin et al. 2002, 2014). Though debatable nowadays, the boundary between folded and plat-formal complexes separates the North Kara plate with the Paleozoic basement and the northern parts of the Taimyr-Severnaya Zemlya fold belt: this subdivision is assumed useful for purposes of seismic stratigraphy and studies of potential oil and gas resources.

Of the Kara Block rock complexes, the Severnaya Zemlya archipelago was proved to be the most representative area, although before 1925 it was absent not only in geological, but in geographical maps.

In the modern structure of the Kara Block, the North-Taimyr-Severnaya Zemlya fold belt is recognized: it underwent successive Baikalian, Caledonian and Hercynian orogenies. It encompasses the entire Northern Taimyr, the archipelagos of Severnaya Zemlya and Nordenskjöld and Izvestiy TCIK islands. Here, the Hutuda-Bolshevik and the Severnaya Zemlya folded zones are distinguished being separated by the Main Severnaya Zemlya deep fault. The core of the Kara Block comprises the North Kara syneclise of the Jurassic-Cenozoic age with underlying gently folded epi-platformal Late Ordovician-Devonian deposits.

The Khutuda–Bolshevik fold-and-thrust zone includes Bolshevik Island, the Izvestia TSIK Islands, as well as the easternmost part of October Revolution Island. The zone is composed of dislocated Late Riphean–Early Cambrian (?) sediments, metamorphosed under sericite-chlorite subfacies of the greenschist facies conditions. These rocks belong to the group of clastic marine flysch formations, whose age by acritarchs was defined as Riphean-Vendian. Recently, the presence in the flysch sandstone of the Cambrian age detrital zircons has been revealed.

On Bolshevik Island and in the east of October Revolution Island, the flysch deposits are intruded by granitoids of a granite-leucogranite formation of presumably Precambrian age and a 320 Ma old diorite-granodiorite. The granodiorite-porphyry and granite-porphyry are accompanied by gold-molybdenum-bearing mineral-ization. Dyke swarms on Bolshevik Island comprise Early–Middle Ordovician trachydolerite, Early Triassic gabbro–dolerite and Late Triassic lamprophyres.

The Late Riphean–Early Cambrian (?) sediments and the granodiorite are overlain with angular unconformity by continental coal-bearing Late Carboniferous-Permian sediments.

The Severnaya Zemlya fold zone is composed of the Lower–Middle Paleozoic folded epi-platformal rocks and fine Lower Permian platform deposits. The zone is located north of the Main Severnaya Zemlya fault and subdivided into two folded subzones: the East-October fold-and-thrust and the October-Pioneer gently folded subzones.

The East-October fold-and-thrust subzone is bounded in the west by the Kirov-Ozernaya strike-slip fault. The subzone comprises the Vendian–Middle Ordovician rocks. These deposits are folded into linear folds of the northeast and submeridional

strike. The stratified rocks (Egiazarov 1959; Makariev et al. 1981; Markovsky et al. 1982a, b; Severnaya et al. 2000) are dominated by intensely dislocated deposits of the Upper Vendian, Cambrian, Lower and Middle Ordovician.

Bottom of the section is composed of marine black—gray limestone—sandstone—mudstone strata. Its lower part contains coarse siliciclastic sediments, the age of which is conditionally defined, according to their position in the section, as the Vendian-Early Cambrian (Proskurnin and Vereshchagin 1989) or Early Cambrian (Lazarenko 1982). The above lying Cambrian deposits are shallow-marine dark-colored clastic rocks containing remains of benthic fauna, mainly trilobites, less often brachiopods and crinoids.

The upper part of the *East-October fold-and-thrust subzone* section is composed of a volcanic-plutonic association with voluminous volcancs of mafic, intermediate and felsic composition of moderately alkalic Na-K and K affinity. The association encompasses stratified sedimentary-volcanic formations, as well as necks, subvolcanic and hypabyssal intrusions. The Severnaya Zemlya fault zone is traced by a chain of intense magnetic anomalies coinciding with the Early–Middle Ordovician rift (possibly back-arc) zone and centers of volcanic-plutonic structures with trachybasalt-trachyandesite-rhyolite and moderately alkalic gabbro-syenite-granite-porphyritic formations (Proskurnin 1995).

The October-Pioner gently folded subzone with a northwestern strike of structures is located westwards of the Kirov-Ozernaya strike-slip fault. Within the zone, the Ordovician, Silurian and Devonian deposits occur. They display results of two types of deformations: Lower and Middle Ordovician rock experienced compression, which formed linear asymmetric folds with reverse fault and thrust of the northwestern strike (Albanova-Ozernaya anticline), while Upper Ordovician to Devonian deposits folded to form concentric folds and reverse faults (Spokoynaya and Pioner-Vavilova brachysynclines).

In the Albanova-Ozernaya anticline, the variegated continental and coastal-marine volcanogenic-carbonate-siliciclastic deposits are exposed. They contain a volcanic admixture, felsic lavas, lenses and veins of gypsum, halite and gypsum grains. In the anticline's crest (river Knizhnaya), a dike swarm of the northwestern strike occurs: these are amphibolized gabbro-dolerites of the Early–Middle Ordovician age.

The gently sloping brachinsinclines (Spokoynaya and Pioner-Vavilova, etc.) are composed mainly of shelf carbonates of the late Ordovician-Silurian and siliciclastic Devonian rocks (Egiazarov 1959; Markovsky et al. 1982a, b; Khapilin 1982; Matukhin and Menner 1999; Severnaya et al. 2000).

The lower part of the Lower Ordovician—Silurian sequence comprises coastal-marine variegated sandstones, dolomites, calcareous dolomites, less often limestones and marls, whose age by coral and conodonts was defined as the Late Ordovician. With an angular and stratigraphic unconformity, it rests upon the Middle Ordovician gypsum along the eastern boundary of the Pioner-Vavilova brachysyncline. The sequence thickness increases from the west to east from 10–15 m to 100–200 m. The Silurian deposits are represented by a complex of shallow-marine mainly carbonate deposits, dominated by bioclastic, algal, stromatolite, and clayey limestones with

scarce dolomite. In the upper part of the section, the rocks have a motley color. Interlayers of sandstones, siltstones, gypsum, argillites, marls occur along with sparse interlayers of ostracod clayey limestones.

The Devonian deposits are widespread in the central and western parts of October Revolution Island (Fig. 3) and almost entirely compose islands Pioner and Komsomolets The Lower Devonian sediments with disconformably rest upon various horizons of the Upper Silurian. The Lower Devonian deposits encompass the lower coastal-marine siliciclastic-carbonate and the upper lagoon-marine carbonate-clastic-sulfate formations. The overlaying deposits of the Middle and lower parts of the Upper Devonian are dominated by continental red-colored clastic complexes containing abundant fossil ichthyofaunas.

The plate complex consists of thin Carboniferous, Permian, Jurassic and Cretaceous sediments sporadically occurring on islands of the archipelago (Fig. 4). Continental sandstone and conglomerate with coal interlayers and traces of plant residues of the Middle Carboniferous–Lower Permian are known on Bolshevik Island; there are also individual outcrops of Jurassic terrigenous deposits. Coastal-marine calcareous sandstone with Permian brachiopods are have been found in the

Fig. 3 Outcrops of the Lower Paleozoic of October Revolution Island (photo by V. Ershova)
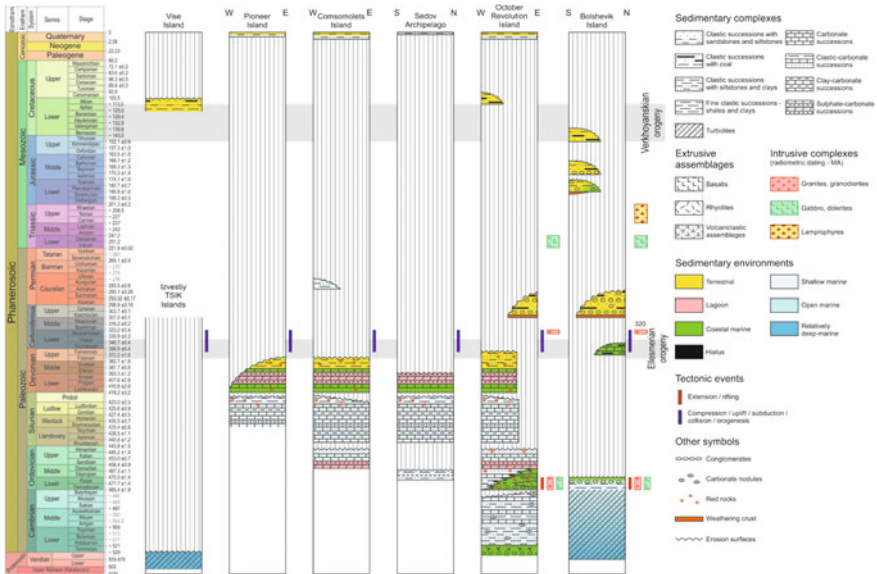
Fig. 4 Tectonostratigraphic charts of the Severnaya Zemlya archipelago

west part of Komsomolets Island. Lower Cretaceous terrigenous continental sediments are typical of some islands of the Kara Sea (Schmidt Island, Vise Island, etc.).

2 Taimyr Peninsula

The Taimyr-Severnaya Zemlya folded region is divided into three zones: North Taimyr–Severnaya Zemlya, Central Taimyr and East Taimyr-Olenek (part of the Verkhoyask belt) (Fig. 5). The first occurs on the Kara basement and is a part of the North Kara terrane. The Central Taimyr and the Eastern Taimyr-Olenek fold systems are parts of the Siberia's Craton. The boundary between the Kara terrane and Siberia Craton goes along the ophiolite suture of the Central Taimyr fold zone. The northern boundary of the Siberia Craton coincides with the Central Taimyr and the Pronchishcheva-Olenek sinistral strike-slip fault zone.

The North Taimyr–Severnaya Zemlya fold zone is composed of metamorphosed and strongly dislocated rocks of the Palaeo- and Neoproterozoic and partly Cambrian ages, as well as variously aged granitoids. It has a fold-and-thrust structure, which was formed during the Baikalian, Salairian and Early Cimmerian tectonic events. The lower parts of the section are composed of black phyllite, meta-siltstone and meta-sandstone of the Upper Palaeoproterozoic or, perhaps, Lower–Middle
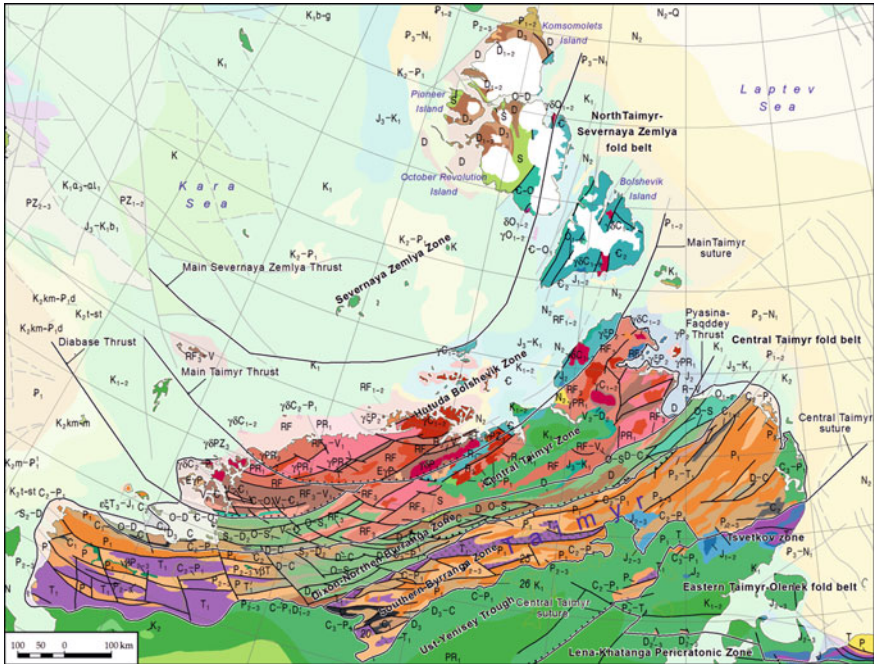
Fig. 5 Geological map of the Taimyr Peninsula

Riphean (Calymmian-Ectasian). Their metamorphic alteration reached amphibolite grade, as a result of which the siliciclastics transformed into gneisses and schists, underwent migmatization and various degree of melting produced gneissose granites of c.1.0 Ga age. The Upper Riphean weakly metamorphosed flysch rest unconformably over the basement. The Cambrian is composed of clastic-carbonate sediments similar to those of the Severnaya Zemlya Archipelago. They are unconformably overlapped by lesser deformed and non-metamorphosed Ordovician deposits with basal conglomerate discontinuous layer. The Precambrian complexes (gneisses and schists) are also found on islands neighboring the Taimyr Peninsula (archipelagos of the Plavnikovy Islands and Nordenskjöld). In the south, this zone is bounded by the Main Taimyr thrust.

The Central Taimyr fold zone is the most complex structure of the Taimyr Peninsula. It is composed of pre-Riphean (?) and Riphean sedimentary, volcanogenic and intrusive rocks that undergone metamorphic and hydrothermal-metasomatic alterations of various facies and types. These metamorphic formations are covered by the Vendian-Lower Carboniferous cover. The zone experienced a powerful compression, which resulted in massive thrusting. There are two allochthonous Precambrian metamorphic complexes: Mamont-Shrenk and Faddey. They are composed of high-metamorphosed clastic and carbonate rocks and metabasites. Two belts of ancient ophiolites, the Chelyuskin (southeastwards of the eponymous Cape) and Stanovskoy

(coast of the Faddey Bay) occur in the zone. They form small bodies (from tens of meters up to 2 km in length and up to tens of meters in width) of metaperidotite and metamorphosed gabbroids. The ophiolites tectonically imbricated with narrow zones of serpentinite mélange, mylonitized green shales or metasomatites. Volcanics are tholeiitic metabasalts of the oceanic and metaryolite-andesite-basalts of the island-arc calc-alkaline series. The Upper Riphean comprises mainly dolomites. All the above-mentioned formations with angular unconformity are overlapped by molasse: clastic rocks, including coarse one, silt-mudstone and horizons of limestones.

The southerly located Early Mesozoic (Early Cimmerian) fold system is 150–200 km wide and more than 1000 km long. It unconformably overlaps the metamorphosed and strongly deformed Upper Proterozoic basement. The Vendian is composed of dolomites that are overlain by the Cambrian clay-carbonate. The Ordovician (Fig. 6), Silurian, Devonian and Lower Carboniferous are composed of either relatively deep-water clay-siliceous-carbonate deposits, or shallow-water limestones, marls and dolomites. The Upper Permian base typically comprises shallow-marine sediments, which are gradually replaced by continental siliciclastic coaliferous units when moving up the section. The Lower Triassic is represented by a trap complex. The Paleozoic and Triassic formations of the South Taimyr zone are intruded by small bodies of alkaline granites, syenites and nepheline syenites of the Late Triassic age. The South Taimyr zone underwent folding in the Pre-Jurassic time. The second, but weaker phase of deformations took place at the Jurassic-Cretaceous boundary.

Fig. 6 Field camp at the Kluevka River, Taimyr

The eastern Taimyr-Olenek fold zone in the Taimyr (the Tsvetkovky gently folded zone) is a fragment of the Verkhoyansk belt. The zone is bounded by the Central Taimyr in the northwest and by the northern coast of the Khatanga Bay in the south. Three complexes are distinguished.

1. Middle Carboniferous-Permian includes gray-colored clastic sediments.
2. Triassic volcaniclastic complex includes volcanic-plutonic associations of hot spots and taphrogenic deposits of the Late Triassic.
3. Jurassic-Neocomian is a clastic poorly coaliferous complex. The deposits form transgressive–regressive rhythms of high orders.

They accumulated under conditions of outer shelf. Pulses of folding occurred at the Permian–Triassic boundary, in the Middle-Late Triassic and Aptian-Albian (Late Cimmerian). During the final Late Triassic and in the Middle-Late Triassic, sub-alkaline basite-dacite cross-cutting bodies of fluidolith of the Carnian Age entraining minerals associated with diamonds (Tsvetkovsky Cape) formed. The youngest igneous rocks in the Eastern Taimyr, are sub-alkaline gabbro-dolerite-quartz-syenite (225–226 Ma), as well as intrusives and breccias of Sr-Ba carbonatite (219–238 Ma), some of which have fluid-explosive or volcanogenic genesis (Proskurnin et al. 2010; Petrov and Proskurin 2010) (Fig. 7).

Fig. 7 Tectonostratigraphic charts of the Taimyr Peninsula

3   New Siberian Islands Archipelago

The New Siberian Islands are an archipelago located in the Eastern Arctic shelf between the Laptev and the East Siberian Seas (Fig. 8). The archipelago comprises three groups of the islands: the Lyakhovsky Islands (Bolshoi and Malyi Lyakhovsky, Stolbovoy); the New Siberian Islands, or the Anzhu Islands (Belkovsky, Kotelny, Bunge Land, Faddeevsky and New Siberia); as well as the De Long Islands (Bennett, Zhokhov, Vilkitsky, Henrietta and Jeannette) which are not big but significantly distant from each other.

In the modern structure, the archipelago of the New Siberian Islands is an orogenic uplift that separates the continent margin platforms and the sedimentary basins of the Laptev and East-Siberian Seas formed upon them.

In the structure of the folded basement of the Lyakhov Islands, several complexes are distinguished, differing in dislocation intensity, as well as the composition and degree of metamorphism of the rock comprising them. One of these is presented by flyschoid greywacke formations with different types of folding and varying degrees of metamorphism. According to the latest views, all flyschoid deposits on the Bolshoi and Malyi Lyakhovsky Islands are from the Late Jurassic-Early Cretaceous (Kuz'michev et al. 2006). In addition, in the southeastern part of the island, a complex of volcanic and metamorphic rocks of the South Anyuy suture is exposed
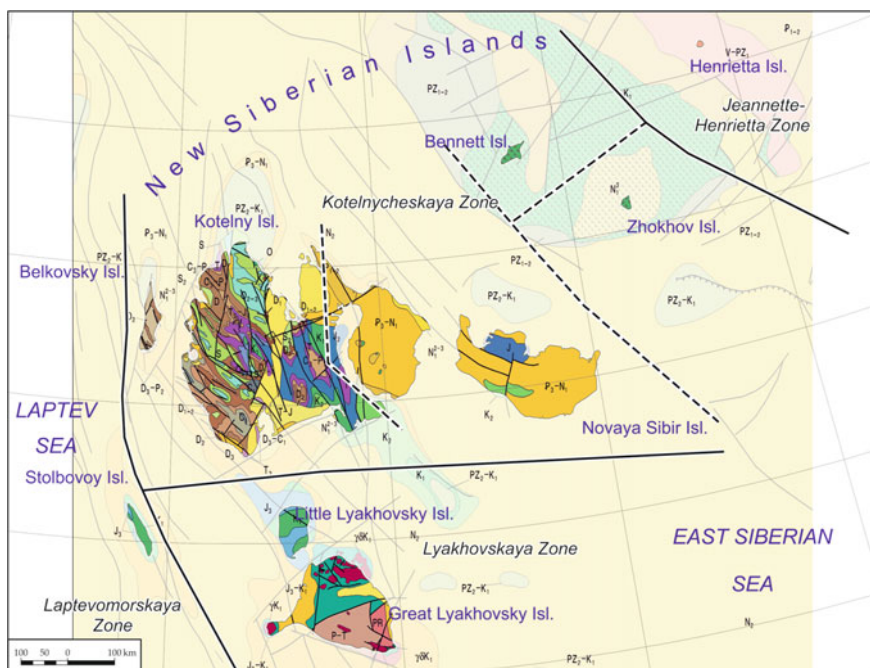
Fig. 8 Geological map of the New Siberian Islands Archipelago

Fig. 9 Pillow lavas on Bolshoi Lyakhovsky Island (by T. Tolmacheva)

(Fig. 9); this occured at the site of the ocean basin as a result of an early Cretaceous collision of the Eurasian and North American continental plates. All complexes on Bolshoi Lyakhovsky Island are broken through by intrusions of grano-diorites and granites of the Apt-Albian age of 122–108 Ma. (Dorofeev et al. 1999).

As paleomagnetic studies have shown, the Anjou and De Long islands belong to a single continental block (Metelkin et al. 2014) with a basement age defined as the Late Riphean (Akinin et al. 2015; Lorenz 2013).

On the Kotelny Island, deposits of the age range from the Ordovician to the lower Cretaceous are collected in folds of the north-west continuation. Here, three structural levels (complexes) can be distinguished: the Ordovician-Middle Devonian carbonates, treated as a deformed cover of the Epibaikalian platform; the Upper Devonian-Carboniferous terrigenous-carbonate intraplate and Upper Paleozoic-Jurassic terrigenous sediment, formed on the passive continental margin. Paleozoic-Jurassic sediments were dislocated and partially eroded in the early Cretaceous. Thermo-chronological studies of samples from Kotelny Island are avaragely aged to 125 ± 22, 106 ± 28 Ma (Prokopiev et al. 2018a, b). Lower Upper retaceous sediments were formed as a result of postfold rifting and are represented by a continental volcanogenic-terrigenous coal-bearing formation containing ignimbrites, rhyolite lavas and units of acidic tuffs (dates of 110–107 ± 2.5 Ma are obtained for ignimbrites). In terms of flora and spore-pollen complexes, the age of these sediments is defined as Apt-Albian and Cenomanian-Turonian, with the Upper Cretaceous deposits occurring on the weathering crust of the Lower Cretaceous rhyolites.

Cenozoic sediments are deposited with erosion on the underlying strata and are represented by thin intraplate terrigenous sediments with carbonaceous interlayers.

On the Faddeyevsky and New Siberia islands, the sediments of the Upper Cretaceous and overlying Cenozoic sediments overlapping it with structural discordance are exposed. These are represented by intraplate coal-bearing terrigenous sediments separated by large stratigraphic discordance on the Upper Cretaceous; Upper Paleocene-Middle Eocene (occurring on a widely developed weathering crust); Oligocene-Middle Iocene; Middle-Upper Miocene and Pliocene-Quaternary stratigraphic sequences.

The section of Bennett Island is composed of terrigenous deposits of the Cambrian and Ordovician and the Early Cretaceous sediments and basalt covers overlying them (Volnov and Sorokov 1961). The Cambrian is represented by sediments of the outer shelf: in the lower part (the Atdaban-May stages of the Cambrian), dark-coloured aleuro-argillites with sandstone interlayers, sandy limestones with trilobite detritus, which are replaced by black shales of the Upper Cambrian–Lower Ordovician. The Ordovician is composed of carbonate and silicyclastic turbidites containing residues of graptolites. This sequence is assumed to be formed under the conditions of a growing marginal continental rift trough (Danukalova 2016). The Ordovician deposits are covered by the weathering crust, formed as a result of Devonian orogeny with the age of tectonic exhumation is 378 ± 38 Ma (Prokopiev et al. 2018a, b). The Lower Cretaceous lies unconformably on the underlying sediments of the Lower Paleozoic. This structural tectonic complex reflects the stage of postorogenic rift genesis and is represented mainly by basalt covers, which, according to petrochemical characteristics, correspond to the traps of the Late Mesozoic high-latitude magmatic province (HALIP). The age of basalts is determined in the range of 106–125 Ma (Fedorov et al. 2005).

The islands of Henrietta and Jeannette are composed of Lower Paleozoic ensialic island-arc volcanogenic-sedimentary complexes: subcontinental gravelites, conglomerates and cross-laminated sandstones in association with the turbidite volcanogenic (tuff)-sedimentary sequences, basalt, andesites, rhyolite and rhyolite covers. These deposits are attributed to the Lower Paleozoic, based on the dating of zircons from igneous and sedimentary rocks. Thermochronological studies of samples from Jeannette Island provide a tectonic exhumation age of 400 ± 25 Ma, and from island Henrietta—$385 + 30$ Ma (Prokopiev et al. 2018a, b).

During the Cenozoic platform stage of development in the Neogene-Quaternary, within the boundaries of the De Long block, volcanic activity took place, as presented on the Zhokhova and Vilkitsky islands in the form of alkaline basalts and alkaline-ultrabasic volcanic rocks (foidites) (Akinin et al. 2015).

On the islands of the Laptev Sea (Belkovsky Island and Stolbovoy Island), Paleozoic and Neocom deposits are exposed (Fig. 10), with angularity blocked by Paleogene-Neogene (Eocene and Oligocene—Lower Miocene) coal-bearing sands and clays (Kuz'michev et al. 2013). On Belkovsky Island, Middle Devonian shallow-water marine limestones are in evidence, which are replaced by sloping clay, clay-siliceous deposits in association with turbidite sequences and units of olistostromes

Fig. 10 Coastal cliff on Stolbovoi Island (photo by M. Kos'ko)

in the upper Devonian-Permian. On Stolbovoy Island, a Volga-Neocom terrigenous turbidite structural tectonic complex is identified, represented by rhythmically bedded sandstones, aleurolites and argillites. The formation of this complex took place in the fore-trough of the closing basin of the South Anyui Ocean against the background of the Late Cimmerian orogenesis. Thermochronological studies of samples from Belkovsky Island give a tectonic exhumation age of 90 ± 11 Ma (Prokopiev et al. 2018a, b).

In 2011 and 2013, VSEGEI organized international geological expeditions to the New Siberian Islands. The goal was to study the best-exposed and most representative Paleozoic and Mesozoic geological sections, as well as varying in age and composition magmatic and metamorphic formations; and to collect rock samples for subsequent studies of mineral composition, as well as for isotope and paleomagnetic studies and paleogeographic reconstructions. During the expeditions, all the islands were visited, including Jeannette Island, where geologists had not been for over 70 years.

Large Russian and foreign geological surveys, mining companies, universities (Aarhus University, Denmark; BGR, Goethe University Frankfurt on the Main, Univ. Erlangen, Germany; Total, Sorbonne Universities, France; Univ. Siena, Italy; Univ. Uppsala, Stockholm University, Swedish Polar Research Secretariat, Sweden; University of Cambridge, UK). FGBU "VSEGEI", VNIIOkeangeologia, St. Petersburg State University, Moscow State University, DPMGI SB RAS, IPGG SB RAS, NEISRI FEB RAS from Russia) took part in organizing the expeditions. During the expeditions, some data on the Late Riphean age of the Koieinichesky Rise basement
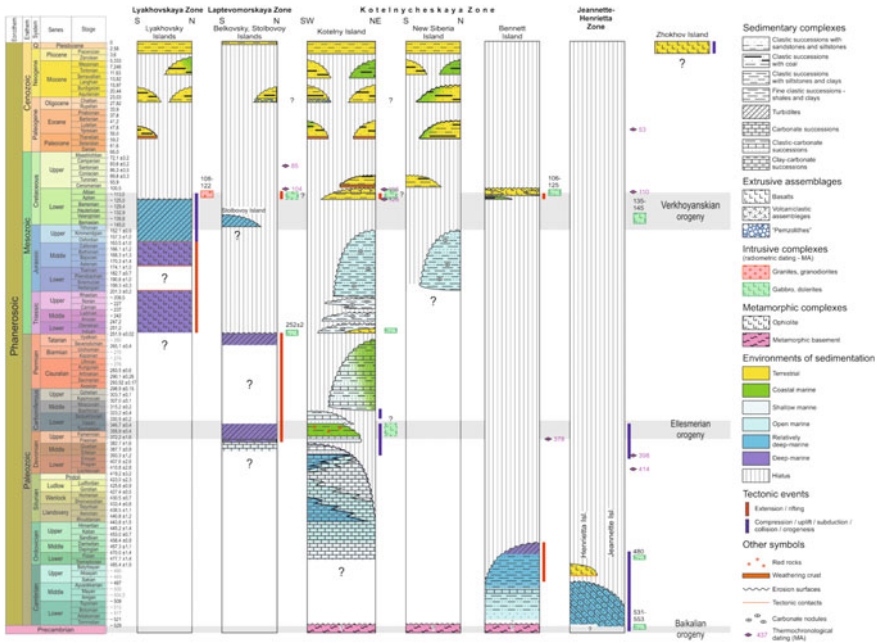
Fig. 11 Tectonostratigraphic charts of the New Siberian Islands Archipelago

were obtained based on the isotope dating of granite and metamorphic xenoliths from Cenozoic basalts of Zhokhov Island. The research findings on volcanogenic-sedimentary island-arc complexes of the Late Riphean–Early Paleozoic prove the presence of the Ellesmerian dislocations on the De Long Islands.

The continuation of the Verkhoyansk fold belt structures to the shelf of the Laptev Sea has been proved on the basis of a study of the geological structure of islands Belkovsky and Stolbovoy and their comparisons with similar coeval formations of continental land (Fig. 11).

4   Wrangel Island

Wrangel Island is located in the front of Mesozoic folded structures of the Arctic continental margin of Chukotka—the Wrangel-Gerald Ridge, to the north and south from South Chukchi and North Chukchi basins. The Wrangel Terrane belongs to the New Siberian-Wrangel fold system in the composition of the Chukchi Mesozoides and has a pronounced fold-thrust structure (Tilman et al. 1970; Kos'ko et al. 1993, 2003; Verzhbitsky et al. 2015) (Fig. 12).

Wrangel Island is built of metamorphic basement and complexly deformed sedimentary cover composed of terrigenous and carbonate Upper Silurian-Middle
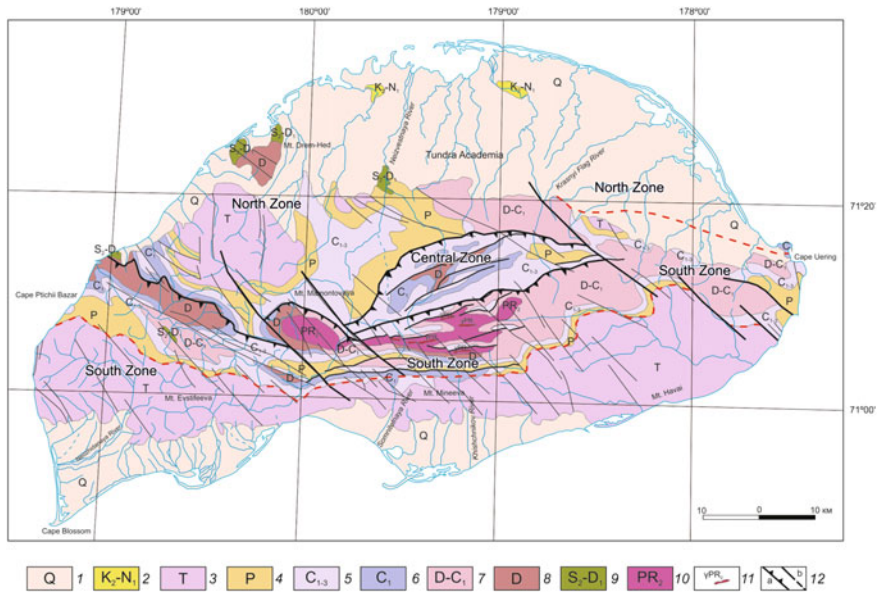
Fig. 12 Geological map and tectonic zones of Wrangel Island (Kos'ko et al. 2003; Sokolov et al. 2017). *1* Quaternary deposits; *2* Upper Cretaceous—Miocene deposits: clays, silts, sands and gravels; *3* Triassic deposits: mudstones, sandstones, siltstones; *4* Permian deposits: mudstones, limestones, sandstones, cherts and gravelits; *5* Lower and Middle Carboniferous deposits: limestones, siltstones, clay shists and phyllites; *6* Lower Carboniferous deposits: conglomerates, mudstones, limestones, dolostones, gypsum, acid and basic volcanic rocks; *7* Devonian and Lower Carboniferous deposits: sandstones, siltstones, conglomerates, carbonate and volcanic rocks; *8* Devonian deposits: sandstones, siltstones, mudstones, quarzites, conglomerates, limestones; *9* Upper Silurian and Lower Devonian deposits: limestones, dolostones, sandstones, siltstones, shales; *10* Upper Proterozoic, Wrangel Complex: meta-volcanics of acid, basic and intermediate compositions, metasandstones, schists; *11* Late Proterozoic granitoides; *12* structural boundaries: a—normal faults; b—other

Devonian, mainly terrigenous Lower-Middle Devonian, carbonate-terrigenous Upper Devonian-Lower Carboniferous, terrigenous-carbonate Upper Carboniferous, carbonate-terrigenous Permian and turbidite Upper Triassic complexes.

The metamorphic basement is composed of dislocated metavolcanic and metasedimentary rocks with single lenses and layers of marbled limestone. The granitoid and amphibolite bodies of the basements are metamorphosed in greenschist and epidoteamphibolite facies (Kos'ko et al. 2003). Current geochronological data (U-Pb zircon age of 594–598 and 700–630 Ma (Kos'ko et al. 1993, 2003; Luchitskaya et al. 2015) shows that it belongs to the Neoproterozoic age.

The Upper Silurian-Middle Devonian strata as thick as 1500 m are composed of quartzite sandstone, quartzite, silty and argillaceous shale with interbeds of limestone, gravelite and conglomerate are exposed to the north-west, in the Drum Head Mountains (Ganelin et al. 1989). Rare limestones contain corals, bryozoans and

brachiopods (Ganelin et al. 1989; Kos'ko et al. 2003). The gravelite and conglomerate contain pebbles of quartz, quartzite, micaceous and quartz-mica schists. Marble and recrystallized limestone are exposed in the eastern part of the island (north of Cape Waring). The thickness of the carbonate section is about 400 m.

The Lower–Middle Devonian is represented by sandstone, siltstone, and shale with conglomerate and gravelite horizons (Kos'ko et al. 1993, 2003; Sokolov et al. 2015). In the Central Ridge, basal conglomerates overlap the Wrangel complex with unconformity and contain pebbles of granite, granite-gneiss and metamorphic schist, as well as mafic metaeffusive fragments. The thickness of the complex is 500–1000 m.

The Upper Devonian-Lower Carboniferous is represented by interbedded dolomite, dolomitized sandy-silty-clayey rocks, polymictic sandstone, siltstone, calcareous rocks with interlayers of gypsum conglomerate and gravelite. The thickness of the Upper Devonian-Lower Carboniferous sediments varies from 500 to 800 m.

The Upper Carboniferous is mainly composed of various organogenic and organogenic-clastic limestones with subordinate shale and mudstone interbeds. The limestone is characterized by flint interlayers and lenses. In the lower part, there are conglomerates with fragments of quartzite, multi-coloured shale and granite, and carbonate rocks have graded bedding: calcirudites, calcarenites and calcilutites are distinguished. The upper part of the section is composed of alternating limestone and shale. The total thickness of the Upper Carboniferous reaches 1200 m.

The Permian in the lower part is composed of alternating bituminous limestone and silty-clayey rocks with rare interlayers of finegrained sandstone. Above, there is a black shale sequence with interbeds of siltstone and aleuropelite. In the upper part, there are horizons of rhythmic alternation of sandstone, siltstone and mudstone, which makes them similar to Triassic turbidite. The thickness of the complex is 1000–1200 m.

The Triassic consists of a sequence of terrigenous turbidite, which is characterized by rhythmic intercalation of dark sandstone, siltstone and shale. The Carian-Norian age has been determined based on rare fauna finds (Kos'ko et al. 2003; Sokolov et al. 2017). The thickness of the complex is 1200–2000 m.

Three tectonic zones have been identified within the island: Northern, Central and Southern, each of which has structural, stratigraphic and lithologic features (Sokolov et al. 2017).

Northern zone. Characteristic features of the zone are: (1) the lack of metamorphic basement outcrops; (2) occurrence of Upper Silurian-Lower Devonian sediments in the base of the section; (3) the Upper Silurian-Lower Devonian complex is crushed into the folds of submeridional strike that distinguishes it from the structural parageneses of the younger Wrangel Island complexes of sublatitudinal strike. The structural plan of the Upper Silurian-Lower Devonian complex was formed under conditions of sublatitudinal compression and is considered to be a result of Ellesmerian deformations (Verzhbitsky et al. 2015; Sokolov et al. 2017).

Fig. 13 Lower Carboniferous gypsum-bearing strata, Central zone, Krasny Flag River

Central zone. The zone consists of two structural stages. The lower one is composed of metamorphosed basalts and acid volcanic rocks and intensely deformed carbonate-terrigenous Devonian-Lower Carboniferous complex (Fig. 13). The age of zircons from acid volcanic rocks is 598.6 ± 7.5 and 594.4 ± 7.1 Ma (U-Pb, SHRIMP-II), from basalts 500–600 Ma (U-Pb, LA-ICP-MS) (Luchitskaya et al. 2015; Sokolov et al. 2017). The upper structural stage is composed of slightly deformed Lower and Upper Carboniferous-Permian limestone, which lie with sharp unconformity and erosion on volcanogenic strata. Coeval complexes of the Northern and Southern zones are characterized by intensive fold-thrust deformations of the northern vergence.

Southern zone. The most complete sections are widespread there, including the metamorphic basement and the overlying sedimentary cover in the stratigraphic range from the Devonian (Fig. 14) to the Triassic.

There are two large thrusts within the Southern zone. Along the Main Thrust in the Central Mountains, the rocks of the Wrangel complex are overthrust onto Devonian and Carboniferous sediments (Ganelin et al. 1989). The Mineev Thrust is located to the south and in most places is distinctly expressed in relief. Along the thrust, the Triassic sediments gently overlap and cut the structural plan of the Paleozoic complexes.

Fold-thrust deformations are of sublatitudinal strike and northern vergence. They formed in the Chukchi (Late Cimmerian) phase of deformations at the end of the Early Cretaceous. The structures are deformed by dextral and sinistral shift faults

Fig. 14 Lower-Middle Devonian basal conglomerate, Southern zone, Central Mountains

of northwestern strike (Kos'ko et al. 1993, 2003; Verzhbitsky et al. 2015), some of which intersect and displace structures of the Northern, Central and Southern zones. They formed during the Chukchi (Late Cimmerian) phase of deformations in the late Early Cretaceous (Fig. 15).

5 Continental Eastern Arctic

The onshore part of the eastern Russian Arctic comprises the Siberian platform and surrounding—the Verkhoyansk-Kolyma orogenic region (VKOR) and the Novosibirsk-Chukotka fold system in the east. The northern VKOR includes the Verkhoyansk-Chersky orogenic belt consisting of the Verkhoyansk fold-and-thrust belt in the west and the Kolyma-Omolon superterrane in the east (Parfenov et al.
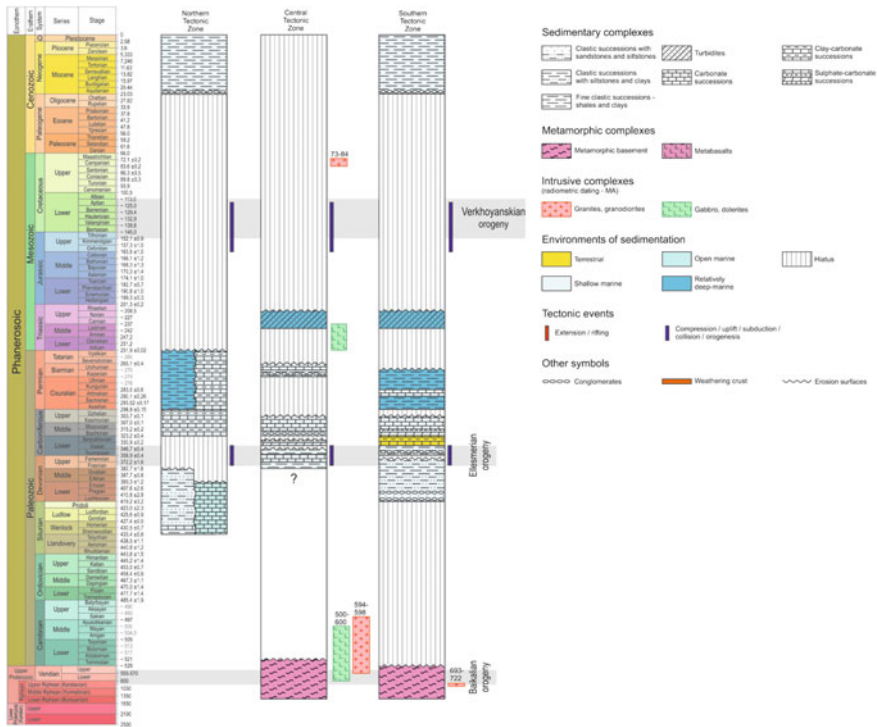
Fig. 15 Tectonostratigraphic charts of Wrangel Island

2003; Prokopiev, 2000; Khudoley and Prokopiev 2007). In plan, the VKOR forms an orocline known in literature as the Kolyma loop (Zonenshain et al. 1990a, b). Further to the east, the VKOR borders along the South Anyui suture zone (accretionary wedge terrane) on the continental part of the Novosibirsk-Chukotka fold system including Chukotka terrane. The eastern and south-eastern parts of the Kolyma-Omolon superterrane and the Chukotka cratonal terrane are overlapped by the Okhotsk-Chukotka volcano-plutonic belt (Parfenov et al. 1993a, b, 2003).

The sedimentary cover of the northeastern Siberian platform is made of clastic-carbonate, volcanogenic, and volcaniclastic rocks of Proterozoic, Paleozoic, and Mesozoic age. Magmatic formations include the Early Cambrian rift-related bimodal complex, Middle Paleozoic, Permo-Triassic and Mesozoic kimberlites, fields of intrusive and effusive Permo-Triassic traps, and plutons composed of Middle Paleozoic ultra-mafic-alkali rocks. The Archean and Early Proterozoic rocks of the crystalline basement of the Siberian platform are exposed in the Aldan shield, in the western part of the same name anteclise, and in the Olenek uplift ahead of the front of the Verkhoyansk-Kolyma orogenic region. Rift-related basins of Late Precambrian and Middle Paleozoic age (Khastakh, Sukhano-Motorchuna, and Kyutyungde) are located within the Anabar anteclise (Prokopiev et al. 2001).

The Lena-Anabar basin made of Upper Paleozoic and Mesozoic rocks and the more northerly Olenek fold belt extend sublatitudinally along the Laptev Sea coast. Limbs of anticlines and cores of synclines within the belt limits are composed of Jurassic and Lower Cretaceous rocks, while Triassic and Upper Permian sandstones and siltstones are exposed in the cores of anticlines.

Outer and inner zones can be identified within the Verkhoyansk fold-and-thrust belt extending along the eastern margin of the Siberian platform. The outer zone includes the Priverkhoyansk foreland basin made of Late Jurassic-Cretaceous clastic rocks and the frontal part of the Verkhoyansk fold-and-thrust belt. The Kular-Nera slate belt (terrane) and the Polousnyi-Debin terrane are located in the inner zone (Prokopiev 2000).

The Verkhoyansk fold-and-thrust belt sedimentary strata initially formed along the passive continental margin of the Siberian (North-Asian) craton. These strata comprise close to Siberian platform margin mainly Carboniferous and Permian deposits which change to Triassic and Jurassic rocks further to the east. This is thick sedimentary wedge (up to 15 km) traditionally called the Verkhoyansk clastic complex which lies on top of the Late Precambrian-Lower Paleozoic clastic-carbonate shelf sediments and Middle Paleozoic rift deposits, exposed in the north along the platform boundary, and comprises clastic shallow-marine, deltaic and open shelf sediments prograding eastwards (Tectonics, geo-dynamics, and metal-logeny…, 2001; Prokopiev et al. 2008). Late Mesozoic transverse granitic belts [140–100 Ma (Prokopiev et al. 2018a, b)] penetrate the Verkhoyansk fold-and-thrust belt.

The Kular-Nera and the Polousnyi-Debin terranes are composed of repeatedly deformed Upper Permian-Jurassic elastics predominated by shale, siltstone, sand-stone, and tuffs (Fig. 16). Olistostrome horizons are also present. The Upper Jurassic deposits of the northern Polousnyi synclinorium are mainly characterized by a clayey composition of sediments with sporadic andesite, basaltic andesite, and basalt belonging to the Svyatoi Nos-Oloy magmatic arc. The Late Cenozoic deposits of the Primorsky lowland overlap the deposits of these terranes in the north.

The Kolyma-Omolon superterrane is located to the east of the Kular-Nerra terrane and consists of terranes of various geodynamic affinity that were amalgamated into a single block in the late Middle Jurassic. The northern part of the superterrane comprises the Omulevka terrane and the Nagondzha turbidite terrane while the central part includes the Alazeya island-arc and Kenkel'da accretionary wedge terranes. To the north, the rocks of the Berezovka turbidite and the Oloy and Khetachan island-arc terranes are exposed.

The Omulevka terrane stretches for 1000 km along the southwestern and north-western margins of the Kolyma-Omolon superterrane, and has a width of 100–150 km. The terrane is composed mainly of Ordovician-Early Carboniferous and, to a lesser extent, Upper Paleozoic-Early Mesozoic deposits. Pre-Ordovician formations are composed of metamorphic rocks. Along with the primary sedimentary rocks, they include felsic and intermediate volcanic rocks. Several types of rock associ-ations are identified in the Ordovician-Lower Carboniferous deposits: bioherm of the carbonate platform, red-colored sulfate-bearing lagoonal and shallow marine
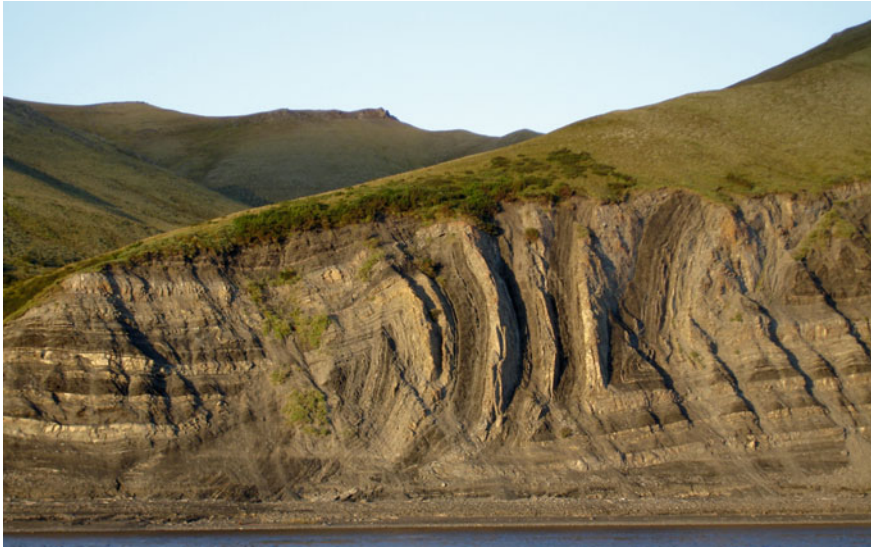
Fig. 16 Deformed Permian deposits of the frontal part of the Verkhoyansk fold-thrust belt in the estuary of the Lena River (photo by A. Prokopiev)

dolomites and marls, turbidites with slump folds, as well as deep-water shales with Ordovician graptolites and basalts. Late Paleozoic strata are composed of deep-water deposits. The Triassic, Lower and lower Middle Jurassic deposits mainly comprise fine-grained clastic rocks.

The Nagondzha turbidite terrain stretches for 450 km as a narrow strip to the north and west of the Omulevka terrane. The terrane is composed of repeatedly deformed Late Paleozoic and Early Mesozoic strata. The oldest Carboniferous-Permian deposits consist of hemipelagic volcaniclastic and carbonate-clastic rocks. The Middle Triassic (Ladinian) and lower units of the Upper Triassic sediments are composed of distal turbidites. The overlying Upper Triassic-Lower Jurassic deposits are composed of rhythmically intercalated siltstone, shale and sandstone. The upper part of the section is composed of Bathonian-Callovian clastic deposits with olistostromes. The Berezovka turbidite terrane is composed of Upper Devonian–Triassic volcaniclastic and carbonate sediments. The Oloy island arc terrane adjacent to the northern part of Berezovka terrane is represented by metamorphic Middle–Upper Devonian rhyolites, tuffs, siltstones, limestones and sandstones, and Carboniferous clastic strata. They are overlain with unconformity by volcaniclastic rocks. The Khetachan island-arc terrane is formed by the folded Upper Triassic and Lower Jurassic volcaniclastic strata which are unconformably overlain by Kimmeridgian-Volgian volcanic rocks of the Svyatoi Nos-Oloy island arc.

The Alazeya island-arc and Kenkel'da accretionary wedge terranes comprise the central part of the Kolyma loop. The Alazeya terrane extends to the south-west of the Khetachan terrane and is composed of Carboniferous-Early Jurassic predominantly

volcaniclastic rocks, which are deformed into gentle open folds. The Kenkel'da terrane is adjacent to the north-western part of the Alazeya terrane. The terrane consists of unknown age rocks: metabasalts (oceanic tholeiites and olivine basalts), which are associated with quartzites, amphibole-mica-quartz, actinolite-epidote-chlorite, chlorite and glaucophane schists; greywackes, tuffs, interlayers and lenses of gravelites, silicites, jasper, pelitomorphic limestone and rare basalt layers. The intrusive rocks of the terrane are represented by tonalites, plagiogranites and gabbro-diorites. The Kenkel'da and Alazeya terranes are overlapped with unconformity by slightly deformed Middle and Upper Jurassic shallow-water marine sediments with conglomerates at the base (Parfenov et al. 2003).

In the west of the Kolyma-Omolon superterrane ophiolites with associated metamorphic rocks obducted in Late Mesozoic time crop out in tectonic sheets (Oxman et al. 1995; Oxman 2003; Parfenov et al. 2003).

The axial part of the Verkhoyansk-Chersky orogenic belt is cut by granitoid plutons of the Late-Jurassic-Early Cretaceous [156–144 Ma (Akinin et al. 2009)] Main (Kolyma) and the Early Cretaceous [137–100 Ma (Layer et al. 2001)] Northern batholith belts. Along the Omulevka terrane and adjacent areas of the Polousnyi-Debin terrane there extends the Uyandina-Yasachnaya magmatic arc composed of Oxfordian-Volgian volcanogenic-sedimentary rocks.

The South Anyui accretionary wedge terrane (suture) extends along the northern margin of the VKOR and the Novosibirsk-Chukotka fold system. It can be traced by linear magnetic and gravity anomalies to the north-west for 400 km under a cover of Cenozoic sediments from the lower reaches of the Kolyma R. to the coast of the East Siberian Sea. The terrane is composed of Callovian and Oxfordian pillow basalt, greywacke, shale, and subordinate chert as well as Lower Cretaceous turbidite. Glaucophane shale and fragments of ophiolites are reported. All deposits are very complexly and repeatedly deformed. Flat-lying Al-bian-Late Cretaceous volcanic rocks of the Okhotsk-Chukotka belt overlap the terrane (Katkov et al. 2010; Sokolov et al. 2014, 2015; Ganelin 2015).

The Chukotka terrane (a fragment of the Late Paleozoic-Early Mesozoic passive margin) is represented by intensely deformed and metamorphosed Precambrian rocks in the greenschist and amphibolite fades, clastic-carbonate Paleozoic deposits, and is dominated by thick terrigenous Triassic turbidites (Tuchkova 2011; Tuchkova et al. 2014). The earlier Phanerozoic tectonic events in Chukotka are associated with the Ellesmerian orogeny, as indicated by early Carboniferous granitoids (Luchitskaya et al. 2015). Permo-Triassic basalts and dolerite sills are known in the east of the terrane (Ledneva et al. 2011). Upper Jurassic-Lower Cretaceous volcaniclastic deposits are widespread in several small depressions. The rocks of the terrane are intensely and repeatedly deformed, and in the east are penetrated by Late Jurassic granite plutons. Metamorphic core complexes of Late Mesozoic age are reported. In the southwest of the terrane, the Triassic folded deposits are unconformably overlain by the shallow-water marine sedimentary and volcanic Upper Jurassic deposits and penetrated by the Late Mesozoic granites of the Nutesyn magmatic arc (Katkov et al. 2010). The uppermost sue cession comprises the Hauterivian-Barremian continental clastic deposits (Sokolov et al. 2014; Ganelin 2015). The northern part of the terrane
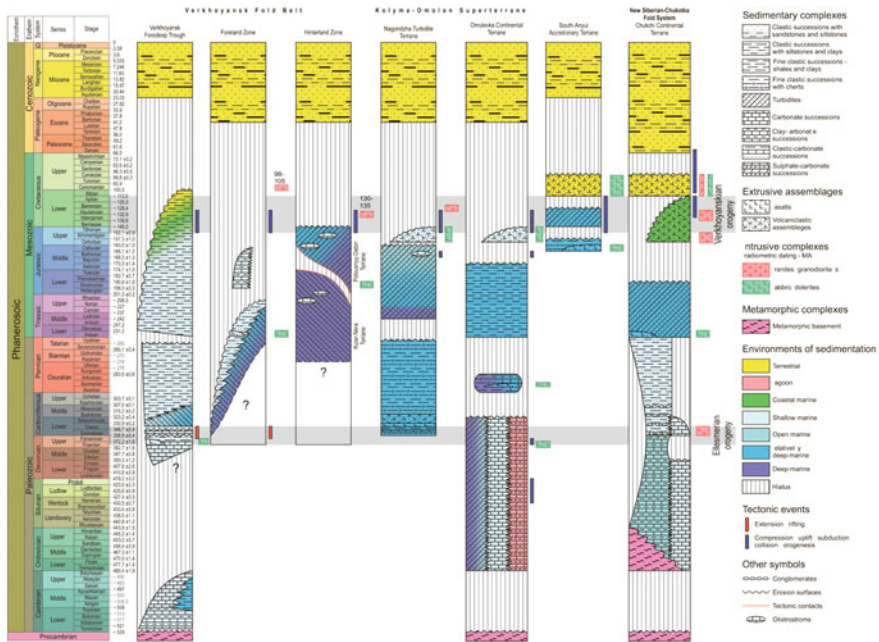
Fig. 17 Tectonostratigraphic charts of the continental eastern Arctic

is hidden under the East Siberian and Chukchi seas, in the southwest it borders on the South Anyui terrane: and in the south and southeast it is covered by Upper Cretaceous volcanic rocks of the Okhotsk-Chukotka volcanic belt (Fig. 17).

References

Akinin VV, Prokopyev AV, Toro H, Miller EL, Vuden J, Goryachev NA, Alshevsky AV, Bakharev AG, Trunilina VA (2009) U-Pb-SRIMP age of granitoids of the Main batholithic belt (NE Asia). Dokl RAS. 426(2):216–221 (in Russian)

Akinin VV, Gottleib E, Miller E, Sobolev NN (2015) Age and composition of basement beneath the De Long archipelago, Arctic Russia, based on zircon U-Pb geochronology and O-Hf isotopic systematic from crustal xenoliths in basalts of Zhokov Island. Arctos

Danukalova MK (2016) The geological history of the territory of the Bennett and Kotelny islands in the Early Paleozoic. a dissertation for the degree of candidate of geological and mineralogical sciences. GIN RAS, 179 p (in Russian)

Daragan-Sushchova LA, Petrov OV, Daragan-Sushchov YI, Rukavishnikova DD (2009) Structural style of the Laptev Sea. In: Proceeding of RAO/CIS offshore 2009 "the international conference and exhibition for oil and gas resources development of the Russian Arctic and continental shelf", pp 321–327 (in Russian)

Dorofeev VK, Blagoveshchenskiy MG, Smirnov AN, Ushakov VI (1999) Novosibirsk islands. Geological structure and mineralogy. VNIIOkeangeologiya, St. Petersburg, 130 p (in Russian)

Egiazarov BKh (1959) Geological structure of the Severnaya Zemlya archipelago. In: Proceedings of NIIGA, vol 94. L.: Gosgeoltekhizdat, 138 p (in Russian)

Fedorov PI, Flerov GB, Golovin DI (2005) New data on the age and composition of volcanic rocks of Bennetta Island (Eastern Arctic). Rep Acad Sci 400(5):666–670 (in Russian)

Ganelin VG, Matveev AV, Kropacheva GS (1989) Upper paleozoic sediments of Wrangel Island. VSEGEI, Leningrad, 87 p (in Russian)

Ganelin AV (2015) Ophiolites of Western Chukotka (structure, age, composition, geodynamic setting). GIN RAS, Moscow, 31 p (in Russian)

Gee DG (2002) October revolution Island tectonics: Swedarctic expedition 2002. In: Rickberg S (ed) Polarforskningssekretariatet Arbok 2002. Polarforsknings-sekretariatet, Stockholm, pp 75–79

Katkov SM, Miller EL, Toro J (2010) Structural paragenes and age of deformation of the Anyui-Chukotka fold system (Northeastern Russia). Geotectonics 44(5):61–80 (in Russian)

Khapilin AF (1982) Stratigraphy of the Devonian deposits of the Severnaya Zemlya archipelago. Collection scientific. Tr. Sevmorgeologiya/ L., pp 103–119 (in Russian)

Khudoley AK, Prokopiev AV (2007) Defining the eastern boundary of the North Asian craton from structural and subsidence history studies of the Verkhoyansk fold-and-thrust belt. In: Sears JW, Harms TA, Evenchick CA (eds) Whence the mountains? Inquiries into the evolution of orogenic systems: a volume in honor of Raymond A. Price: geological society of America special paper, vol 433, pp 391–410

Kos'ko MK, Cecile MP, Harrison JC, Ganelin VG, Khandoshko NG, Lopatin VG (1993) Geology of Wrangel Island, between the Chukchi and East Siberian Seas, Northeastern Russia. Geol Surv Canada Bull 461:101

Kos'ko MK, Avdyunichev VV, Ganelin VG, Opekunov AY, Opekunova MG, Cecile MP, Smirnov AN, Ushakov VI, Khandozhko NV, Harrison JC, Shulga YD (2003) The Wrangel Island: geology, metallogeny, geoecology, vol 200. SPb.: VNIIOkeangeologia, 137 p (in Russian)

Kuz'michev AB, Solov'ev AV, Gonikberg VE, Shapiro MN, Zamzhitskiy OE (2006) Syncollisional Mezozoic clastic sediments on large Lyakhovsky Island (Novosibirskian Island), vol 14, No 1. Strztigrafiya. Geologicheskaya korrelyatsiya, pp 48–68 (in Russian)

Kuz'michev AB, Aleksandrova GN, Herman AB, Danukalova MK, Simakova AN (2013) Paleogene-Neogene sediments of Belkov Island (New Siberian Islands): characteristics of sedimentary cover in the eastern Laptev shelf. Stratigr Geol Correl 21(4):421–444

Kuznetsov NB (2008) Cambrian Orogen Protouralide-Timanide: structural evidence of a collisional nature. DAN 423(6):774–779 (in Russian)

Layer PW, Newberry R, Fujita K, Parfenov LM, Trunilina VA, Bakharev AG (2001) Tectonic setting of the plutonic belts of Yakutia, Northeast Russia, based on 40Ar/39Ar and trace element geochemistry. Geology 29(2):167–170

Lazarenko NP (1982) Correlation of Cambrian deposits of the Severnaya Zemlya archipelago with deposits of Cambrian adjacent territories. Geology of the Severnaya Zemlya archipelago. L.: PGO "Sevmorgeologiya", pp 169–176 (in Russian)

Ledneva GV, Pease VL, Sokolov SD (2011) Permo-Triassic hypabyssal mafic intrusions and associated tholeiitic basalts of the Kolyuchinskaya Bay, Chukotka (NE Russia): links to the Siberian LIP. J Asian Earth Sci 40:737–745

Lorenz H (2013) Geochronology of crustal xenoliths and detritalzircons from the De Long islands. 3P Arctic conference andexhibition, Stavanger, Norway, abstract 90177

Luchitskaya MV, Sokolov SD, Katkov SM, Kotov AB, Natapov LM, Belousova EA (2015) Late Paleozoic granitoids of Chukotka: peculiar features of composition and the location in the structure of Russian Arctic. Geotectonics 2015(4):1–27 (in Russian)

Makariev AA, Lazarenko NP, Rogozov YuG (1981) New data on Cambrian deposits of the Severnaya Zemlya archipelago. Lithology and paleogeography of the Barents and Kara Seas. L, NIIGA, pp 97–109

Markovsky VA, Makaryev AA (1982a) Ordovician deposits of the Severnaya Zemlya archipelago. Geology of the Severnaya Zemlya archipelago. L.: Sevmorgeo, pp 22–39 (in Russian)

Markovsky VA, Smirnova MA (1982b) Silurian deposits of the Severnaya Zemlya archipelago. Geology of the Severnaya Zemlya archipelago. L.: Sevmorgeo, pp 39–60

Matukhin RG, Menner VVl (1999) Stratigraphy of the Silurian and Devonian of the Severnaya Zemlya archipelago. Novosibirsk, 174 p (in Russian)

Metelkin DV, Vernikovsky VA, Tolmacheva TYu, Matushkin NYu, Zhdanova AI (2014) The first paleomagnetic data for the Early Paleozoic deposits of the Novosibirsk Islands (East Siberian Sea): on the formation of the South-Anyuy suture and tectonic reconstruction of Arctida. Lithosphere 3:11–31 (in Russian)

Oxman VS (2003) Tectonic evolution of Mesozoic Verkhoyansk-Kolyma belt (NE Asia). Tectonophysics 365:45–76

Oxman VS, Parfenov LM, Prokopiev AV, Timofeev VF, Tretyakov FF, Nedosekin YD, Layer PW, Fujita K (1995) The Chersky Range ophiolite belt, Northeast Russia. J Geol 103(5):539–556

Parfenov LM, Natapov LM, Sokolov SD, Tsukanov NV (1993a) Terrane analysis and accretion in North-East Asia. Geotectonics 1:68–78 (in Russian)

Parfenov LM, Natapov LM, Sokolov SD, Tsukanov NV (1993b) Terrane analysis and accretion in North-East Asia. Island Arc 2:35–54

Parfenov LM, Berzin NA, Khanchuk AI, Badarch G, Belichenko VG, Bulgatov AN, Dril SI, Kirillova GL, Kuzmin MI, Nokleberg U, Prokopyev AV, Timofeev VF, Tomurtogo O, Yan Kh (2003) Model for the formation of orogenic belts in Central and North-East Asia. Pac Geol 6:7–42

Petrov OV, Proskurin VF (2010) Early Mesozoic carbonatites in folded formations of the Taimyr Peninsula. Dokl Earth Sci 435(2):1592–1595

Pogrebitsky YE (1976) Geodynamic system of the Arctic Ocean. Sov Geol 12:3–22 (in Russian)

Prokopiev AV (2000) The Verkhoyansk-Chersky collisional orogeny. Pac Geol 15:891–904

Prokopiev AV, Toro J, Miller EL, Gehrels GE (2008) The paleo-Lena River—200 m.y. of transcontinental zircon transport in Siberia. Geology 36(9):699–702

Prokopiev AV, Ershova VB, Anfinson O, Stockli D, Powell J, Khudoley AK, Vasiliev DA, Sobolev NN, Petrov EO (2018a) Tectonics of the New Siberian Islands archipelago: Structural styles and low-temperature thermochronology. J Geodyn 121:155–184

Prokopiev AV, Borisenko AS, Gamyanin GN, Fridovsky VYu, Kondratyeva LA, Anisimova GS, Trunilina VA, Vasyukova EA, Ivanov AI, Travin AV, Koroleva OV, Vasiliev DA, Ponomarchuk AV (2018b) Age lines and geodynamic conditions of the formation of deposits and magmatic formations of the Verkhoyansk-Kolyma folded region. Geol Geophys 59(10):1542–1563 (in Russian)

Proskurnin VF (1995) New volcanic-plutonic association of the Severnaya Zemlya and the features of its metalliferous content, vol 1. Taimyr Subsoil, Norilsk, pp 93–100 (in Russian)

Proskurnin VF, Vereshchagin MF (1989) A new type of basic magmatism of the northern framing of the Siberian platform (late Riphean complex of alkaline gabborides of Taimyr). In the book: "Basic magmatism of the Siberian platform and its metallogeny." Abstracts of all-union use on october 18–20, Yakutsk, pp 75–76 (in Russian)

Proskurnin VF, Listkov AG, Gavrish AV, Vanyunin NV (2002) Metallogenic analysis and prospects for economic development of the Taimyr-Severnaya Zemlya gold province. Taimyr Mineral Potential. Issue 5. SPb.: VSEGEI Publishing House, pp 10–42 (in Russian)

Proskurnin VF, Petrov OV, Bagdasarov EA, Rozinov MI, Tolmacheva EV, Larionov AN, Bil'skaya IV, Gavrish AV, Mozoleva IN, Petrushkov BS (2010) Origin of Carbonatites of Eastern Taimyr deduced from an isotopic and geochemical study of zircons. Geology of ore deposits, vol 52, No 8, pp 711–724 (published in Zapiski RMO (Proceedings of the Russian mineralogical society), No. 1, pp 19–36)

Proskurnin VF, Petrushkov BS, Gavrish AV, Bagaeva AA, Vinogradova NP, Larionov AN, Vernikovsky VA, Metelkin DV, Vernikovskaya AE, Matushkin NY (2014) Rhyolite-granite association in the central Taimyr zone: evidence of accretionary-collisional events in the neoproterozoic the article was translated by the authors. Russ Geol Geophys 55(1):18–32 (in Russian)

Ravich MG (1954) Precambrian of Taimyr. In: Korzhinsky DS, Obruchev SV, Vodtransizdat L-M (eds) Proceedings of NIIGA; Issue 76. State Publishing House of Water Transport, 312 p (in Russian)

Severnaya Z, Gramberg IS, Ushakova VI (eds) (2000) Geological structure and mineralogy. SPb.: VNIIOkeangeologiya Publishing House, 187 p (in Russian)

Sokolov SD, Ledneva GV, Tuchkova MI, Luchitskaya MV, Ganelin AV, Verzhbitsky VE (2014) Chukchi Arctic continental margins: tectonic evolution, link to the opening of the Amerasia Basin. In: Fairbanks A, Stone DB, Grikurov GE, Clough JG, Oakey GN, Thurston DK (eds) ICAM VI: Proceedings of the international conference on Arctic Margins VI. A.P. Karpinsky Russian Geological Research Institute (VSEGEI), St. Petersburg, pp 97–114

Sokolov SD, Tuchkova MI, Ganelin AV, Bondarenko GE, Leier P (2015) Tectonics of the South Anyui suture (Northeast Asia). Geotectonics 1:5–30 (in Russian)

Sokolov SD, Tuchkova MI, Moiseev AV, Verzhbitsky VE, Malyshev NA, Gushchina MYu (2017) Tectonic zonality of Wrangel Island (Arctic). Geotectonics 1:3–18 (in Russian)

Tectonics, geodynamics and metallogeny of the territory of the Republic of Sakha (Yakutia) (2001) M: MAIK "Science/Interperiodica" (in Russian)

Tilman SM, Bogdanov NA, Bialobrzegsky SG, Chekhov AD (1970) Geological structure of Wrangle Island. Geology of the USSR. T. XXVI. Islands of the Soviet Arctic. M.: Nedra, pp 377–404 (in Russian)

Tuchkova MI (2011) Lithology of terrigenic rocks from Mesozoic fold belt of the continental margin (Great Caucasus, North-East Asia), vol 600. Trans. of geological Institute Russian Academy of Sciences, LAP, 334 p (in Russian)

Tuchkova MI, Sokolov SD, Khudoley AK, Hayasaka Y, Moiseev AV (2014) Permian and Triassic deposits of Siberian and Chukotka passive margins: sedimentation setting and provenance. In: Fairbanks A, Stone DB, Grikurov GE, Clough JG, Oakey GN, Thurston DK (eds) ICAM VI: proceedings of the international conference on Arctic Margins VI. A.P. Karpinsky Russian Geological Research Institute (VSEGEI), St. Petersburg, pp 61–96

Uflyand AK, Natapov LM, Lopatin VM, Chernov DV (1991) About tectonic nature of Taimyr. Geotectonics 6:76–93 (in Russian)

Vakar VA, Voronov PS, Egiazarov BK (1958) Taymyr-Severnaya Zemlya Fold area. Geological structure of the USSR. V. III. Tectonics. M.: Gosgeoltekhizdat, pp 88–94 (in Russian)

Vernikovsky VA (1996) Geodynamic evolution of the Taimyr folded region. Publishing House SB RAS, Novosibirsk, 203 p (in Russian)

Verzhbitsky VE, Sokolov SD, Tuchkova MI (2015) Present-day structure and stages of tectonic evolution of Wrangel Island, Russian Eastern Arctic region. Geotectonics 49(3):165–192

Volnov DA, Sorokov DS (1961) The geological structure of the Bennetta Island. Sbornik po geologii I neftegazonosnosti Arktiki, vol 16. Gotoptekhizdat, Leningrad, pp 5–18 (in Russian)

Zabiyaka AI (1971) Structure-facies zoning of the Precambrian in Taimyr. Geology and mineral resources of the Krasnoyarsk Territory. Kraen. Book Publisher, Krasnoyarsk, pp 132–136 (in Russian)

Zonenshain LP, Kuzmin MI, Natapov LM (1990a) Geology of the USSR: a plate tectonic synthesis. In: Page BM (ed) Geodynamics Series, vol 21. American Geophysical Union, Washington, D.C

Zonenshain LP, Kuzmin MI, Natapov LM (1990b) Tectonics of lithospheric plates of the USSR, vol 2. M.: Nedra. Book, 334 p (in Russian)

Correlation of Chukotka, Wrangel Island and the Mendeleev Rise

M. I. Tuchkova, S. P. Shokalsky, S. D. Sokolov, and O. V. Petrov

Abstract The paper analyzes Mendeleev Rise sandstones as compared with Triassic sediments of continental Chukotka and Wrangel Island. The study of sedimentological characteristics showed that in the samples, there is gradual maturation of clastic material from the south (continental Chukotka) to the north (Mendeleev Rise). Moreover, in the samples from the Mendeleev Rise, there is no geochemical evidence of redeposition of clastic material, but severe weathering of the rocks from the provenance area has been recorded. High content of clastic quartz with microfractures (18% of all counted grains) in the sample from the Mendeleev Rise indicates that there is continental land in the vicinity from which quartz grains were eroded. Southwards, the amount of the quartz with microfractures decreases: in the Triassic sandstone of Wrangel Island, it occupies 8% and in the samples from Chukotka 3%. Analysis of lithological data indicates the presence of a large continental block in the northern part of the eastern Arctic, near which Upper Triassic shallow-marine deposits of the Mendeleev Rise were formed.

Paleogeographic reconstructions of the Triassic time indicate the existence of a large basin in the present-day northeastern Arctic (Kos'ko 2007; Blakey 2018; Golonka 2011; Scotese 2011, etc.). Studying Triassic turbidite deposits of Chukotka and Wrangel Island made it possible to establish a northern provenance area (Tuchkova 2011; Tuchkova et al. 2014).

Northern provenance area, which was named the Crockerland, was also found for the Triassic sediments of the Sverdrup Basin (Embry and Dixon 1994; Anfinson et al. 2016). Shatsky (1935) assumed the existence of the Hyperborea continent in the

M. I. Tuchkova (✉) · S. D. Sokolov
Geological Institute, Russian Academy of Sciences (GIN RAS), 7 Pyzhevksy per., Moscow 119017, Russia
e-mail: tuchkova@ginras.ru

S. P. Shokalsky · O. V. Petrov
Russian Geological Research Institute (VSEGEI), 74 Sredny Prospect, St. Petersburg 199106, Russia

center of the present-day Eastern Arctic. Later, in mobilist paleotectonic reconstructions, this continental block was named Arctida (Zonenshain et al. 1990). Concepts about Arctida were described in literature (Kuznetsov 2006; khain and Filatova 2009; Laverov et al. 2013; Vernikovsky et al. 2013). In the modern structure, fragments of tectonically dispersed Arctida can be found in Taimyr, Severnaya Zemlya, New Siberian Islands, Chukotka, and Alaska.

In these publications, it is supposed that main structures of Central Arctic Uplifts of the Arctic Ocean (Lomonosov Ridge, Mendeleev, Alpha and Chukchi Rises, Makarov and Podvodnikov Basins) also belong to this ancient continent. Modern structural style of the Eastern Arctic was formed during the Mesozoic and Cenozoic as a result of tectonic rearrangement and relative movements of large continental blocks to form the Amerasian Basin in the Early Cretaceous and the Eurasian basin in the Cenozoic.

It is shown (Sokolov et al. 2015; Sokolov et al. 2014) that when the Proto-Arctic (South-Anyui) ocean was closed, a large continental block, the Chukotka microcontinent, became part of Eurasia. The collision of the Chukotka microcontinent with structures of the active margin of Siberia took place in the Hauterivian-Barremian. In the Triassic, the Chukotka microcontinent was part of the Arctic Canada. Turbidite accumulated on the passive margins of the North American continent. Now they are widespread in Chukotka and Wrangel Island, where they are rather well studied (Tuchkova 2011; Tuchkova et al. 2009, 2014).

There is no information on the composition of the Triassic deposits on the vast water area of the Russian shelf of the Eastern Arctic, since they form part of the acoustic basement, which is overlapped by the Aptian-Albian and possibly Hauterivian-Barremian deposits (Drachev 2011; Verzhbitsky et al. 2012; Nikishin et al. 2014; Arctic Basin … 2017). Undeformed or slightly deformed Triassic deposits are widespread north of the Wrangel-Herald front of Late Mesozoic deformations. According to seismic data, they are part of the sedimentary cover of the North Chukchi Trough.

In the area of Central Arctic Uplifts, Triassic sediments were not found among the rocks raised from the seabed by Russian and foreign scientific expeditions: R/V *Academician Fedorov* (*Arctic* 2000, 2005, 2007), icebreakers *Healy* (2008, 2009) and *Polarstern* (2008).

During the Russian expedition *Arctic-2012,* on escarps and steep slopes of underwater mountains of the Mendeleev Rise, sampling was carried out using not only traditional methods (dredge, grabbing excavator, box corer, bottom sampler), but also for the first time deep-sea core drilling at a shallow depth (up to 2 m) and sampling with manipulators of the research submarine. Bottom-stone material is dominated by carbonaceous rocks, mainly dolomite; terrigenous rocks (sandstone, siltstone, mudstone) occupy 20–25%. Geochronological studying detrital zircons testifies to the Triassic age of several sandstone samples, including fine-grained quartz sandstone with carbonate cement from a boulder taken by the submarine from the escarp of the steep southeastern slope of the Shamshur Seamount (Morozov et al. 2013).

The purpose of this work was to compare sandstone of Chukotka, Wrangel Island, and Mendeleev Rise for the restoration of Triassic paleogeography in the Russian offshore sector of the Eastern Arctic.

1 Geologic Framework

In the tectonic zoning of the Russian offshore sector of the Eastern Arctic, the most difficult is the correlation of individual blocks located on the continent, islands and the Arctic shelf. Previously, tectonic structures of Taimyr, New Siberian Islands, Wrangel Island and significant areas of the Arctic shelf were referred to the Eastern Arctic fold system, which borders the Hyperborean Platform in the north (Tectonics… 1980). Later, tectonic setting was performed on the basis of terrane analysis (Parfenov et al. 1993a, b; Nokleberg et al. 1994; Geodynamics… 2006; Sokolov 2010). In the Chukotka fold area, there are the New Siberian-Wrangel, Anyui-Chukotka, and South Anyui fold systems, which consist of separate terranes and subterranes (Figs. 1 and 2). The New Siberian-Wrangel fold system includes the Kotelny, Bennett and Wrangel terranes. The Anyui-Chukotka fold system includes the Chukchi and East Chukchi (Bering) terranes.
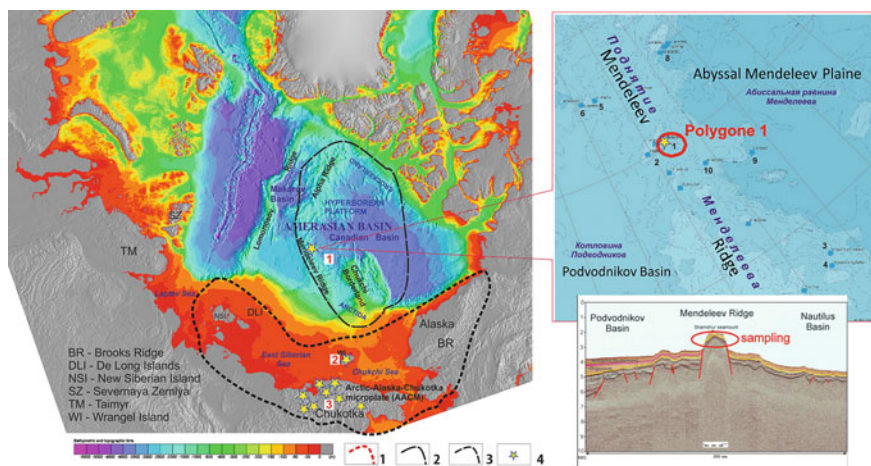
Fig. 1 Map of the Arctic Region. 1—Alaska-Chukotka microcontinent and 2—Hyperborean platform. 3—Contemporary outline of the ancient paleocontinent (Hyperborean Platform, Arctida, Crockerland), cited from (Metelkin et al. 2005; Laverov et al. 2013, with simplifications). 4—Position of the examined sections. Red numbers in the map indicate sampling points: 1—Mendeleev Rise, sample USO-4, 2—Wrangel Island; 3—Chukotka terrane. In the inset—at the top: a fragment of the Mendeleev Rise map with a marked sampling point position at polygon 1 (red oval); an asterisk shows the position of sample USO-4. Below—a fragment of the seismic line of Shamshur Mt. with an area of underwater sampling
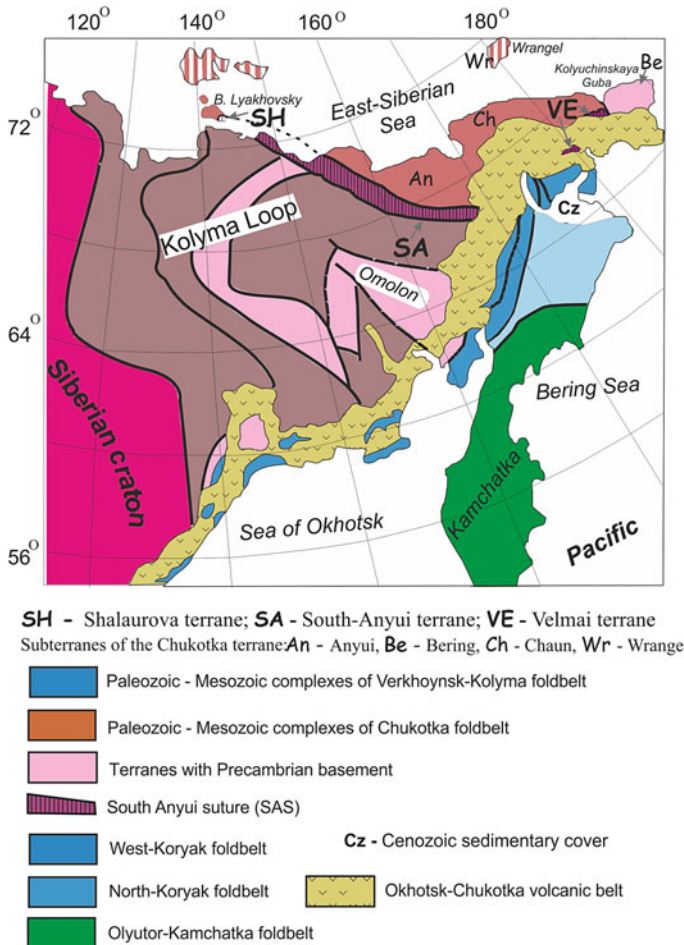
Fig. 2 Tectonic scheme of Northeast Asia, according to (Sokolov et al. 2010)

Structures of the Chukotka fold area were resulted from the Chukchi (Late Cimmerian) phase of deformations in the late Early Cretaceous during the collision of the Chukotka microcontinent with structures of the active margin of Siberia (Parfenov et al. 1993a, b; Sokolov 2010; Sokolov et al. 2015). Traces of Ellesmerian deformations have been identified on New Siberian Islands, Wrangel Island, and in Chukotka (Verzhbitsky et al. 2015; Luchitskaya et al. 2015; Sokolov et al. 2017). The South Anyui suture, a result of the Proto-Arctic (South Anyui) ocean closure, separates Arctic structures of the Chukotka fold area from the Pacific structures of the Verkhoyansk-Kolyma fold area.

Triassic deposits accumulated on passive margins of the Chukotka microcontinent. At present, they are widespread within the Chukotka, Wrangel and South Anyui terranes. The most complete sections were preserved in the Anyui-Chukotka
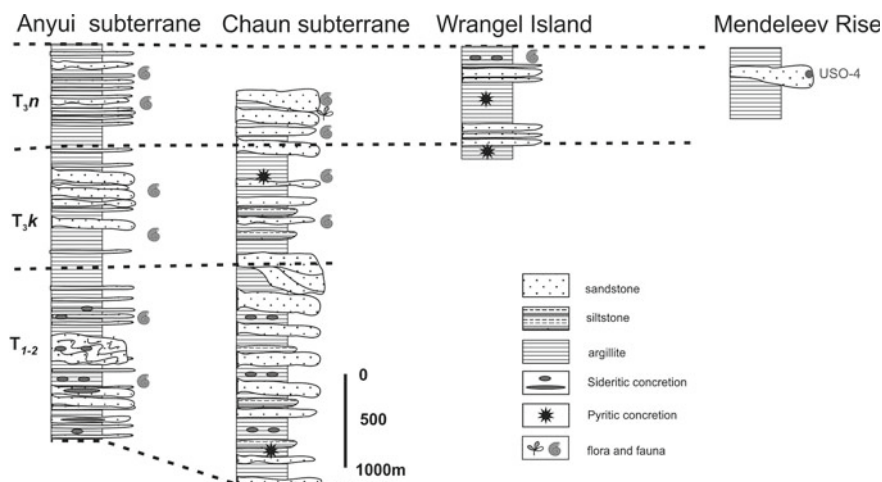
Fig. 3 Structure of the Triassic sections in Chukotka, Wrangel Island, and Mendeleev Rise

fold system. Facies analysis made it possible to identify deposits of the shelf, continental slope, and sea-plain with the southward deepening of the sedimentary basin (Tuchkova, 2011; Tuchkova et al. 2009, 2014). The Wrangel and South Anyui terranes also contain Upper Triassic deposits. The former is characterized by proximal facies of turbidite (Kos'ko et al. 2003), and the latter, by distal turbidite, which occupy the lower structural position among the South Anyui suture allochthons.

Chukotka terrane. Triassic sediments are represented by three rock sequences: Lower-Middle Triassic, Carnian and Norian (Fig. 3) The lower rock sequence is represented by interlayering of fine rhythmic siltstone with interbedded sandstone and argillite, which ratio can vary in different sections (Tuchkova et al. 2007, 2009). Up the section, the amount of sandstone and the thickness of the rhythms increase. The sandstone is characterized by graded, laminar, and oblique layering. There are landslide textures and inclusions of mudstone fragments of the underlying layer. The sequence contains a large number of siderite nodules. The nodules can be small oval-shaped (Fig. 4a) and concretionary interlayers with uneven lower boundary and gradation structure of the layer (Fig. 4b).

Lower-Middle Triassic deposits contain numerous gabbro-dolerite dikes, sills and stocks (Tectonics… 1980; Ledneva et al. 2011).

Carnian sandstones are structureless, there are graded and cross-bedded series, traces of slumping and erosion in the bottom of layers, as well as upward coarsening of deposits up to the emergence of small-pebble conglomerates.

Norian deposits are characterized by fine rhythmic structure with abundant *Monotis* shell remains and trace fossils. Large plant fragments occur.

Fig. 4 Photographs of the Triassic deposits: **a** single oval siderite concretions in the Lower-Middle Triassic, Vernitakayveem River, Chukotka terrane; **b** single small concretions and concretionary interbeds in the sediments of the Lower-Middle Triassic reference section, Enmynveem River, Chukotka terrane; **c** bed of calcareous sandstone in the Upper Triassic deposits, Krasnaya River, Wrangel Island; **d** large single concretion in the Upper Triassic deposits, Chertov Ravine, Wrangel Island; **e** sample of calcareous silt-sandstone (USO-4), Shamshur Mt., Mendeleev Rise; **f** sawn sample USO-4 structureless sandstone

Wrangel terrane. On Wrangel Island, Upper Triassic deposits are only known, which are mainly represented by the Norian and upper part of the Carnian stages (Kos'ko et al. 2003). Contact between Triassic, Permian and older deposits is tectonic (Sokolov et al. 2017). The lower part of the Triassic section is composed

of interbedded siltstone-mudstone and sandstone with dominating fine-grained varieties. The upper part of the section is dominated by sandstones.

Sandstone is grey, sometimes greenish-grey, fine- to medium-grained, mostly structureless, although there are interlayers with graded-bedding. At the base of the sandstone beds, traces of sediment flow and slightly rounded large (10–12 cm across) flattened mudstone intraclasts are recorded. The thickness of the sandstone beds is 10–30 cm; sometimes it can reach 50–60 cm or more. Some interlayers consist of calcareous sandstone with carbonate cement, in which Norian faunistic remains are embedded. In the section, these beds are notable for the well-expressed uneven lower boundary of the layer (Fig. 4c). In some sandstones, there are large single siderite nodules (Fig. 4d). Thin rubbly rocks are characterized by laminar stratification and thin-rhythmical alternation of mudstone and siltstone.

Mendeleev Rise. Quartz sandstone was found among the silicoclastic rocks in the bottom rock collection (Morozov et al. 2013). It is characterized by a high silica content of up to 98%, often cross-bedded structure, illite or carbonate dolomite-calcite, sometimes recrystallized cement. High maturity and good sorting of detrital material typical of sedimentary rocks of the craton platform cover are recorded (Morozov et al. 2013).

On the Shamshur Seamount (Fig. 3), research submarine manipulator raised dense, hard grey rocks with brownish incrustation oxidized to a depth of 1 cm (sample USO-4, Fig. 4e, f). In addition, two samples of uncemented silty sandstone (samples SS-63 and SS-65) were selected from the Arctica-2012 collection. These samples (described below) are also classified as Upper Triassic based on the age of the youngest detrital zircon population (205–233 Ma).

2   Petrographic Data

In mainland Chukotka, the Lower-Middle Triassic sandstone is characterized by grains of silty dimension and a clay matrix content of more than 15%. According to the classification of F. Pettijohn, they are defined as lithic greywackes (Fig. 5). In Upper Triassic sandstone of Chukotka and the Wrangel Island, matrix content is 3–10%, so they are classified as lithic arenite (Tuchkova et al. 2007, 2009). Sample USO-4 also belongs to the lithic arenite (Fig. 5). Samples SS-63 and SS-65 can be assigned to the same group conditionally, since they are not cemented.

Chukotka terrane. In lithic greywacke of the Anyui subterrane, the clay matrix content varies from 15 to 30%. The ratio of rock-forming components is as follows: quartz 19–47%, feldspars 7–32%, rock fragments 29–68% (Tuchkova 2011; Tuchkova et al. 2009, 2014). Low- and medium-metamorphosed rocks were identified in the rock fragments. Some of them contained fragments of altered mafic effusive.
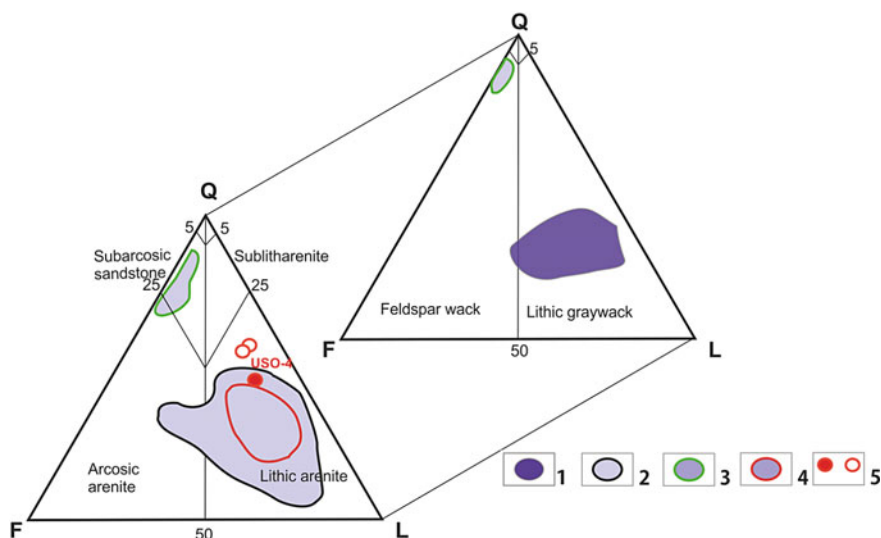
Fig. 5 Classification diagram of sandstones from Chukotka, Wrangel Island, and Mendeleev Rise (classification fields are based on Pettijohn 1975). In the diagram, the composition of sandstones from: 1—Lower-Middle Triassic; 2 to 4—Upper Triassic: 2—Anyuy subterrane, 3—Chaun subterrane, 4—Wrangel Island, 5—samples from the Mendeleev Rise: red circle—sample USO-4, red circle with white filling—samples SS-65 and SS-63

In lithic arenites, quartz occupies 12–46%, feldspars, 9–68%, rocks fragments, 14–68%. The rock fragments are dominated by metamorphic rocks becoming more and more diverse from the Lower to Upper Triassic.

Concretions and concretion interlayers in Lower-Middle Triassic sections are represented by micrite or calcareous silty sandstone (Fig. 6a, b). Cement is dominated by calcite and Mg–Fe calcite, clastic grains are poorly or practically unsorted, rock fragments of different degree of roundness occupy 5–15% per thin section (Fig. 6b). Pyrite grains sometimes can be found (Fig. 6a). In the upper part of the lower Triassic section of the Enmynveem River, undeterminable microfauna is present in the most fine-grained carbonate concretions (Tuchkova et al. 2007).

In the sandstone of the Chaun subterrane, quartz grains occupy 45%, feldspars 20%, rock fragments 26%. Among the rock fragments, there are rhyolite and fine-grained metamorphic rocks of quartz-micaceous composition. In addition, biotite and muscovite can be found as well as chloritized mica, in places sideritized.

Wrangel Island. Upper Triassic sandstone and siltstone belong to the lithic arenite. The rocks are cleavage; ferriferous carbonate, which corrodes clastic grains, occurs as spots in thin sections. The sorting of grains is poor and medium, the grain size ranges from 0.15 to 0.25 mm, the cement is of chlorite-micaceous composition (Fig. 6c). Sandstone composition consist of quartz (20–40%), feldspars (plagioclase, microcline) (34–62%), rock fragments (11–23%) including clasts of granite, cherts, fragments of sedimentary and micaceous shale, altered fragments of mafic and felsic effusives; dehydrated biotite have been also identified.

Dimensions of clastic grains in sandstone beds with basal calcite cement vary from 0.1 to 0.4 mm. The grains are angular and semi-rounded, the edges are intensively corroded by carbonate mineral enclosing clastic grains and debris of faunal remains. Many clastic grains are replaced by calcite (Fig. 6d). Quartz and granitoid rock fragments are dominated; Feldspars are completely replaced by calcite.

Mendeleev Rise. Sample USO-4 is a fine-grained quartz-feldspar sandstone (Fig. 6e). There is no initial matrix in the rock, but basal calcite cement with embedded clastic grains is present. The cement is composed of calcite and dolomite, Mg-calcite is present also. Clastic material is dominated by quartz; there are feldspar, mica, fragments of schist, granite and limestone, effusives of acidic composition. Quartz grains are characterized by predomination of grains with microfractures filled with clay or a mixture of clay minerals (Fig. 6f).

X-ray phase analysis showed that main minerals are quartz (70%), calcite (about 20%), dolomite (about 15%), illite, and K–Na feldspar (not more than 5%).
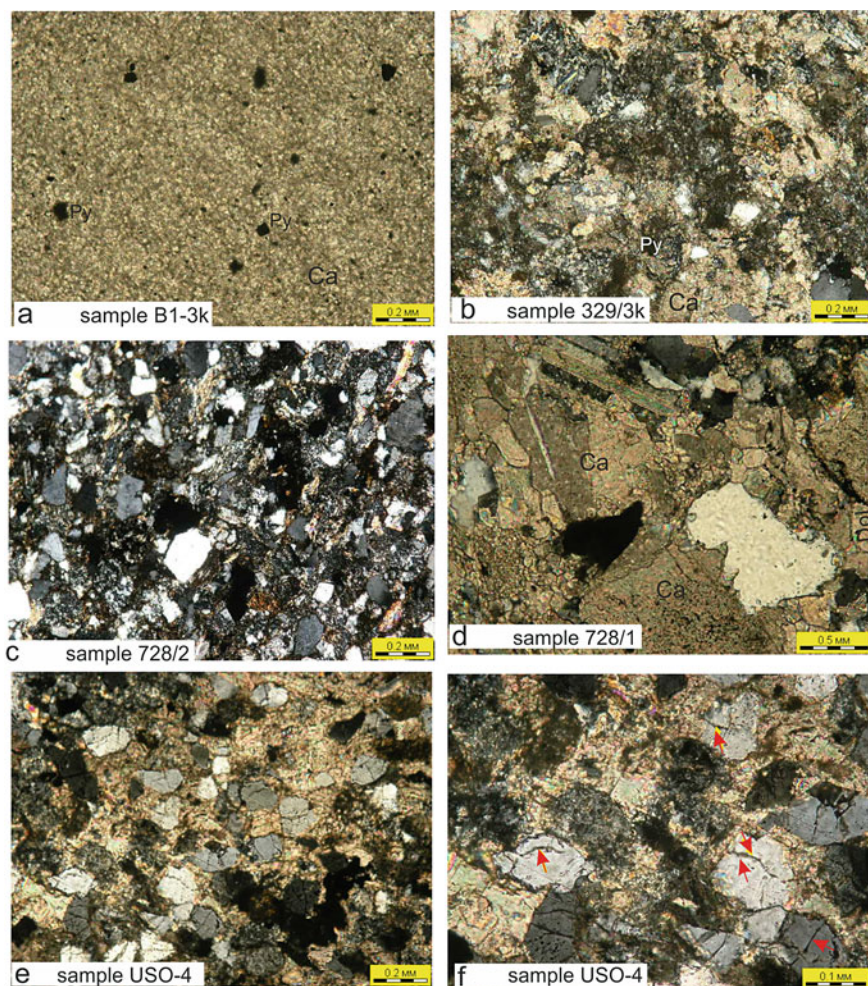
Fig. 6 Photomicrographs of the Triassic nodules and sandstones from Chukotka, Wrangel Island, and Mendeleev Rise: **a** concretion, carbonate rock consisting mainly of calcite (Ca), contains single pyrite (Py) grains, Enmynveem River, Anyuy subterrane, Chukotka; **b** concretionary interbed, fine-grained calcareous sandstone with clastic grains of quartz, feldspar, and mica, Enmynveem River, Anyuy subterrane, Chukotka; **c** sandstone, lithite arenite, with chlorite mica cement, Wrangel Island, Krasnaya River; **d** calcareous sandstone, Krasnaya River, Wrangel Island; calcite (Ca) and dolomite (Dol) in cement; **e** calcareous silt-sandstone is composed mainly of quartz, Mendeleev Rise; **f** quartz fragments with microcracks, along which clay mineral develops (red arrows), Mendeleev Rise

3 Geochemical Data

Chemical composition of sedimentary rocks and the content of impurity elements in them are widely used for deciphering the composition of provenance areas and sedimentary environments in sedimentary basins. This paper analyzes the geochemical features of sample USO-4 in comparison with the data on the Triassic sandstones from Chukotka and Wrangel Island. Diagrams and relationships were used that show the composition of the provenance area, the level of maturation and redeposition of the rock components. The data of whole analysis make it possible to determine the similarity and difference in the composition of rocks and to determine their classification affiliation.

In Pettijohn's diagram (Fig. 7), sample USO-4 occupies a position in the field of quartz arenites, whereas samples of the Triassic sandstones from Chukotka and Wrangel Island are characterized by a less mature composition and occupy greywacke and lithic arenite fields.

In addition, the maturity of deposits by the degree of mechanical sorting can be estimated on the basis of the "titanium module", i.e. by TiO_2/Al_2O_3 ratio (Interpretation of geochemical data 2001). It is believed that the maximum value of 0.09 is characteristic of mature rocks, such as quartzites and quartz sandstones. For sample USO-4, this index is 0.048, which is quite comparable with the samples from Wrangel Island (TiO_2/Al_2O_3 is 0.04–0.06) and somewhat lower in comparison with Chukotka (0.05–0.08). Such a low index may indicate that the sandstones from the Mendeleev Rise were formed at the expense of a more mature clastic matter, which underwent considerable weathering.

To determine the degree of weathering, the CIA (Chemical Index of Alteration) is used, which is an indicator of climate in the erosion area (Nessbitt and Young 1982;
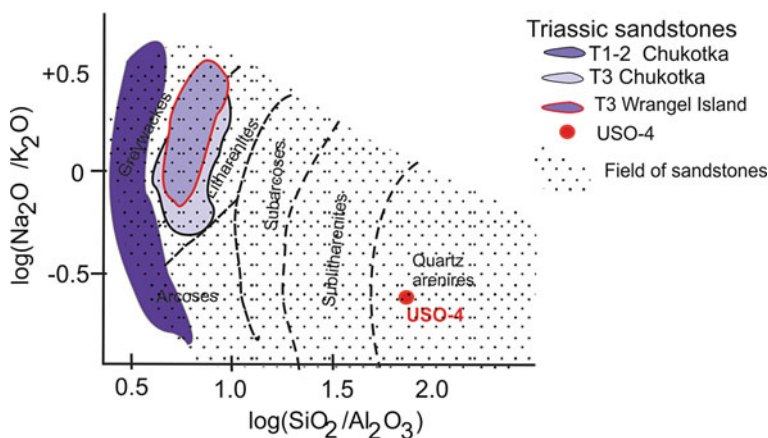
Fig. 7 Classification diagram after Pettijohn (1975) showing distribution of major components in the Triassic sandstones of the Anyuy-Chukotka fold belt

Visser and Young 1990). In the diagram (Fig. 8), sample USO-4 occupies a position in the field with a high level of weathering, although in composition it occupies a position close to the average shale.

Another important parameter is the level of redeposition of clastic material. To determine the level of resedimentation, a diagram is used that reflects Th/Sc–Zr/Sc ratio (Fig. 9). The proportions of these elements are not subject to significant changes in the process of sediment transformation into rock and are characterized by similar
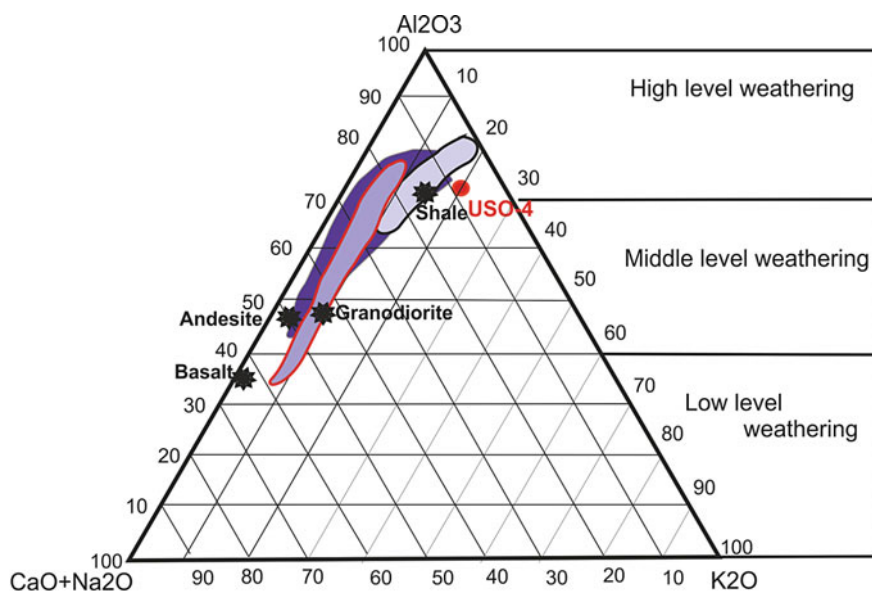
Fig. 8 Al_2O_3–$CaO + Na_2O$–K_2O diagram (Nesbitt and Young 1984) showing compositions for the Triassic sandstone of Chukotka, Wrangel Island and samples (molar proportions). Average values for basalt, andesite, and granodiorite are from McLennan et al. (2003). For legend see Fig. 7

Fig. 9 Diagrams Th/Sc versus Zr/Sc, illustrating the sedimentary recycling of the Triassic samples of Chukotka –Wrangel Island– (USO-4), diagrams by McLennan et al. (2003). For legend see Fig. 7
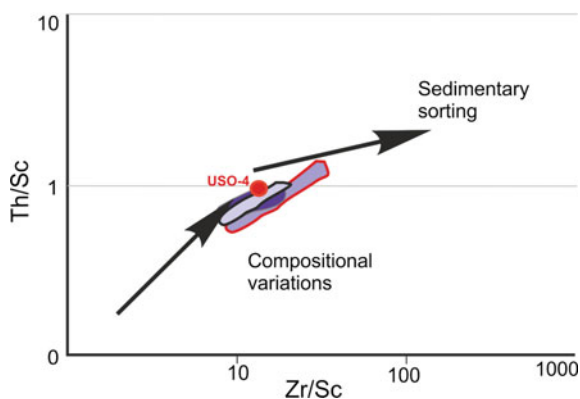
behaviour during sedimentation. Sample USO-4 is at the boundary of the recycling trend and the field of the composite variety of sandstones. Compared with the samples from Chukotka, it is characterized by high recycling, whereas in comparison with the field of samples from Wrangel Island it occupies the middle position.

In addition to this diagram, the analysis of Th/Sc ratio shows a tendency to increase from the continental sections of Chukotka (avg. 0.52) to Wrangel Island (avg. 0.78) and in sample USO-4 is 1.082.

Based on this parameter, it is possible to evaluate the possibilities of using diagrams reflecting the composition of provenance areas. In the case of repeated redeposition of clastic material, the use of genetic diagrams is difficult and undesirable. In this case, the geochemical parameters of sample USO-4 can be assessed, since the position of this sample lies on the boundary between the recycled and non-recycled rocks.

Preliminary conclusions about the prevailing provenance area can be made on the basis of the $CaO + MgO-Na_2O + K2O-SiO_2/10$ diagram analysis (Fig. 10). In connection with the fact that, according to petrographic data, there is carbonate cement in sandstone from sample USO-4, CaO content was recalculated to $CaCO_3$ by the standard procedure described in (Kossovskaya and Tuchkova 1988). After the procedure, sample USO-4 occupies the field of felsic (granite) source area and is in relation to the samples from Chukotka and Wrangel Island in the area of the most mature rocks. A similar conclusion is obtained on the basis of DF1-DF2 diagram analysis, according to which sample USO-4 occupies a position in the field of quartz sandstones.
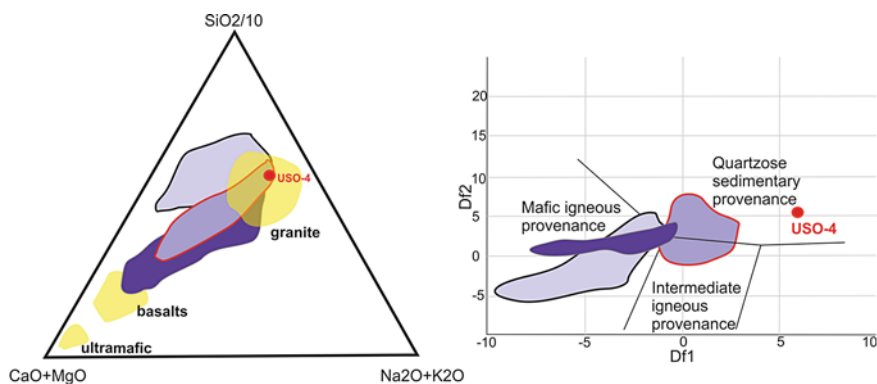

Fig. 10 Discriminant diagrams illustrating the compositions of assumed provenances for samples of the Triassic sandy rocks of Chukotka—Wrangel Island—Mendeleev Rise. In the left diagram after McLennan et al. (2003). In the right discriminant diagram for major component provenance, after Roser and Korsch (1988). Discriminants and fields are $DF1 = 30.6038\ TiO_2/Al_2O_3 - 12.541$ $Fe_2O_3(total)/Al_2O_3 + 7.329\ MgO/Al_2O_3 + 12.031\ Na_2O/Al_2O_3 + 35.42\ K_2O/Al_2O_3 - 6.382.\ DF_2$ $= 56.500\ TiO_2/Al_2O_3 - 10.879\ Fe_2O_3(total)/Al_2O_3 + 30.875\ MgO/Al_2O_3 - 5.404\ Na_2O/Al_2O_3$ $+ 11.112\ K_2O/Al_2O_3 - 3.89.$ For legend see Fig. 7

In more detail, the composition of the sources areas can be determined by analyzing a diagram constructed from Co/Th–La/Sc ratios (Fig. 11). In this diagram, the sandstones from Chukotka, Wrangel Island, and the Mendeleev Rise are characterized by a composition close to the average composition of the continental crust. At the same time, there is an increase in the role of felsic rocks from the Lower Triassic to the Upper Triassic sandstones.

In the diagram constructed from La/Th–Hf ratio, the field of Triassic sandstones is characterized by a mixed composition of felsic and mafic provenance areas (Fig. 12). Points of Chukotka, Wrangel Island, and Mendeleev Rise sandstones form the fields, practically coinciding with each other.

Fig. 11 Discriminant diagram of Co/Th versus La/Sc showing various provenances for clastic rocks: fields: (i) erosion of rocks that are close to the average composition of the continental crust (granodiorites), (ii) increase of the role of mafic rocks, (iii) increase of the role of felsic rocks. From Gu et al. (2002). For legend see Fig. 7
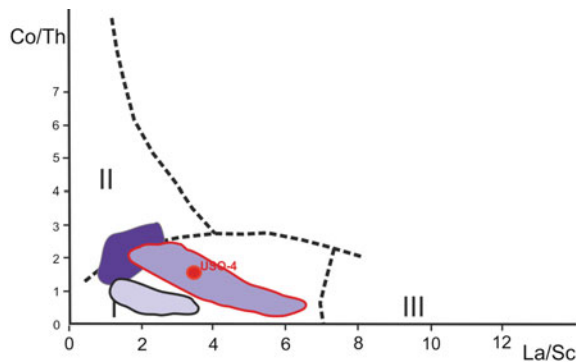
Fig. 12 Hf versus La/Th plot (after Floyd and Leveridge 1987; Gu 1994) for the sandstones of the Chukotka—Wrangel Island—Mendeleev Rise. For legend see Fig. 7
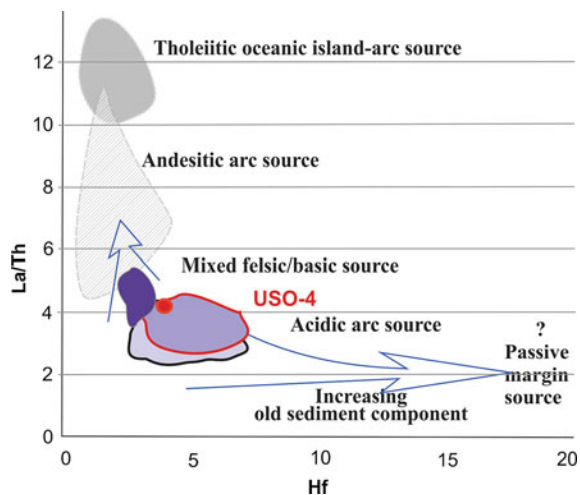
4   U-Pb Dating

Samples from the Triassic deposits of the Chukotka terrane are characterized by practically identical age spectra of zircons (Fig. 13). The youngest population of zircons with the ages of 235–260 Ma is the most numerous. The Upper Triassic samples comprise a small population of old zircons with peaks at 1200, 1500, 1800, 2000 Ma, 5–18 grains each.

Detrital zircons in sandstones from Wrangel Island have a maximum in the range of to 282–331 Ma, with peaks at 210, 305, and 410 Ma. Older populations of zircons are less widespread; however, they have many small peaks in the range 800–1500 Ma and a slightly higher maximum in the range 600–2400 Ma (15–30 grains).

Detrital zircons from the Mendeleev Rise sandstone are characterized by the distribution of populations typical of the Triassic sandstones from Wrangel Island and Chukotka. The most numerous group of zircon grains covers the interval 235–425 Ma with peaks at 205, 235, 250, 300, 405 Ma. Older zircons are represented by individual grains with ages from 550 to 2500 Ma.

Thus, the correlation of the Triassic sequences in Chukotka and Wrangel Island shows gradual deepening of the marine basin from north to south, supply of clastic material from the north with the help of several small river systems operating on the shelf and a large underwater prodelta that moved sediments to a deeper area. A
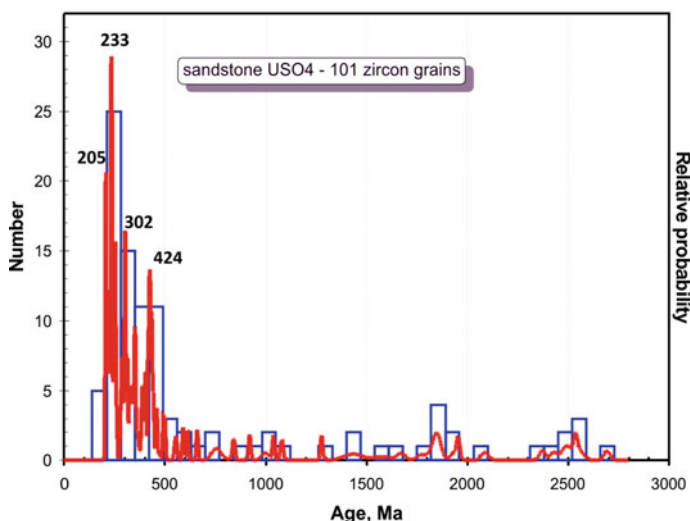
Fig. 13 Distribution of U–Pb detrital zircon ages in the Triassic clastic rocks of Chukotka, Wrangel Island and Mendeleev Rise; **a** sample USO-4; **b** relative probability distribution diagram for detrital zircon U-Pb ages from Triassic sandstones from the Wrangel Island (samples 641/1, 728/1, 497/3, 06/47, and sample C145741 from Miller et al. 2006); **c** relative probability distribution diagram for detrital zircon U-Pb ages from the Triassic sandstones from Chukotka (Upper Triassic samples: 417/4, 06/12-5, L-23-6-1, L11-2-1, 09/321; Lower-Middle Triassic samples: L19-2-1, B-1-5, 09/358 and samples from Miller et al. 2006)

sample of calcareous sandstone from the Mendeleev Rise can be roughly correlated with carbonate (siderite) concretions from the Lower-Middle Triassic sandstones of Chukotka and an interlayer of carbonate sandstones from Wrangel Island.

Comparison of petrographic and geochemical composition of sample USO-4 with coeval sandstones from Chukotka and Wrangel Island shows that the mineral composition of USO-4 sandstone is characterized by the highest content of carbonate cement. A similar type of cement in the Triassic sandstones of the region occurs mainly in the concretionary interlayers of the Lower-Middle Triassic of Chukotka, or in single sandstone beds from the Triassic sequences of Wrangel Island containing numerous faunal remains.

Petrographically, the sandstone from sample USO-4 refers to lithic arenites and is characterized by an increased content of quartz and other stable rock-forming component. Two other non-cemented samples are also most likely lithic arenites. In the Chukotka-Wrangel-Mendeleev Rise line, all three samples from the Mendeleev Rise are sandstones of the most mature composition with quartz content of about 45%.

Quartz grains in the samples are specific; they are characterized by numerous microfractures healed by a clayey mineral. Moreover, when studying sandstone with an electron microscope (SEM), kaolinite was found in some feldspar grains. Kaolinite replaces clastic feldspar, both around the periphery and in the central part of the grains.

The presence of quartz grains with microfractures in the Mendeleev Rise sandstones indicates the arrival of sandy material from nearby land (Table 1). Quartz

Table 1 Composition of Quartz grains with and without microfractures in sandstones and siltsandstones of Chukotka, Wrangel Island and Mendeleev Rise

Mendeleev Rise, Shamshure Mt.					
	USO-4	SS-65	SS-63		
Q without microfractures	80	20	22		
Q with microfractures	14	9	4		
Q all	**94**	**29**	**26**		

Wrangel Island					
	724/1	729/01	708/6	626/1	728/2	729/2
Q without microfractures	32	43	63	59	55	55
Q with microfractures	5	4	5	2	9	2
Q all	37	47	68	61	64	57

Chukotka					
	456/12	400/3-2-1	400/2sand	400/5b	457/1	453/1
Q without microfractures	42	54	50	62	38	29
Q with microfractures	1	2	1	2	2	1
Q all	43	56	51	64	40	30
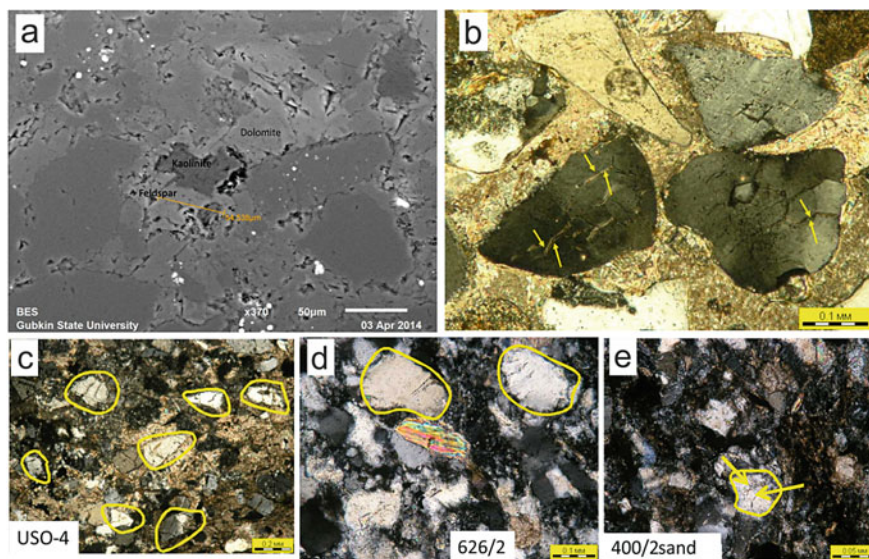
Fig. 14 a photomicrograph of silty sandstone with relics of kaolinite replacing feldspar (in the centre). Sample USO-4, Mendeleev Rise, scanning electron microscope; **b** photomicrograph of the thin section with rounded quartz grains, with microfracture, in which chlorite-mica mixture develops (yellow arrows), continental coal deposits, sandstone, Permian, Anabar River, thin section with analyzer; **c** silty sandstone, quartz grains with different degree of roundness, with microfracture, in which chlorite-mica and sometimes kaolinite are determined, sample USO-4, Mendeleev Rise, thin section with analyzer; **d** fine-grained sandstone, quartz grains, subrounded, micro cracks with chlorite-mica are present, sample 626/2, Wrangel Island, Khishnikov River, thin section with analyzer; **e** silty sandstone, single quartz grain with a relic of microfracture, sample 400/2, Chukotka, Maly Anyuy River, thin section with analyzer

grains of this type are observed mainly in continental environments and are associated with eolian action (Fig. 14). During transportation, such grains crack and crumble, so their preservation is possible only at a short distance with the rapid burial and sediment lithification.

The number of quartz grains with microfractures from the Mendeleev Rise's samples is to 30% of all quartz grains. In the Triassic sandstones from Wrangel Island, the number of such quartz grains is 7–14%. In the Triassic sandstones from Chukotka, the amount of quartz grains with microfractures is no more than 2%. Thus, sandstones from the Mendeleev Rise are the closest to the continental deposits in this parameter.

Based on the analysis of the Th/Sc–Zr/Sc diagram for sample USO-4 is located on the border with the clinic (Fig. 9), which indicates that the sandstone components are not recycled and all genetic geochemical diagrams can be applied to the image. Provenance area for sample USO-4 (Fig. 13) suggests a complex of rocks close to the average composition of the continental crust (granodiorite).

Petrochemical parameters also indicate the most mature composition of rock from the Mendeleev Rise. In Pettijohn's classification diagram (Fig. 7), quartz arenites from the Mendeleev Rise differ from the Upper Triassic sandstones of Wrangel Island and Chukotka, which are in the field of lithic arenites. Older, Lower-Middle Triassic sandstones of Chukotka differ from the Mendeleev Rise sandstones even more, since they are in the field of lithic greywacke.

Sandstones from the Mendeleev Rise have the most mature composition, but they did not undergo intensive recycling. At the same time, the level of weathering in the provenance area, determined by the CIA index in sandstones, is very high, i.e. the area of erosion was for a long time in the zone of weathering. Persistent minerals in the rocks have been preserved, and only relics have remained of unstable ones, in particular, kaolinite replacing feldspars, and clay minerals that heal microfracture in detrital quartz, enclosed in carbonate cement.

5   Results of the Studies

Thus, in the Triassic deposits in the Chukotka-Wrangel-Mendeleev Rise line, there is a distinct trend in the change of deep-sea sediments with ever shallower ones with an ever more mature composition of rocks, which indicates a consistent approach to the continental source of detrital material. At the same time, the amount of quartz grains grown in continental environment increases in sandstones.

Position of this continental land is currently being established approximately, as evidenced by continuing discussions. However, the lithology and paleogeography of the Triassic deposits make it possible to clarify this situation. The Proto-Arctic Ocean, which was connected with the Paleo-Ural Ocean, had existed during the Paleozoic and before the beginning of the Late Jurassic. During the Permian-Triassic, the Proto-Arctic Ocean diminished in size as a result of the Paleo-Ural Ocean closure and collision of the Kara block with Siberia, and turned into the Pacific Bay (Laverov et al. 2013). Turbidites of Chukotka, Wrangel Island, and South Anyuy suture accumulated in its northern passive margin during the Triassic (Tuchkova 2011; Tuchkova et al. 2014). Sandstones of the Mendeleev Rise, occupying the most northern position, (in modern coordinates) are the shallowest facies. The presence of the northern provenance area is also confirmed by sedimentological observations (Tuchkova 2011; Tuchkova et al. 2014). These data contradict the notion of the Baltic as a source area (Miller et al. 2010, 2017).

U-Pb dating of detrital zircons in the Triassic sandstones from Wrangel Island shows a strong influence of the Paleozoic zircons with ages in the range 250–500 Ma in all the analyzed samples (Fig. 7). It is obvious that their source was the Paleozoic granitoids of the Caledonides and Ellesmerides. As mentioned above, in the age spectra of sandstones, an important role is played also by Precambrian detrital zircons.

Thus, there is no doubt today in the existence of the ancient continental block with a high standing during the Late Paleozoic–Early Mesozoic, as the source area of sediments in peripheral paleobasins such as Sverdrup and the marginal basins

of the East Siberian Shelf. At the same time, questions about the age and spatial boundaries of this continental block are now being actively discussed.

6   Conclusions

1. Genesis of the Triassic quartz sandstones from the Shamshur Seamount in the northern part of the Mendeleev Rise occurred in coastal-marine settings close to the continental ones. In the Triassic terrigenous deposits of Wrangel Island and Chukotka southward, the paleogeographic conditions become more marine, with the formation of local prodelta and inter-delta sites; in the same direction, the petrographic composition of sandstones becomes more mature, without recycling.
2. Systematically analyzed from the south (from Chukotka) to the north (from Wrangel Island to the Mendeleev Rise) petrographic, geochemical, and geochronological data indicate the existence of a long-lived provenance area in the Central Arctic Uplifts area; the source is characterized by a long exposure, a high degree of weathering and the absence of significant tectonic rearrangements.
3. Source area for the Triassic sandstones of Eastern Chukotka was mainly Paleozoic rocks, as well as ancient Proterozoic granite and metamorphic rocks.

References

Anfinson OA, Embry AF, Stockli DF (2016) Geochronologic constraints on the Permian-Triassic Northern source region of the Svedrup Basim, Canadian Arctic Islands. Tectonophysics 691:206–219. https://doi.org/10.1016/j.tecto.2016.02.041

Blakey R (2018) Global paleogeography. http://www2.nau.edu/rcb7/globaltext2.html

Drachev SS (2011) Tectonic setting, structure and petroleum geology of the Siberian Arctic offshore sedimentary basins. In: Spencer AM, Embry AF, Gautier DL, Stoupakova AV, Sørensen K (eds) Arctic petroleum geology, vol 35. Geological Society, London, Memoirs, pp 369–394. https://doi.org/10.1144/m35.25

Embry AF, Dixon J (1994) The age of the Amerasia Basin. In: Thurston D, Fujita K (eds) Proceedings international conference on Arctic Margin 1992. US Minerals Management Service, Anchorage, AK, Reports, MMS94_0040, pp 289–294

Floyd PA, Leveridge BE (1987) Tectonic environment of the Devonian Gramscatho basin, south Cornwall: framework mode and geochemical evidence from turbiditic sandstones. J Geol Soc 144:531–542

Geodynamics, magmatism and metallogeny of the East of Russia (2006) Book 1. Dalnauka, Vladivostok, 572 p (in Russian)

Golonka J (2011) Phanerozoic palaeoenvironment and palaeolithofacies maps of the Arctic region. In: Spencer AM, Embry AF, Gautier DL, Stoupakova AV, Sørensen K (eds) Arctic petroleum geology, vol 35. Geological Society, London, Memoirs, pp 79–129. https://doi.org/10.1144/m35.6

Gu XX (1994) Geochemical characteristics of the Triassic Tethys-turbidites in northwestern Sichuan, China: implications for provenance and interpretations of the tectonic setting. Geochim Cosmochim Acta 58:4615–4631

Gu XX, Liu JM, Zheng MH, Tang JX, Qi L (2002) Provenance and tectonic setting of the Proterozoic turbidites in Hunan South China: geochemical evidence. J Sediment Res 72:393–407

Hain VE, Filatova NI (2009) From hyperborea to arctida: toward the precambrian craton of the Central Arctic. Doklady AN 428(2):220–224 (in Russian)

Kaminsky VD (ed) (2017) The Arctic Basin (geology and morphology). VNIIOkeangeologiya, St. Petersburg, 291 p (in Russian)

Kos'ko MK (2007) Terrains of the East Arctic shelf of Russia. Rep Acad Sci 413(1):71–74 (in Russian)

Kos'ko MK, Avdyunichev VV, Ganelin VG, Opekunov AY, Opekunova MG, Cecile MP, Smirnov AN, Ushakov VI, Khandozhko NV, Harrison JC, Shulga YD (2003) The Wrangel Island: geology, metallogeny, geoecology, vol 200. SPb.: VNIIOkeangeologia, 137 p

Kossovskaya AG, Tuchkova MI (1988) On the problem of mineralogical-petrochemical classification and the genesis of sandy rocks. Lithol Miner 2:8–24 (in Russian)

Kuznetsov NB (2006) Cambrian collision of the Baltic and Arctida, Protouralid—Timanide orogen and its erosion products in the Arctic. Dokl RAS 411(6):788–793 (in Russian)

Laverov NP, Lobkovsky LI, Kononov MV, Dobretsov NL, Vernikovsky VA, Sokolov SD, Shipilov EV (2013) Geodynamic model of tectonic evolution of the Arctic in the Mesozoic and Cenozoic and the problem of the outer boundary of the Russia's continental shelf. Geotectonics 1:3–35 (in Russian)

Ledneva GV, Pease VL, Sokolov SD (2011) Permo-Triassic hypabyssal mafic intrusions and associated tholeiitic basalts of the Kolyuchinskaya Bay, Chukotka (NE Russia): links to the Siberian LIP. J Asian Earth Sci 40:737–745. https://doi.org/10.1016/j.jseaes.2010.11.007

Luchitskaya MV, Sokolov SD, Katkov SM, Kotov AB, Natapov LM, Belousova EA (2015) Late Paleozoic granitoids of Chukotka: peculiar features of composition and the location in the structure of Russian Arctic. Geotectonics 4:1–27

McLennan SM, Bock B, Hemming SR, Hurowitz JA, Lev SM, McDaniel DK (2003) The role of provenance and sedimentary processes in geochemistry of sedimentary rocks. In: Lentz D (ed) Geochemistry of sediments and sedimentary rocks: evolutionary considerations to mineral deposit-forming environments. St. John's, Geol. Assoc. of Canada, pp 7–38

Metelkin DV, Vernikovsky VA, Kazansky AY, Belonosov IV (2005) Siberian craton as a supercontinent Rodinia: analysis of paleomagnetic data, vol 404, No 3. Dokl RAS, pp 389–394 (in Russian)

Miller EL, Toro J, Gehrels G, Amato JM, Prokopiev A, Tuchkova MI, Akinin VV, Dumitru TA, Moore TE, Cecile MP (2006) New insights into Arctic paleogeography and tectonics from U-Pb detrital zircon geochronology. Tectonics 25:TC3013. https://doi.org/10.1029/2005tc001830

Miller EL, Gehrels GE, Pease V, Sokolov S (2010) Stratigraphy and U-Pb detrital zircon geochronology of Wrangel Island, Russia: implications for Arctic paleogeography. AAPG Bull 94(5):665–692

Miller EL, Akinin VV, Dumitru TA, Gottlieb ES, Grove M, Meisling K, Seward G (2017) Deformational history and thermochronology of Wrangel Island, East Siberian Shelf and coastal Chukotka, Arctic Russia. In: Pease V, Coakley B (eds) Circum-Arctic lithosphere evolution, vol 460. Geological Society, London, Special Publications. https://doi.org/10.1144/SP460.7

Morozov AF, Petrov OV, Shokalsky SP, Kashubin SN, Kremenetsky AA, Shkatov MYu, Kaminsky VD, Gusev EA, Grikurov GE, Rekant PV, Shevchenko SS, Sergeev SA, Shatov VV (2013) New geological evidence grounding the continental nature of the Central Arctic Uplifts. Reg Geol Metallogeny 53:34–56 (in Russian)

Nessbitt HW, Young GM (1982) Early proterozoic climates and plate motions inferred from major element chemistry of lutites. Nature 299:715–717

Nesbitt HW, Young GM (1984) Prediction of some weathering trends of plutonic and volcanic rocks based on thermodynamic and kinetic considerations. Geochim Cosmochim Acta 48:1523–1534

Nikishin AM, Malyshev NA, Petrov EI (2014) Geological structure and history of the Arctic ocean. EAGE publication, CJSC GEOSurvey GIN, Moscow, p 123

Nokleberg WJ, Parfenov LM, Monger JWH, Baranov BV, Byalobzhesky SG, Bundtzen TK, Feeney TD, Fujita K, Gordey SP, Grantz A, Khanchuk AI, Natal'in BA, Natapov LM, Norton IO, Patton WW, Jr, Plafker G, Scholl DW, Sokolov SD, Sosunov GM, Stone DB, Tabor RW, Tsukanov NV, Vallier TL, Wakita K (1994) Circum-North Pacific tectonostratigraphic terrane map. U.S. Geological Survey Open-File Report 94-714 (2 sheets, scale 1:5 000 000, 1 sheets, scale 1:10 000 000), 433 p

Parfenov LM, Natapov LM, Sokolov SD, Tsukanov NV (1993a) Terrane analysis and accretion in North-East Asia. Geotectonics 1:68–78 (in Russian)

Parfenov LM, Natapov LM, Sokolov SD, Tsukanov NV (1993b) Terrane analysis and accretion in North-East Asia. Island Arc 2:35–54

Pettijohn FJ (1975) Sedimentary rocks. Harper & Row, New York, p 628

Roser BP, Korsch RJ (1988) Provenance signatures of sandstone-mudstone suites determined using discriminant function analysis of major-element data. Chem Geol 67:119–139

Scotese CR (2011) PALEOMAP Project. http://www.scotese.com/earth.htm

Shatsky NS (1935.) On tectonics of the Arctic. Geology and mineral resources of the USSR's North. Glavsevmorput, Leningrad, pp 149–165 (in Russian)

Sklyarov EV (ed) (2001) Interpretation of geochemical data. M.: Internet Engineering, 288 p (in Russian)

Sokolov SD (2010) Essay on the tectonics of Northeast Asia. Geotectonics 6:60–78 (in Russian)

Sokolov SD, Ledneva GV, Tuchkova MI, Luchitskaya MV, Ganelin AV, Verzhbitsky VE (2014) Chapter 4: Chukchi Arctic continental margins: tectonic evolution, link to the opening of the Amerasia Basin. In: Stone DB, Grikurov GE., Clough JG, Oakey GN, Thurston DK (eds) ICAM VI: Proceedings. VSEGEI, St. Petersburg, pp 97–114

Sokolov SD, Tuchkova MI, Ganelin AV, Bondarenko GE, Leier P (2015) Tectonics of the South Anyui suture (Northeast Asia). Geotectonics 1:5–30 (in Russian)

Sokolov SD, Tuchkova MI, Moiseev AV, Verzhbitsky VE, Malyshev NA, Gushchina MYu (2017) Tectonic zonality of Wrangel Island (Arctic). Geotectonics 1:3–18 (in Russian)

Tectonics of the continental margins of the northwestern Pacific Ocean (1980) In: Leytes AM, Fedorovsky VS, Tilman CM, Shilo NA (eds). Nauka Publisher, Moscow, 285 p

Tuchkova MI, Bondarenko G Ye, Buyakaite MI, Golovin DI, Galuskina IO, Pokrovskaya EV (2007) Results from sedimentological and radiometric studies of the Upper Triassic deposits of the Chukotka microcontinent. Geotektonika 5:76–96 (in Russian)

Tuchkova MI (2011) Lithology of terrigenic rocks from Mesozoic fold belt of the continental margin (Great Caucasus, North-East Asia), vol 600. Trans. of Geological Institute Russian Academy of Sciences, LAP, 334 p (in Russian)

Tuchkova MI, Sokolov S, Kravchenko-Berezhnoy IR (2009) Provenance analysis and tectonic setting of the Triassic clastic deposits in Western Chukotka, Northeast Russia. Stephan Mueller Spec Publ Ser 4:177–200

Tuchkova MI, Sokolov SD, Khudoley AK, Verzhbitsky VE, Hayasaka Y, Moiseev AV (2014) Permian and triassic deposits of Siberian and Chukotka passive margins: sedimentation setting and provenance. In: Stone DB, Grikurov GE, Clough JG, Oakey GN, Thurston DK (eds) ICAM VI proceedings. VSEGEI, St. Petersburg, pp 61–96

Vernikovsky VA, Metelkin DV, Tolmacheva TYu, Malyshev NA, Petrov OV, Sobolev NN, Matushkin NYu (2013) On the problem of paleotectonic reconstructions in the Arctic and the tectonic unity of the New Siberian Islands terrane: new paleomagnetic and paleontological data. Proc Russ Acad Sci 451(4):423–429

Verzhbitsky VE, Sokolov SD, Frantzen EM, Little A, Tuchkova MI, Lobkovsky LI (2012) The South Chukchi Sedimentary Basin (Chukchi Sea, Russian Arctic): age, structural pattern, and hydrocarbon potential. In: Gao D (ed) Tectonics and sedimentation: implications for petroleum systems, vol 100. AAPG Memoir, pp 267–290

Verzhbitsky VE, Sokolov SD, Tuchkova MI (2015) Present-day structure and stages of tectonic evolution of Wrangel Island, Russian Eastern Arctic region. Geotectonics 49(3):165–192

Visser JNJ, Young GM (1990) Major element geochemistry and paleoclimatology of the Permo-carboniferous glaciogene Dwika Formation and post-glacial mudrocks in Southern Africa

Zonenshain LP, Kuzmin MI, Natapov LM (1990) Tectonics of lithospheric plates of the USSR, vol 2. M.: Nedra, 334 p (in Russian)

Tectonic Model and Evolution of the Arctic

O. V. Petrov, S. N. Kashubin, S. P. Shokalsky, S. D. Sokolov, E. O. Petrov, and M. I. Tuchkova

Abstract A key achievement of compilation of the Tectonic Map of the Arctic is a creation of a modern plate-tectonic model of the Circumpolar Arctic. This model demonstrates that the Arctic structure is determined by interaction of three lithosphere plates: two continental—North American and Eurasian—and one oceanic—namely Pacific. Modern seismicity serves as an indicator of tectonic processes and outlines boundaries of lithosphere plates.

1 Tectonic Model of the Arctic

The main achievement of geological and tectonic studies within the framework of the work on the creation of the Tectonic Map of the Arctic (TeMAr) and the Tectonic Stratigraphic Atlas of the eastern regions of Russia and the north-east of the Atlantic region (Hopper et al. 2014) involves the construction of a state-of-the-art tectonic model of the Arctic region.

The tectonic model of the Arctic region is based on up-to-date seismicity data indicating all present-day tectonic processes along the boundaries of lithospheric plates (Fig. 1). The belts of shallow earthquakes in the spreading zone of the Mid-Atlantic Ridge and the Gakkel Ridge on the border of the North American and Eurasian lithospheric plates form a narrow chain of seismic activity, which is characterised by shallow earthquake foci, no more than 35–45 km in depth. The boundaries of the Pacific Ocean lithospheric plate are delineated by a wide band of deep-focus earthquakes. Here, the deepest foci of earthquakes are presented, up to 300 km and deeper. On the continental shelf of the Laptev Sea and the land of Northern Eurasia,

O. V. Petrov (✉) · S. N. Kashubin · S. P. Shokalsky · E. O. Petrov
Russian Geological Research Institute (VSEGEI), 74 Sredny Prospect, St. Petersburg 199106, Russia
e-mail: vsgdir@vsegei.ru

S. D. Sokolov · M. I. Tuchkova
Geological Institute, Russian Academy of Sciences (GIN RAS), 7 Pyzhevksy per, Moscow 119017, Russia

187
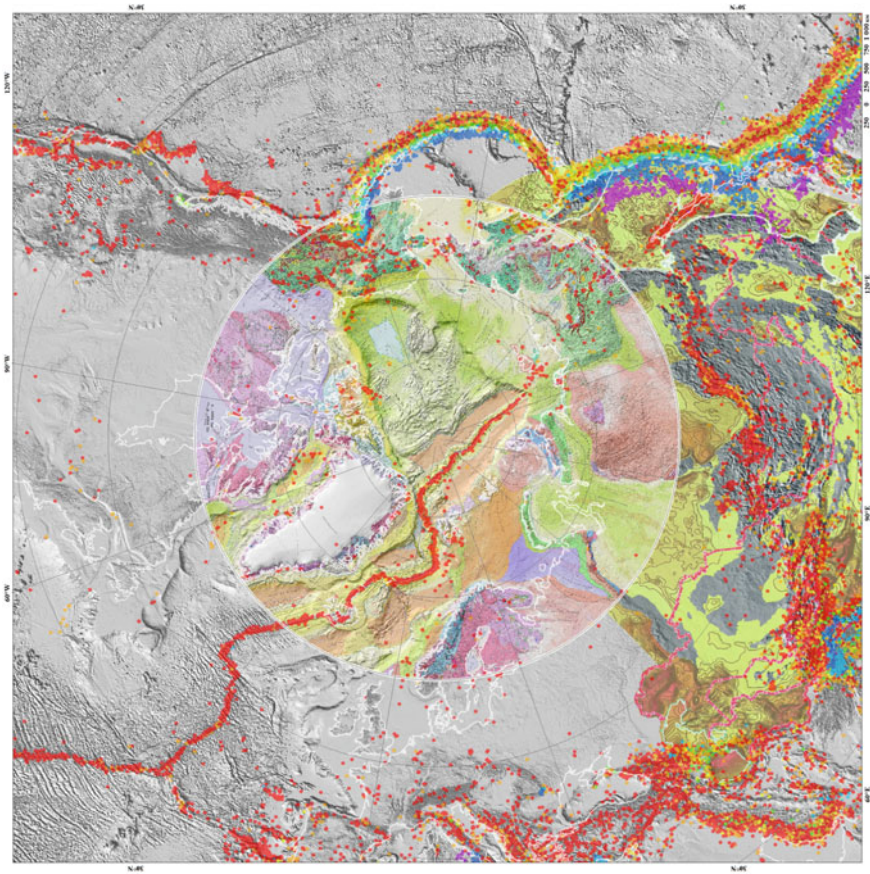
Fig. 1 Tectonic map of the Arctic superposed bathymetry map and scheme of modern seismicity
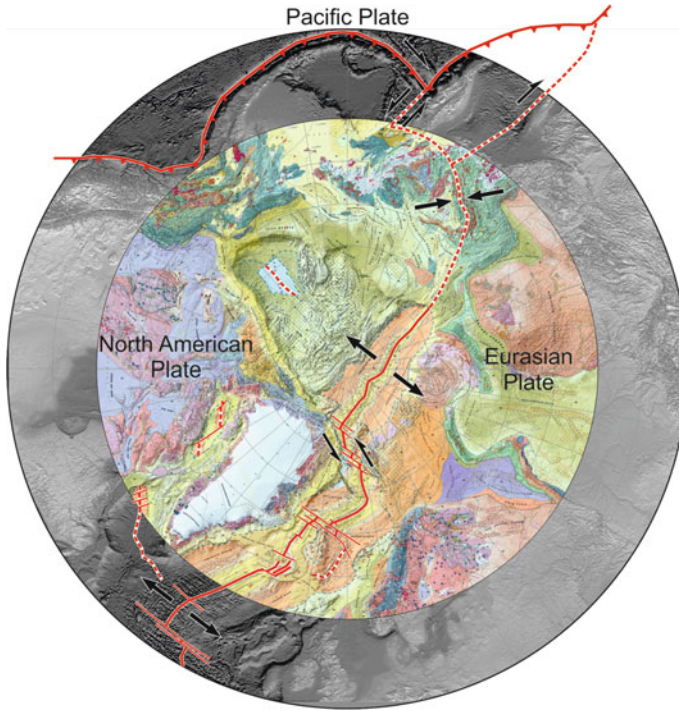
the boundary of the North American and Eurasian lithospheric plates is marked by small-focus seismic activity with an areal distribution of epicentres (www.iris.edu).

According to the latest plate-tectonic model, the present-day tectonic structure of the Arctic is determined by the interaction of three lithospheric plates: two continental North American and Eurasian and Pacific Oceanic (Figs. 2 and 3).

The Pacific Oceanic Plate, plunging at different velocities under the North American and Eurasian plates largely determines the kinematics and the age of the boundaries of the lithospheric plates. This is evidenced by the different nature of the subduction zones on the east and west coasts of the Pacific Plate.

On the west coast, interaction of the Pacific and Eurasian lithospheric plates with the formation of active island arcs and marginal basins is observed. Subduction processes of the Andean type are characteristic of the eastern margin of the Pacific Ocean with a gentle subsidence of the oceanic plate and the formation of coastal ridges. The age of the border margins of the Pacific Ocean plate from the

Fig. 2 Tectonic superposed bathymetry map showing boundaries of three lithosphere plates: two continental—North American and Eurasian—and one oceanic—Pacific

North American and Eurasian lithospheric plates is different due to the pronounced asymmetry of the Pacific mid-ocean ridge. The Eurasian and the North American Plates are bordered by the ancient Jurassic-Cretaceous part of the Pacific Plate and Paleogene-Neogene part, respectively.

Due to the different subsidence rates of the Pacific Ocean plate under the North American and Eurasian continental plates, the position of the boundary between the latter varied in the Late Mesozoic-Cenozoic interval. In the early Cretaceous, the boundary between the North American and Eurasian plates passed along the nascent continental rift within the present Canadian Basin. This boundary clearly separates the marginal basins of the Eurasian and North American plate. The formation of high-latitude Early and Late Cretaceous magmatic province, represented today by manifestations of tholeitic and alkaline magmatism in the Svalbard region, on Franz Josef Land, in Arctic Canada and on the Alfa-Mendeleev Rise, is associated with this stage of geodynamic development of the Arctic.

In the Early Paleogene, a change in the kinematics of the North American and Eurasian Plate led to the formation of a young Arctic Ocean defined by the Gakkel Ridge, as well as the Nansen and Amundsen basins. The initial stage of continental rifting and the formation of a new boundary of the North American and Eurasian
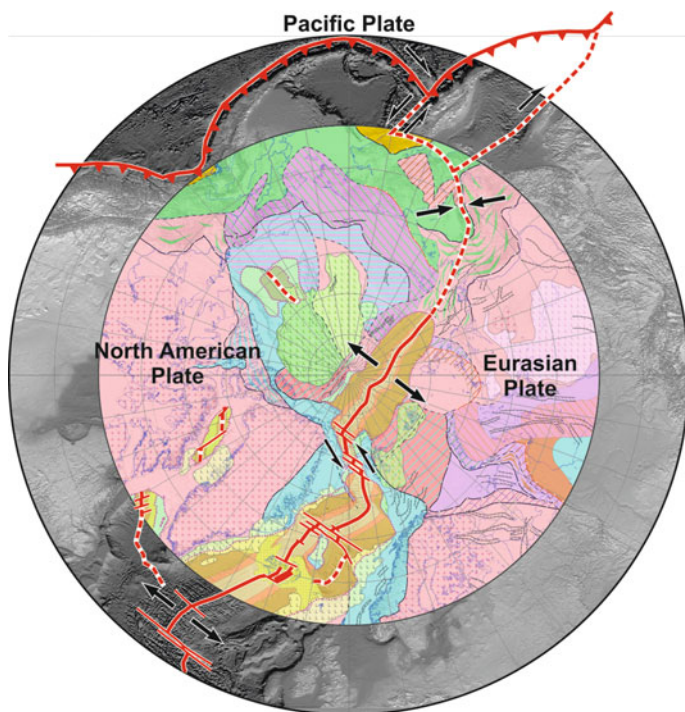
Fig. 3 Tectonic zoning of the Arctic with the lithosphere plates boundaries

lithospheric plates are fixed by manifestations of alkaline magmatism, including in the north of Greenland and on the New Siberian Islands.

The Nansen and Amundsen basins are underlain by a young oceanic crust. The thin (6–8 km) earth crust in the Amundsen basin possesses a two-layer structure (Petrov et al. 2016). The relatively thin low-velocity layer (presumably formed by sedimentary rocks with basalt interlayers) overlaps the thin crystalline crust, which corresponds to the lower mafic crust in its velocity parameters. Such thickness and structural characteristics of the earth's crust are typical of the oceans, as well as the deep-sea soundings of up to 4 km in the Amundsen basin.

The contemporary boundary of the North American and Eurasian continental plates can be traced in the Laptev Sea through a series of following rift depressions, including Ust-Lena, South Laptev, Omoloy Graben and others, which were formed in the Late Cretaceous and Paleogene (Fig. 6). In the continental part of the North-East of Russia, the lithospheric plate boundary passes through the Momsk rift zone presenting itself a series of neotectonic Paleogene-Neogene depressions linearly extended in the north-west direction with manifestations of Cenozoic alkaline-gabbroid magmatism.

At the marginal part of the Eurasian plate within the Barents-Kara passive margin, the crust, which has a thickness of 35–40 km, appears to consist of a three-layer structure (Petrov et al. 2016; Sakoulina et al. 2015, 2016; Roslov et al. 2009; Sakoulina et al. 2000). The thick sedimentary cover is underlain by crystalline crust represented by the upper, low-velocity and—apparently, mostly acidic-crust, and the lower, higher-speed and—possibly—more mafic crust. Such thickness and structure are characteristic of the crust in shallow marginal continental seas.

The Amerasian basin is located within the margin part of the North American Plate and includes the region of the Central-Arctic uplifts, composed by the continental-type crust and modified by deep-water rift induced basins of Podvodnikov and Makarov.

In recent years, earth crust of Alpha and Mendeleev Rises has been studied using Russian and Canadian deep seismic sounding profiles (Petrov et al. 2016; Poselov et al. 2011; Lebedeva-lvanova et al. 2006; Funck et al. 2011; Kashubin et al. 2016, 2018). The crust of the Alpha and Mendeleev Rises was identified to be similar to the crust of the Lomonosov Ridge, yet having greater thickness (32–34 km compared to 17–19 km of the Lomonosov Ridge) due to the increased thickness of the lower crust. This is likely to be due to magmatic underplating, which, in turn, led to intraplate basite volcanism and the HALIP formation in this part of the Arctic.

The crust on the Lomonosov Ridge was studied both in the central part of the Arctic Ocean and in the regions of its junction with Greenland and Eastern Siberia. Russian and Danish-Canadian studies have shown the presence of an intermediate (meta-sedimentary) complex and a two-layer structure of the crystalline crust under the sedimentary cover (Poselov et al. 2011; Jackson et al. 2010). The total thickness of the crust of the Lomonosov Ridge comprises 17–19 km. At present, the continental character of the Lomonosov Ridge is recognised by most Arctic researchers (Jokat 2005; Mooney 2007 etc.).

The crust of the Podvodnikov basin is thinner than that of the surrounding uplifts, reaching a value of 14–27 km. However, its crystalline part is comprised of two layers. The most likely explanation for this is the rift character of the sedimentary basin, formed as a result of stretching of the continental crust followed by its subsidence to depths of 3.5–4 km (Petrov et al. 2016; Kashubin et al. 2013; Lebedeva-lvanova et al. 2011).

Thus, the Amerasian basin is found to be underlain primarily by continental crust, thinned and processed to varying degrees by Cretaceous trap basalt magmatism and characterised by a mosaic magnetic field. The relict of the Cretaceous oceanic crust in the Amerasian basin is assumed only in a limited area of the central Canadian basin (according to the refracted wave velocities) as well as, according to some Canadian and American researchers (Miller et al. 2017), in the Makarov basin.

The results are reflected in the map of the crustal thickness of the Circumpolar Arctic (Fig. 4), which includes seismic profiling and interpolation data constructed from the correlation between the depth of the Moho discontinuity, topography and gravitational anomalies. The areas of continental crust, reduced continental crust and oceanic crust highlighted on the map are also reflected in maps of magnetic and
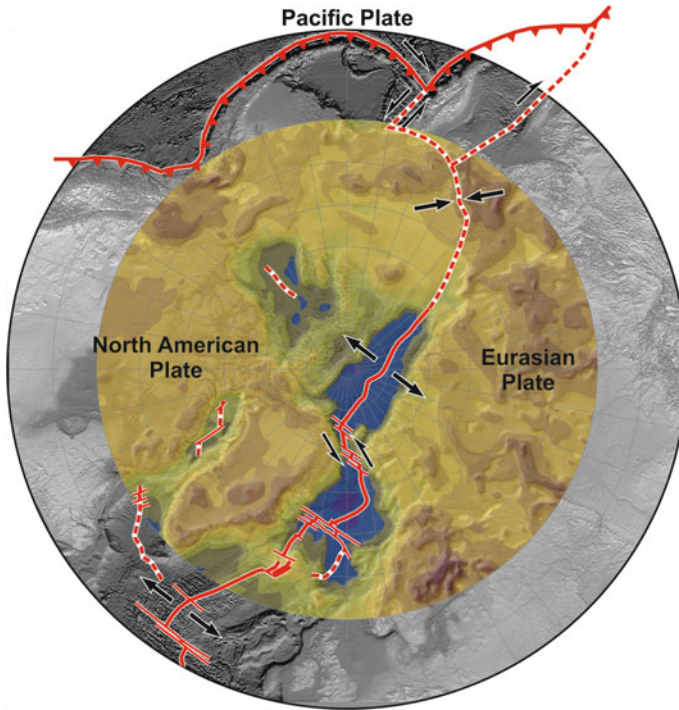
Fig. 4 The map of earth's crust thickness shows that the earth's crust in the Canada, Podvodnikov and Makarov basins has a structure typical for deep sedimentary basins such as South Barents or Peri-Caspian depressions

gravitational fields; these are in good agreement with all current data obtained from studying Arctic islands and carrying out geological sampling of the Arctic seabed.

An analysis of the crustal thickness of the Podvodnikov and Makarov basins—as well as of the Canadian basin—showed that they have a structure typical of inland deep-water sedimentary basins, such as the South Barents Sea or the Peri-Caspian depressions.

The map of the sedimentary cover shows that this reaches a thickness of more than 6–12 km within the Podvodnikov, Makarov and Canadian basins (Fig. 5). This is similar to the sedimentary cover thickness in the South Barents Sea and Peri-Caspian depressions, but is not typical of the oceanic floor (Fig. 6).

Geological testing of underwater escarps carried out by Russian and international expeditions in the Arctic from 2000 to 2016 established that the consolidated sedimentary cover of the zone of Central-Arctic uplifts is composed of terrigenous-carbonate formations aged from upper Vendian to Permian and formed in epicontinental, mostly shallow waters. This overlaps with the poorly lithified, predominantly terrigenous sediments of Meso-Cenozoic origin. All igneous intrusive and effusive formations are represented by a platform trap formation.
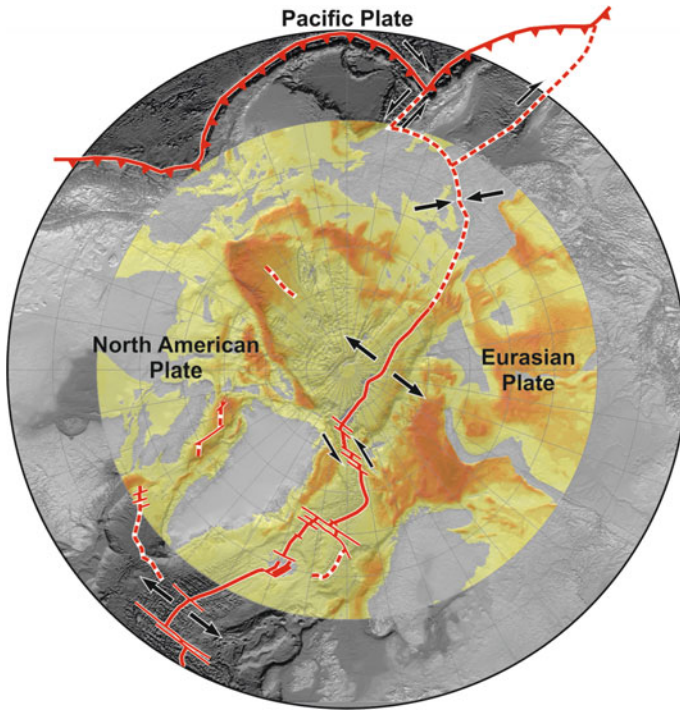
Fig. 5 The map of the sedimentary cover thickness of the Circumpolar Arctic

An analysis of the seismic profiles of the SRM CDP, which intersect all the major tectonic structures of the aquatorial part of the eastern regions of the Russian Arctic, showed close geological connections between the deep-water uplifts of the Central Arctic and the structures of the adjacent shallow-water shelf. The composite profiles presented in the atlas intersect all the most important tectonic structures of the eastern regions of the Russian Arctic.

The composite seismic profile Es10z22m–AR 1401 (1527 km long) crosses the shelf of the East Siberian Sea and the Podvodnikov basin. This profile illustrates continuous tracking of seismic complexes from the shelf to the deepwater part of the North Arctic Ocean. The minimum thickness of sediments (0–3.0 km) is recorded in the south-east along the profile ES10z22m to a stake of 180 km. In the area of this stake there is a serious disturbance in seismic dataset. The basement in the southern block at shallow depths is divided into blocks and characterised by the absence of a constant reflector as well as relatively low velocities (from 4.1 to 4.5 km/s). All these features are characteristic of the young Cimmerian basement. To the north of the 180 km stake, there is a sharp increase in the number of seismic complexes (up to 5), as well as in the thickness of sediments (up to 19 km). The same record structure is traced further northward into the deep-sea part of the Arctic Ocean, into
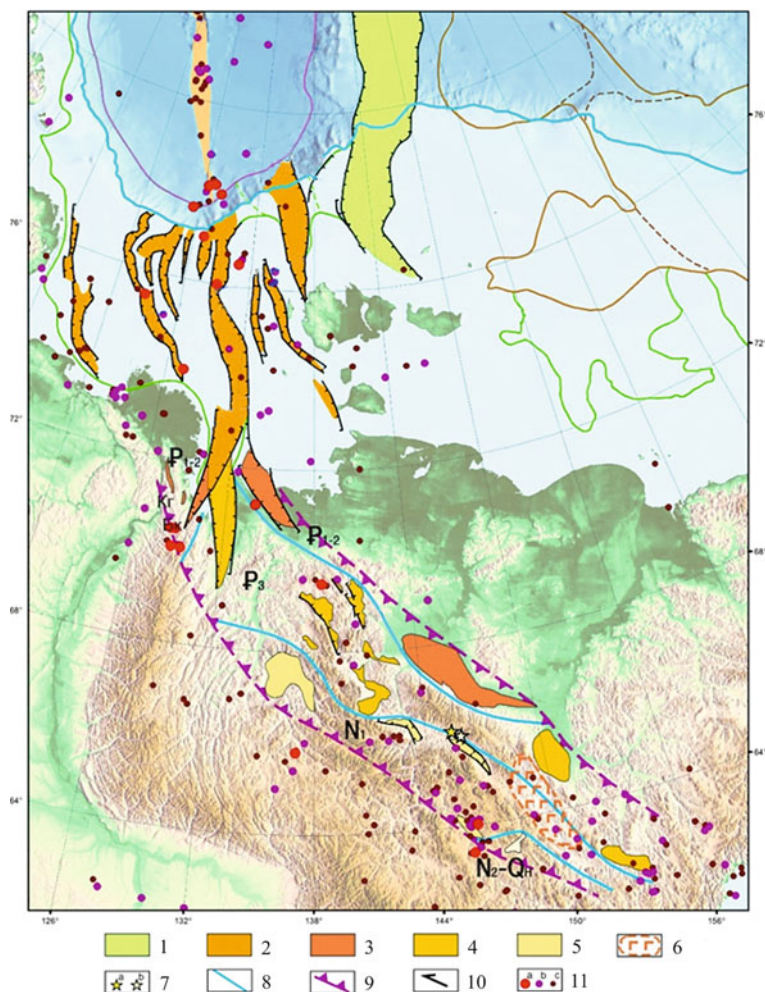
Fig. 6 The Laptev Basin depressions and the Momsky rift system. 1 to 5—age of the basins: 1—Late Cretaceous; 2—Oligocene (P3); 3—Paleocene-Eocene (P1–2), 4—Miocene (N1), 5—Pliocene-Eopleistocene; 6—areal of Early Eocene sodium alkaline-gabbroid magmatism; 7—Cenozoic volcanoes: a—Miocene (Urasa-Khaya volcano), b—Neopleistocene (Balagan-Tas volcano); 8—boundaries of the Mom-sky rift system; 9—boundaries of zones according to the age of riftogenic depressions; 10—general direction of shear movements; 11—earthquakes epicenters

the Podvodnikov basin, along the AR 1401 profile to a stake of 700 km (see paper of Daragan-Sushcheva et al. in this volume).

The AR1402 and AR1406 seismic profiles were obtained by JSC "MAGE" in 2014 as a result of seismic work at the R/V "Akademik Fedorov". The composite profile starting in the north of the East Siberian Sea (AR1402) crosses the De Long uplift, the Podvodnikov basin, the Toll saddle (AR1406), the Makarov basin and the

Lomonosov Ridge. The section along the AR1402–AR1406 profile, as well as the previously mentioned ES10z22m–AR 1401 profile, gives an idea of the structure and characteristics of the sedimentary cover during the transition from the shelf of the East Siberian Sea to the deep part of the Arctic Ocean. The stratigraphic volume of the pre-Cenozoic part undergoes significant changes: the greatest thickness is observed within the limits of the Zhokhovsky trough and the Podvodnikov basin (up to 7–8 km). The most ancient complex, composed of Carboniferous-mid-Permian sediments, lies between the basement and the PU horizon, which is mapped only in the north of the East Siberian Sea within the stakes of 700–725 km.

According to the plate-tectonic model, the region of the Central-Arctic uplifts comprises the marginal part of the North American Continental Plate and all modem tectonic processes within it belong to the in-traplate (Fig. 7). At present, the Neoproterozoic (Epigrenville) craton modified by the Mesozoic-Cenozoic structures is confidently asserted to occupy the entire polar region, including islands, shelves and the Central Arctic uplifts of the Amerasian basin. This plate tectonic model confirms the assumptions of Academicians N. S. Shatsky, Yu. M. Push-charovsky, V. E. Khain, Soviet and Russian scientists L. P. Zonenshain, L. M. Natapov and others, who, in the middle of the last century, identified this structure as the Hyperborea platform, known in later literature as Arktide.
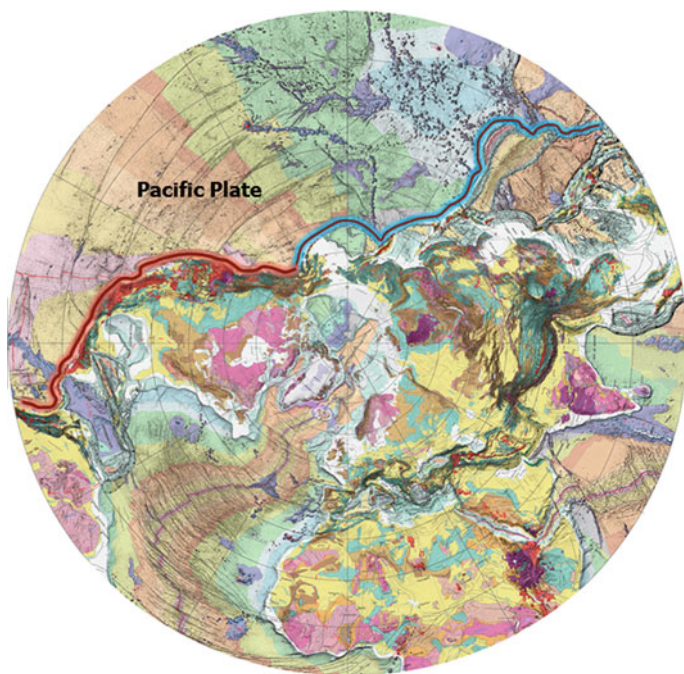
Fig. 7 Geological map of the Northern Hemisphere compiled by Commission for the Geological Map of the World (CGMW) and subduction zones of Pacific oceanic plate submerges under the North-American (red) and Eurasian (blue) plates

Thus, the modern plate-tectonic model of the Arctic is based on a set of reliable geological data on this territory, obtained over the past 15 years as a result of geological and geophysical work by geological services, national academies of sciences and universities of Russia, USA, Canada, Norway, Denmark, Germany and France. These works were supported by the UNESCO Commission for the Geological Map of the World (CGMW), the International Union of Geological Sciences (IUGS), the International Commission on Stratigraphy (ICS) and national programmes for the scientific substantiation of the extension of the continental shelf (ECS).

In particular, this work includes data on modern seismicity accumulated in the Global Seismographic Network in recent years (www.iris.edu) (Figs. 8 and 9), which includes data on potential fields formed on the basis of the magnetic and gravitational field maps included in the set of additional maps for the Tectonic Map of the Arctic. This also comprises more than 300 seismic profiles of the DSS with a total length
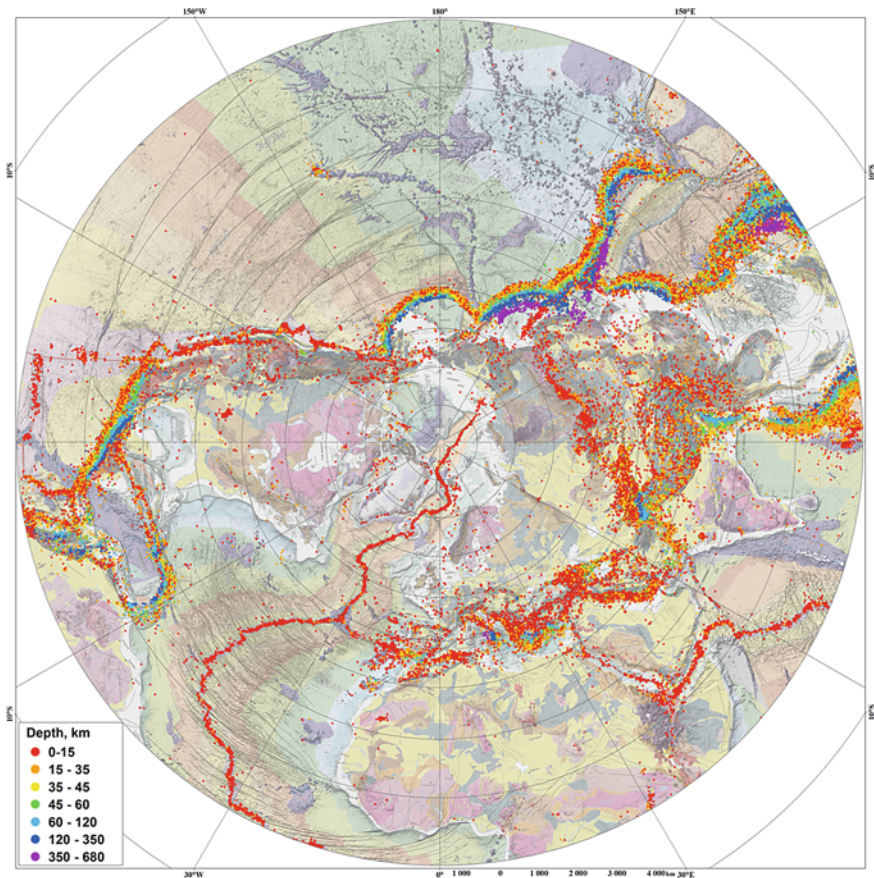
Fig. 8 Scheme of modern seismicity of Northern Hemisphere [data from Global Seismographic Network (www.iris.edu)]
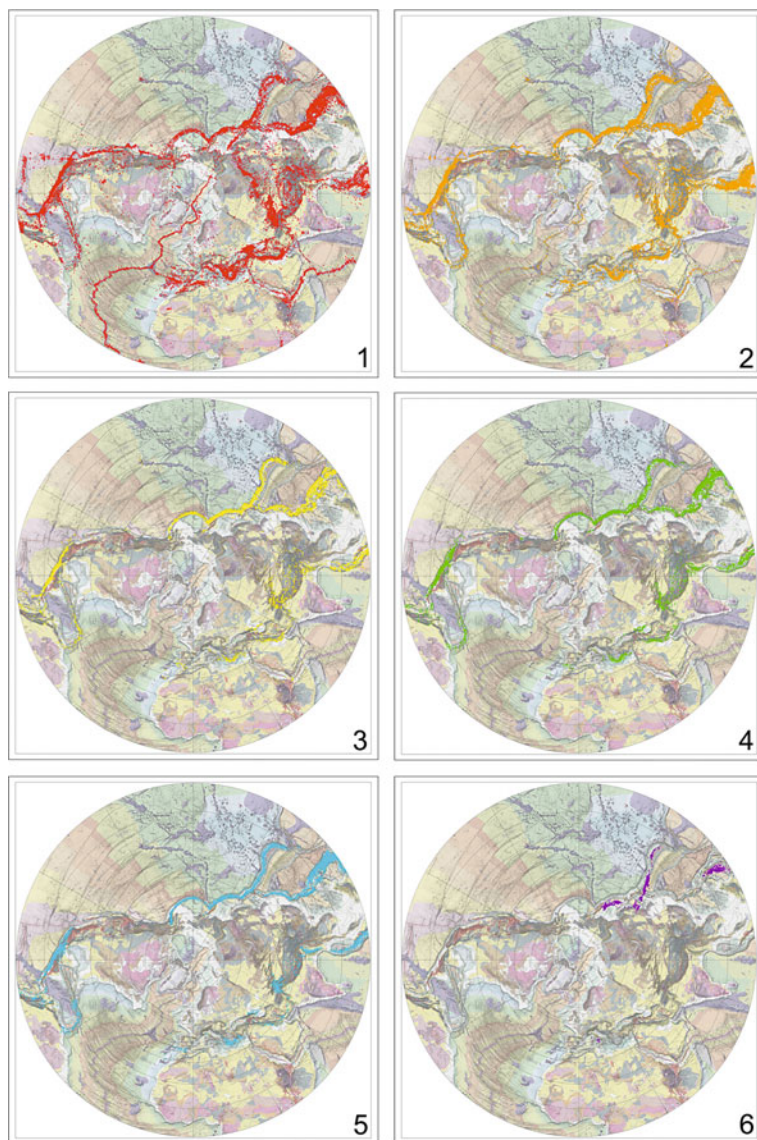
Fig. 9 Scheme of earthquake centers depths

of over 140,000 km, obtained during national and international geophysical studies of the continental shelves and deep-water areas of the North American and Eurasian lithospheric plates. The obtained geological and geophysical data is reflected in the maps of the thickness of the earth's crust and sedimentary cover. These are the results of a comprehensive study of bottom-rock material and materials of deep-water drilling from the Lomonosov Ridge, Alpha and Mendeleev Rises and Chukchi

Plateau (expedition Arctic-2004; 2005; 2012, Polarstern-2006, Heally-2002, etc.), as well as new data on geological structure, isotopic geochronology and geo-chemistry of sedimentary strata of arctic islands and continental land-mass.

The combined geological and geophysical data collected by the international community in recent years thus permitted the achievement of a significant break-through in scientific knowledge of the deep structure of the Arctic basin, providing a reliable basis for the creation of a state-of-the-art Arctic plate tectonic model.

2   Tectonic Evolution of the Eastern Arctic

Tectonic zoning of the Arctic displays distinct relationship between geological structures, crustal types, and the consolidated basement age. There are several major stages of folding in the tectonic evolution of the Arctic: (1) Baikalian or Timanian (Late Vendian—Early Cambrian), Ellesmerian (Late Devonian—Early Carboniferous), Chukchi or Brooks (late Early Cretaceous), and Eurekan (Middle Eocene). Each epoch followed the closure of paleoceanic basins and completed the formation of fold belts.

Formation of the lithosphere structures of the Eastern Arctic took place under the impact of three oceans (Paleo-Asiatic, Atlantic, Pacific) and is closely related to their tectonic history, which is clearly expressed in paleotectonic reconstructions.

The Paleo-Asiatic Ocean was linked with the Pacific via the Polar Urals and Taimyr. After the closure of the paleocean at the end of the Paleozoic and the formation of the Central Asian Fold Belt, the location of the emerging continental and oceanic structures predetermined further tectonic history of the Eastern Arctic in the Mesozoic.

The preserved "Pacific" branch of the Paleo-Asiatic Ocean, the Proto- Arctic Ocean neighboured the Pacific, whose influence is clearly pronounced in geodynamic settings of the active margin with the formation of island arcs and back-arc basins (Fig. 10).

At the same time, in the tectonic evolution of the Arctic, divergent processes typical of the Atlantic took place resulting in the formation of passive margins. For the Eastern Arctic, the influence of the Atlantic was the most distinct in the Cenozoic, when the Eurasian ocean basin formed.

Thus, Eastern Arctic structures formed under the influence and superposition of geodynamic regimes of the Atlantic-type passive continental margin and the active margin of the Pacific Ocean, and the closure of the Paleo-Asian Ocean predetermined the Mesozoic history of the Eastern Arctic and the spatial distribution of continental and oceanic structures.

Formation of the main types of Arctic structures, the way we see it today, started in the Early Mesozoic (Fig. 11).

By the Early Mesozoic (210 Ma), the Ural paleocean had already closed, and in its place, on the border between Euroamerica and Siberia, the oceanic basin (the Proto-Arctic Ocean) remained in the form of a large Pacific Bay (Zonenshain et al.
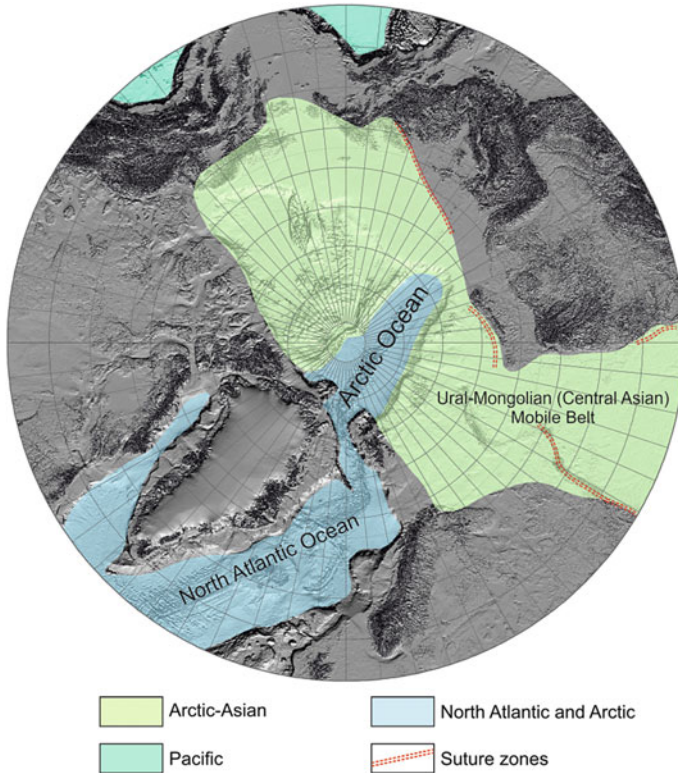
Fig. 10 Map of relationships of recent oceans and Fold Belts in the Arctic. The maps show the relationships between domains with different styles of tectonic evolution: Indo-Atlantic style with spreading-collision events (Scandinavian Caledonides, Appalachian, east Greenland and others) and Pacific accretionary style—with numerous ancient and recent island arcs and marginal seas (whole Arctic-Asian domain and Pacific domain of Russian Northeast and Far East)

1990a, b, Lawver et al. 2002; Sokolov et al. 2014, 2015). The Proto-Arctic Ocean comprised the ocean basins of South Anui and Angayucham.

The northern, American continental margin was passive. Turbidite features the Triassic sediments, which accumulated on the shelf, continental slope, and foothills (Tuchkova 2011). The sandstone composition (Tuchkova et al. 2014) evidences the continental provenance area, which could be the Hyperborean platform (Shatsky 1935), Arctida (Zonenshain et al. 1990a, b) or Crockerland (Embry 1993) in accordance with various reconstructions.

At the end of the Permian and the beginning of the Triassic, in the north of the Siberian continent, intraplate trappean volcanism became widespread. At the same time, the passive Arctic margin of Chukotka underwent destruction (Tectonics… 1980; Ledneva et al. 2011). Numerous sills and hypabyssal bodies of diabase, gabbro and dolerite feature Permian-Lower Triassic sediments of Chukotka. Tuff and basalt that are geochemically similar to the Siberian platform trap (Ledneva et al.
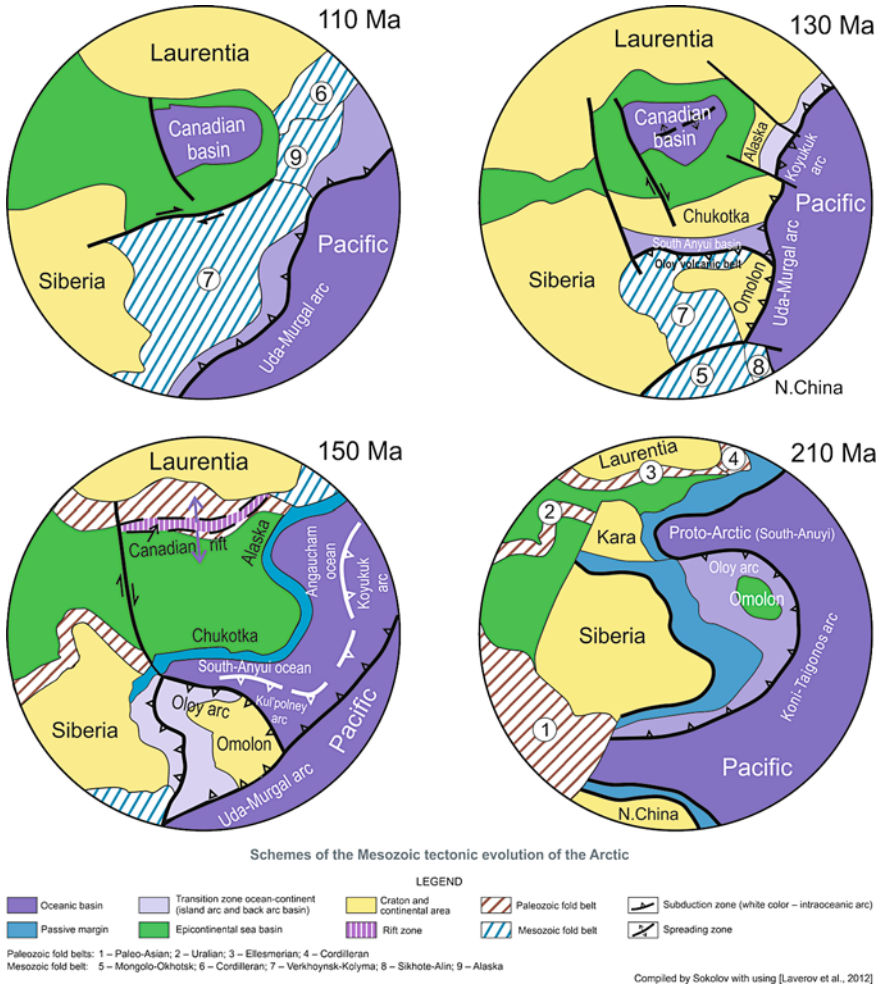
Fig. 11 Schemes of the Mesozoic tectonic evolution of the Arctic

2011, 2014) occur sporadically. The processes of stretching and destruction of the continental crust were interrelated with plume tectonics and the break-up of Pangea (Sokolov et al. 2014).

The southern, Siberian margin of the South Anyui Ocean basin was active. The Alaiai-Oloi island-arc terranes were located along the convergent boundary (Sokolov et al. 2014; Ganelin 2015). The Koni-Taigonos (Koni-Mural according to Parfenov et al. 1993a, b) Island Arc (Sokolov 1992; Sokolov and Tuchkova 2015) occurred on the border with the Pacific. Behind the convergent boundary, there was a system of marginal seas and island arcs with the Omolon and Okhotsk microcontinents.

In Triassic sediments of the passive margin of Siberia, shallow-water shelf facies were replaced eastwards by a more deep-water continental slope and a foot (Parfenov

et al. 1993a, b). Lithologically, they differ significantly from the Triassic sediments of Chukotka and accumulated on different continental margins (Tuchkova et al. 2014).

At the turn of the Middle and Late Jurassic and in the Late Jurassic (150–130 Ma), significant restructuring took place in continental and oceanic structures. Between Siberia and the Pacific Ocean, there were two zones of convergence. In the north-west of the Pacific along the new convergent boundary, the Udsko-Murgal island-arc system was formed, under which the Pacific Ocean lithosphere was subducted. The Uyandina-Yasachnaya island arc emerged in the Verkhoyansk region, near the Siberian continent (Zonenshain et al. 1990a, b). The subduction caused movement and accretion of terrains of the Kolyma Loop and subsequent collision of the Kolyma-Omolon superterrain (Parfenov et al. 1993a, b).

In the Oxfordian-Cimmerian (150–130 Ma), spreading in the Proto-Arctic (South-Anyui) ocean was accompanied by intra-oceanic subduction in the Kulpollney island arc (Sokolov et al. 2015). As of the Volgian, a new stage in the tectonic evolution of the ocean begins. The ocean began to close and turned into the syncollision South-Anyui basin, which kept being filled with terrigenous sediments. At the same time, the convergent border with Siberia restructured and the Oloy volcanic belt was formed on the amalgamated terrains of the Kolyma Loop. The subduction reduced the turbiditic oceanic basin. After the accretion of the Kulpolney Arc, the continental lithosphere of the Chukchi microcontinent began to subduct, which resulted in its collision with the active margin of Siberia. The geodynamic model of the formation and location of the main types of paleostructures can be seen on reconstructions.

In Alaska, the oceanic crust of the Angayucham Basin kept being merged in the subduction zone of the Koyukuk island arc (Moore et al. 1994; Plafker and Berg 1994; Nokleberg et al. 2000a, b). The island arc was in existence for 160–120 million years.

The merge of the oceanic lithosphere southward in the subduction zones of the Kulpolney and Koyukuk island arcs as well as the Oloy volcanic belt caused tension, rupture and separation of the Alaska-Chukotka microplate from the continental margin of Arctic Canada. Riftogenesis began in the Early Jurassic and resulted in the formation of the oceanic crust of the Canada Basin (Embry 1993; Grantz et al. 1990, 2011). According to Shephard et al. (2003), Grantz et al. (2011), the riftogenesis lasted for 195–142 million years, and the spreading lasted for 142–126 (or 120) million years.

It should be noted that the Hauterivian-Barremian reduction and closure of the ocean process occurred simultaneously with the spreading in the Canada Basin. The spreading in the Canada Basin stopped as soon as the collision and the formation of the South Anyui suture in Chukotka and the Kobuk suture in Alaska was over.

The South Anyui suture was formed at the beginning of the Aptian (Fig. 12). Post-collisional granites are 117–108 million years old (Katkov et al. 2010). The collision of the Chukchi microcontinent with the structures of the active Siberian margin resulted in the formation of the Arctic margin of Eurasia in Eastern Arctic. A large continental block, including Chukotka, the shelf with islands and the structures of the Central Arctic elevations (the Mendeleev Rise, the Chukchi Plateau) joined the Asian continent and became its part (Sokolov et al. 2014, 2015).
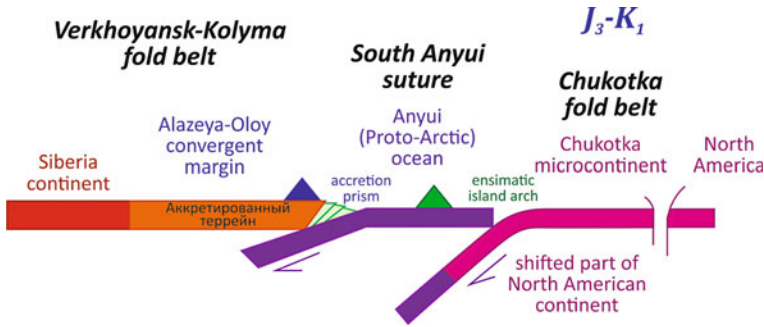
Fig. 12 Geodynamic model of the South Anyui suture. (1) Northern margin (North America) of the Proto-Arctic ocean was passive, and its southern margin (Siberia) was active. There was two south dipping subducted zone: Oloy volcanic belt along Alazeya-Oloy convergent margin and Kul'polney ensimatic arc. Chukotka microcontinent was a shifted block of North America continent. (2) During collision, the passive margin of the Chukotka microcontinent, subducted below the active margin of the North Asian continent. (3) In result of collision the large continental block (Chukotka microcontinent included Chukotka Peninsula, Chukchi Plato, Mendeleeva Uplift. Podvodnikov basin) accreted to Siberia and became a part of Eurasia

Later, in the Aptian-Albian in response to extension, the Ainakhkurgen, Nutesyn and other orogenic depressions filled in volcanic-sedimentary deposits were formed, and the granite-metamorphic domes grew larger (Bering… 1997; Luchitskaya et al. 2010).

Intense intraplate volcanism (HALIP, 120–110 Ma) and continental riftogenesis are typical of this stage of development in the Arctic. The formation of the South Chukchi Trough (Verzhbitsky et al. 2009; Miller and Verzhbitsky 2009) and the synrift complexes of the Podvodnikov Basin and the Chukchi Plateau (Arctic… 2017) takes its beginning in the studied area.

In the Eastern Arctic, the formation of the Mesozoic folded belts completed by the Aptian–Albian. The spatial position and relation of the continents acquired modern outlines. The Okhotsk-Chukotka volcanic belt emerged on the Pacific margins of Eurasia (the Late Albian–Early Campanian). Since that time, the geodynamic regime of regional extension and thermal immersion has prevailed in the Eastern Arctic. There are several stages of riftogenesis related to the formation of the Arctic Ocean (Drachev 2011; Grantz et al. 2011; Arctic… 2017, etc.).

The formation of the Eurasian Ocean basin started in the late Cretaceous-Early Paleogene. As a result, the Lomonosov Ridge began to move away from the Barents-Kara continental margin. The first stage of rifting occurred in the Late Cretaceous–Early Eocene (80–55 Ma), the second stage corresponds to the late Middle Miocene–Late Miocene (Franke et al. 2001; Drachev 2011). Thick sedimentary cover had been accumulated in the Canada Basin during the Late Cretaceous (Mosher et al. 2012a, b).

Seismic lines across the Eurasian margin of the Eastern Arctic clearly show extensional structures in the form of grabens and semi-grabens of different ages (Jokat

et al. 2003; Arctic Basin… 2017). There are submeridional structures extending from the land to the shelf and to the deep-water part (Vinogradov et al. 2016). The Lower Cretaceous, Brookian, post-Campanian, pre-Miocene and Messinian unconformities have been identified in seismic sections.

The extension of the continental crust was periodically accompanied by volcanic activities. Volcanic rocks, dredged and drilled in the Alpha-Mendeleev Rise, correspond to continental basalts (Mukasa et al. 2015; Morozov et al. 2013). In the Podvodnikov Basin, the Early Cretaceous synrift complex of the same age as the first stage of HALIP volcanism (130–110 Ma) and the Late Cretaceous one associated with the last stage of HALIP (90–80 Ma) have been distinguished.

Along with the general regime of extension, fold-thrust structures were formed on continental margins of Arctic Canada and Alaska. In northern Alaska, the Middle Late Cretaceous and Early Cenozoic deformations lead to the junction of the southern flank of the Colville Basin and the Brooks Fold Belt (Moore et al. 2002). Apatite tracks determine the time of deformations of 60, 45 and 23 Ma (O'Sullivan et al. 1997).

The collision of Greenland and the Ellesmere Islands in the Paleocene and Eocene (Eurekan deformation) resulted in the accumulation of detrital sediments in the Sverdrup Basin and the formation of fold-and-thrust structures in the eastern part of the basin (Harrison et al. 1999; Von Gosen and Piepjohn 2003).

Geodynamic model. When developing tectonic models, it is necessary to explain why the opening of the Eurasian Basin in the Cenozoic was accompanied by the extension in the Eastern Arctic. Attempts to explain such a geodynamic regime by compensation in the subduction zone (Zonenshain et al. 1990a, b, Scotese 2011) turned out to be unsuccessful after ascertaining the composition and age of volcanic rocks from the Alpha Ridge and the Mendeleev Rise.

Analysis of geological and geophysical information, including tomography data for the Northern Pacific and the Arctic, made it possible to propose a new geodynamic model developed by the RAS staff (Lobkovsky et al. 2011; Laverov et al. 2013; Lobkovsky 2011) (Fig. 13).

Seismic tomography data for North-East Asia and the North-West Pacific evidence that the cold matter submerging into the subduction zone reaches the transition zone between the upper and lower mantle and changes its direction of movement and then passes into the extended horizontal layer of cold mantle matter, which spreads out to distances of first thousand kilometers under the Eurasian continent (Zhao et al. 2010).

In this case, a recurrent ascending upper mantle flow emerges, which creates the effect of dragging the Arctic lithosphere towards the Pacific Ocean and provides regional sublatitudinal extension that began in the Aptian–Albian (Lobkovsky et al. 2011; Laverov et al. 2013). As a result, blocks in the form of Alpha and Mendeleev Rises separated from the Barents-Kara margin (Fig. 13). The separation and subsequent moving apart of the Alpha and Mendeleev Rises took place 110 to 60 million years ago and were accompanied by rift-related extension of the Makarov and Podvodnikov Basins.
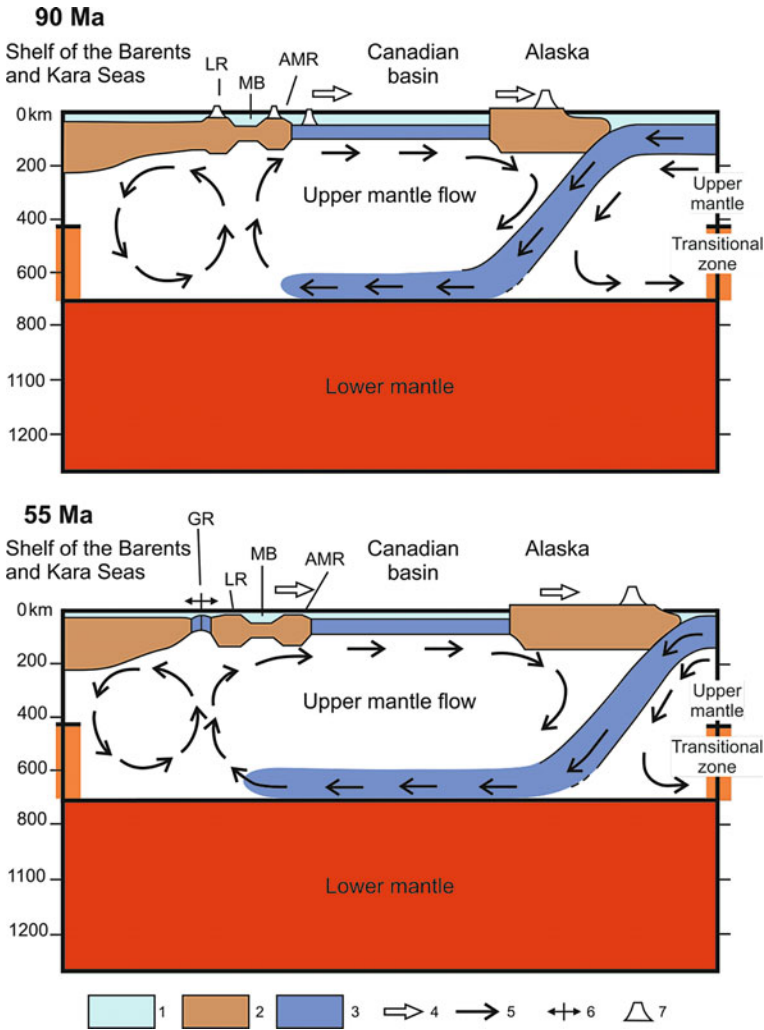
Fig. 13 Model of the upper mantle cell under the continent caused by the Pacific lithosphere subduction (Laverov et al. 2013). 1—ocean water layer, 2—continental lithosphere, 3—ocean lithosphere; 4—continental blocks movement vector towards the Pacific subduction zone due to the convection cell of the upper mantle, 5—direction of flows in the upper mantle and transitional zone, 6—spreading in the Eurasian Basin, 7—magmatism manifestations. Abbreviations: *AMR* the Alpha-Mendeleev Ridge, *GR* the Gakkel Ridge, *LR* the Lomonosov Ridge, *MB* Makarov Basin

Later, the opening of the Eurasian Basin began in the Cenozoic accompanied by the formation of a system of submeridional grabens and horsts.

References

Bering Strait Geologic Field Party (1997) Koolen metamorphic complex, northeastern Russia: Implications for the tectonic evolution of the Bering Strait region. Tectonics 16:713–729

Drachev SS (2011) Tectonic setting, structure and petroleum geology of the Siberian Arctic offshore sedimentary basins. In: Spencer AM, Embry AF, Gautier DL, Stoupakova AV, Sørensen K (eds) Arctic petroleum geology, vol 35. Geol. Soc., London, Mem, pp 369–394

Embry A (1993) Crockerland—the northern source area for the Sverdrup Basin, Canadian Arctic Archipelago. In: Vorren, Bergsager E, Dahl-Stamnes O, Holter E, Johansen B, Lie E, Lund T (eds) Arctic geology and petroleum potential, vol 2. T. Norwegian Petroleum Society, Special Publication, pp 205–216

Franke D, Hinz K, Oncken O (2001) The Laptev Sea Rift. Mar Pet Geol 18:1083–1127

Funck T, Jackson HR, Shimeld J (2011) The crustal structure of the Alpha Ridge at the transition to the Canadian Polar Margin: results from a seismic refraction experiment. J Geophys Res 116:B12101. https://doi.org/10.1029/2011JB008411

Ganelin AV (2015) Ophiolites of Western Chukotka (structure, age, composition, geodynamic setting). GIN RAS, Moscow, 31 p (in Russian)

Grantz A, May SD, Taylor PT, Lawver LA (1990) Canada basin. In: Grantz A, Johnson L, Sweeney JF (eds) The Arctic Ocean region. The geology of North America. L. Geological Society of America, Boulder, CO, pp 379–402

Grantz A, Hart PE, Childers VA (2011) Geology and tectonic development of the Amerasia and Canada Basins, Arctic Ocean. In: Spencer AM, Embry AF, Gautier DL, Stoupakova AV, Sørensen K (eds) Arctic petroleum geology, vol 35. Geological Society London, Memoirs, pp 771–799

Harrison JC, Mayr U et al (1999) Correlation of Cenozoic sequences of the Canadian Arctic region and Greenland; implications for the tectonic history of northern North America. Bull Can Pet Geol 47:223–254

Hopper JR, Funck T, Stoker MS, Arting U, Peron-Pinvidic G, Doornenbal H, Gaina C, Danmarks geologiske undersøgelse (2014) Tectonostratigraphic atlas of the North-East Atlantic region. Geological Survey of Denmark and Greenland, Copenhagen, 338 p

Jackson HR, Dahl-Jensen T, the LORITA working group (2010) Sedimentary and crustal structure from the Ellesmere Island and Greenland continental shelves onto the Lomonosov Ridge, Arctic Ocean. Geophys J Int 182:11–35

Jokat W (2005) The sedimentary structure of the Lomonosov Ridge between 88 °N and 80°N. Geophys J Int 163:698–726

Jokat W, Ritzmann O, Schmidt-Aursch MC, Drachev S, Gauger S, Snow J (2003) Geophysical evidence for reduced melt production on the Arctic ultraslow Gakkel mid-ocean ridge. Nature 423:962–965

Kaminsky VD (ed) (2017) The Arctic Basin (geology and morphology). VNIIOkeangeologiya, St. Petersburg, 291 p (in Russian)

Kashubin SN, Pavlenkova NI, Petrov OV, Milshtein ED, Shokalsky SP, Erinchek YuM (2013) Crust types in the Circumpolar Arctic. Reg Geol Metallogeny 55:5–20 (in Russian)

Kashubin SN, Petrov OV, Artemieva IM, Morozov AF, Vyatkina DV, Golysheva YuS, Kashubina TV, Milshtein ED, Rybalka AV, Erinchek YuM, Sakulina TS, Krupnova NA (2016) Deep structure of the Earth's crust and upper mantle of the Mendeleev Rise along the Arctic-2012 DSS line. Reg Geol Metallogeny 65:16–35 (In Russian)

Kashubin SN, Petrov OV, Milshtein ED, Vinokurov IYu, Androsov EA, Golysheva YuS, Efimova NN, Yavarova TM, Morozov AF (2018) The structure of the earth's crust of the junction zone of the Mendeleev Rise with the Eurasian continent (according to geophysical data). Reg Geol Metallogeny 74:5–18 (in Russian)

Katkov SM, Miller EL, Toro J (2010) Structural paragenes and age of deformation of the Anyui-Chukotka fold system (Northeastern Russia). Geotectonics 44(5):61–80 (in Russian)

Laverov NP, Lobkovsky LI, Kononov MV, Dobretsov NL, Vernikovsky VA, Sokolov SD, Shipilov EV (2013) Geodynamic model of tectonic evolution of the Arctic in the Mesozoic and Cenozoic

and the problem of the outer boundary of the Russia's continental shelf. Geotectonics 1:3–35 (in Russian)

Lawver LA, Grantz A, Gahagan LM (2002) Plate kinematic evolution of the present Arctic region since the Ordovician. In: Miller EL, Grantz A, Klemperer SL (eds) Tectonic evolution of the Bering Shelf–Chukchi Sea–Arctic Margin and adjacent land masses. Special Papers, vol 360. Geological Society of America, Boulder, Colorado, pp 333–358

Lebedeva-Ivanova NN, Zamansky YY, Langnen AE, Sorokin MY (2006) Seismic profiling across the Mendeleev Ridge at 82 °N evidence of continental crust. Geophys J Inter 165:527–544

Lebedeva-Ivanova NN, Gee DG, Sergeyev MB (2011) Chapter 26 Crustal structure of the East Siberian continental margin, Podvodnikov and Makarov basins, based on refraction seismic data (TransArctic 1989–1991). In: Spencer, Embry, Gautier, Stoupakova and Sørensen (eds) Arctic petroleum geology, vol 35. Geological Society of London, pp 395–411

Ledneva GV, Pease VL, Sokolov SD (2011) Permo-Triassic hypabyssal mafic intrusions and associated tholeiitic basalts of the Kolyuchinskaya Bay, Chukotka (NE Russia): links to the Siberian LIP. J Asian Earth Sci 40:737–745

Ledneva GV, Bazylev BA, Layer PW, Ishiwatari A, Sokolov SD, Kononkova NN, Tikhomirov PL, Novikova MS (2014) Intra-plate gabbroic rocks of permo-triassic to early-middle triassic dike-and-sill province of Chukotka (Russia). In: Stone DB, Grikurov GE, Clough JG, Oakey GN (eds) ICAM VI: proceedings of the international conference on Arctic Margins VI. VSEGEI, Petersburg, pp 115–156

Lobkovsky LI (2011) Tectonics of deformable lithospheric plates: generalization of the classic concept, vol 5. Geology of Seas and Oceans, Moscow, pp 24–25 (in Russian)

Lobkovsky LI, Verzhbitsky VE, Kononov MV, Shreider AA, Garagash IA, Sokolov SD, Tuchkova MI, Kotelkin VD, Vernikovsky VA (2011) Geodynamic model of the evolution of the Arctic region in the Late Mesozoic—cenozoic and the problem of the external border of the continental shelf of Russia. Arctic. Ecol Econ 1:104–115 (in Russian)

Luchitskaya MV, Sokolov SD, Bondarenko GE, Katkov SM (2010) Composition and geodynamic setting of granitoid magmatism in the Alyaramaut Uplift (West Chukotka). Geochemistry 9:946–972 (in Russian)

Miller EL, Verzhbitsky VE (2009) Structural studies near Pevek, Russia: implications for formation of the East Siberian Shelf and Makarov Basin of the Arctic Ocean. In: Stone DB, Fujita K, Layer PW, Miller EL, Prokopiev AV, Toro J (eds) Geology, geophysics and tectonics of Northeastern Russia: a tribute to Leonid Parfenov. EGU Stephan Mueller Publication Series, vol 4, pp 223–241

Miller EL, Meisling KE, Anikin VV et al (2017) Circum-Arctic Liotsphere Evolution (CALE) Transect C: displacement of the Arctic Alaska-Chutkotka microplate towards the Pacific during the opening of the Amerasia Basin in the Arctic. In: Pease V, Coakley B (eds) Circum-Arctic litosphere evolution, vol 460. Geol. Soc. London, Spec. Publ. https://doi.org/10.1144/sp460.9

Mooney WD (2007) Crust and lithospheric structure—global crustal structure. In: Romanowicz B, Dziewonski A (eds) Treatise on geophysics, vol 1: seismology and structure of the Earth. Elsevier, pp 361–417

Moore ThE, Dumitru TA, Adams KE et al (2002) Origin of the Lisbume Hills-Herald Arch structural belt: stratigraphic, structural, and fission-track evidens from the Cape Lisbum area, Northwestern Alaska. In: Miller EL et al (eds) Tectonic evolution of the Bering Shelf-Chukchi Sea-Arctic Margin and adjacent landmasses. Geol. Soc. Amer., Boulder, pp 77–109

Moore TE, Wallace WK, Bird KJ, Karl SM, Mull CG, Dillon JT (1994) Geology of northern Alaska. In: Plafker G, Berg HC (eds) The geology of Alaska. Geology of America v. G-1. Geological Society of America, Boulder, Colorado, pp 535–554

Morozov AF, Petrov OV, Shokalsky SP, Kashubin SN, Kremenetsky AA, Shkatov MYu, Kaminsky VD, Gusev EA, Grikurov GE, Recant PV, Shevchenko SS, Sergeev SA, Shatov VV (2013) New geological data substantiating the continental nature of the Central Arctic Uplifts area. Reg Geol Metallogeny 53:34–56 (in Russian)

Mosher DC, Shimeld J, Hutchinson D, Chian D, Lebedova-Ivanova N, Jackson R (2012) Canada Basin revealed. Society of petroleum engineers—Arctic technology conference, vol 2. https://doi.org/10.4043/23797-ms

Mosher DC, Shimeld JW, Chian D, Lebedeva-Ivanova N, Li Q, Hutchinson D, Edwards B, Mayer L, Chapman B (2012) In: Stone DB, Clough JG, Thurston DK (eds) Sediment distribution in Amerasian Basin, Arctic Ocean. Geophys. Institute Report UAG-R-335/. University of Alaska, Fairbanks, Alaska, pp 148–149

Mukasa SB, Mayer LA, Aviado K, Bryce J, Andronikov A, Brumley K, Blichert-Toft J, Petrov OV, Shokalsky SP (2015) Alpha/Mendeleev Ridge and Chukchi Borderland 40Ar/39Ar Geochronology and geochemistry: character of the first submarine intraplate lavas recovered from the Arctic Ocean. Geophysical Research Abstracts, vol 17, EGU2015-8291-2

Nokleberg WJ, Scotese CR, Khanchuk AI, Monger JWH, Dawson KM, Norton IO, Parfenov LM (2000) Dynamic computer model for the Phanerozoic tectonic and metallogenic evolution of the Circum-Pacific. Geol. Society of America Abstracts with Programs, vol 32, No 6, p 59

Nokleberg WJ, Parfenov LM, Monger JWH, Norton IO, Khanchuk AI, Stone DB, Scotese CR, Scholl DW, Fujita K (2000) Phanerozoic tectonic evolution of the Circum-North Pacific. Professional paper 1626.U.S. Geological Survey, 122 p

O'Sullivan PB, Murphy JM, Blythe AE (1997) Late Mesozoic and Cenozoic thermotectonic evolution of the central Brooks Range and adjacent North Slope foreland basin, Alaska: Including fission track results from the Trans-Alaska crustal transect (TACT). J Geophys Res 102(B9):20821–20845. https://doi.org/10.1029/96JB03411

Parfenov LM, Natapov LM, Sokolov SD, Tsukanov NV (1993a) Terrane analysis and accretion in North-East Asia. Geotectonics 1:68–78 (in Russian)

Parfenov LM, Natapov LM, Sokolov SD, Tsukanov NV (1993b) Terrane analysis and accretion in North-East Asia. Island Arc 2:35–54

Petrov O, Smelror M, Morozov A, Shokalsky S, Kashubin S, Artemieva IM, Grikurov G, Sobolev N, Petrov E, Ernst RE (2016) Tectonic model and map of the Arctic region (TeMAr). Earth Science Review

Plafker G, Berg HC (1994) Overview of the geology and tectonic evolution of Alaska. In: Plafker G, Berg HC (eds) The geology of Alaska. Geological Society of America, Boulder, CO, Geology of North America, G-1, pp 989–1021

Poselov VA, Avetisov GP, Kaminsky VD et al (2011) Russian Arctic geotraverses. FGUP VNIIOkeangeologia, St. Petersburg, 172 p (in Russian)

Poselov V, Butsenko V, Chernykh A, Glebovsky V, Jackson HR, Potter DP, Oakey G, Shimeld J, Marcussen C (2011) The structural integrity of the Lomonosov Ridge with the North American and Siberian continental margins. In: ICAM VI: Proceedings of the international conference on Arctic Margins VI, Fairbanks, Alaska, May 2011, pp 233–258. http://www2.gi.alaska.edu/icam6/proceedings/web/

Roslov YuV, Sakoulina TS, Pavlenkova NI (2009) Deep seismic investigations in the Barents and Kara Seas. Tectonophysics 472:301–308

Sakoulina TS, Telegin AN, Tikhonova IM, Verba ML, Matveev YI, Vinnick AA, Kopylova AV, Dvornicov LG (2000) The results of deep Seismic investigation on Geotravers in the Barents Sea from Kola peninsula to Franz-Jozeph Land. Tectonophysics 329:319–331

Sakoulina TS, Pavlenkova GA, Kashubin SN (2015) Structure of the earths crust in the northern part of the Barents-Kara region along the 4-AR DSS profile. Russ Geol Geophys 56(11):1622–1633 (in Russian)

Sakoulina TS, Kashubin SN, Petrov OV, Morozov AF, Krupnova NA, Dergunov NT, Razmatova AV, Tabyrets SN, Kashubina TV, Yavarova TM (2016) The deep structure of the earth's crust and upper mantle of the North-Chukot trough along the GSL Dream-line profile. Reg Geol Metallogeny 68:52–65 (In Russian)

Scotese CR (2011) Paleogeographic reconstructions of the Circum-Arctic Region since the Late Jurassic. Search and Discovery Article #30193. Adapted from oral presentation at AAPG Annual Convention and Exhibition, Houston, Texas, April 10–13, 2011. Posted September 30, 2011

Shatsky NS (1935) On tectonics of the Arctic. Geology and mineral resources of the USSR's North. Glavsevmorput', Leningrad, pp 149–165 (in Russian)

Shepherd GM, Pologruto TA, Svoboda K (2003) Circuit analysis of experience-dependent plasticity in the developing rat barrel cortex. Neuron 38:277–289

Sokolov SD (1992) Accretionary tectonics of the Koryak-Chukotka segment of the Pacific belt. Trans. of Geological Institute Russian Academy of Sciences, 479, Moscow, Nauka, 182 p (in Russian)

Sokolov SD, Tuchkova MI (2015) Mesozoic tectono-stratigraphic terranes of the Koryak-Chukotka region. Special Paper Geol Soc Am 513:461–481

Sokolov SD, Ledneva GV, Tuchkova MI, Luchitskaya MV, Ganelin AV, Verzhbitsky VE (2014) Chukchi Arctic continental margins: tectonic evolution, link to the opening of the Amerasian Basin. In: Fairbanks A, Stone DB, Grikurov GE, Clough JG, Oakey GN, Thurston DK (eds) ICAM VI: Proceedings of the international conference on Arctic Margins VI. A.P. Karpinsky Russian Geological Research Institute (VSEGEI), St. Petersburg, pp 97–114

Sokolov SD, Tuchkova MI, Ganelin AV, Bondarenko GE, Leier P (2015) Tectonics of the South Anyui suture (Northeast Asia). Geotectonics 1:5–30 (in Russian)

Tectonics of the continental margins of the northwestern Pacific Ocean (1980) In: Leytes AM, Fedorovsky VS, Tilman CM, Shilo NA (eds) Nauka Publisher, Moscow, 285 p

Tuchkova MI (2011) Lithology of terrigenic rocks from Mesozoic fold belt of the continental margin (Great Caucasus, North-East Asia), vol 600. Trans. of Geological Institute Russian Academy of Sciences, LAP, 334 p (in Russian)

Tuchkova MI, Sokolov SD, Khudoley AK, Hayasaka Y, Moiseev AV (2014) Permian and Triassic deposits of Siberian and Chukotka passive margins: sedimentation setting and provenance. In: Fairbanks A, Stone DB, Grikurov GE, Clough JG, Oakey GN, Thurston DK (eds) ICAM VI: Proceedings of the international conference on Arctic Margins VI. A.P. Karpinsky Russian Geological Research Institute (VSEGEI), St. Petersburg, pp 61–96

Verzhbitsky VE, Sokolov SD, Tuchkova MI (2009) Tectonics, stages of structural evolution and oil and gas prospects of the shelf of the Chukchi Sea (Russian Arctic). Geology of the polar connections of the Earth. XLII Mater Tecton Appl 1:85–90 (in Russian)

Vinogradov VA, Gusev EA, Rekant PV, Pyatkova MN (2016) Specific features of sedimentary cover formation in the Taimyr-Alaska area of the Arctic (in terms of structural relations in the shelf-ocean system). Petrol Geol Theor Appl Stud 11(1) (in Russian)

Von Gosen W, Piepjohn K (2003) Eurekan transpressive deformation in the Wandel Hav Mobile Belt (northeast Greenland). Tectonics 22(4):1039, 13–28

Zhao D, Piraino F, Liu L (2010) The structure and dynamics of the mantle under East Russia and adjacent regions. Geol Geophys 51(9):1188–1204 (in Russian)

Zonenshain LP, Kuzmin MI, Natapov LM (1990a) Geology of the USSR: a plate tectonic synthesis. In: Page BM (ed) Geodynamics series, vol 21. American Geophysical Union, Washington, DC

Zonenshain LP, Kuzmin MI, Natapov LM (1990) Tectonics of lithospheric plates of the USSR, vol 2. M.: Nedra, Book. 334 p (in Russian)